

ISSN 2312-4334

MINISTRY OF EDUCATION AND SCIENCE OF UKRAINE

East European Journal of Physics

No 2. 2019

2019

East European Journal of Physics

EEJP is an international peer-reviewed journal devoted to experimental and theoretical research on the nuclear physics, cosmic rays and particles, high-energy physics, solid state physics, plasma physics, physics of charged particle beams, plasma electronics, radiation materials science, physics of thin films, condensed matter physics, functional materials and coatings, medical physics and physical technologies in an interdisciplinary context.

Published quarterly in hard copy and online by V.N. Karazin Kharkiv National University Publishing.
ISSN 2312-4334 (Print), ISSN 2312-4539 (Online)

The editorial policy is to maintain the quality of published papers at the highest level by strict peer review.

Approved for publication by the Academic Council of the V.N. Karazin Kharkiv National University (June 24, 2019, Protocol No. 7). EEJP registered by the order of Ministry of Education and Science of Ukraine № 747 of 13.07.2015, and included in the list of scientific specialized editions of Ukraine, which can be published results of dissertations for the Ph.D. and Dr.Sci. degree in physical and mathematical sciences.

Editor-in-Chief

Azarenkov N.A., V.N. Karazin Kharkiv National University, Kharkiv, Ukraine

Deputy editor

Girka I.O., V.N. Karazin Kharkiv National University, Kharkiv, Ukraine

Executive Secretary

Hirnyk S.A., V.N. Karazin Kharkiv National University, Kharkiv, Ukraine

Editorial Board

Adamenko I.N., V.N. Karazin Kharkiv National University, Ukraine

Akulov V.P., City University of New York, USA

Antonov A.N., Institute of Nuclear Research and Nuclear Energy, Sofia, Bulgaria

Barannik E.A., V.N. Karazin Kharkiv National University, Ukraine

Beresnev V.M., V.N. Karazin Kharkiv National University, Ukraine

Berezynoy Yu.A., V.N. Karazin Kharkiv National University, Ukraine

Bizyukov A.A., V.N. Karazin Kharkiv National University, Ukraine

Bragina L.L. STU Kharkiv Polytechnical Institute, Ukraine

Broda B., University of Lodz, Poland

Budagov Yu.A., Joint Institute of Nuclear Research, Dubna, Russia

Dovbnya A.M., NSC Kharkiv Institute of Physics and Technology, Ukraine

Dragovich B.G., University of Belgrade, Serbia

Duplij S.A., Westfälische Wilhelms-Universität Münster, Mathematisches Institut, Münster, Germany

Garkusha I.E., NSC Kharkiv Institute of Physics and Technology, Ukraine

Gofman Yu., Jerusalem College of Technology, Israel

Grekov D.L., NSC Kharkiv Institute of Physics and Technology, Ukraine

Karnaukhov I.M., NSC Kharkiv Institute of Physics and Technology, Ukraine

Khodusov V.D., V.N. Karazin Kharkiv National University, Ukraine

Kondratenko A.N., V.N. Karazin Kharkiv National University, Ukraine

Korchin A.Yu., NSC Kharkiv Institute of Physics and Technology, Ukraine

Krivoruchenko M.I., Institute for Theoretical and Experimental Physics, Moscow, Russia

Lazurik V.T., V.N. Karazin Kharkiv National University, Ukraine

Mel'nik V.N., Institute of Radio Astronomy, Kharkiv, Ukraine

Merenkov N.P., NSC Kharkiv Institute of Physics and Technology, Ukraine

Neklyudov I.M., NSC Kharkiv Institute of Physics and Technology, Ukraine

Noterdaeme J.-M., Max Planck Institute for Plasma Physics, Garching, Germany

Nurmagambetov A.Yu., NSC Kharkiv Institute of Physics and Technology, Ukraine

Onyschenko I.M., NSC Kharkiv Institute of Physics and Technology, Ukraine

Ostrikov K.N., Plasma Nanoscience Centre Australia, Clayton, Australia

Peletminsky S.V., NSC Kharkiv Institute of Physics and Technology, Ukraine

Pilipenko N.N., NSC Kharkiv Institute of Physics and Technology, Ukraine

Radinschi I., Gheorghe Asachi Technical University, Iasi, Romania

Slyusarenko Yu.V., NSC Kharkiv Institute of Physics and Technology, Ukraine

Smolyakov A.I., University of Saskatchewan, Saskatoon, Canada

Shul'ga N.F., NSC Kharkiv Institute of Physics and Technology, Ukraine

Tkachenko V.I., NSC Kharkiv Institute of Physics and Technology, Ukraine

Voyevodin V.M., NSC Kharkiv Institute of Physics and Technology, Ukraine

Yegorov O.M., NSC Kharkiv Institute of Physics and Technology, Ukraine

Editorial office

Department of Physics and Technologies, V.N. Karazin Kharkiv National University

Kurchatov av., 31, office 402, Kharkiv, 61108, Ukraine

Tel: +38-057-335-18-33,

E-mail: eejp@karazin.ua,

Web-pages: <http://periodicals.karazin.ua/eejp> (Open Journal System)

Certificate of State registration No.20644-10464P, 21.02.2014

ORIGINAL PAPERS

- Algebraization in Stability Problem for Stationary Waves of the Klein-Gordon Equation** 5
Nataliia Goloskubova, Yuri Mikhlin
Алгебраїзація в задачі стійкості стаціонарних хвиль рівняння Клейна-Гордона
Н.С. Голоскубова, Ю.В. Міхлін
- Research of the Syngle Crystal and Multilayer Composite Detectors Response Under Irradiation by Fast Neutrons** 11
Volodymyr Ryzhikov, Gennadiy Onyshchenko, Ivan Yakymenko, Sergei Naydenov, Alexandr Opolonin, Sergei Makhota
Дослідження відгуку монокристалічних та багатошарових детекторів на опромінення швидкими нейтронами
В.Д. Рижиков, Г.М. Оницько, І.І. Якименко, С.В. Найденов, О.Д. Ополонін, С.В. Махота
- Novel Phosphonium Dye TDV1 as a Potential Fluorescent Probe to Monitor DNA Interactions with Lysozyme Amyloid Fibrils** 19
Olga Zhytniakivska, Uliana Tarabara, Kateryna Vus, Valeriya Trusova, Galyna Gorbenko, N. Gadjev, Todor Deligeorgiev
Новий фосфонієвий барвник як потенційний флуоресцентний зонд для дослідження взаємодії ДНК з амілоїдними фібрилами лізоциму
О. Житняківська, У. Тарабара, К. Вус, В. Трусова, Г. Горбенко, Н. Гаджев, Т. Делігеоргієв
- Study of Advanced Nanoscale ZRN/CRN Multilayer Coatings** 27
Olga Maksakova, Alexander Pogrebnyak, Vyacheslav Beresnev, Vyacheslav Stolbovoy, Sónia Simoês, Dosym Yerbolatuly
Дослідження перспективних нанорозмірних ZRN/CRN багатошарових покриттів
О.В. Максакова, О.Д. Погребняк, В.М. Береснев, В.О. Столбовий, С. Симоєс, Д. Єрболатули
- Effect of Silicon Surface Treatment on the Electrical and Photoelectric Properties of Nanostructured MoO_x/N-Si Heterojunctions** 33
Mykhailo Solovan, Taras Kovalyuk, Pavlo Maryanchuk
Вплив обробки поверхні кремнію на електричні і фотоелектричні властивості наноструктурованих гетеропереходів MoO_x/N-Si
М.М. Солован, Т.Т. Ковалюк, П.Д. Мар'янчук
- Regularities of Changes in Kearns Texture Coefficient at Cold Rolling of Zr-2.5%Nb Alloy** 39
Viktor Grytsyna, Dmitry Malykhin, Tetiana Yurkova, Kostiantyn Kovtun, Tetiana Chernyayeva, Gennadiy Kovtun, Vira Kornyejeva, Olena Slabospitskaya, Irina Tantsura, Viktor Voyevodin
Закономірності змін текстурного параметра кернса при холодній прокатці сплаву Zr-2.5%Nb
В.М. Грицина, Д.Г. Малихін, Т.С. Юркова, Г.П. Ковтун, К.В. Ковтун, В.В. Корнєєва
О.А. Слабоспицька, І.Г. Танцюра, Т.П. Черняєва, В.М. Воєводін
- Investigation of Silicon and Manganese Solubility in Cementite of Iron-Based Alloys** 46
Natalia Filonenko, Alexander Babachenko, Ganna Kononenko
Дослідження розчинності силіцію та мангану в цементиті сплавів на основі заліза
Н.Ю. Філоненко, О.І. Бабаченко, Г.А. Кононенко
- Solubility of Boron and Carbon in Ferrite of the Fe-B-C System Alloys** 52
Natalia Filonenko
Розчинність бору та карбону в фериті сплавів системи Fe-B-C
Н.Ю. Філоненко
- GEANT4 Modeling of Energy Spectrum of Fast Neutrons Source for the Development of Research Technique of Heavy Scintillators** 58
Viktoriia Lisovska, Tetiana Malykhina, Valentina Shpagina, Ruslan Timchenko
GEANT4-моделювання енергетичного спектру джерела швидких нейтронів для напрацювання методики дослідження важких сцинтиляторів
В.В. Лісовська, Т.В. Малихіна, В.О. Шпагіна, Р.М. Тимченко

East European Journal of Physics

No 2 2019

- Improvement of Properties of Self-Injected and Accelerated Electron Bunch by Laser Pulse in Plasma, Using Pulse Precursor** 64
Vasyl Maslov, Denys Bondar, Iryna Levchuk, Ivan Onishchenko
Поліпшення властивостей самоінжектованного і прискореного електронного згустку лазерним імпульсом в плазмі використанням передвісника
В.І. Маслов, Д.С. Бондар, І.П. Левчук, І.М. Онищенко
- Uniform Focusing of Sequence of Relativistic Positron Bunches in Plasma** 69
Vasyl Maslov, Denys Bondar, Iryna Levchuk, Sofiia Nikonova, Ivan Onishchenko
Однорідне фокусування послідовності релятивістських позитронних згустків у плазмі
В.І. Маслов, Д.С. Бондарь, І.П. Левчук, С.А. Ніконова, І.М. Онищенко
- METHODOLOGY OF SCIENCE
- Formalization of Cognition Process as an Additional Component Responsible for Development of Theoretical Physics** 75
Jaroslaw Kaczmarek
Формалізація процесу пізнання як додаткового компонента, відповідального за розвиток теоретичної фізики
Ярослав Качмарек
- HISTORY OF SCIENCE
- Institute of Theoretical Physics after A.I. Akhiezer** 113
Alla Tanshina
Институт теоретической физики имени А.И. Ахиезера
Алла Таньшина

PACS: 05.45-a; 46-40.Ff

ALGEBRAIZATION IN STABILITY PROBLEM FOR STATIONARY WAVES OF THE KLEIN-GORDON EQUATION

 Nataliia Goloskubova*,  Yuri Mikhlin**

National Technical University "KhPI",
Kyrpychev str. 2, Kharkiv, Ukraine

*E-mail: nataligoloskubova1992@ukr.net, **E-mail: muv@kpi.kharkov.ua

Received February 1, 2019; revised February 13, 2019; accepted April 15, 2019

Nonlinear traveling waves of the Klein-Gordon equation with cubic nonlinearity are considered. These waves are described by the nonlinear ordinary differential equation of the second order having the energy integral. Linearized equation for variation obtained for such waves is transformed to the ordinary one using separation of variables. Then so-called algebraization by Ince is used. Namely, a new independent variable associated with the solution under consideration is introduced to the equation in variations. Integral of energy for the stationary waves is used in this transformation. An advantage of this approach is that an analysis of the stability problem does not need to use the specific form of the solution under consideration. As a result of the algebraization, the equation in variations with variable in time coefficients is transformed to equation with singular points. Indices of the singularities are found. Necessary conditions of the waves stability are obtained. Solutions of the variational equation, corresponding to boundaries of the stability/instability regions in the system parameter space, are constructed in power series by the new independent variable. Infinite recurrent systems of linear homogeneous algebraic equations to determine coefficients of the series can be written. Non-trivial solutions of these systems can be obtained if their determinants are equal to zero. These determinants are calculated up to the fifth order inclusively, then relations connecting the system parameters and corresponding to boundaries of the stability/instability regions in the system parameter space are obtained. Namely, the relation between parameters of anharmonicity and energy of the waves are constructed. Analytical results are illustrated by numerical simulation by using the Runge-Kutta procedure for some chosen parameters of the system. A correspondence of the numerical and analytical results is observed.

KEY WORDS: the Klein-Gordon equation, stationary waves stability, Ince algebraization

The nonlinear Klein-Gordon equation appears in different physical problems, namely, in problems of wave propagation through a region of weak superconductivity (so-called Jefferson transition), motion of dislocations in crystals, propagation of waves in ferromagnetic materials, propagation of laser pulses in a two-phase medium, studying surfaces with negative Gaussian curvature, relativistic effects etc. [1-4]. Besides, it can be considered as useful mathematical model to describe a behavior of various types of traveling waves. Among the articles on the stability of nonlinear traveling waves, we highlight the paper [5], where the stability of traveling waves in some general distributed nonlinear system is considered, and the paper [6], where the stability of traveling waves in some nonlinear chain is analyzed. A variety of analytical, numerical and hybrid techniques are used to study travelling waves and their properties in [7]. In the presented paper the Klein-Gordon equation with cubic nonlinearity is used to represent new method for studying the stability of traveling waves. Namely, the so-called Ince algebraization [8] is used. Note that this approach was successfully used earlier in study of the stability of nonlinear normal vibration modes in nonlinear systems with a finite number of degrees of freedom [9-11]. Besides, this procedure is similar to one proposed in the paper [5] for the stability of traveling waves problem, but results on such stability problem for concrete systems are not presented in this publication. The Ince algebraization is based on a choice of the new independent variable, determining the traveling wave under consideration. An advantage of the proposed approach is that we do not need to use a specific form of the solution under consideration in analysis of the stability problem.

The present paper aims at contributing of the Ince algebraization to the problem of nonlinear wave stability. Our task is to use the proposed approach in regard of the equations in variations for the traveling waves of the nonlinear Klein-Gordon equation. Numerical simulation illustrates obtained theoretical results.

THE GENERAL MODEL. STATIONARY TRAVELING WAVES

One considers the Klein-Gordon equation with cubic nonlinearity:

$$\frac{\partial^2 u}{\partial t^2} - c_0^2 \frac{\partial^2 u}{\partial x^2} + \omega_0^2 u = -qu^3 \quad (1)$$

Stationary traveling waves are presented in the following form:

$$u = \Phi(\varphi): \text{ where } \varphi = kx - \omega t \quad (2)$$

where φ is the wave phase. Substituting (2) into equation (1), we obtain the following ordinary differential equation for describing traveling waves:

$$\frac{d^2 \Phi}{d\varphi^2} (\omega^2 - c_0^2 k^2) + \omega_0^2 \Phi + q\Phi^3 = 0 \quad (3)$$

The energy integral here is written as follows:

$$\frac{1}{2} \left(\frac{d\Phi}{d\varphi} \right)^2 (\omega^2 - c_0^2 k^2) + \omega_0^2 \frac{\Phi^2}{2} + q \frac{\Phi^4}{4} = h. \tag{4}$$

In addition, from equation (3) we can obtain the following relation, which will be used later in analysis of the traveling wave stability:

$$\frac{d^2\Phi}{d\varphi^2} = \frac{-\omega_0^2\Phi - q\Phi^3}{\omega^2 - c_0^2 k^2}. \tag{5}$$

Besides, from the equation (4) we get the following relation which will be also used later:

$$\left(\frac{d\Phi}{d\varphi} \right)^2 = \frac{2 \left(h - \omega_0^2 \frac{\Phi^2}{2} - q \frac{\Phi^4}{4} \right)}{\omega^2 - c_0^2 k^2}. \tag{6}$$

EQUATION IN VARIATIONS

To study the stability of stationary waves, we write out, first of all, the linearized equation in variations $V(t, x)$ obtained for the solution (2). One has from the equation (3) the following:

$$\frac{\partial^2 V}{\partial t^2} = c_0^2 \frac{\partial^2 V}{\partial x^2} - V(\omega_0^2 + 3q\Phi^2), \tag{7}$$

where the function $\Phi(\varphi)$ is determined by the equation (3).

As the first step, we now introduce the independent variables φ, t instead of the variables x, t . The variational equation (7) in the new variables is rewritten as follows:

$$\frac{\partial^2 V}{\partial \varphi^2} (\omega^2 - c_0^2 k^2) - 2\omega \frac{\partial^2 V}{\partial \varphi \partial t} + \frac{\partial^2 V}{\partial t^2} = -V(\omega_0^2 + 3q\Phi^2). \tag{8}$$

Then we use the separation of variables as $V = e^{st} \check{z}(\varphi)$ and the additional transformation:

$$\check{z}(\varphi) = e^{A\varphi} W, \tag{9}$$

where $A = \frac{s\omega}{\omega^2 - c_0^2 k^2}$. As a result, instead of the equation (8) we get the following ODE in variations:

$$\frac{d^2 W}{d\varphi^2} (\omega^2 - c_0^2 k^2) = -W(B - \omega_0^2 - 3q\Phi^2), \tag{10}$$

where $B = \frac{s^2}{c_0^2 k^2 - \omega^2}$.

Note that since the parameter s^2 is presented in equation (10), in the case of real values of the parameter s , they can be both positive and negative. In view of the transformation (9), this leads to increase of the variations, that is, to instability. Thus, stability can be observed only under the condition that $s^2 < 0$. One has from here that for the stability there should be the following inequalities:

$$B > 0, \text{ if } c_0^2 k^2 - \omega^2 < 0 \text{ and } B < 0, \text{ if } c_0^2 k^2 - \omega^2 > 0. \tag{11}$$

Then, as a new independent variable, instead of φ , the variable Φ , determining the traveling wave under consideration, is chosen. Now, after some transformations, the equation of variations can be presented as,

$$2 \frac{d^2 W}{d\Phi^2} \left(h - \omega_0^2 \frac{\Phi^2}{2} - q \frac{\Phi^4}{4} \right) - \frac{dW}{d\Phi} (\omega_0^2 \Phi + 3q\Phi^3) + W(B - \omega_0^2 - 3q\Phi^2) = 0, \tag{12}$$

whose singular points are obtained when coefficient near the second derivative is equal to zero. One has the following:

$$h - \omega_0^2 \frac{\Phi^2}{2} - q \frac{\Phi^4}{4} \equiv (\Phi - \Phi_0)G(\Phi, \Phi_0) = 0, \tag{13}$$

where Φ_0 is a root of this equation.

The transformation to the equation in variations to the form of equation with singular points (12) is the so-called algebraization by Ince of the stability problem which was first presented in [8]. An advantage of this approach is that an analysis of the stability problem does not need to use the specific form of the solution $\Phi(\varphi)$.

CONSTRUCTION OF BOUNDARIES OF THE STABILITY/INSTABILITY REGIONS

It is shown in [8] that boundaries of the stability/instability regions in the parameter space of the variational equation with singular points are determined by solutions presented in the following series:

$$W = z^r(a_0 + a_1z + \dots). \quad (14)$$

Here r is one of two indices of the variational equation singularity [12], and $z = (\Phi - \Phi_0)$. To determine the indices of the singular point Φ_0 , we introduce the series (14) into equation (12). Collecting the terms with the lowest degree of z , we obtain the following equation to determine these indices:

$$r(r-1)(-\omega_0^2\Phi_0 - q\Phi_0^3) - r(\omega_0^2\Phi_0 + 3q\Phi_0^3) = 0. \quad (15)$$

It follows that

$$r_1 = 0 \quad \text{and} \quad r_2 = -\frac{2q\Phi_0^2}{\omega_0^2 + q\Phi_0^2}. \quad (16)$$

Substituting now the series (14) corresponding to the zero index to the equation in variations (12) and equating the coefficients with the same degrees by z , we get the following infinite recurrent system (17) of linear homogeneous algebraic equations to determine coefficients of the series:

$$\begin{aligned} z^0: & 4a_2 \left[h - \omega_0^2\Phi_0^2 - \frac{q}{4}\Phi_0^4 \right] - a_1(\Phi_0\omega_0^2 + q\Phi_0^3 - B + \omega_0^2 + 3q\Phi_0^2) - a_0 \left(-B + \omega_0^2 + 3q\Phi_0^2 + \frac{q}{4}\Phi_0^4 \right) = 0 \\ z^1: & 12a_3 \left(h - \frac{\omega_0^2}{2}\Phi_0^2 - \frac{q}{4}\Phi_0^4 \right) - a_2(4\Phi_0\omega_0^2 + 4q\Phi_0^3 + 2\omega_0^2 + 6q\Phi_0^2) + a_1(B - 2\omega_0^2 - 6q\Phi_0^2) - 6a_0q\Phi_0 = 0 \\ z^2: & -15a_3(\Phi_0\omega_0^2 + \Phi_0^3q) + a_2(B - 5\omega_0^2 - 12q\Phi_0^2) - 9a_1q\Phi_0 - 3a_0q = 0, \end{aligned} \quad (17)$$

etc.

The system (17) has a non-trivial solution if its determinant is equal to zero. This determinant was calculated up to the fifth order inclusively, and, thus, the relation connecting the system parameters was obtained; as a result, boundaries of the stability/instability regions in the system parameter space can be constructed. Note that boundaries obtained by calculation of determinants of the fourth and fifth orders are close, so, we did not calculate determinants of the highest order than five.

Substituting the series (14) corresponding to the root r_2 into the equation in variations (12) and equating the coefficients with the same degrees by z , we obtain the infinite recurrent system of linear algebraic homogeneous equations for determining the expansion coefficients. Due to bulkiness of these algebraic equations, we present here only two first ones of them by equations (18):

$$\begin{aligned} z^{r_2-1}: & 2 \left[h - \omega_0^2 \frac{\Phi_0^2}{2} - q \frac{\Phi_0^4}{4} \right] \left\{ \frac{2q\Phi_0^2}{\omega_0^2 + q\Phi_0^2} \left[\frac{2q\Phi_0^2}{\omega_0^2 + q\Phi_0^2} - 1 \right] + \frac{2q\Phi_0^2}{\omega_0^2 + q\Phi_0^2} \right\} a_1 - 2a_0 \frac{2q\Phi_0^2}{\omega_0^2 + q\Phi_0^2} \left[\frac{2q\Phi_0^2}{\omega_0^2 + q\Phi_0^2} - 1 \right] \left[(\omega_0^2\Phi_0 + q\Phi_0^3) \right] - \\ & \frac{2q\Phi_0^2}{\omega_0^2 + q\Phi_0^2} a_0 (\omega_0^2\Phi_0 + 3q\Phi_0^3) = 0 \\ z^{r_2}: & a_0 6q\Phi_0 (\omega_0^2\Phi_0 + q\Phi_0^3) \left[h - \omega_0^2 \frac{\Phi_0^2}{2} - q \frac{\Phi_0^4}{4} \right] + a_0 3q\Phi_0 (2 + 2\omega_0^2\Phi_0 + 2q\Phi_0^3) \left[h - \omega_0^2 \frac{\Phi_0^2}{2} - q \frac{\Phi_0^4}{4} \right] + a_0 2(\omega_0^2 + \\ & 3q\Phi_0^2)^2 \left[h - \omega_0^2 \frac{\Phi_0^2}{2} - q \frac{\Phi_0^4}{4} \right] - 2a_0 (\omega_0^2 + 3q\Phi_0^2)^3 + a_0 [-\omega_0^2\Phi_0 - q\Phi_0^3] (\omega_0^2 + 3q\Phi_0^2) (2 + 2\omega_0^2\Phi_0 + \\ & 2q\Phi_0^3) + a_0 \left[-\frac{\omega_0^2}{2} - q \frac{3\Phi_0^2}{2} \right] (\omega_0^2\Phi_0 + q\Phi_0^3) (2 + 2\omega_0^2\Phi_0 + 2q\Phi_0^3) + a_1 [-\omega_0^2\Phi_0 - q\Phi_0^3] (\omega_0^2\Phi_0 + q\Phi_0^3) (2 + \\ & 2\omega_0^2\Phi_0 + 2q\Phi_0^3) + a_1 \left[-\frac{\omega_0^2}{2} - q \frac{3\Phi_0^2}{2} \right] \left[(2 + 4\omega_0^2\Phi_0 + 4q\Phi_0^3) (\omega_0^2 + 3\Phi_0^2q) \right] + a_2 (2 + 2\omega_0^2\Phi_0 + 2q\Phi_0^3) (\omega_0^2\Phi_0 + \\ & q\Phi_0^3) + a_1 [4\omega_0^2 + 12\Phi_0^2] \left[h - \omega_0^2 \frac{\Phi_0^2}{2} - q \frac{\Phi_0^4}{4} \right] + a_1 [-\omega_0^2\Phi_0 - q\Phi_0^3] (4 + 4\omega_0^2\Phi_0 + 4q\Phi_0^3) + 4a_2 \left[h - \omega_0^2 \frac{\Phi_0^2}{2} - \right. \\ & \left. q \frac{\Phi_0^4}{4} \right] - a_0 [\omega_0^2 + 3\Phi_0^2q] [\omega_0^2\Phi_0 + q\Phi_0^3] - a_1 (\omega_0^2\Phi_0 + q\Phi_0^3) [\omega_0^2\Phi_0 + q\Phi_0^3] - a_0 (1 + \omega_0^2\Phi_0 + q\Phi_0^3) [\omega_0^2 + \\ & 3\Phi_0^2q] + a_0 [B - \omega_0^2 - 3q\Phi_0^2] = 0. \end{aligned} \quad (18)$$

The resulting system has a nontrivial solution if its determinant is equal to zero. This determinant was calculated up to the fourth order inclusive, and, thus, the relation connecting the system parameters was obtained; so, boundaries

of the stability/ instability regions in the system parameter space are constructed. Note that boundaries obtained by calculation of determinants of the fourth and fifth orders are also close in this case.

Boundaries of the stability/ instability regions in some places of the system parameters are presented in Figs. 1,2. Here we fix the traveling wave amplitude, namely, it is assumed that $\Phi_0 = 1$; the frequency $\omega = 1.5$; $c_0 = 1$; $k = 0.1$. The boundaries in the place of the parameters B, h for index r_1 are chosen in Fig. 1, where the parameter B varies in the interval $[2.9...3.2]$; the system energy h varies in the interval $[0..0.1]$. Here and further the dimensionless parameter of

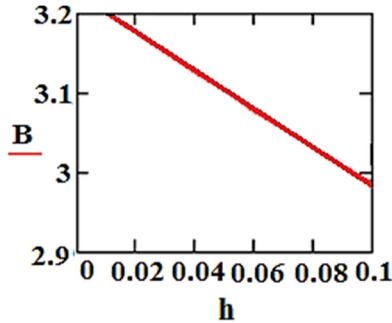


Fig. 1. The boundary between stability/ instability regions in the place (B, h) for index r_1 .

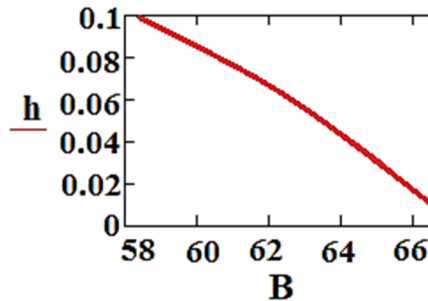


Fig. 2. The boundary between stability/ instability regions in the place (B, h) for index r_2 .

anharmonicity q is calculated from the equation (13); $c_0^2 k^2 - \omega^2 = -2.24$. The boundaries in the place of the parameters B, h for index r_2 are presented in Fig. 2, where the parameter B varies in the interval $[58...66.5]$; the system energy h varies in the interval $[0..0.1]$. In Figs. 1,2 regions of stability are situated on the left side of the obtained boundaries. In Fig.3 the system parameters are chosen as $\Phi_0 = 1$; $\omega = 0.5$; $c_0 = 1$; $k = 0.6$. The boundaries in the place of the parameters (B, h) for index r_2 are chosen in Fig. 3, where the parameter B varies in the interval $[-5...0]$; the system energy h varies in the interval $[0..0.1]$; the parameter q is calculated from the equation (12); $c_0^2 k^2 - \omega^2 = 0.11$. Region of stability is disposed above the boundary showed in Fig. 3.

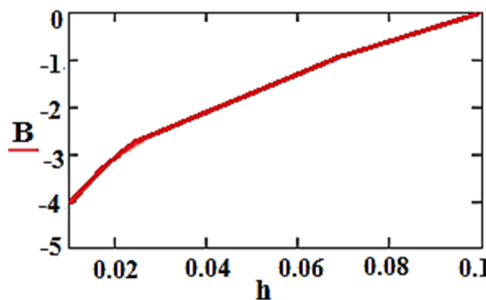


Fig. 3. The boundary between stability/ instability regions in the place (B, h) for index r_2 .

The Runge-Kutta test for the equation in variations (10) shows limited/ unlimited solutions when parameters are chosen from the stability/ instability regions obtained earlier. The same fixed parameters as were used above are used in the calculations. In Fig. 4 the limited solutions of the variational equation are shown. These solutions are chosen in the stability region in the place (B, h) presented in Fig.1. Namely, the system energy $h = 0.05$, the dimensionless parameter $B = 3.1$, the dimensionless parameter $q = -4.43$ are used for Fig. 4a. Fig. 4b is obtained for $h=0.04, B = 60, q = -4.34$.

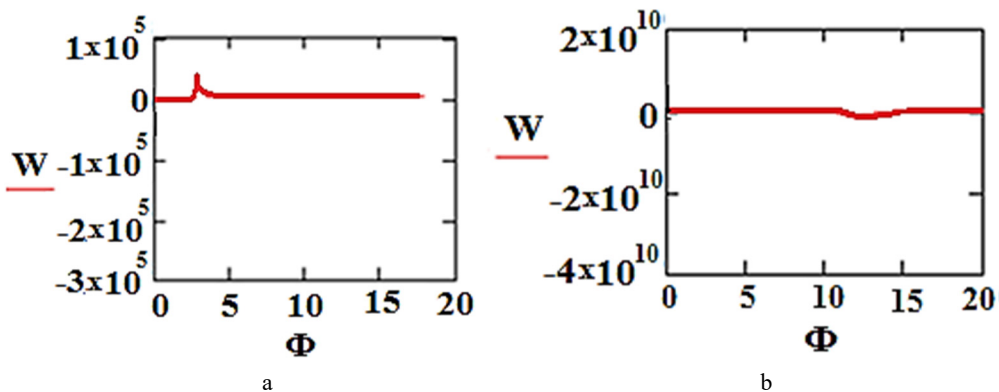


Fig. 4. Limited solutions of the equation in variations chosen in region of stability.

Calculations are made for $h = 0.05, B = 3.1$ (a) and for $h=0.04, B = 60$ (b). Other parameters correspond to ones used for Fig. 1.

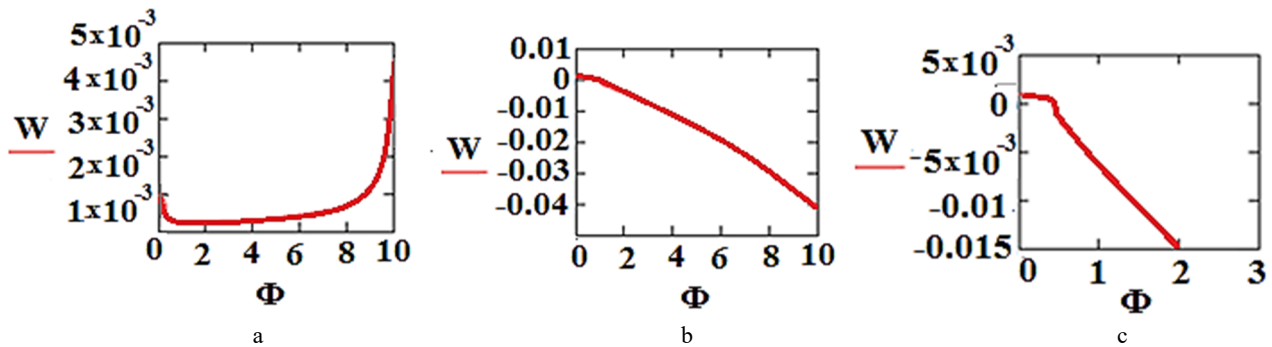


Fig. 5. Unimited solutions of the equation in variations chosen in regions of instability.

Calculations are made for $h=0.08, B = 3.18$ (a), for $h = 0.06, B = 3.15$ (b), and for $h = 0.09, B = 66$ (c). Other parameters correspond to ones used for Fig. 1,2.

Increasing solutions of the equation in variations are presented in Fig. 5. Namely, the solution presented in Fig. 5a is chosen in the instability region showed in Fig. 1; here $h=0.08, B = 3.18, q = -4.18$. The solution presented in Fig. 5b is also chosen in this instability region; here $h=0.06, B = 3.15, q = -4.26$. The solution presented in Fig. 5c is chosen in the instability region showed in Fig. 2 when $h=0.09, B = 66, q = -4.1$.

Then the limited and unlimited solutions of the variational equation obtained by the Runge-Kutta test are shown in Fig. 6 for regions of stability/ instability presented in Fig. 3. Parameters used in numerical calculations are the same. Namely, the limited solution from the region of stability is presented in Fig. 6a for $h=0.01, B = -1, q = -0.42$. The unlimited solution from the region of instability is shown in Fig. 6b for $h=0.04, B = -4, q = -0.26$.

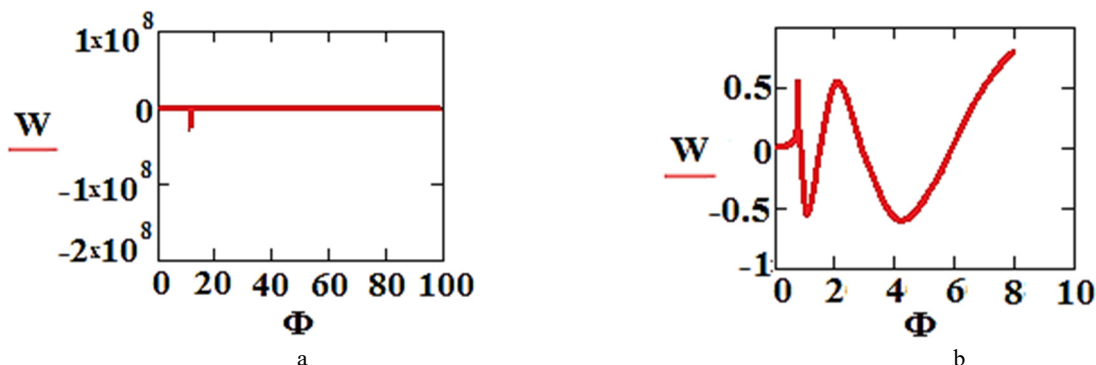




Fig. 6. Limited solution (a) and unlimited solution (b) of the equation in variations.

Calculations are made for $h=0.01, B = -1$ (a) and for $h=0.04, B = -4$ (b). Other parameters correspond to ones used for Fig. 3.

CONCLUSION

We can conclude that the Ince algebraization can be successfully used to analyze stability of nonlinear traveling waves of the Klein-Gordon equation with cubic nonlinearity. Boundaries of the stability/ instability regions in place of the system parameters are obtained by analysis of the linearized equation in variations which is transformed to equation with singular points when the variable connected with solution under consideration is chosen as a new independent variable. Solutions corresponding to these boundaries are constructed in power series. Numerical simulation illustrates this analysis of the traveling wave stability. It seems that the method of algebraization can be used in the stability analysis of other types of nonlinear traveling and standing waves.

ORCID-IDs

Nataliia Holoskubova  <https://orcid.org/0000-0003-2399-0177>, Yuri Mikhlin  <https://orcid.org/0000-0002-1780-9346>

REFERENCES

- [1]. G.B. Whitham, *Linear and Nonlinear Waves*, (Wiley, New York, 1999).
- [2]. V. Benci and D. Fortunato, *Variational Methods in Nonlinear Field Equations. Springer Monographs in mathematics.* (Springer, Switzerland, 2014).
- [3]. A.D. Polyaniin and V.F. Zaitsev, *Handbook of Nonlinear Partial Differential Equations*, (Boca Raton, Chapman & Hall/CRC, 2004).
- [4]. O. Waldron and R. A. Van Gorder, *Physica Scripta*, **92**(10), 105001, 2017, doi:10.1088/1402-4896/aa86fa.
- [5]. E.I. Yakubovich, in: *Нелинейные волны [Nonlinear waves]*, (Nauka, Moscow, 1979), 62-67. (in Russian)
- [6]. N. Budinsky and T. Bountis, *Physica D*, **8**(3), 445—452 (1983), doi: 10.1016/0167-2789(83)90236-1.
- [7]. A. Ghazaryan, S. Lafortune and V. Manukian, *Philosophical Transactions of The Royal Society A. Mathematical Physical and Engineering Sciences*, **376**(2117), 20180001 (2018), doi: 10.1098/rsta.2018.0001.

- [8]. R.L. Ince, *Ordinary Differential Equations*. (Longmans Green, London, 1926).
- [9]. Yu.V. Mikhlin and A.L. Zhupiev, *Int. J. of Non-Linear Mechanics*, **32**(2), 393-409, (1997), doi: 10.1016/S0020-7462(96)00047-9.
- [10]. Yu.V. Mikhlin, T.V. Shmatko and G.V. Manucharyan, *Computer & Structures*, **82**(31), 2733–2742, 2004, doi: 10.1016/j.compstruc.2004.03.082.
- [11]. K.V. Avarmov, Yu.V. Mikhlin, *Нелинейная динамика упругих систем. Т.1. Модели, методы, явления (Издание 2-е исправленное и дополненное) [Nonlinear Dynamics of Elastic Systems, V.1]* (IKI, Moscow-Izhevsk, 2015). (in Russian)
- [12]. A.F. Vakakis, L.I. Manevitch, Y.V. Mikhlin, V.N. Pilipchuk and A.A. Zevin, *Normal Modes and Localization in Nonlinear Systems*, (Wiley, New York, 1996).

АЛГЕБРАИЗАЦИЯ В ЗАДАЧЕ СТЙКІСТІ СТАЦІОНАРНИХ ХВИЛЬ РІВНЯННЯ КЛЕЙНА-ГОРДОНА

Н.С. Голоскубова, Ю.В. Міхлін

Національний технічний університет "Харківський політехнічний інститут",
61002, Україна, м. Харків, вул. Кирпичева 2

Розглянуто нелінійні бігучі хвилі рівняння Клейна-Гордона з кубічною нелінійністю. Ці хвилі описуються звичайним диференціальним рівнянням другого порядку, що має інтеграл енергії. Лінеаризоване рівняння у варіаціях для таких хвиль трансформується у звичайне диференціальне рівняння за допомогою розподілення змінних. Потім використовується так звана алгебраїзація за Айнсом. А саме, у рівняння в варіаціях вводиться нова незалежна змінна, що пов'язана з рішенням, яке розглядається. Під час такої трансформації використовується інтеграл енергії для стаціонарних хвиль. Перевага такого підходу зв'язана з тим, що для аналізу проблеми стійкості не треба використовувати специфічний вигляд рішення, що розглядається. В результаті такої алгебраїзації рівняння у варіаціях зі змінними за часом коефіцієнтами перетворюється у рівняння з особливими точками. Знайдено індекси особливих точок. Отримано необхідні умови стійкості хвиль. Рішення рівнянь у варіаціях, що відповідають межах регіонів стійкості / нестійкості в просторі параметрів системи побудовано у вигляді степеневих рядів за новою незалежною змінною. Можуть бути виписані нескінченні рекурентні системи алгебраїчних рівнянь для розрахунку коефіцієнтів цих рядів. Нетривіальні розв'язки таких систем можуть бути отримані, якщо їх визначники дорівнюють нулю. Ці визначники розраховано до п'ятого порядку включно, а потім отримано зв'язки між параметрами системи і відповідні межі регіонів стійкості/ нестійкості в площині параметрів системи. А саме, встановлено зв'язки між параметрами ангармонізму та енергії хвилі. Аналітичні результати проілюстровано чисельним моделюванням за допомогою процедури Рунге-Кутти. Спостерігається відповідність чисельних та аналітичних результатів.

КЛЮЧОВІ СЛОВА: рівняння Клейна-Гордона, стійкість стаціонарних хвиль, алгебраїзація за Айнсом

АЛГЕБРАИЗАЦИЯ В ЗАДАЧЕ УСТОЙЧИВОСТИ СТАЦИОНАРНЫХ ВОЛН УРАВНЕНИЯ КЛЕЙНА-ГОРДОНА С КУБИЧЕСКОЙ НЕЛИНЕЙНОСТЬЮ

Н.С. Голоскубова, Ю.В. Михлин

Національний технічний університет "Харківський політехнічний інститут"
61002, Україна, г. Харьков, ул. Кирпичева 2

Рассмотрены нелинейные бегущие волны уравнения Клейна-Гордона с кубической нелинейностью. Эти волны описываются обыкновенным дифференциальным уравнением второго порядка, которое имеет интеграл энергии. Линейризованное уравнение в вариациях для таких волн преобразуется в обыкновенное дифференциальное уравнение при помощи разделения переменных. Затем используется так называемая алгебраизация по Айнсу. А именно, новая независимая переменная, которая связана с решением, которое рассматривается, вводится в уравнение в вариациях. При этом используется интеграл энергии для стационарных волн. Преимущество такого подхода состоит в том, что для анализа проблемы устойчивости не нужно использование специфической формы решения, которое рассматривается. В результате подобной алгебраизации уравнение в вариациях с переменными по времени коэффициентами преобразуется в уравнение с особыми точками. Найдены индексы особых точек. Решения уравнений в вариациях, которые отвечают границам областей устойчивости/неустойчивости, построены в виде степенных рядов по новой независимой переменной. Могут быть выписаны бесконечные рекуррентные системы алгебраических уравнений для определения коэффициентов этих рядов. Нетривіальні рішення таких систем можуть бути отримані, якщо їх визначники рівні нулю. Ці визначники обчислено до п'ятого порядку включительно, а потім отримано зв'язки між параметрами системи і відповідні межі областей стійкості/ нестійкості в площині параметрів системи. А саме, встановлені зв'язки між параметрами ангармонізму та енергії волни. Аналітичні результати ілюструються чисельним моделюванням при допомозі процедури Рунге-Кутти. Наблюдается соответствие численных и аналитических результатов.

КЛЮЧЕВЫЕ СЛОВА: уравнения Клейна-Гордона, устойчивость стационарных волн, алгебраизация по Айнсу

PACS: 29; 29.40.Mc; 29.40.-n

RESEARCH OF THE SINGLE CRYSTAL AND MULTILAYER COMPOSITE DETECTORS RESPONSE UNDER IRRADIATION BY FAST NEUTRONS

 Volodymyr Ryzhikov¹,  Gennadiy Onyshchenko^{1,2*},  Ivan Yakymenko²,
 Sergei Naydenov^{1,3}, Alexandr Opolonin¹, Sergei Makhota¹

¹*Institute for Scintillation Materials, STC "Institute for Single Crystals", National Academy of Sciences of Ukraine
60 Nauky Ave., 61001 Kharkiv, Ukraine*

²*V.N. Karazin Kharkiv National University, 4 Svobody Sq., Kharkiv, 61022, Ukraine*

³*Institute for Single Crystals, STC "Institute for Single Crystals", National Academy of Sciences of Ukraine
60 Nauky Ave., 61001 Kharkiv, Ukraine*

*E-mail: gennadiy.m.onyshchenko@karazin.ua

Received April 15, 2019; revised May 20, 2019; accepted June 3, 2019

The object of this work was to study the response of the detectors based on the oxide scintillators under irradiation by a flux of fast neutrons from ²³⁹Pu-Be source by counting photomultiplier tube pulses. In the process of the research the counting efficiency of the detectors was measured in units of $(\text{pulse} \times \text{s}^{-1} \times \text{cm}^{-2}) / (\text{neutron} \times \text{s}^{-1} \times \text{cm}^{-2})$ for single-crystal and multilayer composite detectors ZWO (ZnWO₄), CWO (CdWO₄), BGO (Bi₄Ge₃O₁₂, composite). The measured response for ZWO detector was ~ 64 pulse/neutron, for CWO ~ 36 pulse/neutron, for BGO ~ 0.44 pulse/neutron. The detectors response was registered by a fast preamplifier with the operation speed of up to 500 MHz, based on high-speed operational amplifiers with voltage feedback. The statistical error of measurement for the neutron registration efficiency by the broadband channel made 7% for the detectors with the effective thickness of ~ 40-50 mm, which is due to the spherical geometry of the experiment. The formation of the detector response is affected by the following parameters of neutron reactions: cross section of inelastic and resonant scattering of scintillator nuclei, density of composite nuclei levels, resonance region width, lifetimes of long-lived states and their number. The measured values of the counting efficiency of fast neutrons registration are accounted for the fact that the inelastic scattering reaction for some nuclei is the starting point that triggers the cascade process of the nuclear states discharge. The registration of the cascade of the discharge gamma-quanta, ranging from nanoseconds to a few microseconds, causes an increase in the detector counting efficiency and, as a consequence, an increase in the detector sensitivity to neutron detection. The observed increase in the counting efficiency of secondary gamma quanta is realized when the neutrons are slowed down in the detectors having sufficiently noticeable thickness and appropriate isotopic composition.

KEY WORDS: detector, fast neutrons, excited states, countable efficiency, density of nuclear levels

Creation of highly sensitive detectors for the neutron and gamma-neutron radiation monitoring systems is the issue of the day. The objective of this work is studying the response of single-crystal and multilayer composite detectors under their irradiation by fast neutrons, aimed at creation of compact and efficient detectors of neutron and gamma-neutron radiation intended for control of the illegal transportation of fissile and radioactive materials. In [1, 2] it was shown that the mechanism of inelastic scattering ($n, n'\gamma$) can be used for registration of the fast neutrons by detector, in which heavy oxide scintillators are utilized as the working material [3-5]. Fast neutrons in this detector are registered by counting pulses induced by the secondary gamma quanta.

In the process of slowing down the fast neutrons in oxide detectors with the thickness of 4-5 cm and above, the resonance region energies (~ 1-100 keV) are achieved. In the case of elastic resonant scattering, the nuclei emit prompt gamma quanta, since the lifetime of the composite nucleus is short. At the inelastic resonance scattering ($n, n'\gamma$)_{res} the escaped neutron has a small energy and, consequently, a highly probability to be captured by the nuclei in (n, γ) reaction. Daughter compound nuclei with a short and mean lifetime of the states are excited. Thus, in the process of slowing down, the fast neutrons excite a chain of genetically bound nuclear states and generate gamma rays from ($n, n'\gamma$) and ($n, n'\gamma$)_{res} reactions [6, 7].

Thus, the inelastic scattering reaction ($n, n'\gamma$) is the starting point that triggers the cascade process of formation and decay of the excited nuclei states in the crystals under study.

If the lifetimes of nuclear states are in the range from nanoseconds to tens of microseconds, then the detector response registration causes an increase in the detector counting efficiency and, as a result, an increase in its sensitivity to gamma-neutron flux.

This paper presents the measurement data and the analysis of contributions of the conversion mechanisms during the fast neutrons slowing down to the genetically bound cascades of gamma-quanta from inelastic and resonant inelastic scattering of fast neutrons on the nuclei of single-crystal and multilayer oxide ZWO, BGO, CWO detectors.

RESEARCH METHODS

The fast neutrons response in the detectors under study is formed by gamma quanta scattered in the detector, and it should be noted, that the spectrum has no evident peculiarities and, in general, is a superposition of several exponents. In this case, it is very important to correctly determine the lower registration threshold of the detector under study.

To estimate the registration efficiency we used the parameter "counting" efficiency or "pulse/particle" i.e. the ratio of the detector counting rate from 1 cm² to the number of particles captured by the detector on the area of 1 cm² per 1 s,

© Volodymyr Ryzhikov, Gennadiy Onyshchenko, Ivan Yakymenko, Sergei Naydenov, Alexandr Opolonin,

Sergei Makhota, 2019

i.e. $\text{pulse} \times \text{s}^{-1} \times \text{cm}^{-2} / \text{neutron} \times \text{s}^{-1} \times \text{cm}^{-2}$. The choice of this parameter allows correct estimation of the sensitivity to neutrons of the detectors operating on the principle of registration of the secondary products, which are different from the incident particle.

In the process of scattering and slowing down in the detector material having linear dimensions $\sim 3\text{-}5$ cm the energy of the fast neutrons decreases from 10 MeV to several keV or less. This makes it possible to use for the detection purposes the mechanisms, which are specific for low-energy regions, and have high interaction cross sections and level densities, for example, resonant inelastic scattering, and which, ultimately produce the chains of gamma quanta.

The nuclear reaction analysis based on thermodynamic model [8] allows approximately estimating the average energy of the emitted neutron, the average excitation energy of the compound, and that of the daughter nuclei, which is equal to $\sim 1.5\text{-}3$ MeV. This energy is quite sufficient to excite at least one lower energy level in the nuclei of medium and large atomic weight scintillators (for example, W, Zn, Cd, Bi), whose decay causes gamma quanta emission.

With the decay of nuclear states excited in reactions with neutrons, in addition to the prompt gamma quanta from $(n, n'\gamma)$ reaction, the emission of the delayed gamma quanta from the compound nucleus $(A + 1, Z)$, the daughter nucleus (A, Z) and secondary neutrons capable to re-capture are possible [11].

The quanta in the lifetime range for the excited states from nanoseconds to tens of microseconds are of practical interest. It is the combination of the prompt and delayed quanta that forms genetically bound chains, which efficiently enhance the events statistics.

Radiometric characteristics of the single-crystal detectors ZWO, CWO and multi-layer composite detector BGO, irradiated by fast neutrons from ^{239}Pu -Be source were measured using a broadband ($\Delta f = 500$ MHz) counting channel.

The broadband channel efficiently registers the signals with the duration of ~ 0.7 ns – 1000 ns and amplitude of > 2 mV. The total dark noise of the photomultiplier tube (PMT) and the noise of electronics are ~ 10 mV.

In this time domain the prompt gamma-quanta signals, arising in inelastic and resonant inelastic reactions of the neutron scattering, and signals of the nuclei long-lived nuclear states decay may be observed.

The structural scheme of the experiment in spherical geometry is shown in Fig. 1.

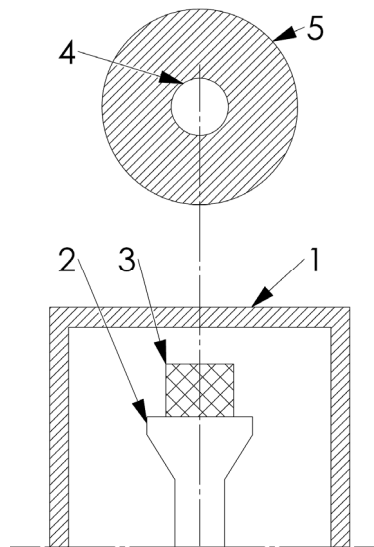


Fig. 1. Structural scheme for measuring the efficiency of fast neutrons registration in spherical geometry:

1 – 5 mm thick lead shield to attenuate the noise background in the low-energy region; 2 – photomultiplier R1307; 3 – scintillator under study; 4 – neutron source ^{239}Pu -Be; 5 – $\varnothing 100$ mm lead ball, with $\varnothing 20 \times 50$ mm well; detector - source distance - 1000 mm.

In this work the "spherical" geometry was used (Fig. 2) [9]. In case the isotropic neutron source is surrounded by a thick spherically symmetric layer of the matter, that can only scatter the neutrons (elastically and inelastically), but not absorb them, the number of neutrons, emitted into outer space, will not change. Scattering in the beam directed to the detector (front hemisphere) is compensated for by scattering into the detector from other points of the ball (rear hemisphere). Due to the spherical symmetry of the entire device, the number of neutrons passing through every square centimeter of the spherical surface will also remain unchanged.

Lead spherical shield has practically no effect on the number of elastically and inelastically scattered neutrons, with the exception of neutrons absorbed in the lead ball due to the reaction of radiation capture (n, γ) . Thus, the scattering ball does not change the neutron counting rate in the detector, and the spherical shield ball performs the function of attenuation of only gamma quanta, but not of the neutron flux, what, in fact, is necessary for the efficiency measurement technique.

We can say that the scattering in the shield ball is compensated for by the experiment geometry. The compensation is carried out by the entire volume of the ball, especially, if the absorber thickness is insignificant, as compared to the distance between the source and the detector, and the ball shape is close to ideal.

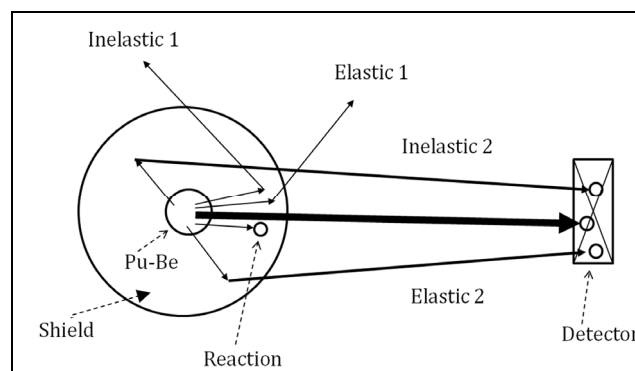


Fig. 2. Processes of fast neutrons scattering (\rightarrow) and absorption (\circ) in "spherical" geometry

One of the disadvantages of spherical geometry is an increase in the effective size of the neutron source and, as a result, the need to perform measurements at large distances (~ 1 m) as compared to the "narrow" geometry, what also requires a more intensive source. The deviation from the law of inverse squares for the neutron source in the range of 1-1.2 m does not exceed 3%, for the distance of 0.5 m, the error increases to 30%. Besides, the shape of the neutron spectrum undergoes some distortion.

Note, that if the counting rate is measured both with a ball and without it, then it is possible to determine the cross section for radiation capture reaction in the matter of the spherical sample. The coefficient of the neutron absorption in the shield sphere sample was measured for the concrete type of the neutron source and shield sphere ball of a certain diameter and chemical composition, the determined attenuation coefficient was used further in studies of scintillators of any size. The constancy of the absorption coefficient correction turns out to be the determining factor, if it is necessary to carry out accurate measurements with a large number of detectors of different size, for which it is difficult to take into account the attenuation factor in shadow geometry due to the significant effect of the accumulation factor. In addition to improving the measurement accuracy by eliminating the influence of the neutron accumulation factor, the spherical geometry also allowed to reduce the effect of the scattered gamma quanta excited by a neutron source in the walls of the laboratory room. As a source of neutrons the $^{239}\text{Pu-Be}$ source with the neutron flux of $0.95 \times 10^5 \text{ neutron} \times \text{s}^{-1}$ was used. The source was placed inside $\text{Ø}100$ mm lead ball, with $\text{Ø}20$ mm well. The size of the source: $\text{Ø} 20 \times 30$ mm. The lead ball, besides the main task to reduce the effect of the accumulation factor in the material of the ball, at the same time attenuates the accompanying gamma radiation from $^{239}\text{Pu-Be}$ source. In the neutron source there is an accompanying high-energy gamma radiation from the reactions: $^4\text{He} + ^9\text{Be} \rightarrow ^{13}\text{C}^* \rightarrow ^{12}\text{C}^* + n \rightarrow ^{12}\text{C} + n + \gamma$ ($E_\gamma = 4.43$ MeV), $^{13}\text{C}^* \rightarrow ^{13}\text{C} + \gamma$ ($E_\gamma = 3.68$ MeV).

The correction to the efficiency of fast neutrons detection by registering gamma rays with the energy $E_\gamma = 4.43$ MeV for the ZWO oxide scintillator with a size $\text{Ø}56 \times 40$ mm made ~ 0.08 . In this case, the γ/n ratio for $^{239}\text{Pu-Be}$ source was taken equal to 0.71 [10], the absorption of gamma quanta with the energy of 4.43 MeV in 40 mm thick lead was ~ 0.15 , the absorption efficiency of gamma quanta with the energy of 4.43 MeV in ZWO with a thickness of 50 mm was ~ 0.8 .

The correction to the fast neutrons absorption in the shield lead ball subject to the radiative capture reaction (n, γ) was determined experimentally using $^6\text{LiI}(\text{Eu})$ detector and made $\sim 2.5\%$. The size of $^6\text{LiI}(\text{Eu})$ scintillator was: $\text{Ø}15 \times 10$ mm, ^6Li enrichment was 96%. The thermal peak ($\alpha + t$) for $^6\text{LiI}(\text{Eu})$ had the gamma equivalent of 3.98 MeV, fast neutrons were registered in the energy range of $3.98 \text{ MeV} \div 10 \text{ MeV}$. The correction for the gamma quanta with energy $E = 4.43$ MeV was taken into account.

The contribution of the scattered fast neutrons from the walls of the laboratory room did not exceed 3%. The correction was determined using $^6\text{LiI}(\text{Eu})$ detector by measuring the deviation from the law of inverse squares when registering the fast neutrons. The contribution of the scattered gamma radiation in the range of "source-detector" distance $R = 1 \div 2$ m did not exceed $\sim 1\%$. The correction was determined by measuring the deviation from the law of inverse squares when registering ^{137}Cs quanta.

An additional lead shield, 5 mm thick, served as a shield against the background gamma radiation. The coefficient of the background attenuation by 5 mm thick lead in the range of 10 keV-150 keV was ~ 3 .

Multilayer composite detectors (Fig. 3) are of particular interest for detection of fast neutrons [12-14]. The energy registration efficiency (measured at the output pulse time $\tau = 1 \mu\text{s}$) for the fast neutrons, detected by composite detectors $100 \times 100 \times 40$ mm in size, turned out to be comparable with that for the single-crystal detectors $\sim 10 \times 10 \times 10$ mm in size [5], what allows using them to create large-size neutron detectors.

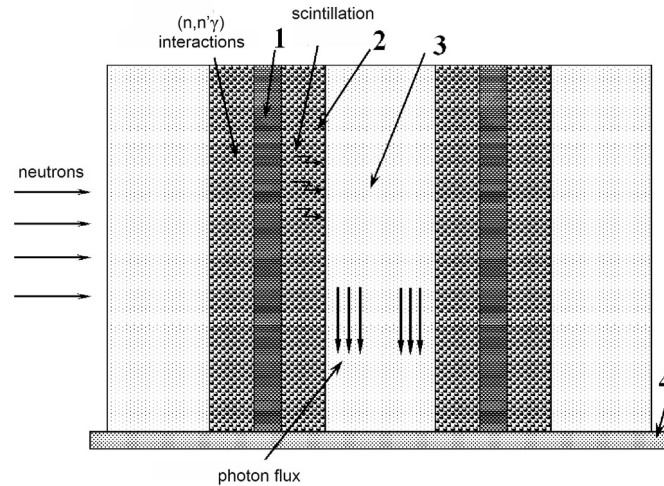


Fig. 3. The structure of the composite multilayer detector

1 – reflector; 2 – solution of scintillation granules ($\varnothing \sim 300$ microns) in optical rubber; 3 – light guide, $\varnothing 5$ mm; 4 – photomultiplier tube window.

The statistical error of the neutron detection efficiency measurement by the broadband channel was 7% for the detectors with an effective thickness of ~ 40 mm. The time of the data accumulation was 5 exposures 20 minutes each at the source irradiation and the same values for the background accumulation.

Fig. 4 shows a block diagram of the measuring channels, which comprises Hamamatsu R1307 photomultiplier with the channel baseline noise level of 5 mV at the photomultiplier voltage of 1100 V and a low-noise broadband amplifier [6, 7]. As the major recorder a pulse counter with bandwidth $\Delta f \sim 200$ MHz was used. The linear spectrometric amplifier with the output pulse time $\tau = 1 \mu s$ and Wilkinson analog-digital converter (ADC) with 2048 channels present an auxiliary channel, which serves to control the registration threshold.

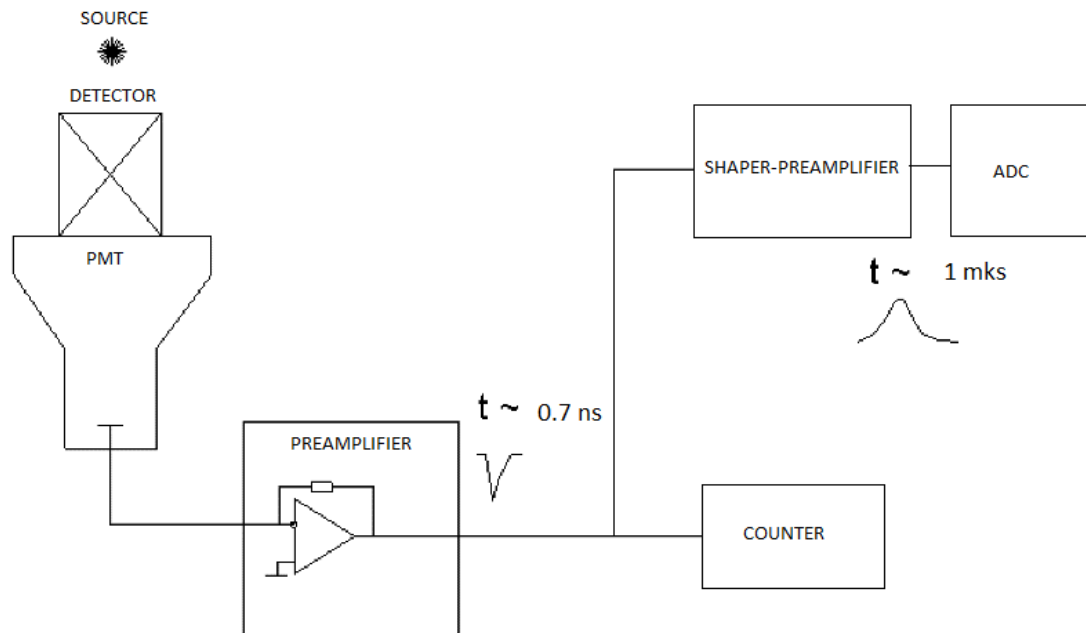


Fig. 4. Structural diagram of the measuring channels

Fig. 5 shows the circuit of the broadband pulse amplifier used to amplify the response signals from the detector. The proper rise time of the amplifier is 0.7 ns ($\Delta f \sim 500$ MHz), the first stage is made according to the transimpedance amplifier circuit (current-to-voltage converter), the total amplification factor for the next 5 stages makes at least 32, the baseline noise in the absence of PMT is 5 mV, the baseline noise with the connected photomultiplier is 10 mV, active elements “Analog Devices 4817” are used.

Fig. 6 shows the signal shapes in the broadband ($\tau = 7$ ns, with PMT taken into account, the upper figure) and in the narrowband ($\tau = 1 \mu s$, the lower figure) channels when the fast neutrons are detected by ZWO.

Fig. 7 shows the counting characteristic of the broadband channel ($\tau = 7$ ns) as a function of the registration threshold. The operating point of the measurements corresponded to the registration threshold of ~ 10 mV.

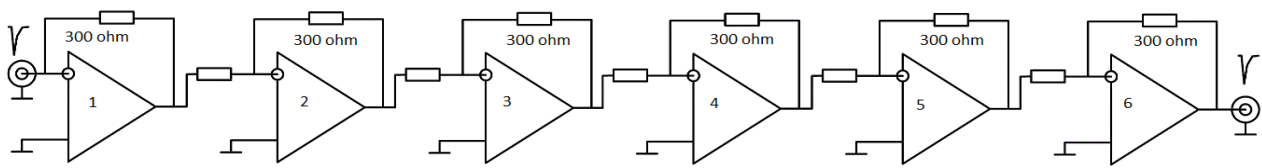


Fig. 5. Circuit of the broadband pulse amplifier.

Op1-Op6 – Analog Devices 4817. The value of the input resistors Op2-Op6 in the circuits of inverted inputs is 150 Ohms.

Fig. 8 represents on a logarithmic scale the hardware spectrum, which is registered by a narrow-band channel ($\tau = 1 \mu\text{s}$) in the process of interaction of the fast neutrons from ^{239}Pu -Be source with ZWO detector. In the left part of the figure we can see the right-hand slope of the PMT noise distribution (exponent 1), which gradually passes into the region of the detector desired signal (exponent 2).

The starting-point of the desired signal area is in the 160-th channel, what corresponds to $\sim 10 \text{ mV}$. The peak observed at the beginning of the scale is the right-hand slope of the PMT dark pulses distribution.

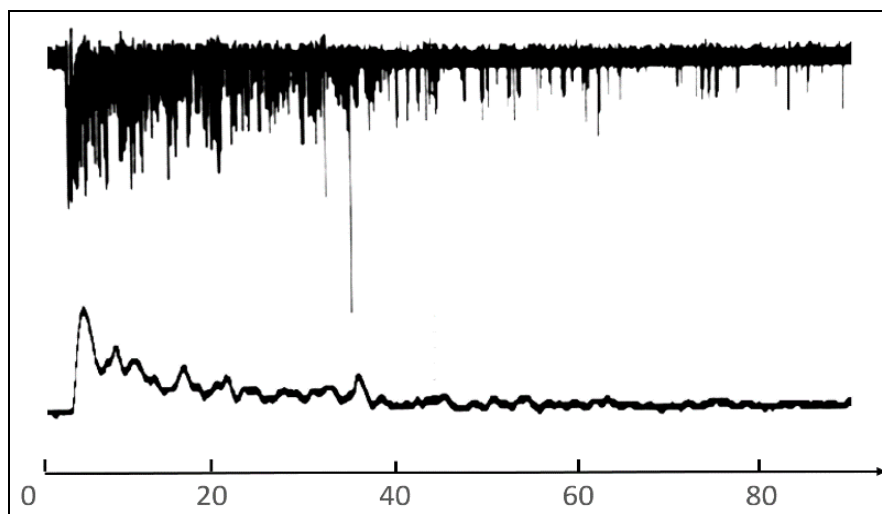


Fig. 6. Wave shapes for ZWO detector in the broadband ($\tau = 7 \text{ ns}$, the upper figure) and narrowband ($\tau = 1 \mu\text{s}$, the lower figure) channel. X axis – time, μs .

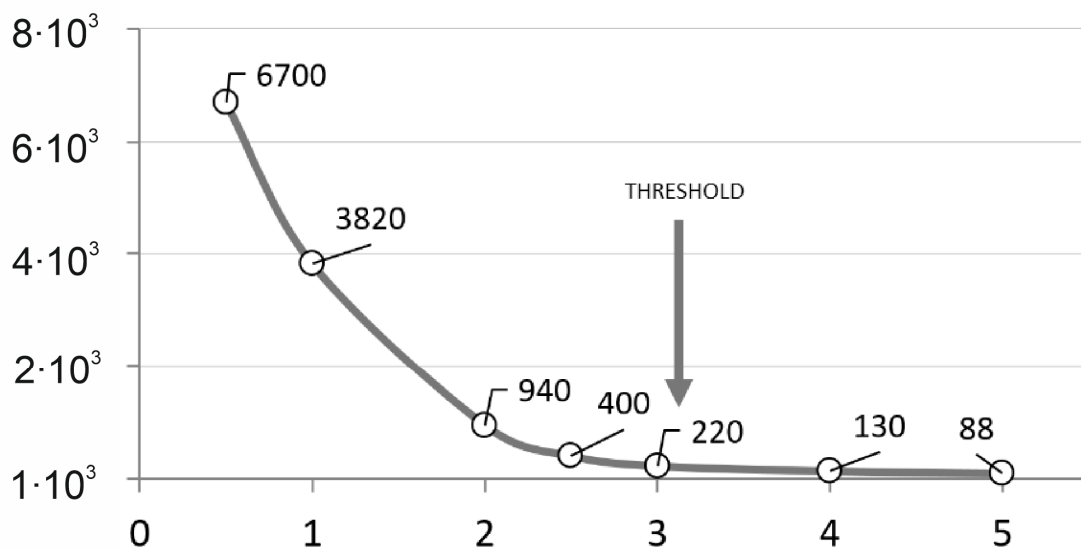


Fig. 7. The counting characteristic of the broadband channel as a function of the registration threshold. X axis is the registration threshold in relative units, Y axis is the counting rate, pulse/sec.

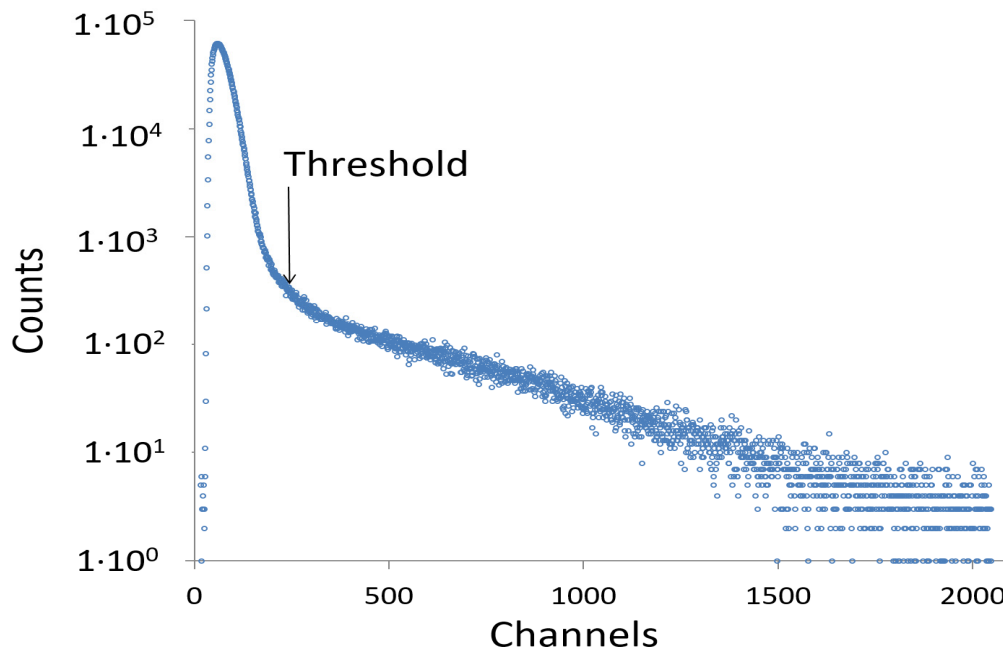


Fig. 8. The hardware spectrum on a logarithmic scale, which is registered in the narrowband channel ($\tau = 1 \mu\text{s}$) at the interaction of fast neutrons from ^{239}Pu -Be source with ZWO detector. The scintillator size is $\text{Ø}56 \times 40 \text{ mm}^3$. The position of the vertical arrow corresponds to the threshold $\sim 10 \text{ mV}$. X axis is the channel number. Y axis is the number of pulses.

THE RESULTS

In this work the experimental values of the response to the fast neutrons of ^{239}Pu -Be source for the detectors: BGO (multilayer) – 0.44 pulse/neutron, ZWO (single-crystal) – 64 pulse/neutron, CWO (single-crystal) – 36 pulse/neutron are obtained (Fig. 9). The data are represented in units “pulse/neutron” ($\text{pulse} \times \text{s}^{-1} \times \text{cm}^{-2} / (\text{neutron} \times \text{s}^{-1} \times \text{cm}^{-2})$, counting efficiency), i.e. as a ratio of the rate of counting, taken from 1 cm^2 of the detector input window, to the neutron flux density.

Counting efficiency

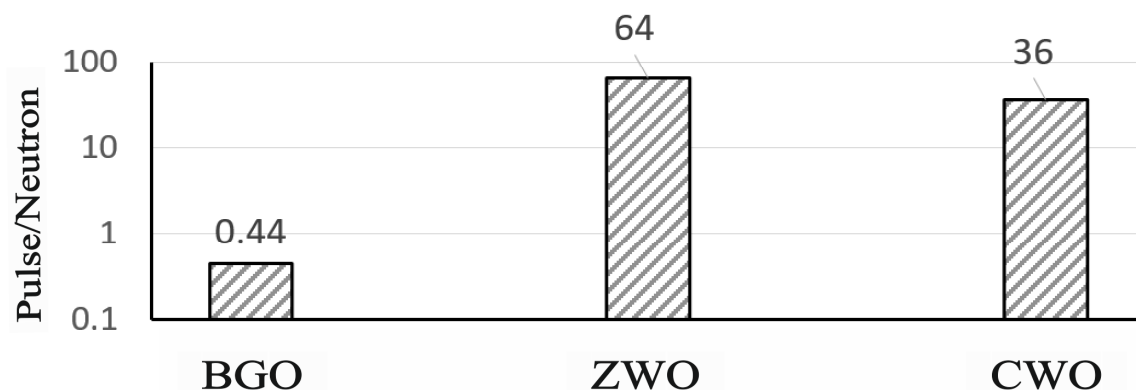


Fig. 9. Response to fast neutrons for the detectors: BGO (multilayer) – 0.44 pulse/neutron, ZWO (single-crystal) – 64 pulse/neutron, CWO (single-crystal) – 36 pulse/neutron. The ordinate axis is the ratio of the rate of counting, taken from 1 cm^2 of the detector input window, to the neutron flux density (pulse/neutron).

The obtained results for the counting efficiency of fast neutrons registration can be explained, firstly, by registration of prompt gamma quanta from the reactions of inelastic scattering $(n, n'\gamma)_{in}$, elastic and inelastic resonant scattering, and, secondly, by registration of genetically bound decay quanta of mean- and long-lived states of excitation nuclei from the reactions of inelastic scattering, elastic and inelastic resonant scattering and resonant radiation capture. This is contributed to by the use, as a fast preamplifier, the current-to-voltage converter with the operating frequency of 500 MHz ($\tau = 0.7 \text{ ns}$).

It should be noted that the registration efficiency of the composite detectors in the counting mode proved to be comparable with that of single-crystal detectors when operating in the spectrometric mode [5]. This indicates to the possibility of creating fast neutron composite detectors of considerable size and high sensitivity as an alternative to He-3 counters.

CONCLUSION

In this work the experimental values of the response to the fast neutrons from ^{239}Pu -Be source for BGO, ZWO and CWO detectors were obtained. A significant increase in the counting efficiency of fast neutrons registration for ZWO and CWO detectors was found out. At that, the efficiency of fast neutrons detection by the multilayer composite detector BGO turned out to be comparable with that of the single-crystal detectors, when operating in the spectrometric mode [5].

The experimental results can be explained by registration of a significant number of cascade gamma-quanta induced by the neutron reactions with scintillator nuclei during the neutrons slowing-down in the detector material. In reactions with neutrons the cascades of secondary gamma quanta, which are genetically bound with the primary inelastic scattering neutron, emitted during the decay of the excited nuclear states, may be produced.

The parameters affecting the increase of the efficiency of fast neutrons detection during their slowing down in the matter of the detectors under study are as follows: inelastic scattering cross section, cross sections in the resonance region, width of the resonance region, density of nuclear levels of compound nuclei [11], lifetime and energy of the excited levels and their number.





It was the use of the fast operation channel, that increased the counting efficiency by about two orders of magnitude for gamma quanta of the short-lived nuclear states (~ 1 -100 ns) by ZWO, CWO single-crystal detectors, as compared to the registration method, which utilizes the spectrometric registration mode, in which a significant suppression of response pulses from the short-lived nuclear states is observed.

Thus, the application of the counting mode for registration of the response of the oxide scintillators allows creating the detectors alternative to the existing ^3He counters for the radiation fields monitoring.

ACKNOWLEDGMENTS

The authors are indebted to Mrs. G.E. Vetrova for assistance in preparing the English version of this paper.

ORCID IDs

Volodymyr Ryzhikov  <https://orcid.org/0000-0002-2833-2774>, Gennadiy Onyshchenko  <https://orcid.org/0000-0001-6945-8413>, Ivan Yakymenko  <https://orcid.org/0000-0002-0194-837>, Sergei Naydenov  <https://orcid.org/0000-0002-5585-763X>,

REFERENCES

- [1]. M. Anelli, G. Battistoni, S. Bertolucci, C. Bini, P. Branchini, C. Curceanu, G. De Zorzi, A. Di Domenico, B. Di Micco, A. Ferrari, P. Gauzzi, S. Giovannella, F. Happacher, M. Iliescu, M. Martini, S. Miscetti, F. Nguyen, A. Passeri, A. Prokofiev, P. Sala, B. Sciascia and F. Sirghi, *Nuclear Instruments and Methods in Physics Research A*, **581**, 368-372 (2007), doi: 10.1016/j.nima.2007.08.005.
- [2]. L.L. Nagornaya, V.D. Ryzhikov, B.V. Grinyov, L.A. Piven', G.M. Onyshchenko and E.K. Lysetska, *Abstracts IEEE Nuclear Science Symposium*, (Dresden, Germany, 2008).
- [3]. B. Grinyov, V. Ryzhikov, L. Nagornaya, G. Onishchenko and L. Piven', Patent of USA. US 8.058.624 B2 (15 November 2011).
- [4]. V.D. Ryzhikov, B.V. Grinyov, G.M. Onyshchenko, L.A. Piven, O.K. Lysetska, O.D. Opolonin, S.A. Kostioukevitch, and C.F. Smith; *Proceedings Volume 9213, Hard X-Ray, Gamma-Ray, and Neutron Detector Physics XVI*, 92131B (San Diego, California, 2014), doi: 10.1117/12.2058185.
- [5]. V.D. Ryzhikov, S.V. Naydenov, G.M. Onyshchenko, L.A. Piven, T. Pochet and C.F. Smith, *Nuclear Instruments and Methods in Physics Research Section A: Accelerators, Spectrometers, Detectors and Associated Equipment*, **903**, 287-296 (2018), doi: 10.1016/j.nima.2018.06.074.
- [6]. I. Yakymenko, B. Grinyov, V. Ryzhikov, G. Onyshchenko, S. Naydenov, O. Opolonin and S. Makhota, *Sixth International Conference "Engineering of scintillation materials and radiation technologies ISMART"*, (Minsk, 2018), pp. 46.
- [7]. V.D. Ryzhikov, G.M. Onishenko, I.I. Yakimenko, S.V. Najdenov, A.D. Opolonin and S.V. Mahota, *XVII конференция по физике высоких энергий и ядерной физике [XVII Conference on High Energy Physics and Nuclear Physics]*, (NSC "KIPT", Kharkiv, 2019), pp. 96.
- [8]. J.M. Blatt and V.F. Weisskopf, *Theoretical Nuclear Physics*, (2010).
- [9]. A.I. Abramov, Ju.A. Kazanskij and E.S. Matushevich, *Основы экспериментальных методов ядерной физики [Fundamentals of experimental methods in nuclear physics]*, (Energoatomizdat, Moscow, 1985), pp. 488.
- [10]. G. Venkataraman, Dayashankar and J.S. Jayakar, *Nuclear Instruments and Methods*, **82**, 49-50, (1970), doi: 10.1016/0029-554X(70)90323-X.
- [11]. T. Egidy and D. Bucurescu, *Physical Review C*, **72**, 044311 (2005), doi: 10.1103/PhysRevC.72.044311.
- [12]. V.D. Ryzhikov, S.V. Naydenov, T. Pochet, G.M. Onyshchenko, L.A. Piven and C.F. Smith, *IEEE Trans. Nuclear Sciences*, **65**(9), 2547-2553 (2018), doi: 10.1109/TNS.2018.2825642.
- [13]. V.D. Ryzhikov, V.O. Litychevskij, G.M. Onishchenko, L.O. Piven et al, Patent UA 109524 C2, (25 August 2015), (in Ukrainian).
- [14]. V.D. Ryzhikov, S.V. Naydenov, T. Pochet, G.M. Onyshchenko, L.A. Piven and C.F. Smith, *EPJ Web of Conferences*, **170**(5), 07010 (2018), doi: 10.1051/epjconf/201817007010.

ДОСЛІДЖЕННЯ ВІДГУКУ МОНОКРИСТАЛІЧНИХ ТА БАГАТОШАРОВИХ ДЕТЕКТОРІВ НА ОПРОМІНЕННЯ ШВИДКИМИ НЕЙТРОНАМИ**В.Д. Рижиков¹, Г.М. Онищенко^{1,2}, І.І. Якименко², С.В. Найденов^{3,1}, О.Д. Ополонін¹, С.В. Махота¹**¹*Інститут Сцинтиляційних Матеріалів, НТЦ "Інститут Монокристалів" НАН України**пр. Науки, 60, 61001, Харків, Україна*²*Харківський Національний Університет імені В. Н. Каразіна**пл. Свободи, 4, Харків, 61022, Україна*³*Інститут Монокристалів, НТЦ "Інститут Монокристалів", НАН України**пр. Науки, 60, 61001, Харків, Україна*

Метою цієї роботи було вивчення відгуку детекторів на основі оксидних сцинтиляторів при опроміненні потоком швидких нейтронів джерела $^{239}\text{Pu-Be}$ шляхом реєстрації імпульсів ФЕП. У процесі досліджень вимірювалася лічильна ефективність детекторів в одиницях $(\text{імпульс} \times \text{с}^{-1} \times \text{см}^{-2}) / (\text{нейтрон} \times \text{с}^{-1} \times \text{см}^{-2})$ для монокристалічних і багатошарових композитних детекторів ZWO (ZnWO_4), CWO (CdWO_4), BGO ($\text{Bi}_4\text{Ge}_3\text{O}_{12}$). Вимірний відгук для детектора ZWO склав ~ 64 імпульс/нейтрон, для CWO ~ 36 імпульс/нейтрон, для BGO ~ 0.44 імпульс/нейтрон. Відгук детекторів реєструвався ширококутовим передпідсилювачем з швидкодією до 500 МГц, виконаним із застосуванням швидкодіючих операційних підсилювачів зі зворотним зв'язком по напрузі. Статистична похибка вимірювань значення ефективності реєстрації нейтронів ширококутовим трактом становила 7% для детекторів з ефективною товщиною $\sim 40\text{-}50$ мм, що обумовлюється використанням сферичної геометрії експерименту. На формування відгуку детектора впливають наступні параметри нейтронних реакцій: перерізи непружного і резонансного розсіювання ядер сцинтиляторів, щільність рівнів складених ядер, ширина резонансної області, час життя ядерних станів і їх кількість. Виміряні значення лічильної ефективності реєстрації швидких нейтронів пояснюються тим, що реакція непружного розсіювання для деяких ядер є відправною точкою, що ініціює каскадний процес створення та розрядки ядерних станів. Реєстрація каскаду розрядних гамма-квантів, починаючи від наносекунд до одиниць мікросекунд, викликає збільшення ефективності реєстрації детектора і, як наслідок, збільшення чутливості детектора до детектування нейтронів. Спостережуване збільшення лічильної ефективності вторинних гамма-квантів реалізується при уповільненні нейтронів в детекторах досить помітною товщини і відповідного ізотопного складу.






КЛЮЧОВІ СЛОВА: детектор, швидкі нейтрони, збуджені стани, лічильна ефективність, щільність ядерних рівнів**ИССЛЕДОВАНИЕ ОТКЛИКА МОНОКРИСТАЛЛИЧЕСКИХ И МНОГОСЛОЙНЫХ КОМПОЗИТНЫХ ДЕТЕКТОРОВ ПРИ ОБЛУЧЕНИИ БЫСТРЫМИ НЕЙТРОНАМИ****В.Д. Рижиков¹, Г.М. Онищенко^{1,2}, И.И. Якименко², С.В. Найденов^{3,1}, А.Д. Ополонин¹, С.В. Махота¹**¹*Інститут Сцинтиляційних Матеріалів, НТЦ "Інститут Монокристалів" НАН України**пр. Науки, 60, 61001, Харків, Україна*²*Харківський Національний Університет імені В.Н. Каразіна**пл. Свободи, 4, Харків, 61022, Україна*³*Інститут Монокристалів, НТЦ "Інститут Монокристалів", НАН України**пр. Науки, 60, 61001, Харків, Україна*

Целью настоящей работы являлось исследование отклика детекторов на основе оксидных сцинтиляторов при облучении потоком быстрых нейтронов источника $^{239}\text{Pu-Be}$ путем регистрации импульсов ФЭУ. В процессе исследований измерялась счетная эффективность детекторов в единицах $(\text{импульс} \times \text{с}^{-1} \times \text{см}^{-2}) / (\text{нейтрон} \times \text{с}^{-1} \times \text{см}^{-2})$ для монокристаллических и многослойных композитных детекторов ZWO (ZnWO_4), CWO (CdWO_4), BGO ($\text{Bi}_4\text{Ge}_3\text{O}_{12}$). Измеренный отклик для детектора ZWO составил ~ 64 импульс/нейтрон, для CWO ~ 36 импульс/нейтрон, для BGO ~ 0.44 импульс/нейтрон. Отклик детекторов регистрировался широкополосным предварительным усилителем с быстродействием до 500 МГц, выполненным на быстродействующих операционных усилителях с обратной связью по напряжению. Статистическая погрешность измерений значения эффективности регистрации нейтронов широкополосным трактом составляла 7% для детекторов с эффективной толщиной $\sim 40\text{-}50$ мм, что обуславливается использованием сферической геометрии эксперимента. На формирование отклика детектора оказывают влияние такие параметры реакций с нейтронами, как величины сечения неупругого и резонансного рассеяния ядер сцинтиляторов, плотность ядерных уровней составных ядер, ширина резонансной области, времена жизни изомерных состояний, их количество. Измеренные значения счетной эффективности регистрации быстрых нейтронов объясняются тем фактором, что реакция неупругого рассеяния является стартовым процессом, который запускает каскадный процесс разрядки ядерных изомерных состояний. Регистрация каскада гамма-квантов разрядки в интервале от единиц наносекунд до единиц микросекунд приводит к увеличению счетной эффективности детектора и, как следствие, к повышению чувствительности детектора к обнаружению нейтронов. Наблюдаемое увеличение счетной эффективности вторичных гамма-квантов реализуется при замедлении нейтронов в детекторах достаточно заметной толщины и подходящего изотопного состава.

КЛЮЧЕВЫЕ СЛОВА: детектор, быстрые нейтроны, возбужденные состояния, счетная эффективность, плотность ядерных уровней

PACS: 87.14.C++c, 87.16.Dg

NOVEL PHOSPHONIUM DYE TDV1 AS A POTENTIAL FLUORESCENT PROBE TO MONITOR DNA INTERACTIONS WITH LYSOZYME AMYLOID FIBRILS

 Olga Zhytniakivska¹,  Uliana Tarabara^{1*},  Kateryna Vus¹,  Valeriya Trusova¹,
 Galyna Gorbenko¹, N. Gadjev², Todor Deligeorgiev²

¹*Department of Nuclear and Medical Physics, V.N. Karazin Kharkiv National University
4 Svobody Sq., Kharkiv, 61022, Ukraine*

²*Faculty of Chemistry and Pharmacy, Sofia University, "St. Kliment Ohridski" 1
blv. J. Bourchier, Sofia, 1164, Bulgaria*

*E-mail: uliana.tarabara@gmail.com

Received 15 April 2019, revised May 5, 2019; accepted May 8, 2019

The applicability of the novel cationic phosphonium dye TDV1 to monitor the complexation between DNA and pathologically aggregated proteins, amyloid fibrils, was tested using the optical spectroscopy and molecular docking techniques. TDV1 has been found to be highly emissive in buffer solution and is characterized by one well-defined fluorescence peak attributed to the dye monomers. The association of the dye with the double stranded DNA was followed by the enhancement of monomer fluorescence coupled with a bathochromic shift of the emission maximum. The addition of fibrillar lysozyme (LzF) to TDV1-DNA mixture led to the further enhancement of fluorescence intensity of the monomeric dye form coupled with a hypsochromic shift of the emission maximum and an appearance of a second long-wavelength peak. An assumption has been made that the fluorescence enhancement augmenting with increasing the protein concentration in the TDV1/DNA system is produced by the interaction of the free TDV1 monomers with lysozyme fibrils as well as by the LzF-induced conformational alterations of DNA. The long-wavelength peak emerging in the presence of LzF is presumably a consequence of the J-aggregate formation upon the TDV1 association with lysozyme fibrils. The molecular docking studies showed that TDV1 monomers are incorporated into the fibril grooves associating with 7 β -strands in such a way that the dye long axis is parallel to the fibril axis. The most energetically favorable position of TDV1 is the S60-W62/G54-L56 groove in the lysozyme fibril core. In contrast, the TDV1 dimers seem to associate with the more hydrophilic side of the model β -sheet. Cumulatively, the results from the absorption and fluorescence measurements, together with the molecular docking analysis are consistent with the minor groove mode of the TDV1 binding to dsDNA. The electrostatic interactions seem to play a predominant role in the TDV1 complexation with the double stranded DNA, while the hydrophobic interactions and steric hindrances are supposed to be influential in the association of TDV1 with fibrillar lysozyme.

KEYWORDS: Phosphonium dye, fibrillar lysozyme, DNA, J-aggregates

Over the past decade the phenomenon of protein self-assembly into supramolecular aggregates, amyloid fibrils, attracts ever growing interest due to its involvement in the molecular etiology of a number of debilitating disorders including Parkinson's, Alzheimer's, Huntington's, Creutzfeldt-Jakob diseases, type II diabetes, etc. Although a consensus about the origin of such pathologies has been reached and is presented by the amyloid cascade hypothesis, the initial molecular events underlying fibril formation remain unclear [1]. The factors, such as the abnormal partial unfolding or folding of the proteins arising from the mutations, oxidative or heat stress or destabilization of the protein structure at the lipid-water interfaces are supposed to play essential role in amyloid growth [2,3]. Furthermore, a series of recent investigations provide evidence for the potential involvement of non-proteinaceous cofactors in the formation of amyloid deposits [4-7]. For instance, heparan sulfate, is reported to be linked with the amyloid disorders [4-5]. Likewise, the analysis of the brain tissues from victims of Alzheimer's disease revealed the presence of nucleic acids in the neurofibrillary tangles, intracellular inclusions composed of the tau protein and in the senile plaques consisting of the A β peptides [7]. Despite an undeniable evidence for the presence of polyanions in amyloid deposits, the questions whether and how they affect fibrillogenesis, are still unclear. It has been demonstrated that RNA stimulates the prion protein conversion in vitro [8]. Kampers and co-workers have uncovered the ability RNA to provoke the aggregation of the microtubule-associated protein tau into Alzheimer-like paired helical filaments [9,10]. Moreover, the double-stranded DNA has been found to promote the fibrillation of α -synuclein [11,12]. Remarkably, DNA is capable of strong associating with the mature fibrils of human muscle acylphosphatase, human lysozyme and hen egg white lysozyme [13,14]. There is also evidence that the cytotoxic action of soluble protein oligomers can be limited by the nucleic acids [15]. Despite great advances in the understanding the mechanisms behind the interactions of glycosaminoglycans and nucleic acids with fibrillar protein aggregates, little is known about the molecular scale details of this process. However, several studies have demonstrated that electrostatic interactions prevail in the polyelectrolyte-amyloid fibril complexes [13,14]. A variety of powerful techniques, including an agarose gel based assay, circular dichroism, fluorescence and absorption spectroscopy, small-angle x-ray scattering, electron microscopy are currently used to monitor the DNA binding to amyloid fibrils. The complex nature of the interactions between the amyloid fibrils and polyanions like nucleic acids requires the development of sophisticated, although simple approaches, one of which involves the application of the extrinsic fluorescent dyes.

Among a variety of fluorescent compounds currently used in the DNA and amyloid fibrils studies an important place belongs to the dyes of cyanine family [16-20]. To exemplify, the oxazole yellow homodimer, which has

previously been employed mainly as a DNA-intercalating probe, appeared to be suitable for in vitro amyloid sensing [16]. The ability to detect the protein fibrillar aggregates and to stain the double stranded DNA has been also shown for the mono-, tri-, penta- and heptamethine cyanine dye [17-20], styryl cyanine dyes [21,22], merocyanines [23], to name only a few. An extensive application of cyanines in the studies of amyloid fibrils and DNA is dictated by their favorable spectral properties, such as, particularly, high extinction coefficients, intensive absorption in a wide spectral region, from UV to NIR, high fluorescence intensity and quantum yield increase upon the dye binding to nucleic acids or proteins, etc. Another interesting property of the cyanines is their ability to form the self-associates stabilized by the van-der Waals, H-bonding, electrostatic, steric, hydrophobic and stacking interactions [24,25]. Dictated by the geometry of the molecules within the aggregate, both the H- and J-aggregates have been observed. The aggregate type depends on the spatial arrangement of the transition dipoles of individual dye molecules and can be easily identified by the spectroscopic means [26]. Kasha has long proposed that the interaction between the transition dipoles of tightly packed molecules generates a splitting of the excited states into exciton levels [26]. For the J-aggregates, the lower exciton is allowed, thus resulting in a bathochromically shifted absorption, whereas for the card-pack H-arrangements only the upper state transition is allowed, giving rise to the hypsochromic shift of the absorption spectra. Importantly, DNA and amyloid proteins have been shown to have a significant impact on the aggregation properties of cyanines [19,27,28]. The remarkable ability of cyanines to interact both with nucleic acids and fibrillar protein assemblies with accompanying changes of the dye spectral properties gives the impetus for their use as effective reporters in tracing the DNA interaction with amyloid fibrils.

In view of this, the aim of the present study was the investigation of the ability of the novel phosphonium cyanine dye TDV1 to monitor the DNA-amyloid protein interactions.

EXPERIMENTAL SECTION

Materials

Hen egg white lysozyme, calf thymus DNA were from Sigma (Sigma, St. Louis, MO, USA). The phosphonium dye TDV1 was provided by Professor Todor Deligeorgiev, University of Sofia, Bulgaria. All other materials and solvents were commercial products of analytical grade and were used without further purification.

Preparation of working solutions

The stock solution of TDV1 was prepared by dissolving the dye in 5 mM sodium phosphate buffer (pH 7.4). The concentration of TDV1 was determined spectrophotometrically, using the extinction coefficient $\epsilon_{480} = 2.1 \times 10^5 \text{ M}^{-1} \text{ cm}^{-1}$. The stock solution of calf thymus DNA was prepared in 10 mM Tris-HCl, 0.5 mM EDTA buffer (pH 7.4) at room temperature with occasional stirring to ensure the formation of a homogenous solution. The concentration of the DNA was determined spectrophotometrically using the extinction coefficient $\epsilon_{260} = 6.6 \times 10^3 \text{ M}^{-1} \text{ cm}^{-1}$. The lysozyme amyloid fibrils (Fig.1) were grown by the incubation of the protein solution (10 mg/ml) in 10 mM glycine buffer (pH 2) at 60 °C for 14 days. The working solution of fibrillar lysozyme was prepared in 5 mM Na-phosphate buffer (pH 7.4). Fibril formation was assessed by the transmission electron microscopy. A 10 μl drop of the protein solution was applied to a carbon-coated grid and blotted after 1 min. A 10 μl drop of 1.5% (w/v) phosphotungstic acid solution was placed on the grid, blotted after 30 s, and then washed 2 times by deionized water and air dried. The resulting grids were viewed by the EM-125 electron microscope (Selmi, Ukraine).

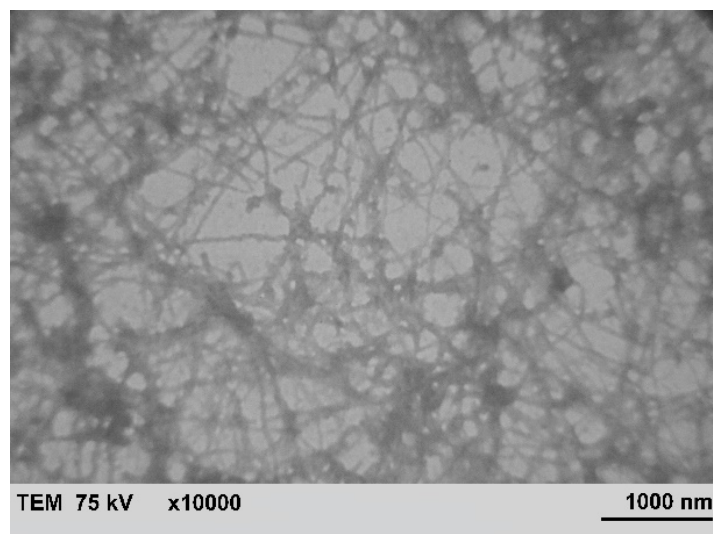


Fig. 1. Transmission electron microscopy image of lysozyme amyloid fibrils. Scale bar is 1000 nm.

Spectroscopic measurements

The absorption spectra of TDV1 were recorded with the spectrophotometer Shimadzu UV-2600 (Japan) at 25 °C. The steady-state fluorescence spectra were recorded with RF6000 spectrofluorimeter (Shimadzu, Japan). The fluorescence measurements were performed at 20 °C using 10 mm pathlength quartz cuvettes. The fluorescence spectra of cyanine dyes were recorded in the range of 500 to 750 nm with the excitation wavelength 480 nm.

Molecular docking study

The molecular docking was performed to identify the possible sites for the TDV1 binding to lysozyme fibrils and to elucidate the nature of the interactions between the dye and fibrillar protein aggregates. The crystal structure of hen egg white lysozyme (PDB ID: 3A8Z) was taken from the Protein Data Bank. The β -structured core of the lysozyme fibril was built from the K-peptide, GILQINSRW (the residues 54-62 of the wild type protein), using the CreateFibril tool as described previously [29]. The structure of TDV1 was built and optimized in Avogadro [30]. The docking models of the dye dimers and the complexes between the dye monomer (or dimer) and fibrillar lysozyme were obtained using the PatchDock algorithm, that is a user-friendly tool for calculation of the optimal structures of the protein-drug and protein-protein complexes. The online-available program searches the transformations of the two interacting molecules (assuming the proteins to be rigid bodies), revealing the maximized surface shape complementarity and minimized number of steric clashes. The top 10 of the obtained conformations were then refined by the FireDock algorithm, that calculates the optimal rearrangement of the side chains in the protein-ligand complex by the Monte Carlo minimization of the binding score function that is essentially determined by the energy of ligand-protein van der Waals interactions and the desolvation free energy.

An interacti examined phosphonium dye TDV1 and the double stranded DNA. The program performs docking using the spherical polar Fourier correlations with the inputs of ligand and receptor in PDB format. The structure of the B-DNA dodecamer d(CGCGAATTCGCG)₂ (PDB ID: 1BNA) was downloaded from the Protein Data Bank (<http://www.rcsb.org/pdb>). The parameters used for the molecular docking include: FFT mode – 3D, correlation type – shape only, grid dimension – 0.6, ligand range – 180, receptor range – 180, distance range – 40, and twist range – 360. The docked complexes were visualized by the Visual Molecular Dynamics (VMD) software.

RESULTS AND DISCUSSION

A widespread approach to monitoring the interactions of small ligands (dyes, drugs, etc.) with biological macromolecules is based on the use of UV-visible absorption spectroscopy. The magnitude of the changes in absorption intensity and other characteristics of the spectral band are usually correlated with the strength of interaction. Therefore, at the first step of study, to assess the sensitivity of the TDV1 to DNA-amyloid protein interactions, the absorption spectroscopy technique was utilized. As shown in Fig. 2, the absorption spectrum of TDV in buffer solution is characterized by one well-defined peak at ~ 470 nm.

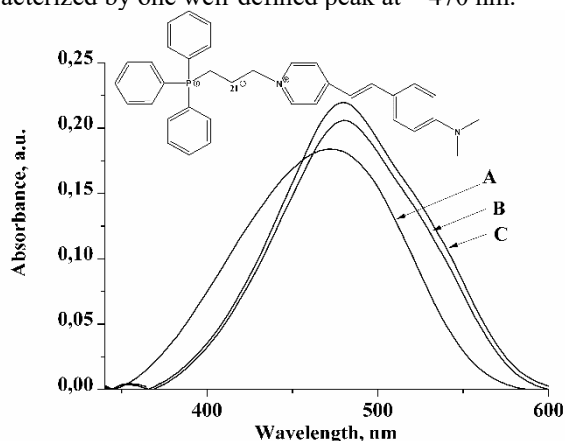


Fig. 2. Absorption spectra of TDV1 in buffer solution (A), in the presence of double stranded DNA (B) and in the combined DNA/fibrillar lysozyme system (C). TDV1 concentration was 11.8 μ M. DNA concentration was 34 μ M. Fibrillar lysozyme concentration was 0.7 μ M. Shown in the inset is the structural formula of TDV1.

In the presence of double stranded DNA significant changes in the dye absorption spectra have been observed pointing to the strong association of TDV1 with the nucleic acid. The addition of DNA was accompanied by a small hyperchromism, ~10 nm bathochromic shift of the absorption maximum coupled with a broadening of the absorption spectra due to appearance of a red-shifted shoulder at 540 nm. A detailed analysis of the available literature on the dye-nucleic acid interactions indicates that hyperchromism is a spectral feature reflecting the non-covalent interactions, particularly the electrostatic and minor groove binding motifs [22,31]. More interesting is the fact of broadening of the absorption spectrum, which can be attributed to the dye aggregation on the DNA template [27]. Generally, the cyanine dyes interact with the DNA minor grooves forming the plane-to-plane H dimers that can be identified easily through the appearance of a new absorption band hypsochromically shifted with respect to the monomer band [20,32,33]. However, for some cyanine dyes the end-to-end aggregation in a minor groove of DNA was observed resulting in the emergence of a new bathochromically shifted absorption band [28,34,35]. It should be noted, that the H-aggregates in the weak

coupling regime possess an absorption band red-shifted relative to the monomeric band [36,37]. The existence of H-aggregates in the weak excitonic coupling regime was firstly proposed by Spano, who described the absorption and emission spectra of the linear H- and J-aggregates with the nearest-neighbor-only coupling (J_0) as a function of the coupling strength [37]. Accordingly, a question arises, whether the aggregates formed on the DNA template are weakly coupled because of the plane-to-plane or end-to-end molecular arrangements? Taken into account that the width of the minor groove does not exceed 1.2 nm, and the TDV1 is a relatively large dye (its length, width and height are 2.26 nm, 0.99 nm and 0.99 nm, respectively), the aggregation of the dye into the face-to-face molecular assemblies (even weakly coupled H-dimers) is blocked by the walls of the minor groove. Therefore, the observed red-shifted shoulder presumably corresponds to the dye head-to-tail dimers formed in the DNA minor groove. The addition of fibrillar lysozyme to the dye-DNA system has been accompanied by a slight increase of the monomer absorption along with a small broadening of the absorption spectrum. However, the observed changes in the absorption spectra in the presence of aggregated protein are too weak to give any realistic explanation since they can be attributed to the dye-LzF interactions as well as to the influence of lysozyme fibrils on the DNA structure.

In view of this, at the next step of the study, to assess the sensitivity of TDV1 to the DNA - amyloid protein interactions, the fluorescence spectra of the dye were recorded in the buffer solution, in the presence of double stranded DNA (Fig. 3) and in the combined dsDNA/LzF systems (Fig. 4). TDV1 appeared to be highly emissive in buffer solution (Fig. 3a). The DNA addition resulted in a significant increase of the fluorescence intensity coupled with a red shift of the emission maximum up to 9 nm (Fig. 3a). The observed fluorescence enhancement is most likely to arise from the rigidification of the fluorophore. Importantly, the absorption spectroscopy data point to the J-dimerization of the cyanine dyes on the DNA template. The end-to-end aggregates are commonly highly fluorescent. However, as can be seen from the TDV1 fluorescence spectra in the presence of DNA, only the fluorescence of monomers takes place. The above discrepancy between the absorption and fluorescent data is most likely to result from the different phosphate-to-dye ratios (P/D). The absorption and fluorescence spectra were measured at the low (*ca.* 2.8) and high (*ca.* 134) P/D ratios, respectively. Generally, when the dye is in excess, cyanines tend to self-associate on the DNA template with the formation of the dye dimers in the minor groove, a tendency well described, in particular, for thiazole orange, Cyan 2 and Hoechst 33258 [34,38]. Further increase of the DNA concentration led to the binding of these dyes predominantly in the monomeric form. It should be noted that similar behavior was observed for acridine orange in the presence of the double stranded DNA [39]. At the high dye/DNA ratios, when the dye is in excess, its dimers bind electrostatically to the phosphate groups, whereas under the conditions of DNA excess strong intercalation is observed [39]. Due to the extended structure of the phosphonium dye under study, the exclusively intercalative binding mode for the TDV1 monomers seems unrealistic. However, the possibility of the “half intercalation” mode of the dye-DNA complexation cannot be ruled out [40]. In this case, the heterocycle with a high basicity accommodates in a more nucleophilic groove whereas heterocycle with a low basicity intercalates into a more electrophilic inter-base space [40].

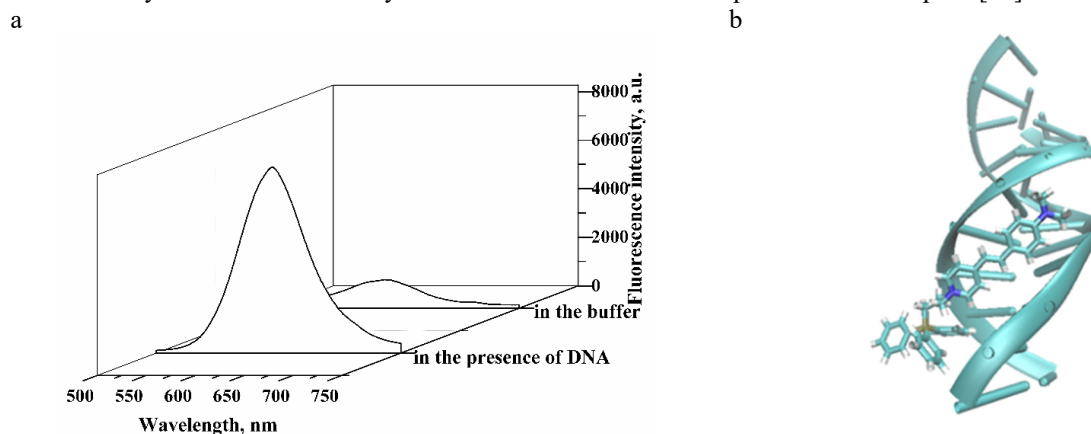


Fig. 3. Fluorescence spectra of TDV1 in buffer solution and in the presence of DNA. TDV1 concentration was 0.32 μM . DNA concentration was 42.8 μM (a). Schematic representation of the energetically most favourable dye complex with the double stranded DNA (b). A NewCartoon drawing method (VMD) is employed to represent the DNA structure, and TDV1 is depicted by Bonds:

In an attempt to ascertain the mode of the dye-DNA binding, the molecular docking studies were performed. A double-stranded DNA dodecamer [d(CGCGAATTCGCG)₂, PDB ID 1BNA] and TDV1 were taken as the input structures. Generally, to predict the best orientation of the ligand molecule within the double stranded DNA helix, the ligands are made flexible to attain different conformations. Therefore, in our docking studies the DNA structure was kept rigid, while the structure of TDV1 was made flexible to provide an energetically favorable docked pose. The molecular docking studies showed that TDV interacts with the minor groove of DNA (Fig. 3b).

The addition of fibrillar lysozyme to the TDV1-DNA mixture led to the 1.3-fold enhancement of the fluorescence intensity of the monomeric dye form coupled with a blue shift of the emission maximum up to 6 nm (Fig. 4a). In addition, a second well-defined peak at 703 nm was appeared. The enhancement of TDV1 fluorescence intensity at

618 nm can be interpreted in terms of the interaction of the free dye monomers with lysozyme fibrils as has been previously observed for the monomethine and trimethine cyanines [18]. However, we cannot rule out that the fluorescence intensity increase is caused by the LzF-induced alterations in the DNA structural state [13, 14]. The observed long-wavelength peak augmenting with the fibrillar lysozyme concentration presumably reflects the J-aggregate formation upon the TDV1 association with fibrils in the presence of DNA. Remarkably, the ability of rhodamine 6G to aggregate on the amyloid fibril template was reported by Hanczyc et al. [41], who demonstrated that the structural differences between the lysozyme and insulin amyloid fibrils promote the formation of the J-type and H-type molecular arrangements of the dye, respectively. The enhanced aggregation of the cyanine dye 7514 in the presence of fibrils was reported also by Volkova et al. [42] who ascribed the band shifted to the long-wavelength region relative to the monomer band to the formation of the J-aggregates. Presumably, the hydrophobic, electrostatic, and van der Waals interactions between the dye and the fibrillar proteins promote the formation of the dye J-aggregates. Notably, typical fibril binding sites for the small organic molecules are represented by the long surface grooves running parallel to the fibril axis, which may induce the end-by-end stacking of the fibril-bound TDV1 molecules, followed by the dye dimerization [43]. The simple docking studies were performed to assess the potential binding sites for TDV1 within the fibril core. As can be seen in Fig. 4 (panels “b” and “c”), the binding sites for TDV1 are represented by grooves formed by the polar and nonpolar amino acid residues. It appeared that TDV1 monomers are incorporated to the fibril grooves similarly to the classical amyloid marker Thioflavin T [44], associating with seven β -strands in such a way that the dye long axis is parallel to the fibril axis (Fig. 4b). The most energetically favorable positioning of TDV1 is provided by the groove S60-W62/G54-L56 of the lysozyme fibril core. In turn, TDV1 dimers seem to associate with a more hydrophilic surface of the lysozyme fibrils that is sterically more accessible for the dyes than the dry “steric zipper” interface [45]. Presumably, the dye-fibril hydrophobic interactions and steric hindrances have the predominant influence on the association of TDV1 with fibrillar lysozyme.

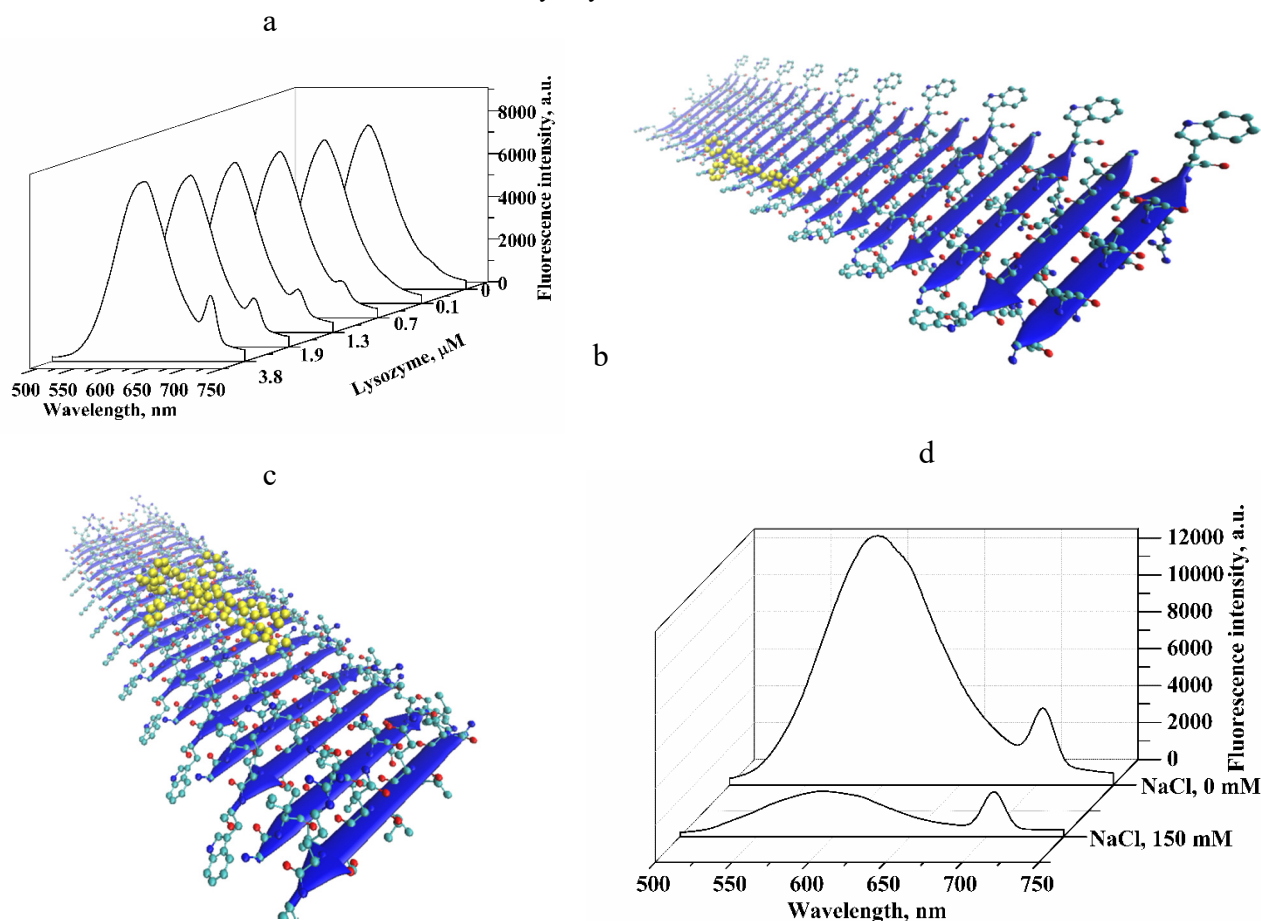


Fig. 4. Fluorescence spectra of TDV1 in buffer solution and in the presence of DNA. TDV1 concentration was $0.32 \mu\text{M}$. DNA concentration was $42.8 \mu\text{M}$. The most energetically favorable TDV1 monomer (b) and dimer (c) complexes with the fibrillar lysozyme, obtained using the molecular docking. Ligand and protein are represented via VDW and New Cartoon/CPK methods, respectively. Panel (d) represents the effect of sodium chloride on the fluorescence spectra of TDV1 in the combined DNA/LzF system. TDV1, DNA and LzF concentrations were $0.3 \mu\text{M}$, $42 \mu\text{M}$ and $3.7 \mu\text{M}$, respectively.

It is crucial to note that the binding of free TDV1 monomers to lysozyme fibrils is not the only reason for the described above enhancement of the fluorescence intensity augmenting with increasing the protein concentration in the TDV1/DNA system (Fig. 4a). Probably, the observed fluorescence increase is produced by the LzF-induced conformational changes of the DNA molecule. Recent studies indicate that the nucleic acid binding to the lysozyme fibrils is nonspecific in nature and occurs presumably through electrostatic interactions [13,14]. The hydrophobicity negatively affects the strength of interactions between the oppositely charged DNA and fibrils since the stronger binding with the negatively charged nucleic acids is peculiar to the native lysozyme in comparison with the fibrillar Lz possessing the exposed hydrophobic regions [13]. The circular dichroism measurements indicate that both the native and fibrillar lysozyme can cause a deformation of the DNA helical structure [14]. Moreover, the hydration pattern near the phosphate groups and ribose rings of DNA helix has been affected by proteins [14]. In view of the above, it is highly probable that fibrillar lysozyme affects the DNA structure in such a manner that the DNA minor grooves (putative TDV1 binding sites) become more accessible to the free dye molecules. An additional argument in favor of our hypothesis that TDV1 fluorescence enhancement at 618 nm is largely determined by the LzF-induced conformational alterations of the DNA rather than by the interaction of the dye monomers with fibrils, comes from the ionic strength effect studies (Fig. 4d). The addition of 150 mM sodium chloride to the TDV1/DNA/LzF mixture resulted in ~ 6-fold decrease in the monomer fluorescence intensity and 2-fold fluorescence reduction of the dimeric dye form at 703 nm. Owing to the cationic nature of TDV1 and the negative polyphosphate skeleton of DNA, the electrostatic interactions seem to play a predominant role in the dye-nucleic acid complexation. It is generally known that in the presence of DNA, Na⁺ ions partly neutralize the negative charges of the DNA phosphate backbone. As a result, the electrostatic attraction between the small molecules and DNA surface is weakened leading to the release of the TDV1 from the DNA minor grooves and concomitant decrease in the monomer fluorescence intensity. The 2-fold fluorescence reduction of the dimeric dye form at 703 nm is probably associated with the formation of atmosphere of Cl⁻ counter-ions around the dye molecules, disrupting in such a way the cyanine dimers by sterical blocking of the end-to-end contacts [46].

CONCLUSIONS

To summarize, the present study was focused on the investigation of the ability of the novel phosphonium cyanine dye TDV1 to monitor the DNA-amyloid protein interactions. The analysis of the fluorescence spectra of TDV1 in the presence of DNA and in the combined DNA/fibrillar lysozyme systems provides evidence for the binding of TDV1 monomers to the DNA minor groove and the association of the dye dimers with the hydrophilic surface of the lysozyme fibril core. The electrostatic interactions seem to be prevalent in the TDV1 complexation with the double stranded DNA. At the same time, the dye-fibril hydrophobic interactions and steric hindrances are supposed to dominate in the TDV1 binding to fibrillar lysozyme. The results obtained suggest that the novel phosphonium dye TDV1 may prove of value in elucidating the mechanisms of DNA interactions with pathogenic protein aggregates associated with the amyloid diseases.

ACKNOWLEDGEMENTS

This work was supported by the Ministry of Education and Science of Ukraine (the Young Scientist project № 0117U004966 “Nano- and microsized liophylic and liophylized self-associated systems: application in modern technologies and biomedicine”) and by the President’s of Ukraine grant No 0118U002284 from the State Fund for Fundamental Research of Ukraine “Development of novel anti-amyloid strategies by high-throughput screening of inhibitors of pathological protein aggregation”.

ORCID IDs

Olga Zhytniakivska <https://orcid.org/0000-0001-9554-0090>, Uliana Tarabara <https://orcid.org/0000-0002-7677-0779>,
Kateryna Vus <http://orcid.org/0000-0003-4738-4016>, Valeriya Trusova <https://orcid.org/0000-0002-7087-071X>,
Galyna Gorbenko <http://orcid.org/0000-0002-0954-5053>

REFERENCES

- [1]. E. Karran, M. Mercken and B. Strooper, *Nature Reviews Drug Discovery*, **10**, 698–712 (2011), doi: 10.1038/nrd3505.
- [2]. J. Adamcik and R. Mezzenga, *Macromolecules*, **45**, 1137–1150 (2012), doi: 10.1021/ma202157h.
- [3]. C.M. Dobson, *Cold Spring Harb. Perspect. Biol.* **9**, 1-14 (2017), doi: 10.1101/cshperspect.a023648.
- [4]. J. Diaz-Nido, F. Wandosell and J. Avila, *Peptides*, **23**, 1323-1332 (2002), doi: 10.1016/S0196-9781(02)00068-2.
- [5]. J. van Horssen, P. Wesseling, L.P. van den Heuvel, R.M. de Waal and M.M. Verbeek, *Lancet. Neurol.* **2**(8), 482–492 (2003), doi: 10.1016/S1474-4422(03)00484-8.
- [6]. J.B. Ancsin, *Amyloid*, **10**, 67-79 (2003), doi: 10.3109/13506120309041728.
- [7]. S.D. Ginsberg, J.E. Galvin, T.S Chiu, V.M. Lee, E. Masliah and J.Q. Trojanowski, *Acta Neuropathol.* **96**(5), 487–494 (1998), doi: 10.1007/s004010050.
- [8]. M.R. Deleault, R.W. Lucassen and S. Supattapone, *Nature*, **425**, 717–720 (2003), doi: 10.1038/nature01979.
- [9]. M. Hasegawa, R.A. Crowther, R. Gakes and M. Goedert, *J. Biol. Chem.* **272**, 33118–33124 (1997), doi: 10.1074/jbc.272.52.33118.
- [10]. T. Kampers, P. Friedhoff, J. Biernat, E.M. Mandelkow and E. Mandelkow, *FEBS Lett.* **399**(3), 344–349 (1996), doi: 10.1016/S0014-5793(96)01386-5.

- [11]. M.L. Hedge and K.S.J. Rao, *Arch. Biochem. Biophys.* **464**(1), 57–69 (2007), doi: 10.1016/j.abb.2007.03.042.
- [12]. D. Cherny, W. Hoyer, V. Subramaniam and T.M. Jovin, *J. Mol. Biol.* **344**, 929–938 (2004), doi: 10.1016/j.jmb.2004.09.096.
- [13]. M. Calamai, J.R. Kumita, J. Mifsud, C. Parrini, M. Ramazzotti, G. Ramponi, N. Taddei, F. Chiti and C. Dobson, *Biochemistry*. **45**, 12806–12815 (2006), doi: 10.1021/bi0610653.
- [14]. S. Ghosh, N.P. Pandey, S. Sen, D.R. Tripathy and S. Dasgupta, *J. Photochem. Photobiol. B.* **127**, 52–60 (2013), doi: 10.1016/j.jphoto.2013.07.015.
- [15]. J.D. Domizio, R. Thang, L.J. Stagg, M. Gagea, M. Zhuo, J.E. Ladbury and W. Cao, *J. Biol. Chem.* **287**, 736–747 (2012), doi: 10.1074/jbc.M111.238477.
- [16]. D.L. Lindberg and E.K. Esbjorner, *Biochem. Biophys. Res. Commun.* **469**, 313–318 (2016), doi: 10.1016/j.bbrc.2015.11.051.
- [17]. V.B. Kovalska, M.Y. Losytsky, O.I. Tolmachev, Y.L. Slominskii, G.M. Segers-Nolten, V. Subramaniam and S.M. Yarmoluk, *J. Fluoresc.* **22**, 1441–1448 (2012), doi: 10.1007/s10895-012-1081-x.
- [18]. K.D. Volkova, V.B. Kovalska, A.O. Balanda, R.J. Vermeij, V. Subramaniam, Y.L. Slominskii and S.M. Yarmoluk, *J. Biochem. Biophys. Meth.* **70**, 727–733 (2007), doi: 10.1016/j.jbbm.2007.03.008.
- [19]. K.Vus, U. Tarabara, A. Kurutos, O. Ryzhova, G. Gorbenko, V. Trusova, N. Gadjev and T. Deligeorgiev, *Mol. Biosyst.* **13**, 970–980 (2017), doi: 10.1039/c7mb00185a.
- [20]. A. Kurutos, O. Ryzhova, U. Tarabara, V. Trusova, G. Gorbenko, N. Gadjev and T. Deligeorgiev, *J. Photochem. Photobiol. A.* **328**, 87–96 (2016), doi: 10.1016/j.jphotochem.2016.05.019.
- [21]. Q. Li, J.-S. Lee, C. Ha, C. B. Park, G. Yang, W. B. Gan and Y.-T. Chang, *Angew. Chem. Int. Ed.* **43**(46), 6331–6335 (2004), doi: 10.1002/anie.200461600.
- [22]. C.V. Kumar, R.S. Turner and E.H. Asuncion, *J. Photochem. Photobiol. A.* **74**, 231–238 (1993), doi: 10.1016/1010-6030(93)80121-O.
- [23]. J. Yan, J. Zhu, K. Zhou, J. Wang, H. Tan, Z. Xu, S. Chen, Y. Lu, M. Cui, L. Zhang, *Chem. Comm.* **53**, 9910–9913 (2017), doi: 10.1039/C7CC05056A.
- [24]. M.K. Johansson, H. Feedder, D. Dick, and R.M. Cook, *J. Am. Chem. Soc.* **124**(24), 6950–6956 (2002), doi: 10.1021/ja025678o.
- [25]. B. Birkan, D. Gulen and S. Ozcelic, *J. Phys. Chem.* **110**, 10805–10813 (2006), doi: 10.1021/jp0573846.
- [26]. M. Kasha, H.R. Rawls and M.A. El-Bayoumi, *Pure. Appl. Chem.* **100**, 17287–17296 (1996).
- [27]. K.S. Hannah and B.S. Armitage, *Acc. Chem. Res.* **37**, 845–853 (2004), doi: 10.1021/ar030257c.
- [28]. M. Wang, G. Silva and B. Armitage, *J. Am. Chem. Soc.* **122**, 9977–9986 (2000), doi: 10.1021/ja002184n.
- [29]. M.R. Smaoui, F. Poitevin, M. Delarue, P. Koehl, H. Orland, and J. Waldspühl, *Biophys. J.* **104**(3), 683–693 (2013), doi: 10.1016/j.bpj.2012.12.037.
- [30]. M.D. Hanwell, D.E. Curtis, D.C. Lonie, T. Vandermeersch, E. Zurek and G.R. Hutchison, *J. Cheminform.* **4**, 17 (2012), doi: 10.1186/1758-2946-4-17.
- [31]. T. Sarwar, S. Rehman, A.A. Husain, H.M. Ishqi and M. Tabish, *Int. J. Biol. Macromol.* **73**, 9–16 (2015), doi: 10.1016/j.ijbiomac.2014.10.017.
- [32]. J.L. Seifert, R.E. Connor, S.A. Kushon, M. Wang and B.A. Armitage, *J. Am. Chem. Soc.* **121**, 2987–2995 (1999), doi: 10.1021/ja984279j.
- [33]. D.E. Wemmer, *Annu. Rev. Biophys. Biomol. Struct.* **29**, 439–461 (2000), doi: 10.1146/annurev.biophys.29.1.439.
- [34]. T.Yu. Ogul'chansky, M.Yu. Losytsky, V.B. Kovalska, S.S. Lukashov, V.M. Yashchuk and S.M. Yarmoluk, *Spectrochim. Acta. A. Mol. Biomol. Spectrosc.* **57**, 2705–2715 (2001), doi: 10.1016/S1386-1425(01)00537-6.
- [35]. G.Ya. Guralchuk, A.V. Sorokin, I.K. Katrunov, S.L. Yefimova, A.N. Lebedenko, Yu.V. Malyukin and S.M. Yarmoluk, *J. Fluoresc.* **17**, 370–376 (2007), doi: 10.1007/s10895-007-0201-5.
- [36]. H. von Berlepsch, C. Böttcher, A. Ouart, C. Burger, S. Dähne, S. Kirstein, *J. Phys. Chem. B.* **104**(22), 5255–5262 (2000), doi: 10.1021/jp000220z.
- [37]. S. Spano, *Acc. Chem. Res.* **43**(3), 429–439 (2010), doi: 10.1021/ar900233v.
- [38]. T. Stokke and T. Steen, *J. Histochem. Cytochem.* **33**(4), 333–338 (1985), doi: 10.1177/33.4.2579998.
- [39]. J. Kapuscinski, Z. Darzynkiewicz and M.R. Melamed, *Biochem. Pharm.* **32**(24), 3679–3694 (1983).
- [40]. S.M. Yarmoluk, S.S. Lukashov, T.Yu. Ogul'chansky, M.Yu. Losytsky and O.S. Kornushyna, *Biopolymers.* **62**, 219–227 (2001).
- [41]. P. Hanczyc, L. Sznitko, C. Zhong and A. Heeger, *ACS Photonics.* **2**(12), 1755–1762 (2015), doi: 10.1021/acsp.20150458.
- [42]. K.D. Volkova, V.B. Kovalska, M.Y. Losytsky, K.O. Fal, N.O. Derevyanko, Y.L. Slominskii, O.I. Tolmachev and S.M. Yarmoluk, *J. Fluoresc.* **21**, 775–784 (2011), doi: 10.1007/s10895-010-0770-6.
- [43]. M. Groenning, M. Norrman, J. Flink, M. Weert, J. Bukrinsky, G. Schluckebier and S. Frokjaer, *J. Struct. Biol.* **159**(3), 483–497 (2007), doi: 10.1016/j.jsb.2007.06.004.
- [44]. M.R.H. Krebs, E.H. C. Bromley and A.M. Donald, *J. Struct. Biol.* **149**, 30–37 (2005), doi: 10.1016/j.jsb.2004.08.002.
- [45]. K.Vus, V. Trusova, G. Gorbenko, R. Sood, E. Kirilova, G. Kirilov, I. Kalnina and P. Kinnunen, *J. Fluoresc.* **24**, 493–504 (2014), doi: 10.1007/s10895-013-1318-3.
- [46]. F.A. Schaberle, V.A. Kuz'min, and I.E. Borissevitch, *Biochim. Biophys. Acta.* **1621**, 183–191 (2003), doi: 10.1016/S0304-4165(03)00057-6.

НОВИЙ ФОСФОНІЄВИЙ БАРВНИК ЯК ПОТЕНЦІЙНИЙ ФЛУОРЕСЦЕНТНИЙ ЗОНД ДЛЯ ДОСЛІДЖЕННЯ ВЗАЄМОДІЇ ДНК З АМІЛОЇДНИМИ ФІБРИЛАМИ ЛІЗОЦИМУ

О. Житняківська¹, У. Тарабара¹, К. Вус¹, В. Трусова¹, Г. Горбенко¹, Н. Гаджев², Т. Делігеоргієв²

¹Кафедра ядерної та медичної фізики, Харківський національний університет імені В.Н. Каразіна
пл. Свободи 4, Харків, 61022, Україна

²Факультет хімії і фармації, Софійський університет, Софія, 1164, Болгарія

За допомогою методів оптичної спектроскопії і молекулярного докінгу проведена оцінка можливості використання нового катіонного фосфонієвого барвника TDV1 для дослідження комплексоутворення між ДНК і патогенними білковими агрегатами, амілоїдними фібрилами. Виявлено, що для мономерів TDV1 характерна висока інтенсивність флуоресценції у

буферному розчині. При взаємодії барвника з подвійною спіраллю ДНК спостерігалось зростання інтенсивності флуоресценції мономерів та відбувався батохромний зсув максимуму флуоресценції. При додаванні фібрилярного лізоциму (LzF) до суміші TDV1-ДНК, поряд з подальшим підвищенням інтенсивності флуоресценції мономерної форми барвника і гіпсохромним зсувом максимуму випромінювання, спостерігалась поява додаткового, довгохвильового піку. Зроблено припущення, що зростання інтенсивності флуоресценції зі збільшенням концентрації білка в системі TDV1/ДНК зумовлене як взаємодією вільних мономерів TDV1 з фібрилами лізоциму, так і конформаційними змінами ДНК, викликаними фібрилами лізоциму. Поява довгохвильового піку, ймовірно, є результатом J-агрегації TDV1 у присутності фібрилярного білка. З використанням методу молекулярного докінгу показано, що мономер TDV1 зв'язується з сімома ланцюгами борозенки фібрил лізоциму таким чином, що їх поздовжня вісь паралельна осі фібрили. Показано, що найбільш енергетично вигідним центром зв'язування є борозенка, сформована амінокислотними залишками S60-W62/G54-L56. В той же час, димери барвника утворюють стабільні комплекси з більш гідрофільною стороною модельного β -листа. Результати, отримані методами флуоресцентної, абсорбційної спектроскопії і молекулярного докінгу свідчать про взаємодію TDV1 з малою борозенкою ДНК. Електростатичні взаємодії, вочевидь, є домінуючими при комплексоутворенні TDV1 з дволанцюговою ДНК, тоді як гідрофобні взаємодії та стеричні чинники є визначальними при асоціації барвника з фібрилярним лізоцимом.

КЛЮЧЕВЫЕ СЛОВА: Фосфонієвий барвник, фібрилярний лізоцим, ДНК, J-агрегати

НОВЫЙ ФОСФОНИЕВЫЙ КРАСИТЕЛЬ КАК ПОТЕНЦИАЛЬНЫЙ ФЛУОРЕСЦЕНТНЫЙ ЗОНД ДЛЯ ИССЛЕДОВАНИЯ ВЗАИМОДЕЙСТВИЯ ДНК С АМИЛОИДНЫМИ ФИБРИЛЛАМИ ЛИЗОЦИМА

О. Житняковская¹, У. Тарабара¹, К. Вус¹, В. Трусова¹, Г. Горбенко¹, Н. Гаджев², Т. Делигеоргиев²

¹Кафедра ядерной и медицинской физики, Харьковский национальный университет имени В.Н. Каразина
пл. Свободы 4, Харьков, 61022, Украина

²Факультет химии и фармации, Софийский университет, София, 1164, Болгария

С помощью методов оптической спектроскопии и молекулярного докинга проведена оценка возможности использования нового катионного фосфониевого красителя TDV1 для изучения комплексообразования между ДНК и патогенными белковыми агрегатами, амилоидными фибриллами. Обнаружено, что TDV1 обладает высокой интенсивностью флуоресценции мономеров в буферном растворе. Ассоциация красителя с двухцепочечной ДНК сопровождалась усилением флуоресценции мономеров в сочетании с батохромным сдвигом максимума испускания. Добавление фибриллярного лизоцима (LzF) к смеси TDV1-ДНК, наряду с дальнейшим увеличением интенсивности флуоресценции мономерной формы красителя и гипсохромным сдвигом максимума излучения мономеров, приводило также к появлению дополнительного, длинноволнового пика. Сделано предположение, что увеличение интенсивности флуоресценции с увеличением концентрации белка в системе TDV1/ДНК обусловлено как взаимодействием свободных мономеров TDV1 с фибриллами лизоцима, так и вызванными фибриллярным лизоцимом конформационными изменениями ДНК. Наблюдаемый длинноволновый пик, предположительно, является результатом образования J-агрегатов при ассоциации TDV1 с фибриллами лизоцима. С использованием метода молекулярного докинга показано, что мономер TDV1 связывается с семью β -тяжами бороздки фибрилл таким образом, что их длинная ось параллельна оси фибрилл. Наиболее энергетически выгодным центром связывания TDV1 является бороздка S60-W62/G54-L56. В то же время, димеры TDV1, по-видимому, образуют стабильные комплексы с более гидрофильной поверхностью модельного β -листа. В совокупности, результаты, полученные методами флуоресцентной и абсорбционной спектроскопии, а также данные молекулярного докинга свидетельствуют о связывании TDV1 с малой бороздкой ДНК. Электростатические взаимодействия, по-видимому, являются преобладающими в связывании TDV1 с двухцепочечной ДНК, тогда как гидрофобные взаимодействия и стерические факторы определяют ассоциацию красителя с фибриллярным лизоцимом.

КЛЮЧЕВЫЕ СЛОВА: Фосфониевый краситель, фибриллярный лизоцим, ДНК, J-агрегаты.

PACS: 68.65.Ac, 68.37.Hk, 61.05.C-, 62.25.-g

STUDY OF ADVANCED NANOSCALE ZrN/CrN MULTILAYER COATINGS

 Olga Maksakova^{1*},  Alexander Pogrebnyak^{1,2}, Vyacheslav Beresnev^{3**},
 Vyacheslav Stolbovoy⁴,  Sónia Simões⁵, Dosym Yerbolatuly⁶

¹Sumy State University, 2, Rymtsky Korsakov Str., 40007 Sumy, Ukraine

²D. Serikbayev East Kazakhstan State Technical University

69, Protozanova Str., 070004, Ust-Kamenogorsk, The Republic of Kazakhstan

³V.N. Karazin Kharkiv National University, 4, Svobody Sq., 61022 Kharkiv, Ukraine

⁴National Science Center Kharkov Institute of Physics and Technology, 1, Akademicheskaya Str., 61108 Kharkiv, Ukraine

⁵University of Porto, R. Dr. Roberto Frias, 4200-465 Porto, Portugal

⁶Sarsen Amanzholov East-Kazakhstan State University

34, 30Gvardeiskoi divisii Str., 070020, Ust-Kamenogorsk, The Republic of Kazakhstan

*E-mail: maksakova.tereshenko@gmail.com, **E-mail: v.beresnev@karazin.ua

Received April 12, 2019; revised May 2, 2019; accepted May 31, 2019

The scientific interest in the investigation of nitride composites as protecting materials in tool and machining industries intensively increases. The good oxidation resistance of CrN single-layer films and high melting point, good chemical and thermal resistance of ZrN compound are motive factors for designing of multilayer composites composed of these metal nitrides. The suggested advantages of ZrN/CrN multilayer coatings as structural materials are the high-temperature resistance, high density and extreme hardness compared to the metal-nitride systems. Experimental ZrN/CrN multilayer coatings were deposited on AISI 321 steel substrates by using a cathodic arc evaporation device equipped with two high-purity metal Cr and Zr targets. Structural, chemical and morphological characteristics together with mechanical properties of multilayer composites were analyzed by X-ray diffraction, scanning electron microscopy, energy-dispersive X-ray spectroscopy and Vickers hardness tester. SEM analysis revealed an increase of roughness and concentration of the droplets on the surface of the coatings when negative bias potential decreased to -70 V. The results of data obtained from the X-ray analysis showed (200) and (111) plane for ZrN and Cr₂N phases as the most intense. The peak positions of ZrN were shifted towards lower diffraction angles comparing with bulk values and indicated a decrease of the inter-planar distance and formation of compressive stresses. The calculated lattice strain values in the ZrN were higher than those of the CrN, indicated a greater presence of dislocations and defects in the lattice of ZrN. The averaged crystallite sizes in ZrN and CrN layers were 11-14 and 7-12 nm, respectively. The maximum value of the Vickers microhardness was found to be 6600HV0.01 that is 2.1 and 1.8 times greater than the corresponding values of binary CrN and ZrN coatings.

KEYWORDS: nitrides, cathodic arc deposition, microstructure, elemental composition, structural-phase state.

The extension of the operational life of industrial equipment, components of installations, cutting, drilling and other machining tools stays a relevant task of science and technology of materials engineering till present. Moreover, nowadays at the stage of an enhanced economy of resources and in going to energy-saving technologies, this issue becomes even more acute. While functioning, the product surface layers undergo the strongest loading, physical, chemical and thermal effects. One of the ways to protect and improve various material properties is to modify it due to deposition of nanostructured thin coatings on its surface.

Cathodic-arc technique is a multipurpose method of coating deposition since the resulted products gain wide industrial distribution because of their suitability for various functional purposes [1, 2]. Transition metal nitride coatings with a thickness of a few microns are one of the most studied and widely used materials. Unfortunately, the possibilities of increasing the hardness and plasticity of the surface layer during the deposition of simple nitrides are practically depleted, since at mid-temperature range mononitrides initiated to be thermally unstable [3-5].

Recently, nanoscale coatings of a complex elemental and phase composition realized through the multilayer coating concept are of considerable interest, since combinations of various elements make it possible to use the best properties of two or several metals and their nitrides [6, 7].

This paper describes the effect of deposition parameters on the structure, elemental and phase composition of multilayer coatings ZrN/CrN, as well as their mechanical characteristics.

EXPERIMENTAL DETAILS

The ZrN/CrN multilayers were fabricated by the cathodic-arc method in a Bulat 6 deposition system [8], which composed of a vacuum chamber, vacuum pumping system, nitrogen supply system that worked at pressure between 10⁻⁵ to 10⁻² Pa, arc power supplies that produced the current from 50 to 200 A, substrate power supply that ensured constant negative bias voltage and automatic rotation system for substrate holder. Within the working chamber, there was an electrode formed by an anode, where the steel substrates were placed, and cathodes with the Zr and Cr targets. Metal targets were in the opposite positions and the substrates were mounted on two sides of a rotating substrate holder between the two targets. Experimental coatings were deposited by alternately rotating the substrates between Cr and Zr targets. The arc current of 100 A was constantly applied for all samples. When the first multilayer ZrN/CrN film started to produce, the chamber was filled with nitrogen at a pressure of 0.03 Pa. For other samples of the coatings, it changed

as the goal of this investigation was to evaluate the influence of deposition conditions on morphology, phase state and mechanical properties of multilayer condensates. Specific details of the deposition process of the multilayer coatings were summarized in Table 1.

The surface and cross-section structure, as well as the chemical composition of the coatings, were analyzed by scanning electron microscopy with energy dispersive X-ray spectroscopy facilities (SEM-EDS) in a FEI Quanta 400 FEG ESEM/EDAX Genesis X4M. For the XRD characterization technique, we used a Panalytical X'Pert Pro MPD diffractometer. Phase identification was realized through the ICDD data. Mechanical properties were evaluated by Vickers microhardness tests in a Struers Duramin-5 using a load of 98 mN (HV0.01).

Table 1.

Deposition conditions of multilayer ZrN/CrN coatings.

Sample number	Arc current I_d , A	Bias voltage U_s , V	Substrate temperature T_s , °C	Nitrogen pressure P_N , Pa	Exposing time t , s	Total deposition time, h	Deposition rate R_d , nm/s	Number of layers
1	100	-70	250	0.04	ZrN:10/CrN:10	1	3.25	354
2				0.43			3.5	
3		-150		0.16			4.5	
4				0.03			2.65	

RESULTS AND DISCUSSION

Morphologic study

The morphology of the PVD-coatings is basically controlled by the process characteristics, i.e. substrate temperature (T_s), working gas pressure (P_N), the negative bias voltage applied to the substrate (U_s) and an arc current (I_d) [9, 10]. During the surface analysis of experimental coatings, it is revealed that micro-relief of the surface is expressed by numerous shallow different-sized depressions due to the growth of crystallites of different sizes. The formation of the droplets with a particle diameter averaged from 2 to 5 microns is observed for all the coatings. Increasing the nitrogen pressure up to 0.43 Pa while the deposition does not introduce any special changes in the surface morphology. However, increasing the energy of the precipitated flow through the bias potential to -200 V significantly reduces the concentration of the droplets on the surface. Probably, with the increase of the substrate bias value, the energetic particles bombardment becomes more intensive and activates the process of cleaning the surface from smaller fractions. Fig. 1a shows the cross-sectional SEM image of the multilayer sample number 4. The heterophase interfaces between ZrN and CrN layers are rather straight and immiscible. The dark contrast layers correspond to the CrN, while lighter ones indicate the binary ZrN. The structure of layers is dense, no boundary porosity or other defects exist.

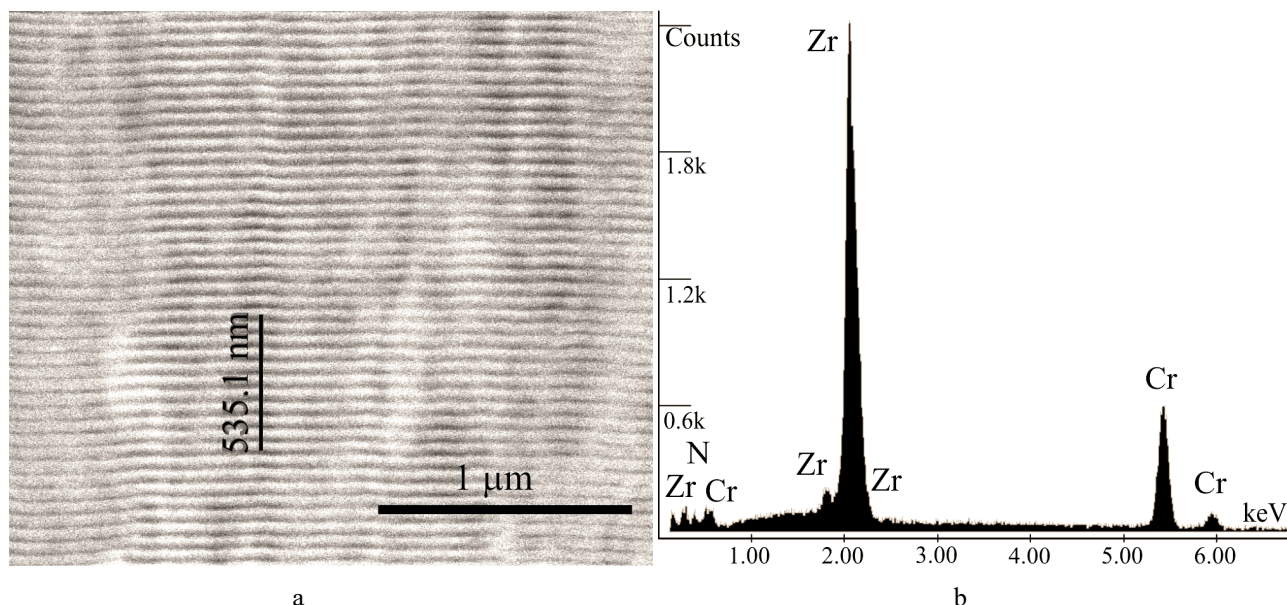


Fig. 1. Cross-sectional SEM image (a) and EDS spectrum (b) of multilayer ZrN/CrN coating number 4

Shown in Fig. 1b EDS spectrum is composed of Zr, Cr and N peaks, that confirms the purity of elemental composition of the coating number 4. The chemical compositions of multilayer ZrN/CrN coatings are generalized in Table 2 together with the total and bilayer thicknesses extracted from SEM images using ImageJ software.

It is seen from data collected via SEM and EDS that obtained coatings have the nanoscale bilayer thickness within the range from 53 to 70 nm and near-stoichiometric or stoichiometric composition as an atomic percentage of nitrogen

changes from 46 to 51. It is obvious, that for experimental coatings there is a tendency to decrease the concentration of metal elements with increasing nitrogen pressure. The lower chromium concentration in comparison with the zirconium concentration is due to the fact that chromium has a lower atomic mass ($\text{Cr} = 51.99 \text{ g/mol}$ vs. $\text{Zr} = 91.22 \text{ g/mol}$), that is, it is a lighter element. The fact is that in the process of coating deposition, when the plasma energy and, accordingly, the intensity of deposition increases, with an increase in P_N , lighter atoms may escape from the surface coating layer, which leads to an increase of another element concentration in the coating.

Table 2.

Characteristics of multilayer ZrN/CrN coatings: average coating thickness, bilayer period and chemical composition.

Sample number	Coating thickness D , μm	Bilayer period λ , nm	Chemical composition, at.%		
			N	Zr	Cr
1	11.5	65	46	30	24
2	12.4	70	50	27	23
3	16.0	90	51	29	20
4	9.4	53	47	35	18

Structural characterization

X-ray diffraction patterns of multilayer ZrN/CrN composites are shown in Fig. 2. As seen in this figure, at all values range of nitrogen pressure there is a clear (200) preferred orientation for ZrN layers and (111) preferred orientation for CrN layers (non-isostructured multilayers). For the coatings deposited at low bias potential, the texture of the ZrN layer with orientation (111) appears at the patterns. This behavior suggests the prerequisites for the cube-on-cube epitaxial growth. Some small contributions of ZrN(220) reflection are identified for samples number 1 and 2, but it disappears for larger values of U_S .

The texture coefficient T_C of (200) plane with respect of (111) plane for ZrN phase and T_C of (111) plane of Cr_2N phase with respect of (111) plane of CrN phase (samples 1 and 2) was calculated by the equation [11]:

$$T_c(hkl) = \frac{I(hkl) / I_0(hkl)}{(1/N) [\sum_N I(hkl) / I_0(hkl)]}, \quad (1)$$

where $I(hkl)$ is the integrated intensity of the diffraction plane calculated using an approximation of the pseudo-Voigt function, $I_0(hkl)$ is the relative intensity of the corresponding plane given in ICDD, and N is the number of reflections.

The evolution of the crystallography texture coefficient in the function of the working gas pressure is clearly observed in Table 3. For the low values of P_N , the texture coefficient values are 2.35 and 1.12 for the ZrN and the Cr_2N , respectively. As the nitrogen pressure increases, the coefficient for both phases lightly and respectively diminishes going to values between 1.51 for the ZrN and 1.07 for the Cr_2N .

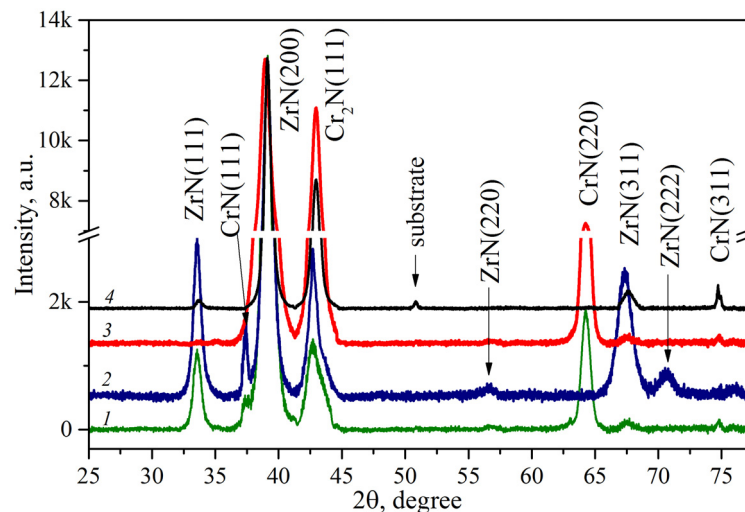


Fig. 2. X-ray diffraction data obtained from multilayer ZrN/CrN coatings

The X-ray method for determining internal stresses is based on the fact that the elastic deformation of the crystal lattice is expressed by the changes in inter-planar distance and diffraction angle in the X-ray patterns. It is necessary to point out one feature of the X-ray method for measuring residual stresses. The X-ray diffraction line is formed as a result of the total reflection from those crystallographic planes for which the Wulff-Bragg condition is satisfied. Thus, all calculations carried out on the basis of measuring the angular positions of X-ray lines provide information on the

stress state of only certain oriented grains of a polycrystalline sample. In this study, the lattice strains ε of ZrN and CrN were calculated according to the following equation based on (200)ZrN and (111)Cr₂N planes [12]:

$$\varepsilon = \frac{d - d_0}{d_0}, \quad (2)$$

where d_0 is the inter-planar distance of distinct (hkl) planes of the residual stress-free lattice and d is the inter-planar distance of the same planes influenced by residual stress. It is obvious from the Table 3 that the strains of the ZrN is greater than those of the CrN, indicating a larger formation of dislocations and defects in ZrN lattice. These dislocations cause the subdivision of the original crystallites of larger size into domains (small crystallites), producing tensile and compressive strains within diminished crystallites [13].

Table 3.

Values of strain-size parameters calculated from X-ray patterns of ZrN/CrN coatings

Sample number	Investigated phase and plane	Experimental diffraction angle 2θ , deg	Standard diffraction angle $2\theta_0$, deg	Experimental inter-planar distance d , nm	Standard inter-planar distance d_0 , nm	Crystallite size L , nm	Texture coefficient T_c	Lattice strain ε , %
1	ZrN (200)	39.10	39.13	0.2305	0.2309	11	2.35	-0.17
	Cr ₂ N(111)	42.77	42.72	0.2111	0.2114	7	1.12	-0.14
2	ZrN(200)	39.12	39.13	0.2302	0.2309	12	1.51	-0.30
	Cr ₂ N(111)	42.77	42.72	0.2112	0.2114	10	1.07	-0.09
3	ZrN(200)	39.10	39.13	0.2305	0.2309	14	2.05	-0.17
	Cr ₂ N(111)	42.79	42.72	0.2112	0.2114	12	-	-0.09
4	ZrN(200)	39.12	39.13	0.2306	0.2309	13	2.67	-0.13
	Cr ₂ N(111)	42.78	42.72	0.2110	0.2114	11	-	-0.18

Peaks obtained from ZrN demonstrate the shift toward lower angles (2θ ranged from 39.10 to 39.12°), that signifies the existence of compressive stresses in ZrN layers. A significant movement of the Cr₂N peaks towards higher angles ($2\theta = 42.77$ and 42.79°) in relation to standard values ($2\theta = 42.72^\circ$) shows the presence of tensile stresses in CrN layers.

Mechanical properties

Hardness values of the multilayer ZrN/CrN coatings measured using the Vickers tip, which is a four-sided pyramid, are presented in Fig. 3. All samples acquire the hardness that overperforms the corresponding value of individual coatings, i.e., CrN and ZrN monolayers. It is observed a hardness-increasing trend as the nitrogen pressure in the vacuum chamber decreases. The highest hardness of 6600HV0.01 is obtained for sample number 2 with stoichiometric composition of 50 at.% N and bilayer period of 70 nm, that is on 51 % and 47 % greater than referent value from ZrN and CrN coatings, respectively.

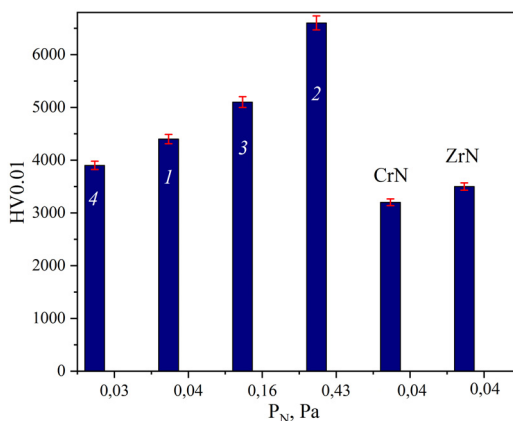


Fig. 3. Variation of microhardness with nitrogen pressure values for the multilayer ZrN/CrN coatings and binary ZrN and CrN coatings.

In general, the increase of the mechanical properties of multilayer coating lies in application of the multilayer concept that possess the following conditions: (i) the presence of many interfaces that blocks the dislocation movement across the interface between ZrN and CrN layers; (ii) coherency strains cause periodical strain-stress fields due to the lattice-mismatch in the multilayer coating; (iii) the formation of the discrete layers in the multilayer system, which observed in the SEM results; (iv) the formation of partial correlation within (111) crystallography direction between ZrN and CrN layers.

CONCLUSIONS

In summary, the morphological and structural-phase characteristics, as well as mechanical properties of multilayer ZrN/CrN coatings grown on stainless steel substrates by the cathodic arc deposition were studied.

It was shown that the surface of the multilayer composited contained droplet particles, which concentration depended on negative bias potential applied to the steel substrate. The total thickness of the obtained films ranged from 9.4 to 16.0 μm , while the bilayer period varied from 53 to 90 nm. The elemental composition of cathodic arc coatings depended on working gas pressure, hence, at high values of P_N formed coatings had the stoichiometric composition (50-51 at.%).





Additionally, different deposition conditions, i.e. nitrogen pressure and substrate bias, promoted the preferred formation of two phases ZrN(200) and Cr₂N(111), but at $U_S = -70$ V the intensive peak of ZrN(111) and reflex of CrN(111) were found on diffraction patterns.

The enhancement in microhardness of multilayer ZrN/CrN coatings was observed for all experimental samples. The maximum value 6600HV0.01 was found for the sample number 2 of stoichiometric composition (51 at.% N) obtained at $P_N = 0.43$ Pa, $U_S = -70$ V. Presented findings prove that multilayer ZrN/CrN coatings are appropriate for use as protective materials due to high hardness. However, the tribological, thermal and oxidation experiments of multilayer ZrN/CrN systems need to be done in order to find out their potential and extend the range of possible applications.

ACKNOWLEDGEMENTS

Presented work was financially supported by budget programs: "Multilayer and multicomponent coatings with adaptive behavior in wear and friction conditions" (No 0118U003579) and "Physical properties of the two-dimensional nanomaterials and metallic nanoparticles" (No. 0117U003923).

ORCID IDs

Olga Maksakova  <https://orcid.org/0000-0002-0646-6704>, Alexander Pogrebnjak  <https://orcid.org/0000-0002-9218-6492>, Vyacheslav Stolbovoy  <https://orcid.org/0000-0001-7734-0642>, Sónia Simoães  <https://orcid.org/0000-0003-4670-4516>

REFERENCES

- [1]. D.M. Sanders, D.B. Boercker, and S. Falabella, IEEE Trans. Plasma Sci. **18**, 883 (1990), doi: 10.1109/27.61499.
- [2]. O. Knotek, W.D. Münz, and T. Leyendecker, J. Vac. Sci. Technol. A Vacuum, Surfaces, Film. **5**, 2173 (1987), doi: 10.1116/1.574948.
- [3]. H. Willmann, P.H. Mayrhofer, P.O.Å. Persson, A.E. Reiter, L. Hultman, and C. Mitterer, Scr. Mater. **54**, 1847 (2006), doi: 10.1016/j.scriptamat.2006.02.023.
- [4]. H.C. Barshilia and K.S. Rajam, J. Mater. Res. **19**, 3196 (2004), doi 10.1557/JMR.2004.0444.
- [5]. A.P. Ehiasarian, P.E. Hovsepian, L. Hultman and U. Helmerson, Thin Solid Films. **457**, 270 (2004), doi: 10.1016/j.tsf.2003.11.113.
- [6]. X.M. Xu, J. Wang, J. An, Y. Zhao and Q.Y. Zhang, Surf. Coatings Technol. **201**, 5582 (2007), doi: 10.1016/j.surfcoat.2006.07.132.
- [7]. A.D. Pogrebnjak, Ya.O. Kravchenko, O.V. Bondar, B. Zhollybekov and A.I. Kupchishin, Prot. Met. Phys. Chem. Surfaces. **54**, 240 (2018), doi: 10.1134/S2070.
- [8]. O.V. Maksakova, S. Simoães, A.D. Pogrebnjak, O.V. Bondar, Ya.O. Kravchenko, T.N. Koltunowicz and Zh.K. Shaimardanov, J. Alloys Compd. **776**, 679 (2019), doi: 10.1016/j.jallcom.2018.10.342.
- [9]. D.M. Mattox, in: Deposition Technologies for Films and Coatings, edited by R.F. Bunshah (Noyes, Park Ridge, NJ, 1982), pp. 63-82.
- [10]. M. Pohler, R. Franz, J. Ramm, P. Polcik and C. Mitterer, Surf. Coatings Technol. **206**, 1454 (2011), doi: 10.1016/j.surfcoat.2011.09.028.
- [11]. C. Agashe, B.R. Marathe, M.G. Takwale and V.G. Bhide, Thin Solid Films. **164**, 261 (1988), doi: 10.1016/0040-6090(88)90146-0.
- [12]. F.H. Chung and D.K. Smith, Industrial Applications of X-Ray Diffraction, 1st ed. (CRC Press, New York, 1999), p. 1024.
- [13]. H.P. Klug and L.E. Alexander, X-Ray Diffraction Procedures for Polycrystalline and Amorphous Materials, 2nd ed. (John Wiley & Sons, New York, 1974), p. 960.

ДОСЛІДЖЕННЯ ПЕРСПЕКТИВНИХ НАНОРОЗМІРНИХ ZrN/CrN БАГАТОШАРОВИХ ПОКРИТТІВ

О.В. Максакова¹, О.Д. Погребняк^{1,2}, В.М. Береснев³, В.О. Столбовий⁴, S. Simoães⁵, Д. Єрболатулі⁶

¹Сумський державний університет, вул. Римського-Корсакова, 2, 40007 Суми, Україна

²Східно-Казахстанський державний технічний університет ім. Д. Серікбаєва
вул. Протозанова, 69, 070004 Усть-Каменогірськ, Республіка Казахстан

³Харківський національний університет імені В.Н. Каразіна, майд. Свободи 4, 61022 Харків, Україна

⁴Національний науковий центр Харківський фізико-технічний інститут, вул. Академічна 1, 61108 Харків, Україна

⁵University of Porto, R. Dr. Roberto Frias, 4200-465 Porto, Portugal

⁶Східно-Казахстанський державний університет імені Сарсена Аманжолова
вул. 30-ї Гвардійської дивізії, 34, 070020 Усть-Каменогірськ, Республіка Казахстан

Науковий інтерес до дослідження нітридних композитів в якості захисних матеріалів в інструментальній та обробній промисловостях інтенсивно зростає. Хороша стійкість до окислення одношарових плівок CrN і висока температура плавлення, хороша хімічна і термічна стійкість ZrN є рушійними факторами для створення багатошарових композитів, в яких використовуються нітриди цих перехідних металів. Передбачувані переваги багатошарових покриттів в якості

конструкційних матеріалів – це висока термостійкість, висока щільність їх структури і покращена твердість у порівнянні з системами нітрид-метал. Багат шарові покриття ZrN/CrN осаджувалися на сталеві підкладки AISI 321 за допомогою вакуумно-дугового пристрою, оснащеного двома металевими мішенями Cr і Zr високої чистоти. Структурні, хімічні та морфологічні характеристики, а також механічні властивості багат шарових композитів були проаналізовані за допомогою рентгенівської дифракції, растрової електронної мікроскопії, енергодисперсійної рентгенівської спектроскопії і твердомира, оснащеного пірамідкою Віккерса. РЕМ-аналіз виявив збільшення шорсткості і концентрації крапель на поверхні покриттів, коли негативний потенціал зсуву знижувався до значення в -70 В. Результати даних, отриманих від рентгеноструктурного аналізу, показали, що найбільш інтенсивними є площини (200) і (111) для ZrN і Cr₂N фази, відповідно. Положення піків ZrN були зміщені в бік менших кутів дифракції в порівнянні з об'ємними значеннями і вказували на зменшення міжплощинної відстані і формування стискаючих напружень. Розраховані значення напруження решітки в ZrN вище, ніж у CrN, що свідчить про більшу наявності дислокацій і дефектів в решітці ZrN. Усереднені розміри кристалітів в шарах ZrN і CrN становили 11-14 і 7-12 нм відповідно. Було встановлено, що максимальне значення мікротвердості по Віккерсу становить 6600HV0.01, що в 2,1 і 1,8 рази більше, ніж відповідні значення бінарних покриттів CrN і ZrN.

КЛЮЧОВІ СЛОВА: нітриди, вакуумно-дугове осадження, мікроструктура, елементний склад, структурно-фазовий стан.

ИССЛЕДОВАНИЯ ПЕРСПЕКТИВНЫХ НАНОРАЗМЕРНЫХ ZrN/CrN МНОГОСЛОЙНЫХ ПОКРЫТИЙ

О.В. Максакова¹, А.Д. Погребняк^{1,2}, В.М. Береснев³, В.А. Столбовой⁴, S. Simões⁵ Д. Ерболатулы⁶

¹ Сумский государственный университет, ул. Римского-Корсакова, 2, 40007 Сумы, Украина

² Восточно-Казахстанский государственный технический университет им. Д. Серикбаева
ул. Протозанова, 69, 070004 Усть-Каменогорск, Республика Казахстан

³ Харьковский национальный университет имени В. Н. Каразина, пл. Свободы 4, 61022 Харьков, Украина

⁴ Национальный научный центр Харьковский физико-технический институт
ул. Академическая, 1, 61108, Харьков, Украина

⁵ University of Porto, R. Dr. Roberto Frias, 4200-465 Porto, Portugal

⁶ Восточно-Казахстанский государственный университет имени Сарсена Аманжолова
ул. 30-й Гвардейской дивизии, 34, 070020 Усть-Каменогорск, Республика Казахстан

Научный интерес к исследованию нитридных композитов как защитных материалов в инструментальной и обрабатывающей промышленности интенсивно возрастает. Хорошая стойкость к окислению однослойных пленок CrN и высокая температура плавления, хорошая химическая и термическая стойкость ZrN являются движущими факторами для создания многослойных композитов, в которых используются нитриды этих переходных металлов. Предполагаемые преимущества многослойных покрытий в качестве конструкционных материалов – это высокая термостойкость, высокая плотность их структуры и чрезвычайная твердость по сравнению с системами нитрид-металл. Многослойные покрытия ZrN/CrN наносились на стальные подложки AISI 321 с использованием вакуумно-дугового устройства, оснащенного двумя металлическими мишенями Cr и Zr высокой чистоты. Структурные, химические и морфологические характеристики, а также механические свойства многослойных композитов были проанализированы с помощью рентгеновской дифракции, растровой электронной микроскопии, энергодисперсионной рентгеновской спектроскопии и твердомера, оснащенного пирамидкой Виккерса. РЕМ-анализ выявил увеличение шероховатости и концентрации капель на поверхности покрытий, когда отрицательный потенциал смещения снижался до значения в -70 В. Результаты данных, полученных от рентгеноструктурного анализа, показали, что наиболее интенсивными являются плоскости (200) и (111) для ZrN и Cr₂N фазы, соответственно. Положения пиков ZrN были смещены в сторону меньших углов дифракции по сравнению с об'ємними значеннями і указывали на уменьшение межплоскостного расстояния и присутствие сжимающих напряжений. Рассчитанные значения напряжений решетки в ZrN выше, чем у CrN, что свидетельствует о большем наличии дислокаций и дефектов в решетке ZrN. Усредненные размеры кристаллитов в слоях ZrN и CrN составляли 11-14 и 7-12 нм соответственно. Было установлено, что максимальное значение микротвердости по Виккерсу составляет 6600HV0.01, что в 2,1 и 1,8 раза больше, чем соответствующие значения бинарных покрытий CrN и ZrN.

КЛЮЧЕВЫЕ СЛОВА: нитриды, вакуумно-дуговое осаждение, микроструктура, элементный состав, структурно-фазовое состояние.

PACS: 71.55.Gs, 72.80.Ey, 73.20.Hb, 73.40.Gk, 73.40.Lq, 85.60.Bt

EFFECT OF SILICON SURFACE TREATMENT ON THE ELECTRICAL AND PHOTOELECTRIC PROPERTIES OF NANOSTRUCTURED MoO_x/n-Si HETEROJUNCTIONS

 Mykhailo Solovan*,  Taras Kovaliuk,  Pavlo Maryanchuk

*Yuriy Fedkovych Chernivtsi National University,
st. Kotsyubyns'kogo 2, 58012, Chernivtsi, Ukraine*

**E-mail: m.solovan@chnu.edu.ua*

Received March 13, 2019; revised April 24, 2019; accepted May 7, 2019

The paper presents the results of studies of the effect of silicon surface treatment on the electrical and photoelectric properties of nanostructured MoO_x/n-Si heterojunctions. The nanostructured heterojunctions MoO_x/n-Si, were prepared by deposition of thin films of molybdenum oxide (*n*-type conductivity) by reactive magnetron sputtering in the universal vacuum system Leybold Heraeus L560 on the nanostructured silicon substrates (*n*-type conductivity), which were made by chemical etching with the assistance of silver nanoparticles. Dark and light volt-ampere (*I* – *V*) characteristics of the heterojunctions under study were measured, the value of the potential barrier height, the values of the serial *R_s* and the shunt *R_{sh}* resistance at room temperature were determined. It was established that the silicon surface treatment does not affect the potential barrier height, but significantly affects the values of serial *R_s* and shunt *R_{sh}* resistance. The electrical and photoelectric properties of the obtained structures were investigated, the dominant mechanisms of current transfer through the heterostructures under forward bias are well described in the framework of emission-recombination and tunneling models with the presence of interface states. The main mechanism for the charge carrier transport through heterojunctions with the reverse bias is the Frenkel–Pool emission. Investigation of photoelectric properties of heterojunctions MoO_x/n-Si was carried out at illumination by white light with intensity *P_{opt}* = 80 mW/cm². It was established that the heterostructure No.5 MoO_x/n-Si with grown nanowires and etched silver nanoparticles has a maximum open-circuit voltage *V_{oc}* = 0.17 V, short-circuit current density *I_{sc}* = 10 mA/cm². The possibilities of using the obtained heterostructures as photodiodes were analyzed.

KEY WORDS: surface treatment, series resistance, current transfer mechanisms, molybdenum oxide, silicon.

In recent years the interest to the research of semiconductor heterojunctions created on the basis of thin films of transition metal oxides has considerably grown up. Molybdenum oxide (MoO_x) has found practical application in electronics and in photovoltaic devices long ago due to high work function of electron and good physical properties: it has a high transmission factor in the visible part of the spectrum [1], a low electrical resistivity [2], the band gap width *E_g* > 3 eV [3, 4]. In our previous work [5] we showed the possibility to form planar photosensitive heterostructures based on silicon and molybdenum oxide. It is known that the expansion of the scope of such heterostructures application is possible by creating nanostructured surfaces of the base material.

The silicon-based nanostructures are attribute components of the up-to-date instrument engineering in the field of electronics, optoelectronics, chemical sensors, as well as for the conversion and accumulation of solar energy. The silicon surface, which is modified by arrays of nanowires, has a low reflection coefficient and a large active area, what allows its successful practical application [6]. Judging by the aforesaid, the creation and study of nanostructured MoO_x/Si heterojunctions is of considerable scientific and practical interest.

The objective of the work is to study the effect of silicon surface treatment on the electrical and photoelectric properties of nanostructured MoO_x/n-Si heterojunctions.

EXPERIMENTAL PART

To grow nanowires the monocrystalline silicon of *n*-type conductance with surface orientation (100) and thickness of 330 μm was used. The resistivity and concentration of the crystals charge carriers at the temperature (295 K) made: $\rho = 6 \text{ Ohm}\cdot\text{cm}$ and $n = 7.4 \cdot 10^{14} \text{ cm}^{-3}$, respectively. The depth of the burial level - Fermi for the base material ($E_c - E_F = 0.27 \text{ eV}$) was determined from the expression for the concentration of equilibrium electrons: $n = 2(2\pi m_n kT/h^2)^{3/2} \exp(-(E_c - E_F)/kT)$.

To remove the native oxide and to purify the surface from the contaminants the silicon plates were chemically etched in 5% solution of hydrofluoric acid (HF) in bi-distilled water for 5 minutes. At the start of the nanowires growing the silicon substrates were washed in an ultrasonic bath in bi-distilled water and in acetone, after washing the substrates were etched in a solution of sulfuric acid and 30% of hydrogen peroxide (H₂O₂) in the appropriate ratio (3:1) to remove the organic contaminants. After purification our samples were immersed in pre-prepared aqueous solutions of 0.02M AgNO₃ and of 5M HF in the ratio (1:1) for 5-10 seconds in order to deposit silver nanoparticles on the substrates [5-6].

After deposition of silver nanoparticles some part of the substrates were taken to create heterostructures, and the others for the next steps to create nanowires. The next step to create nanowires was etching of silicon substrates with silver nanoparticles in the solution of 5M HF and 30% H₂O₂ in the ratio (10:1). Also, after creating nanowires on the

silicon substrate with intercalated silver nanoparticles, some part of the substrates was taken to create heterostructures. The final procedure was etching silver nanoparticles from the substrate itself using nitric acid.

Thin MoO_x films were deposited on the surface of nanostructured monocrystalline Si (size $5 \times 5 \times 0.36$ mm) with orientation (100) in the universal vacuum device Leybold Heraeus L560 by reactive magnetron sputtering of a pure molybdenum target in the atmosphere of argon and oxygen mixture under the forward-current voltage. Before starting the spraying process the vacuum chamber was pumped out to the residual pressure of $5 \cdot 10^{-3}$ Pa. The partial pressures of argon and oxygen were 0.24 Pa and 0.034 Pa, respectively, at the constant magnetron power of 30 W. In the course of spraying process the substrate temperature is maintained at 573 K. The spraying process lasted for 3 minutes.

After finishing the process of deposition of the MoO_x thin films the vacuum chamber was gradually cooled to room temperature and then was opened to replace the molybdenum target with ITO target ($\text{In}_2\text{O}_3\text{-SnO}_2$ 90:10 by mass). The deposition of ITO thin 0.15 μm -thick films, which were used as an antireflection coating, was carried out by the method of magnetron sputtering of the ITO target in the Argon atmosphere under the direct-current voltage.

During the process of deposition the argon pressure in the vacuum chamber was ~ 0.4 Pa. The installed power of the magnetron was ~ 30 W. The deposition process lasted for ~ 5 min. at the substrate temperature of ~ 420 K. To provide the frontal electric contact with the thin MoO_x film the conducting paste was used. To avoid recombination on the rear side of silicon and to ensure a good set of photogenerated charge carriers, we used substrates that previously had rear contact with the built-in internal field. The contact was created by sputtering a layer of the intrinsic hydrogenated amorphous silicon (a-Si:H) with the thickness of ~ 10 nm to passivate the substrate surface, the next layer of hydrogenated amorphous silicon n^+ (a-Si:H) with the thickness of ~ 20 nm, which was heavily doped with phosphorus, to create isotype junction with the barrier height of ~ 0.1 eV on the rear side of Si, and the last layer of Al was deposited by thermal evaporation (the block diagram is shown in the inset of Fig. 1).

RESULTS AND DISCUSSION

ELECTRICAL PROPERTIES OF NANOSTRUCTURED HETEROJUNCTIONS $\text{MoO}_x/\text{n-Si}$

The $\text{MoO}_x/\text{n-Si}$ heterostructures were prepared using the method of reactive magnetron sputtering of molybdenum oxide thin films on the single-crystal n-Si substrates with different surface treatment (Table 1).

Table 1.

Conditions for $\text{MoO}_x/\text{n-Si}$ heterostructures preparation

Sample No. 1	The $\text{MoO}_x/\text{n-Si}$ heterostructure was prepared without chemical treatment of the substrates.
Sample No. 2	The $\text{MoO}_x/\text{n-Si}$ heterostructure: Si substrates were etched in 5% aqueous solution of HF.
Sample No. 3	The $\text{MoO}_x/\text{n-Si}$ heterostructure: silver nanoparticles were deposited on Si substrates.
Sample No. 4	The $\text{MoO}_x/\text{n-Si}$ heterostructure: nanowires with intercalated silver nanoparticles were grown on Si substrates.
Sample No. 5	The $\text{MoO}_x/\text{n-Si}$ heterostructure: nanowires were grown on Si substrates and silver nanoparticles were etched.

Fig. 1 shows the volt-ampere characteristics and dependences of the differential resistance [7] on the applied bias for the $\text{MoO}_x/\text{n-Si}$ heterojunctions with different treatment of Si surface, listed in Table 1.

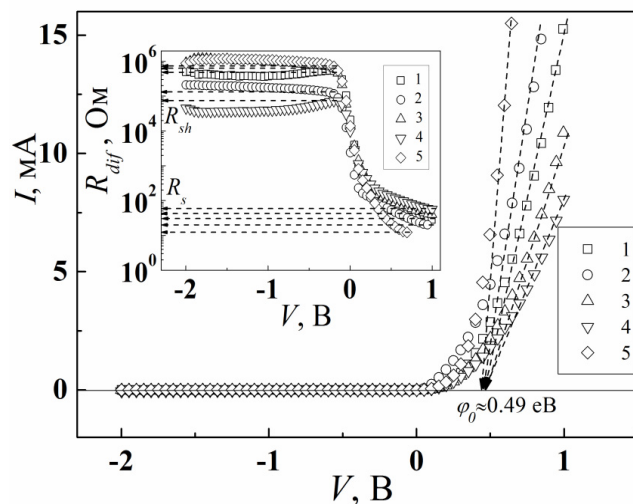


Fig. 1. I - V characteristics of $\text{MoO}_x/\text{n-Si}$ heterojunctions.

The inset shows the dependence of the differential resistance of $\text{MoO}_x/\text{n-Si}$ heterojunctions on the applied voltage (at room temperature)

Table 2 presents the major parameters of heterojunctions subject to the volt-ampere characteristics: heterojunction rectification factor k , the value of the potential barrier height φ_0 , and the value of the series and shunt resistance of heterojunctions.

Table 2.

Parameters of MoO_x/n-Si heterojunctions

Sample	k at $V = 0,7$ V	φ_0 , eV	R_s , Ω	R_{sh} , Ω
1	2.3×10^3	0.49	30	6.1×10^5
2	5.2×10^2	0.49	20	1.3×10^5
3	1.3×10^3	0.49	42	6.7×10^5
4	2.6×10^2	0.49	59	7.4×10^4
5	6.3×10^3	0.49	13	7.5×10^5

As Fig. 1 and Table 2 show, that the Si surface treatment does not affect the height of the potential barrier since its value depends on the difference in the work function of the heterojunction components, and its value can be affected by the electric charge localized on the surface energy states. However, the surface treatment significantly affects the value of the series resistance R_s . Table 2 shows that the substrate surface treatment in HF (sample 2) causes a decrease in the series resistance due to the removal of the native oxide (SiO₂) from the substrate surface, but to determine more precisely the reasons for the series resistance growth an additional research is required. The lowest value of the series resistance for sample No. 5 is stipulated by an increase in the active area of the developed heterojunction surface and by a decrease in the effective length of the base material [8], while the highest values of the rectification factor and shunt resistance indicate that heterostructure No. 5 is the best among all the above-listed ones.

MECHANISMS OF CURRENT TRANSFER IN THE NANOSTRUCTURED MoO_x/n-Si HETEROJUNCTIONS

Forward biases

The analysis of the forward branches of I - V characteristics of MoO_x/n-Si structures built in a semi-log scale (Fig. 2), with the influence of series and shunt resistances taken into account, showed that the dependence $\ln[I - (V - IR_s)/R_{sh}] = f(V - IR_s)$ comprises two straight portions, what indicates to the exponential dependence of the current on the voltage and to the presence of two dominant mechanisms of charge transfer in the voltage range under study. The values of the nonideality factor according to $\Delta \ln[I - (V - IR_s)/R_{sh}] / \Delta (V - IR_s) = e/nkT$, where n is the nonideality factor, determined for the both voltage portions are given in Table 3.

A small value of the potential barrier height $\varphi_0 = 0.49$ eV, as a rule, leads to the flow of the over-barrier current. In the voltage range ($3kT/e < V < 0.2$ V) the dependence $I(V)$ is well described by the expression for the emission-recombination mechanism of current transfer with the influence of the series and shunt resistances taken into account (direct recombination of charge carriers through the energy states on the interface, which is determined by the potential barrier height) [9, 5]:

$$I = I_s \left[\exp\left(\frac{q(V - IR_s(T))}{nkT}\right) - 1 \right] + \frac{V - IR_s}{R_{sh}}, \tag{1}$$

where

$$I_s = B_0 \exp\left(-\frac{\varphi_0(T)}{nkT}\right), \tag{2}$$

B_0 is the coefficient that depends weakly on the temperature, the coefficient n , as a rule, varies from 1 to 2, what correlates well with experimentally obtained values (Table 3).

Table 3.

MoO_x/n-Si heterojunction parameters

Sample	n ($3kT/e < V < 0.2$ V)	n ($0.2 < V < 0.4$ V)	a , B^{-1}
1	1.58	3.64	10.76
2	1.80	5.49	7.68
3	1.66	3.64	10.76
4	1.65	3.77	10.40
5	1.50	2.97	13.20

When the emission-recombination mechanism is dominant, it is considered that the recombination centers are uniformly distributed by energy and are concentrated in a narrow region near the interface.

Taking the logarithm of expression (1) we obtain:

$$\ln\left(I - \frac{V - IR_s(T)}{R_{sh}}\right) = I_s + \frac{q(V - IR_s(T))}{nkT} \quad (3)$$

From the last expression it is evident that the dependences $\ln(I - [V - IR_s]/R_{sh}) = f(V - IR_s)$ should be approximated by straight lines with a slope, what is really observed (Fig. 2).

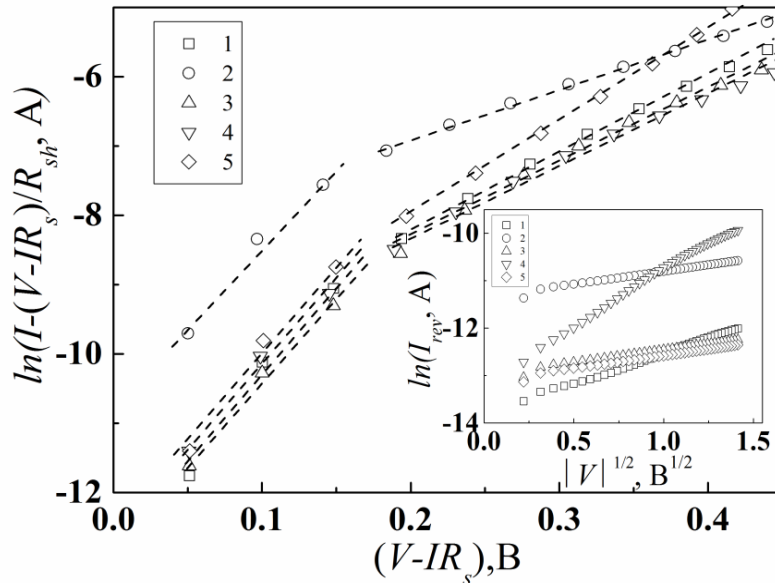


Fig. 2. Forward branches of I - V characteristics of MoO_x/n-Si heterojunctions in a semi-log scale, with the influence of series and shunt resistances taken into account

The inset shows the dependences described by the Frenkel-Poole emission through MoO_x/n-Si heterojunctions at reverse bias.

In the voltage range $0.2 < V < 0.4$ V a small constant slope (a large value of the nonideality factor $n > 2$) of the experimental dependences $\ln(I) = f(V)$ at different temperatures can be considered as an evidence of the tunneling nature of the current transfer mechanism [10]. Straight portions of I - V characteristics with identical slopes occur at sufficiently large biases, where the space charge region is sufficiently thin for direct tunnel effect, which is described by Newman formula for the tunneling mechanism of current transfer with the effect of series resistance taken into account [9, 10]:

$$I = I_t^0 \exp(\beta T) \cdot \exp[\alpha(V - IR_s)], \quad (4)$$

I_t^0 , α , β are constants. The experimental value of α was determined from the dependence $\ln(I) = f(V - IR_s)$ and is shown in Table 3.

Reverse biases

The dependence $I_{rev}(V)$ is well described in the framework of the model based on the Frenkel-Poole emission. The essence of the corresponding processes is the thermal excitation of charge carriers, captured by surface traps, facilitated by electric field [11].

The dependence of the electric field strength on the reverse voltage $E(V)$ in the space charge region of the asymmetric heterojunction was estimated by the formula taken from [5].

The dependence of the reverse current on the voltage ($0.12 < |V| < 2$ V), plotted in coordinates $\ln(I_{rev}) = f(|V|^{1/2})$ is shown in the inset of Fig. 2 and is well approximated by straight lines, what confirms the validity of the proposed mechanism of the current transfer. Curve 4 (for the sample with the intercalated silver nanoparticles) deviates from the others, what is due to formation of silver oxide or silver-containing compounds with dielectric properties in this heterostructure, and as a result some additional traps or recombination centers are formed that affect the current flow.

PHOTOELECTRIC PROPERTIES OF NANOSTRUCTURED MoO_x/n-Si HETEROJUNCTIONS

Figure 3 presents the dark and light I - V characteristics of MoO_x/n-Si heterostructures.

As Fig. 3 shows, at illumination with white light with the intensity of 80 mW/cm² the forward and reverse current I_{light} increases as compared to their values in the dark zone I_{dark} . The heterostructure parameters determined from the dependence $I=f(V)$ had the following values (Table 4).

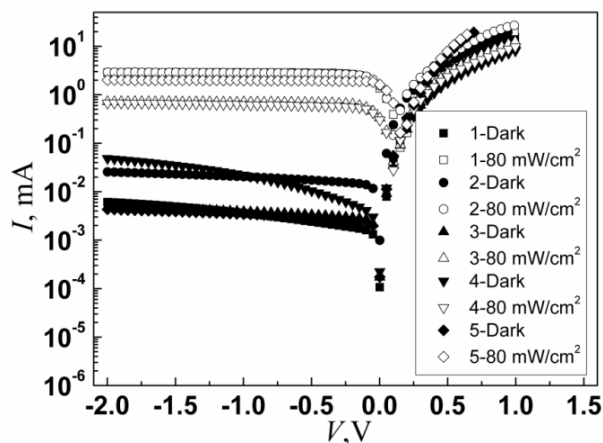


Fig.3. Dark and light I - V characteristics of $\text{MoO}_x/\text{n-Si}$ heterojunctions in a semi-log scale

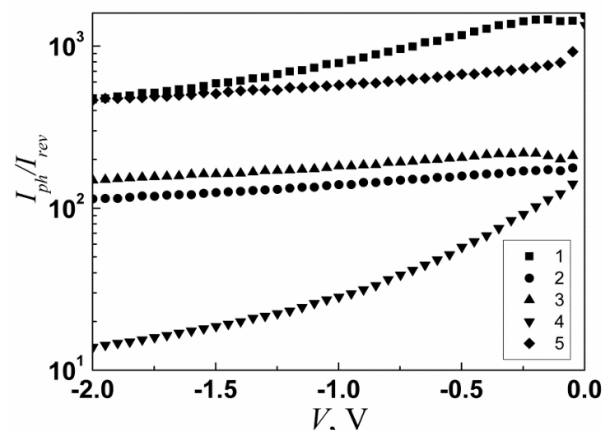


Fig.4. The $I_{ph}/I_{rev}=f(V)$ dependencies of $\text{MoO}_x/\text{n-Si}$ heterojunctions in a semi-log scale

Table 4.

Photoelectric parameters of $\text{MoO}_x/\text{n-Si}$ heterojunctions

Sample	V_{oc} , V	I_{sc} , mA/cm ²
1	0,167	8,56
2	0,113	9,56
3	0,117	2
4	0,11	1,87
5	0,17	10

A large ratio between the photocurrent and the dark reverse current I_{ph}/I_{rev} shows that the heterostructures under study can be used as photodiodes (Fig. 4). At the same time, Fig. 4 shows that for sample 4 (with intercalated silver nanoparticles) the photoelectric parameters are the lowest. Due to the negative effect of the intercalated silver nanoparticles on the current transfer mechanisms, as well as the barrier and photoelectric parameters of the obtained structures, these silver nanoparticles are to be etched in nitric acid when growing nanowires on silicon by the above described method.

Table 4 shows that heterostructure No. 5 has the highest photoelectric parameters among the heterostructures under study, and after their refinement by introducing intermediate layers and high-quality passivation of dangling bonds in silicon they can be used as solar cells.

CONCLUSION

The effect of surface treatment of Si substrates on the electrical and photoelectric properties of $\text{MoO}_x/\text{n-Si}$ heterostructures was studied.

Photosensitive $\text{MoO}_x/\text{n-Si}$ heterojunctions were obtained by the method of reactive magnetron sputtering.

The I - V characteristics were measured. The electrical properties and barrier parameters of the obtained heterostructures were investigated.

The studies have shown that the mechanisms of current transfer through the heterostructures under forward bias are well described in the framework of emission-recombination and tunnel models with the presence of interface states. The basic mechanism for the charge carrier transfer through the heterojunctions at reverse bias is Frenkel-Poole emission.

The authors have found that the heterostructures are photosensitive and can be used as photodiodes.

ORCID IDs

Mykhailo Solovan <http://orcid.org/0000-0002-1077-5702>, Taras Kovaliuk <http://orcid.org/0000-0002-7712-6758>,
Pavlo Maryanchuk <https://orcid.org/0000-0002-5523-4280>

REFERENCES

- [1]. S. Subbarayudu, V. Madhavi and S. Uthanna, Adv. Mat. Lett. **4**(8), 637 (2013), doi: 10.5185/amlett.2012.11466.
- [2]. L.D. López-Carreño, A. Pardo, M. Zuluaga, O.L. Cortés-Bracho, J. Torres, and J.E. Alfonso, Phys. Stat. Sol. (c). **4**, 4064 (2007), doi: 10.1002/pssc.200775931.
- [3]. A.L. Fahrenbruch and R.H. Bube *Fundamentals of Solar Cells. Photovoltaic Solar Energy Conversion* (Academic, New York, 1983).
- [4]. V.V. Brus, M.I. Ilashchuk, Z.D. Kovalyuk, P.D. Maryanchuk and K.S. Ulyanytskyi, Semicond. Sci. Technol. **26**, 125006 (2011).

- [5]. M.M. Solovan, Journal of Nano- and Electronic Physics. **10**(2), 02030 (2018).
 [6]. M.M. Solovan, V.V. Brus, A.I. Mostovyi, P.D. Maryanchuk, I.G. Orletskyi, T.T. Kovaliuk and S.L. Abashin, Semiconductors. **51**(4), 542 (2017).
 [7]. L.A. Kosyachenko, X. Methew, V.V. Motushchuk and V.M. Sklyarchuk, Solar Energy. **80**, 148 (2006).
 [8]. H.P. Parkhomenko, M.M. Solovan and P.D. Maryanchuk, Journal of Nano- and Electronic Physics. **10**(2), 02028 (2018).
 [9]. B.L. Sharma and R.K. Purohit, *Semiconductor heterojunctions*, Vol. 5. (Pergamon Press, New York, 2015), p. 224.
 [10]. A. Fahrenbruch and R. Byub, *Solar cells (theory and experiment)*, (Energoatomizdat, Moscow, 1987), p. 278.
 [11]. S.M. Sze and K. Kwok, *Physics of Semiconductor Devices*, 3rd ed. (Wiley, New Jersey, 2007), p. 815.
 [12]. V.V. Brus, M.I. Iashchuk, V.V. Khomyak, Z.D. Kovalyuk, P.D. Maryanchuk and K.S. Ulyanytsky, Semiconductors, **9**, 1152 (2012).

ВПЛИВ ОБРОБКИ ПОВЕРХНІ КРЕМНІЮ НА ЕЛЕКТРИЧНІ І ФОТОЕЛЕКТРИЧНІ ВЛАСТИВОСТІ НАНОСТРУКТУРОВАНИХ ГЕТЕРОПЕРЕХОДІВ $\text{MoO}_x/n\text{-Si}$

М.М. Солован, Т.Т. Ковалюк, П.Д. Мар'янчук

Чернівецький національний університет імені Юрія Федьковича
вул. Коцюбинського 2, 58012 Чернівці, Україна

У роботі представлено результати досліджень впливу обробки поверхні кремнію на електричні та фотоелектричні властивості наноструктурованих гетеропереходів $\text{MoO}_x/n\text{-Si}$. Наноструктуровані гетеропереходи $\text{MoO}_x/n\text{-Si}$, створено шляхом нанесення тонких плівок оксиду молибдену (n -типу провідності) методом реактивного магнетронного розпилення в універсальній вакуумній установці Leybold Heraeus L560 на наноструктуровані підкладки кремнію (n -типу провідності), які виготовляли шляхом хімічного травлення за участю наночастинок срібла. Виміряні темнові та світлові вольт-амперні характеристики (ВАХ) досліджуваних гетеропереходів, визначено значення висоти потенціального бар'єру, значення послідовного R_s і шунтуючого R_{sh} опорів при кімнатній температурі. Встановлено, що обробка поверхні кремнію не впливає на висоту потенціального бар'єру, але суттєво впливає на величину послідовного R_s та шунтуючого R_{sh} опорів. Досліджено електричні і фотоелектричні властивості отриманих структур, домінуючі механізми струмопереносу через гетероструктури при прямому зміщенні добре описуються в рамках емісійно – рекомбінаційної та тунельної моделей за участю поверхневих станів. Основним механізмом переносу носіїв заряду через гетеропереходи при зворотному зміщенні є емісія Френкеля-Пула. Дослідження фотоелектричних властивостей гетеропереходів $\text{MoO}_x/n\text{-Si}$ проводили при опроміненні білим світлом інтенсивністю $P_{opt} = 80 \text{ мВт/см}^2$. Встановлено, що гетероструктура №5 $\text{MoO}_x/n\text{-Si}$ з вирощеними нанодротоми і витравленими наночастинами срібла має максимальну напругу холостого ходу $V_{oc} = 0,17 \text{ В}$, густину струму короткого замикання $I_{sc} = 10 \text{ мА/см}^2$. Проаналізовано можливості застосування отриманих гетероструктур в якості фотодіодів.

КЛЮЧОВІ СЛОВА: обробка поверхні, послідовний опір, механізми струмопереносу, оксид молибдена, кремній.

ВЛИЯНИЕ ОБРАБОТКИ ПОВЕРХНОСТИ КРЕМНИЯ НА ЭЛЕКТРИЧЕСКИЕ И ФОТОЭЛЕКТРИЧЕСКИЕ СВОЙСТВА НАНОСТРУКТУРИРОВАННЫХ ГЕТЕРОПЕРЕХОДОВ $\text{MoO}_x/n\text{-Si}$

М.Н. Солован, Т.Т. Ковалюк, П.Д. Марьянчук







Черновицкий национальный университет имени Юрия Федьковича
ул. Коцюбинского 2, 58012 Черновцы, Украина

В работе представлены результаты исследований влияния обработки поверхности кремния на электрические и фотоэлектрические свойства наноструктурированных гетеропереходов $\text{MoO}_x/n\text{-Si}$. Наноструктурированные гетеропереходы $\text{MoO}_x/n\text{-Si}$, созданы путем нанесения тонких пленок оксида молибдена (n -типа проводимости) методом реактивного магнетронного распыления в универсальной вакуумной установке Leybold Heraeus L560 на наноструктурированные подложки кремния (n -типа проводимости), которые изготавливали путем химического травления с участием наночастиц серебра. Измерены темновые и светловые вольт-амперные характеристики (ВАХ) изучаемых гетеропереходов, определено значение высоты потенциального барьера, значение последовательного R_s и шунтирующего R_{sh} сопротивлений при комнатной температуре. Установлено, что обработка поверхности кремния не влияет на высоту потенциального барьера, но существенно влияет на величину последовательного R_s и шунтирующего R_{sh} сопротивлений. Исследовано электрические и фотоэлектрические свойства полученных структур, доминирующие механизмы токопереноса через гетероструктуры при прямом смещении хорошо описываются в рамках эмиссионно-рекомбинационной и туннельной моделей с участием поверхностных состояний. Доминирующим механизмом переноса носителей заряда через гетеропереходы при обратном смещении является эмиссия Френкеля-Пула. Исследование фотоэлектрических свойств гетеропереходов $\text{MoO}_x/n\text{-Si}$ проводили при облучении белым светом интенсивностью $P_{opt} = 80 \text{ мВт/см}^2$. Установлено, что гетероструктура №5 $\text{MoO}_x/n\text{-Si}$ с выращенными нанопроводами и витравленными наночастицами серебра имеет максимальное напряжение холостого хода $V_{oc} = 0,17 \text{ В}$, плотность тока короткого замыкания $I_{sc} = 10 \text{ мА/см}^2$. Проанализированы возможности применения полученных гетероструктур в качестве фотодиодов.

КЛЮЧЕВЫЕ СЛОВА: обработка поверхности, последовательное сопротивление, механизмы токопереноса, оксид молибдена, кремний.

PACS: 28.41.Qb, 81.40.Ef, 61.10.Nz, 61.72.Hh

REGULARITIES OF CHANGES IN KEARNS TEXTURE COEFFICIENT AT COLD ROLLING OF Zr-2.5%Nb ALLOY

 Viktor Grytsyna,  Dmitry Malykhin*,  Tetiana Yurkova,  Kostiantyn Kovtun,
Tetiana Chernyayeva,  Gennadiy Kovtun,  Vira Kornyeveva, Olena Slabospitskaya,
Irina Tantsura, Viktor Voyevodin

NSC "Kharkiv Institute of Physics and Technology" NASU
Kharkiv, 61108, st. Akademicheskaya 1, Ukraine

*E-mail: dmitr.malykhin@gmail.com

Received April 15, 2019; revised May 13, 2019; accepted May 16, 2019

X-ray studies of the changes in characteristics of crystallographic texture with cold deformation of Zr-2.5%Nb alloy plates by longitudinal and cross rolling up to 56% at the speed of $5 \dots 10 \text{ sec}^{-1}$ were carried out. The original plates were made from longitudinal fragments and rings cut from $\varnothing 15.0 \times 1.5 \text{ mm}^2$ tube, and were then annealed at $580 \text{ }^\circ\text{C}$. Texture of the plates was studied by the method of inverse pole figures with calculation of the Kearns texture coefficient along the normal to the plate plane. Dependences of the texture coefficient on degrees of deformation of the plates are built. A discrepancy was found between texture coefficient values measured on different sides of the plates, which is associated with the straightening of the original tube fragments and invariance of "c"-axes distribution after subsequent annealing of the initial plates. By introducing corrections to the degree of deformation calculated from the parameters of the cross section of the original tube, such discrepancies were eliminated for the data on cross-rolling of the material. As a result, for both deformation schemes, two stages of changes in the texture coefficient with alloy deformation were revealed: the initial stage of its growth and the subsequent stage of minor changes. Both stages are mainly linear and have the boundary value of the texture coefficient equal to $0.65 \dots 0.68$. To study the structural mechanisms of changes in the texture of the alloy, an original technique of comparative analysis of changes in the texture coefficient of the material and in the distribution of crystallographic orientations is applied. It is established that at the initial stage of changes in the texture coefficient with deformation in both schemes, the rotation of the crystallographic "c" axes of the material occurs abruptly, and it does at angles of more than 60° . This confirms the essential role of twinning in the texture changes of the alloy. In particular, we have shown that the initial stage is significantly dominated by the $\{10\bar{1}2\}\langle\bar{1}011\rangle$ system of tensile twins. Connection of twinning with differences in texture changes at the longitudinal and cross rolling of the alloy is discussed.

KEYWORDS: zirconium alloys, rolling, XRD, texture, twinning

Investigation of crystallographic texture of materials is one of the applied and fundamental problems of materials science. Based on the texture data, one can either calculate or predict a large number of tensor characteristics of products made of materials with low symmetry crystal lattices: coefficient of thermal expansion [1, 2], precipitate orientations [3], mechanical characteristics [4], as well as coefficients of thermal or electrical conductivity, and other characteristics. Products designed for use in nuclear reactors and made from materials with crystallographic anisotropy have a radiation growth, the rate of which also depends on their texture coefficients. This phenomenon is one of the main problems of reactor materials science [5-8].

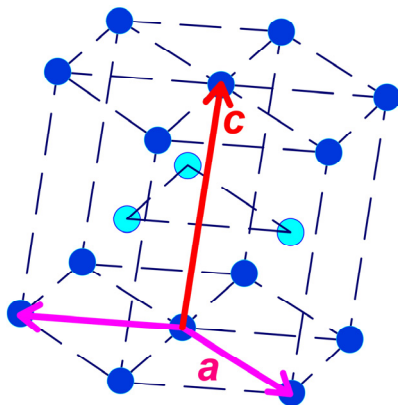


Fig. 1. Crystalline hcp cell and its axes

In contrast to the method of direct pole figures widely used in recent times for texture studies, its prototype – the X-ray method of inverse pole figures (IPFs) [9-11] – has retained its principal advantages of simplicity and accuracy of defining the texture characteristics of materials that have biaxial crystallographic anisotropy and show quantitative relationship with the above characteristics of products. This applies to tubes made of zirconium alloys used in fuel assemblies of reactors on thermal neutrons.

The main characteristic for such analyses is the Kearns texture coefficient (f), introduced for investigation of zirconium alloys [1]. This is a numerical characteristic of directionality of hcp-lattice basal normals of grains in materials – their "c" axes (Fig. 1) – along a given certain direction of the product: $f_j = \langle \cos^2 \alpha_{ji} \rangle$, where α_{ji} are the angles between the "c" axes (from the i -th orientations plurality) and this direction (j). In cases of biaxial crystallographic anisotropy of the above characteristics, for example, for hcp metals, this can be expressed by the following formula [2]:

$$q_j = (q_c - q_a) f_j + q_a \quad (1)$$

where q_j can be one of these characteristics with respect to the j -th direction, and could be represented by its basic values (q_a, q_c). In particular, the radiation growth factor in a given direction of the product – the so-called texture coefficient of radiation growth – can be unambiguously determined by its texture coefficient:

$$G_j = 1 - 3f_j. \quad (2)$$

This coefficient is an important characteristic, which is used to control and predict the radiation resistance of products made of nuclear materials with hcp lattice.

In this work, changes in the texture and texture coefficient of cold-rolled plates of Zr-2.5%Nb alloy are studied. This material is used as a structural material of the central tubes of fuel assemblies and of the pressure tubes in the RBMK reactors. From a fundamental standpoint, the task is to study principles of texture changing of the material and the structural mechanisms accompanying it.

This study is associated with one of the elementary deformation schemes. It is expected that a set of such studies can help improve the texture prediction techniques, texture control criteria and related performance parameters, in particular, the radiation growth parameters of products made of hcp metals – zirconium alloy tubes used in nuclear reactor industry.

The task to precise the regularities obtained in [12], with especial experimental conditions of that, was also envisaged.

EXPERIMENTAL

Preparation of samples

For the research, the material of $\varnothing 15.0 \times 1.5$ mm² tube of Zr-2.5%Nb alloy (finish annealing at 580 °C, 3 hrs.) was used. Table 1 shows the chemical composition of the material.

Table.

Chemical composition of the Zr-2.5%Nb alloy

Elements	Zr	Nb	Fe	Hf	Cr	Sn	O	C	N	Si	H
wt. %	97.4	2.43	0.04	0.01	0.004	–	0.092	0.012	0.0036	0.0025	0.0017

For investigations, longitudinal fragments, obtained by cutting the tube by its by-diameter plane, and rings of the tube were used after their straightening up to the plate shape and subsequent annealing in $1.5 \cdot 10^{-3}$ Pa vacuum at 580 °C for 24 hours.

The investigated surfaces of the samples were pretreated by chemical etching using a reagent with a volumetric combination of water, nitric acid, and hydrofluoric acid in ratio of 9: 5:1.5. The surfaces of the plates were etched up to 65 μ m. This is the initial state of the plates. According to preliminary XRD measurements, it is this etching that eliminated the effects of near-surface non-uniformity of texture characteristics.

Further, the samples were deformed in a rolling mill DUO260 \times 200 at room temperature from 6 to 56% on the whole (5...7% per pass) without intermediate annealing. The rate of deformation was 5...10 s⁻¹. Plates made of rings were rolled in the circumferential direction of the tube.

In view of the revealed differences between the texture coefficient values, texture measurements were carried out on both sides of the plates, and due to it, the corresponding designations of the sides were adopted: “outer” and “inner”. For plates made of rings, changes in the texture coefficient were presented in the coordinates of the deformation of the pre-surface regions, taking into account the preliminary straightening of the tube fragments. The parameters of the tube section were used to calculate an additive correction to the degree of deformation of these areas, which in this case was added with the corresponding sign to the degree of deformation of the plate. This technique was considered permissible due to the identical geometry of the deformation of the pre-surface regions during both straightening and rolling. This guaranteed an absolute error of 0.5% for the aggregated deformation [12].

On the IPFs method

According to the principles of the texture method, the pole density P_{ji} for each i reflection is calculated from the set of integrated intensities I_{ji} of X-ray reflections obtained by ordinary measurement in a given direction (j) [11]:

$$P_{ji} = \frac{1}{R_j} \frac{I_{ji}}{I_{0i}} \quad \left(R_j = \sum_i A_i \frac{I_{ji}}{I_{0i}} \right) \quad (3)$$

where I_{0i} are the reflection intensities for the material in isotropic (non-textured) state; A_i are the statistical weights of the i -th reflection [11] ($\sum A_i = \sum A_i P_{ji} = 1$).

To improve accuracy of the method, precise A_i and I_{0i} values were determined. The A_i values were mathematically calculated using the principle of construction of Wigner-Seitz cells [11] on the sphere of crystallographic orientations (hkl) of crystal reflections. The set of I_{0i} values for a given alloy was obtained by synthesis of the calculated and experimental data. The latter were obtained on the basis of a series of studies on texture destruction of the given alloy by microwave heat treatment [13].

The set of P_{ji} values obtained for the selected measurement directions was used to plot IPFs and to determine the texture coefficient for the selected measuring direction (j), using the statistical summation technique [11]:

$$f_j = \langle \cos^2 \alpha_i \rangle_j = \sum_i A_i P_{ji} \cos^2 \alpha_i \tag{4}$$

According to the results of testing of this method with the adjusted set of initial characteristics, the random error in determining the texture coefficients for the material is about ± 0.003 .

We assume a possibility in principle to analyze the structural mechanisms leading to changes in the texture coefficient of the material and in “c”-axes distributions.

Texture measurements were carried out on the DRON4-07 X-ray diffractometer using the radiation $\text{CuK}\alpha$. To reduce the vertical divergence of X-ray beam in this scheme, the pair of the Soller slits was used.

RESULTS

Figure 2 shows the IPFs plotted according to the results of texture measurements on the original Zr-2.5%Nb tube along its radial, axial, and tangential directions. In the coordinates of longitudinal plate rolling, it corresponds to the normal direction (ND), the rolling direction (RD) and the transverse direction (TD), respectively. The density values of the basal (0002) and prismatic poles ($hki0$) are marked here and below, and a tone scale of P_{ji} values is given.

As Figure 2 shows, the initial tube texture has a basic similarity with the ordinary texture of the plates after rolling in the same direction. We mean a fan-like distribution of the basal normals of the hcp lattice (the “c” axes) in the cross-section plane. For the original sample, data of an X-ray scanning in the neighborhood of the ND have confirmed this, and have shown that, in the coordinates of axial section of the tube, the angular distribution of “c” axes is localized within $\pm 25^\circ$ around ND. Thus, for plates made from longitudinal fragments of the tube and from its rings, the subsequent deformation can be defined, respectively, as longitudinal and transverse rolling.

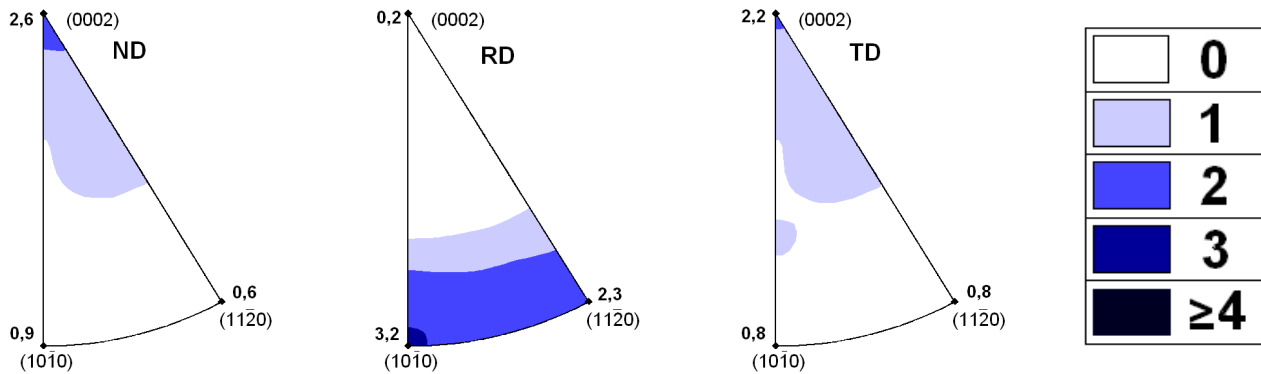


Fig. 2. IPFs of the tube in its three directions, given to the coordinates of longitudinal rolling plate [12]. The values of prismatic and basal pole densities are marked.

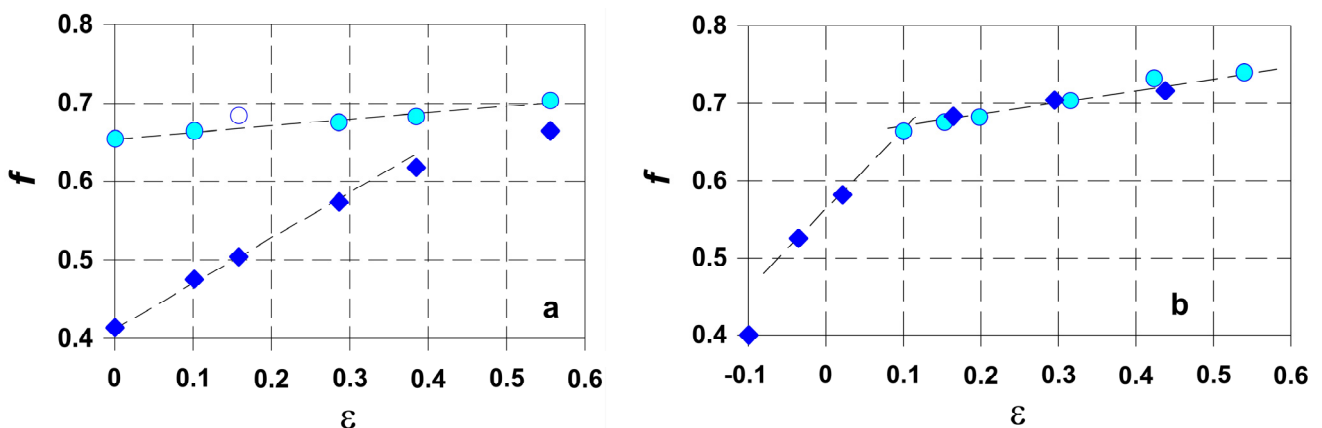


Fig. 3. Changes in the texture coefficient with the degree of plate deformation by longitudinal rolling (a) and of near-surface regions of the cross-rolled plates (b). Data from the plate sides which corresponding to the outer (♦) and inner (○) surface of the tube.

According to the metallographic examination, in the original samples (ann. 580 °C, 24 hrs.), the 20 μm grains were observed. Numerous 0.5 μm β -Nb phase precipitates aligned along the rolling direction were also observed. According to the diffractometer data, the sizes of the mosaic blocks in the material are 150 nm and above, and the strains are $0.7 \cdot 10^{-3}$.

Figure 3a shows graphs of changes in the texture parameter on the “outer” and “inner” surfaces of the plates with the degree of deformation of the plates by longitudinal rolling. Figure 3b presents similar data for the cross rolling of the plates, characterized in that the abscissa axis, according to the above, shows the actual degree of deformation of the

near-surface regions of the plates associated with their preliminary straightening and obtained by addition the corrections to degree of deformation of plate.

DISCUSSION

Features of X-ray measurements of samples are associated with the thickness of the analyzed near-surface layer. For X-ray measurement of zirconium and its alloys in CuK_α radiation, the thickness of such a layer is several microns. The effect of pre-straightening of the tube fragments, as it was meant, leads to differences in X-ray texture data on the different sides of the plates, due to their deformations of different signs. In this case, annealing of the alloy in the single-phase region (below 600 °C), as is known, does not change its texture in terms of “c”-axes distribution. Thus, in the prehistory of the samples, an effect of preliminary deformation of the surfaces remains, equivalent for the cross rolling of the plates in the tube coordinates.

In this regard, the main differences in the data on changes in the texture coefficient for the two differing deformation schemes is that the total effect of the deformation of the surface regions of different sides of the plates can be brought together only for cross rolling. This is shown in Figure 3b and can be regarded as a result of the deformation of continuum of the material. For Figure 3a, data cannot be unambiguously merged, and each of its graphs should be considered separately.

Despite such difficulties, the material of tubes made from zirconium-niobium alloys remains an exceptional subject for textural studies, since it differs from plates, with their usual prehistory, by a more moderate initial texture, – since, according to the analysis of subsequent data, under normal conditions for plate treatment, this alloy will lose the exceptionality after rolling by 60% or more.

Graphical regularities

Despite the above remarks, the moderate character of the initial texture on the “outer” sides of the plates leads to existence of the initial stage, which is characterized by significant changes in the texture coefficient with a degree of deformation (Fig. 3a,b). The texture coefficient is meant is calculated for the direction of the normal to the rolling plane. The subsequent (second) stages (round icons on the graphs) begin at $f \approx 0.65 \dots 0.68$ and are characterized by small linear changes.

It should be noted that for cross rolling of the alloy plates, the boundaries between the stages in these studies (Fig. 3b) and in [12] coincide. At the same time, the second stage in this figure is lower than the previous results by about 0.07. Some differences also occur at the initial stage. In general, such differences are associated with the specifics of the experimental conditions in previous work.

Taking into account the qualitative results of the work [12] and data from other preliminary studies gives grounds to assume that the initial stages of changes in the texture coefficient with the deformation of the plates (Fig. 3) are also mostly linear. Such signs are also shown by the initial stage in Figure 3b. However, with the first acts of deformation (< 5...10%) deviations from linearity may exist. For example, the data of similar studies on hafnium can be regarded in such aspect (deformation up to 5%; [14]). Such deviation was also noticed by us on this alloy after SHF (microwave) quenching and the subsequent initial rolling act by 7%. We associate this effect with the details of the prehistory of the samples. In particular, the last example could be reasonably interpreted as a manifestation of the effect of stress relaxation [12]. Such examples are probably in Figure 3b.

If so, then the rate of change of the texture coefficient with the degree of cross rolling of the plates on the initial stage (Fig. 3b) is significantly lower than in the previous results. In this case, according to the analysis of the results (Fig. 3a,b), the rates of all changes at cross rolling should be about two times higher than at longitudinal rolling.

On mechanisms of texture changes

To study the mechanisms of texture changes, an original technique was used to analyze the character of the correlation of the texture coefficient with the volume fraction of grains, whose “c” axes are oriented within $0 \dots 30^\circ$ with the rolling plane. This fraction of grains gives “prismatic” reflections $(10\bar{1}0)$, $(11\bar{2}0)$, $(21\bar{3}0)$, and other ones, which close to them by crystallographic orientation. On the basis of the obtained data, we determined their portion in the samples (c_p) using the following formula:

$$c_p = \sum_i A'_i P_i. \quad (5)$$

The values of A'_i (5) represent the portions of the space of reflecting orientations that completely or partially falls within the assigned angular limits: $0 \leq A'_i \leq A_i$. Figure 4 presents graphical comparing of the f and c_p values in the near-surface regions of the “outer” and “inner” sides of the plates for the longitudinal and cross rolling.

Despite the fact that the graphs in Figures 3a and 3b have qualitative and quantitative differences, the graphs of the comparison of the data in Figures 4a,b demonstrate a similarity. The figures show that at the initial stage of changes in the texture coefficient, its linear correlation is observed with the fraction of grains, whose “c” axes are deflected more

than 60° from the normal direction of the plates. At that, in the process of deformation, the texture of the plates is formed by orienting the axes along the normal direction, and this is done at angles of $60\text{--}90^\circ$. In this case, in view of the strong correlation, such acts occur abruptly, without intermediate positions.

It should be noted that the value of the derivative in the correlation graphs is approximately minus one. This fits into a simplified scheme of “*c*”-axes directing. According to this scheme, with the rotation of the axes from the rolling plane into the normal direction, the texture coefficient of the reoriented grain fraction varies from zero to one. Totally for the plate, it does by the numerical portion value of these grains. This is possible due to the exclusive activity of twinning with rotations through an angle of $\approx 90^\circ$.

In this regard, it is known that in hcp metals there are systems of compression and tensile twins [15, 16]. Among the last ones, the twins of the system $\{10\bar{1}2\}\langle\bar{1}011\rangle$, turning the “*c*” axes of grains by 85° , are considered as the most active mechanism of texture formation at deformation. It is also considered that these twins, as well as other twinning systems, play an essential role in deformation texture of zirconium and its alloys [16, 17].

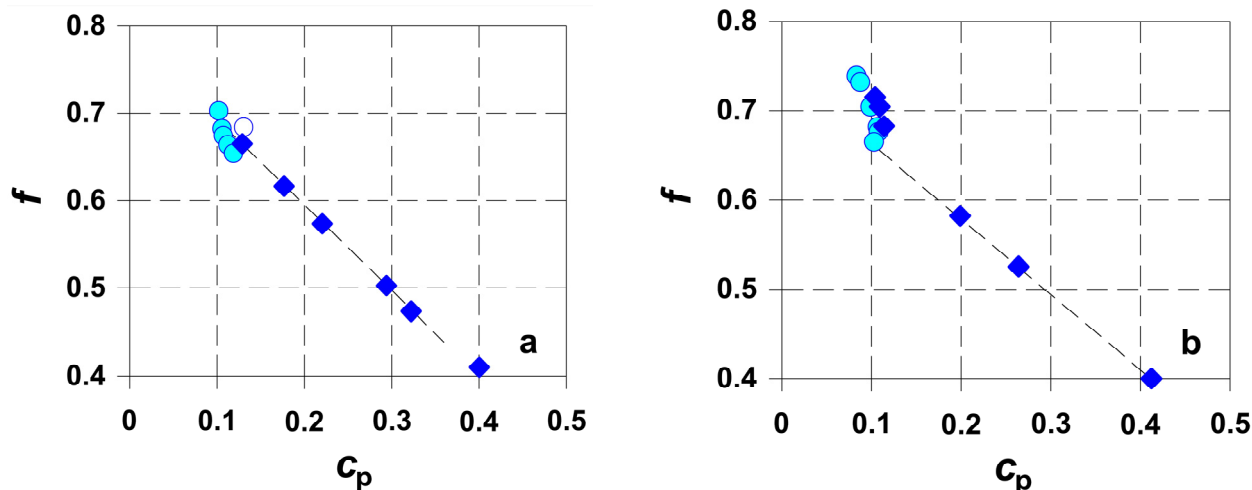


Fig. 4. Matching of the texture coefficient values (Fig. 3) with the numerical part of “*c*” axes orientations within $0\text{--}30^\circ$ from the rolling plane for longitudinal (a) and cross (b) rolling of the plates. Marking of points is the same.

The obtained results confirm this conclusion regarding metals of the titanium subgroup, including zirconium and its alloys. According to our results, the system $\{10\bar{1}2\}\langle\bar{1}011\rangle$ of tensile twins is the main factor for changes in the texture coefficient at the initial stage of deformation.

As noted, such an initial stage exists when the initial values of the texture coefficient (measured in ND) are below 0.65, especially if there is a fraction of orientations of the “*c*” axes in the neighborhood of directions lying in the rolling plane. The dominant activity of such a system was identified, in particular, in zirconium plates, however, under special conditions of deformation [18]. In the studies of this kind, should such initial stage be practically absent, a conclusion might differ [19].

According to preliminary estimates, the results obtained fit into simple geometric schemes of texture coefficient changes at the initial stage of longitudinal and cross rolling of this alloy. This aspect is discussed.

Effect of non-uniformity of deformation of the plates, what could arise along their thickness at rolling process, on their texture will also studied further.

CONCLUSIONS

Using the method of inverse pole figures (IPFs) with X-ray measurements as the basis, we have investigated the crystallographic texture of the Zr-2.5%Nb plates, which were made of straightened segments of the $\varnothing 15.0 \times 1.5$ mm² tube, annealed for 24 hours at 580°C and were cold-worked from 6 to 56% by longitudinal and cross rolling. Calculations of the Kearns texture coefficients for the direction perpendicular to the rolling plane of samples have been carried out. Effects of both near-surface and bulk non-uniformities were taken into account at preparation of the samples and at processing of the results.

The principal character of texture coefficient changes of the material with deformation in both schemes of rolling has been established. In both cases, this involves the existence of an initial stage of significant increase of texture coefficient up to ~ 0.7 , and the subsequent stage of minor changes. It is noted that changes in the texture coefficient at each stage are mainly linear. Rates of the changes have been estimated. Existence conditions for the initial stages are clarified.






The original method of studying the mechanisms of deformation of the alloy in a comparative analysis of changes in the texture coefficient of the material and in its distribution of crystallographic orientations was used. Correlations of the characteristics of the initial stage with the features of the distributions of the “*c*” axes of the hcp lattice in the alloy are established.

It is noted that more than 90% of quantitative changes of the texture coefficient in the initial stage of plate deformation is related to abrupt turns of crystalline fragments through wide angles to the normal direction involved with rolling. This confirms the fact that the texture formation by rolling of Zr-2.5%Nb plates is caused by a dominant role of twinning, especially, at the initial stage. An exclusive activity of the $\{10\bar{1}2\}\langle\bar{1}011\rangle$ system of tensile twins at the initial stage of growth of the texture coefficient has been revealed.

ACKNOWLEDGEMENTS

The authors are grateful to Dr. V.S. Krasnorutsky for promotion of the direction of the researches.

ORCID IDs

Viktor Grytsyna  <https://orcid.org/0000-0003-4341-007X>, Dmitry Malykhin  <https://orcid.org/0000-0003-0259-0211>, Tetiana Yurkova  <https://orcid.org/0000-0003-1264-640X>, Kostiantyn Kovtun  <https://orcid.org/0000-0002-0524-5053>, Gennadiy Kovtun  <https://orcid.org/0000-0003-4242-7697>.

REFERENCES

- [1]. Kearns, WAPD-TM-472, Westinghouse Electric Corporation, Pittsburg, Pa. USA (1965).
- [2]. P.A. Tempest, J. Nucl. Mater. **92**(2-3), 191-200 (1980), doi: 10.1016/0022-3115(80)90102-6.
- [3]. J.J. Kearns and C.R. Woods, J. Nucl. Mater. **20**(3), 241-261 (1966), doi: 10.1016/0022-3115(66)90036-5.
- [4]. V.M. Allen, M. Preuss, J.D. Robson and R.J. Comstock, Mater. Sci. Forum 495-497, 675-80 (2005), doi: 10.4028/www.scientific.net/MSF.495-497.675.
- [5]. J.J. Stobo and B. Pawelski, J. Nucl. Mater. **4**(1), 109 (1961), doi: 10.1016/0022-3115(61)90155-6.
- [6]. E.F. Sturcken and W.R. McDonell, J. Nucl. Mater. **7**(1), 85-91 (1962), doi: 10.1016/0022-3115(62)90196-4.
- [7]. R.A. Murgatroyd and A. Rogerson, J. Nucl. Mater. **79**(2), 302-311 (1979), doi: 10.1016/0022-3115(79)90095-3.
- [8]. A. Rogerson and R.A. Murgatroyd, J. Nucl. Mater. **80**(2), 253-259 (1979), doi: 10.1016/0022-3115(79)90188-0.
- [9]. G.B. Harris, Phil. Mag. **43**(336), 113-123 (1952), doi: 10.1080/14786440108520972.
- [10]. A. Guinier, *Théorie et Technique de la Radiocristallographie*, 2nd ed. (Paris, 1956) 736 p. (in French)
- [11]. P.R. Morris, J. Appl. Phys. **30**(4), 595-596 (1959), doi: 10.1063/1.1702413.
- [12]. V.M. Grytsyna, D.G. Malykhin, T.S. Yurkova, K.V. Kovtun, T.P. Chernyayeva, G.P. Kovtun and V.N. Voyevodin, Physics of Radiation Effect and Radiation Materials Science, **5**(117), 69-74 (2018).
- [13]. V.M. Grytsyna, A. Stukalov, T. Chernyayeva, V. Krasnorutskyy, D. Malykhin, V. Voyevodin, and V. Bryk, J. ASTM International, **2**(8), 1-22 (2005), doi: 10.1520/JAI12339.
- [14]. D. Malykhin, G.P. Kovtun and T.S. Potina, Problems of Atomic Science and Technology **1**, 35-40 (2016).
- [15]. E.A. Calnan and C.J.B. Clews, Phil. Mag. **42**(331), 919-931 (1951), doi: 10.1080/14786445108561320.
- [16]. E. Tenckhoff, J. ASTM International **2**(4), 1-26 (2005), doi: 10.1520/JAI12945.
- [17]. C.N. Tome, R.A. Lebensohn and U.F. Kocks, Acta Metall. Mater. **39**(11), 2667-2680 (1991), doi: 10.1016/0956-7151(91)90083-D.
- [18]. R.J. McCabe, G. Proust, E.K. Cerreta and A. Misra, International Journal of Plasticity, **25**(3), 454-472 (2009), doi: 10.1016/j.ijplas.2008.03.010.
- [19]. Bai-feng Luan, Qing Ye, Jian-wei Chen, Hong-bing Yu, Dong-li Zhou and Yun-chang Xin, Trans. Nonferr. Met. Soc. China **23**(10), 2890-2895 (2013), doi: 10.1016/S1003-6326(13)62811-3.

ЗАКОНОМІРНОСТІ ЗМІН ТЕКСТУРНОГО ПАРАМЕТРА КЕРНСА ПРИ ХОЛОДНІЙ ПРОКАТЦІ СПЛАВУ Zr-2.5%Nb

Грицина В.М., Малихін Д.Г., Юркова Т.С., Ковтун Г.П., Ковтун К.В.,

Корнєєва В.В., Слабоспицька О.А., Танцюра І.Г., Черняєва Т.П., Воєводін В.М.

*Національний Науковий Центр «Харківський фізико-технічний інститут»
61108, Харків, вул. Академічна, 1*

Проведено рентгеновські дослідження закономірностей змін характеристик кристалографічної текстури при холодній деформації пластин зі сплаву Zr-2,5% Nb шляхом поздовжньої і поперечної прокатки до 56% зі швидкістю приблизно $5 \dots 10 \text{ сек}^{-1}$. Вихідні пластини було виготовлено з поздовжніх фрагментів і кілець, вирізаних з труби $\varnothing 15,0 \times 1,5 \text{ мм}^2$, і потім відпалено при $580 \text{ }^\circ\text{C}$. Текстуру пластин досліджено за методом зворотних полюсних фігур з розрахунком текстурного параметра Кернса уздовж нормалі до площини пластин. Побудовано залежності текстурного параметру від ступеня деформації пластин. Виявлено розбіжність значень текстурного параметру, виміряного на різних сторонах пластин, що зв'язується з випрямленням вихідних заготовок труби і незмінністю розподілу кристалографічних осей «с» після наступного віддалу вихідних пластин. Шляхом введення поправок до ступенів деформації, розрахованих за параметрами перетину вихідної труби, такі розбіжності було усунуто для даних з поперечної прокатки матеріалу. В результаті для обох схем деформації виявлено дві стадії змін текстурного параметру з деформацією сплаву: початкову стадію зростання і подальшу стадію незначних змін. Обидві стадії мають, в основному, лінійний характер з граничним значенням текстурного параметру $0,65 \dots 0,68$. Для дослідження структурних механізмів змін текстури сплаву застосовано оригінальний прийом порівняльного аналізу змін текстурного параметру матеріалу та розподілу кристалографічних орієнтацій. Встановлено, що на початковій стадії змін текстурного параметру з деформацією за обома схемами повороти кристалографічних осей «с» матеріалу відбуваються стрибкоподібно на кути більш за 60° . Це підтверджує суттєву роль двійникування у текстурних змінах сплаву. Зокрема, нами показано, що на початковій стадії значно домінує система $\{10\bar{1}2\}\langle\bar{1}011\rangle$ двійників розтягування. Обговорюється зв'язок двійникування з особливостями текстурних змін при поздовжній і поперечній прокатці сплаву.

КЛЮЧОВІ СЛОВА: сплави цирконію, прокатка, рентгенографія, текстура, двійникування

**ЗАКОНОМЕРНОСТИ ИЗМЕНЕНИЙ ТЕКСТУРНОГО ПАРАМЕТРА КЕРНСА
ПРИ ХОЛОДНОЙ ПРОКАТКЕ СПЛАВА Zr-2.5%Nb**

**Грицина В.М., Малыхин Д.Г., Юркова Т.С., Ковтун Г.П., Ковтун К.В.,
Корнеева В.В., Слабоспицкая Е.А., Танцюра И.Г., Черняева Т.П., Воеводин В.Н.**
*Национальный Научный Центр «Харьковский физико-технический институт»
61108, Харьков, ул. Академическая, 1*

Проведены рентгеновские исследования закономерностей изменений характеристик кристаллографической текстуры при холодной деформации пластин из сплава Zr-2,5%Nb путём продольной и поперечной прокатки до 56% со скоростью примерно $5 \dots 10 \text{ сек}^{-1}$. Исходные пластины были изготовлены из продольных фрагментов и колец, вырезанных из трубы $\varnothing 15,0 \times 1,5 \text{ мм}^2$, и затем отожжены при $580 \text{ }^\circ\text{C}$. Текстура пластин исследована методом обратных полюсных фигур с расчётом текстурного параметра Кернса вдоль нормали к плоскости пластин. Построены зависимости текстурного параметра от степени деформации пластин. Выявлено расхождение значений текстурного параметра, измеренного на разных сторонах пластин, что связывается с выпрямлением исходных заготовок трубы и неизменностью распределения кристаллографических осей «с» после последующего отжига исходных пластин. Путём введения поправок к степени деформации, рассчитанных по параметрам сечения исходной трубы, такие расхождения были устранены для данных по поперечной прокатке материала. В результате для обеих схем деформации выявлено две стадии изменений текстурного параметра с деформацией сплава: начальную стадию роста и последующую стадию незначительных изменений. Обе стадии имеют, в основном, линейный характер с граничным значением текстурного параметра $0,65 \dots 0,68$. Для исследования структурных механизмов изменений текстуры сплава применён оригинальный приём сравнительного анализа изменений текстурного параметра материала и распределения кристаллографических ориентаций. Установлено, что на начальной стадии изменений текстурного параметра с деформацией по обеим схемам повороты кристаллографических осей «с» материала происходят скачкообразно на углы более 60° . Это подтверждает существенную роль двойникования в текстурных изменениях сплава. В частности, нами показано, что на начальной стадии значительно доминирует система $\{10\bar{1}2\}\langle\bar{1}011\rangle$ двойников растяжения. Обсуждается связь двойникования с различиями текстурных изменений при продольной и поперечной прокатке сплава.

КЛЮЧЕВЫЕ СЛОВА: сплавы циркония, прокатка, рентгенография, текстура, двойникование

PACS: 61.50.Ah, 64.10.+h

INVESTIGATION OF SILICON AND MANGANESE SOLUBILITY IN CEMENTITE OF IRON-BASED ALLOYS

 Natalia Filonenko^{1,2*},  Alexander Babachenko²,  Ganna Kononenko²

¹State Institution "Dnipropetrovsk Medical Academy of Health Ministry of Ukraine"
9, Vernadsky Str., Dnipro, 49044, Ukraine

²Z.I. Nekrasov Iron and Steel Institute of National Academy of Sciences of Ukraine
1, Ak. Starodubova K.F. sq., Dnipro, 49107, Ukraine

*E-mail: natph2016@gmail.com

Received March 11, 2019; revised March 26, 2019; accepted April 17, 2019

In the paper we obtained the expression of cementite free energy and determined the solubility of manganese and silicon in Fe₃C cementite depending on the temperature. Investigation was carried out for alloys with carbon content of 0.55-0.60 % (wt.), silicon content of 0.95-1.0 % (wt.), manganese content of 0.8-0.9% (wt.), the rest was iron. The smelting of Fe-Mn-Si-C system alloys was carried out in the alundum crucible furnace in argon atmosphere. The cooling rate of alloys after casting was 10 K/s. Microstructure analysis along with X-ray diffraction analysis was used to determine the structural state of the alloys. In addition, the physical characteristics of the alloys studied in this paper were determined, such as alloy chemical dependence of ultimate strength, extension and contraction ratio, impact toughness and hardness. The results obtained in this paper showed that the iron-based alloy with the content of carbon of 0.57 % (wt.), silicon of 0.97 % (wt.) and manganese of 0.85 % (wt.) had the superior microstructure and physical properties. The microstructure of alloys studied in the paper is represented by pearlite, which makes up to 95 % of the volume. In the alloys we revealed the highly dispersed inclusions of Fe_{2.7}Mn_{0.3}C, Fe_{0.25}Mn_{1.4}C_{0.6} and Fe₉SiC_{0.4} carbides, whose volume ratio was up to 1.5 %, the rest was ferrite. As it is known, the structural constituent of pearlite is cementite. The cementite has a significant effect on the physical properties of alloys. Application of quasi-chemical method enables to calculate the free energy of silicon and manganese doped with cementite and to determine the temperature dependence of silicon and manganese content in cementite. It is ascertained that there is a slight increase of carbon content in cementite (up to 28.79 % (atoms)). Manganese can replace up to 12 % of iron atoms, and silicon can replace up to 4.5 % of iron atoms, depending on temperature. The calculated data obtained in this paper are in good agreement with those found experimentally by other authors.

KEYWORDS: Fe-Mn-Si-C alloys, cementite, free energy of cementite, solubility of manganese and silicon in cementite

The up-to-date working conditions of railway wheels require the development of new steels, whose chemical composition, along with the heat treatment, provide increased strength and hardness of metal for wheels with a view to increase their operational properties (wear resistance, resistance to the formation of shelled tread, maximum load on the axle). At the formation of the complex of mechanical properties of railway wheels an important role is played by the morphology and chemical composition of Fe₃C cementite, which is formed in steel during crystallization and thermal treatment of these products. The formation of Fe₃C cementite is known to occur in iron steels and alloys with carbon content of more than 0.01% (wt.) [1]. Cementite has a complex crystal lattice and contains 6.67% (wt.) of carbon. Doping of Fe₃C cementite by metal atoms affects the physical properties of steels and alloys. In the process of doping steels by manganese (regardless of its amount), by chromium (up to 2%), or by stronger carbide-forming elements (tungsten, molybdenum), they dissolve in cementite, partially replacing the atoms of iron in its crystalline lattice. Here, some doped cementite, for example (Fe, Cr)₃C or (Fe, Mn)₃C, is formed, which differs as to its physical properties from the ordinary non-doped cementite Fe₃C. Nickel and silicon are referred to graphite-forming elements that affect decomposition of Fe₃C carbide resulting in the release of free-state carbon, i.e. graphite [1].

The most promising for the railway wheels is doping of steel with such inexpensive basic chemical elements as manganese and silicon. At doping of this kind, the formation of phases (Fe₁₁Si)C₄ and (Fe₁₁Mn)C₄, Fe_{2.7}Mn_{0.3}C [2-4], as well as of cementite Fe₃C doped with manganese and silicon is possible.

The object of this work was to determine the phase composition of the iron-based alloys doped with manganese and silicon, as well as solubility of these elements in cementites depending on the temperature.

MATERIALS AND RESEARCH TECHNIQUES

The research was carried out on the samples of steels with content of carbon of 0.55-0.60% (wt.), silicon 0,95-1,0% (wt.), manganese 0,8-0,9% (wt.), the rest was iron. Melting of the experimental steels and manufacture of the railway wheels from them was carried out under industrial conditions at the enterprises of "INTERPIPE-Ukraine" Company. Fe-Mn-Si-C alloys were molten in the alundum crucible furnace in the argon atmosphere. The rate of cooling of castings was 10 K/s. The samples after moulding had a cylindrical shape and the following dimensions: diameter – 15 mm and height - 30 mm. To determine the chemical composition of the alloy the chemical and spectral analysis was used [5]. The phase composition of the alloys was determined using an optical microscope "Neofot-21". The main results of the X-ray micro-spectral analysis were obtained using an electron microscope JSM-6490 with scanner ASID-4D and a programmable energy-dispersive X-ray microanalyser "LinkSystems 860". The research of mechanical characteristics was performed on the device of SMC-2 model. The wear resistance tests were performed at the load of

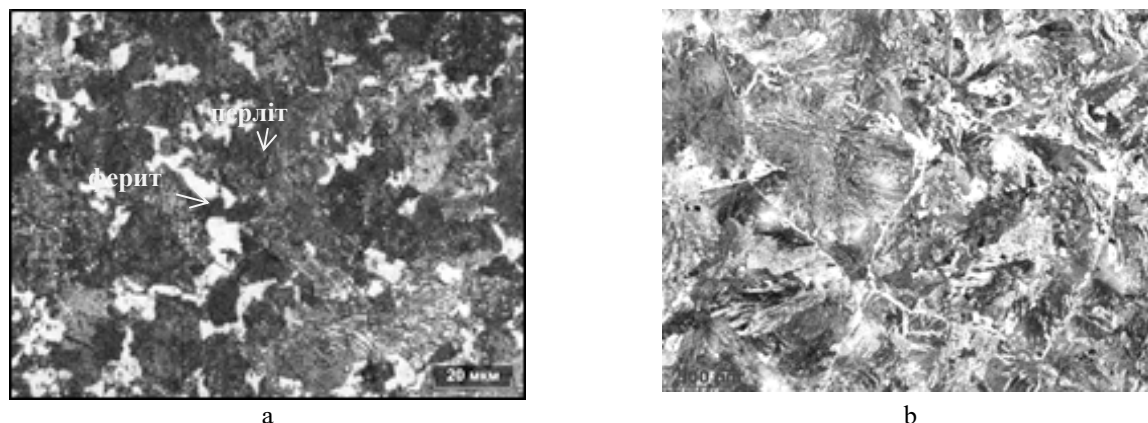


Fig. 2. The microstructure of the alloy containing: a) carbon – 0.58% (wt.), silicon – 0.40% (wt.) and manganese – 0.70% (wt.); b) carbon – 0.65% (wt.), silicon – 0.6% (wt.) and manganese – 0.75% (wt.), $\times 500$

Table 1.

Dependence of the strength limit, extension and contraction ratio, impact toughness and hardness on the chemical composition

Content of chemical elements in alloys, % (wt.)	The strength limit, σ_v , N/mm ²	Relative extension n , δ , %	Relative contraction ψ , %	Impact toughness, KCU _{obed} , J/cm ²	Hardness, HB
C=0.57; Si=0.97; Mn=0.85	1160	12.5	31	27	326
C=0.65; Si=0.6; Mn=0.75	≥ 1020	9	16	18	≥ 320
C=0.58; Si=0.40; Mn=0.7	960	8	14	20	≥ 255

The microstructure of alloys studied in this paper was represented by pearlite, whose bulk fraction was up to 95%. Cementite is the structural component of pearlite, which affects the alloys mechanical properties.

Cementite has a complex structure [4]. The authors of the work gave a definition of the cementite structure and pointed to the peculiarity of the structure of cementite, which consists in the fact that the atoms of iron and carbon form Z-shape chains [7].

Each elementary cell contains 12 iron atoms, 4 of which are located in the FeI (4c) position and 8 – in the FeII (8d) position. In the crystal lattice of carbide Fe₃C the carbon atoms are located in the middle of the prisms.

By the results presented in the paper the crystallographic program “CaRIne v.3.1” was utilized to form the carbide crystal structure.

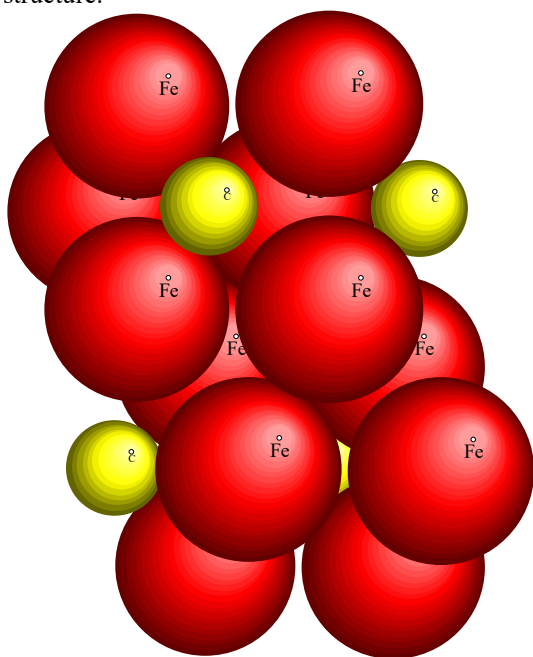


Fig. 3. The structure of Fe₃C carbide

According to the results of the crystal lattice formation the distance between the iron and carbon atoms in the trigonal prism is 1.906 Å, 2.041 Å, 2.064 Å and 2.11 Å, what corresponds to the results given in [3]. The distance between the nearest one to another carbon atoms is 3.12 Å.

To obtain the calculation results of the limit of carbon atoms solubility in the carbide lattice a quasi-chemical method was used [8]. The carbon atoms in the carbide can be conventionally located in two sublattices. The first sublattice (location) consists of carbon atoms containing six nearest iron atoms, two of which belong to the position of iron atoms FeII, and are located at the distance of 2.11 Å, and four – to the position FeI, two of them are located at the distance of 2.04 Å, and two – at the distance of 1.91 Å. The other sublattice consists of two closest carbon atoms, interacting with each other, which are located at the distance of 3.12 Å (Fig. 3).

The interaction of the Fe-C, M-C, and C-C atoms can be considered as follows: the interaction energy of the pairs of atoms: for the first sublattice for the iron atoms position FeII – v_{FeII-C} , v_{MII-C} , for

the position $FeI - v_{MI_1C}, v_{FeI_1C}$, and for two atoms of iron and manganese located at the distance of 1, 91 Å from the carbon atoms $- v_{MI_2C}, v_{FeI_2C}$. For two carbon atoms, located at the distance of 3.12 Å $- v_{CC}$. For the numerical values of the energy of interaction of the pairs of atoms the results given in [9] were used.

The free energy of carbide can be determined by the formula: $F = E - kT \ln W$, where E is the internal energy of Fe_3C phase, W is the thermodynamic probability of the atoms location in the sites of the carbide crystal lattice, $k = 1.38 \cdot 10^{-23}$, J/K is Boltzmann constant, T is absolute temperature.

Thus, the free energy of carbide is determined as follows:

$$\begin{aligned}
 F = & - \sum_{i=1}^2 (N_{FeII} N_{Ci} v_{FeIIC} + N_{MII} N_{Ci} v_{MIIC}) - \sum_{i=1}^2 (N_{FeI_i} N_{Ci} v_{FeI_iC} + N_{MI_i} N_{Ci} v_{MI_iC}) - \\
 & - \sum_{i=1}^2 (N_{FeI_2i} N_{Ci} v_{FeI_2C} + N_{MI_2i} N_{Ci} v_{MI_2C}) - \sum_{i=1}^2 N_{Ci} N_{Ci} v_{CC} - \\
 & - kT ((N_{FeII} + N_{MII}) \ln((N_{FeII} + N_{MII}) - 1) - N_{FeII} \ln(N_{FeII} - 1) - N_{MII} \ln(N_{MII} - 1) + \\
 & + (N_{FeI_1} + N_{MI_1}) \ln((N_{FeI_1} + N_{MI_1}) - 1) - N_{FeI_1} \ln(N_{FeI_1} - 1) - N_{MI_1} \ln(N_{MI_1} - 1) + \\
 & + (N_{FeI_2} + N_{MI_2}) \ln((N_{FeI_2} + N_{MI_2}) - 1) - N_{FeI_2} \ln(N_{FeI_2} - 1) - N_{MI_2} \ln(N_{MI_2} - 1) + \\
 & + (N - N_{Me}) \ln((N - N_{Me}) - 1) - N_C \ln(N_C - 1),
 \end{aligned} \tag{1}$$

where $N_{Me} = N_{FeII} + N_{MII} + N_{FeI_1} + N_{MI_1} + N_{FeI_2} + N_{MI_2}$, N_C is the number of carbon atoms, N is the total number of sites in the lattice, respectively.

To calculate the solubility of carbon in cementite the solution of the system of equations should be found:

$$\frac{\partial F}{\partial N_{FeII}} = 0, \quad \frac{\partial F}{\partial N_{MII}} = 0, \quad \frac{\partial F}{\partial N_{FeI_1}} = 0, \quad \frac{\partial F}{\partial N_{MI_1}} = 0, \quad \frac{\partial F}{\partial N_{FeI_2}} = 0, \quad \frac{\partial F}{\partial N_{MI_2}} = 0 \quad \text{та} \quad \frac{\partial F}{\partial N_C} = 0. \tag{2}$$

The resulting system of equations (2) is transcendental. Usually the solution of such equations can be obtained graphically or numerically. But in the framework of this problem it is expedient to consider an asymptotic solution of the equations. For this we present the logarithm included in each of the equations of the system (2) in the form of Taylor series (this is acceptable in case of its convergence):

$$\begin{aligned}
 \frac{\partial F}{\partial N_{FeII}} = & - \sum_{i=1}^2 N_{Ci} v_{FeIIC} - kT \left(\frac{(-1)^{n-1} (N_{FeII})^n}{n} + \sum_{n=1}^{\infty} \frac{(-1)^n (N_{FeII})^{n+1}}{(N_{MII})^{n+1} (n+1)} - \sum_{n=1}^{\infty} \frac{(-1)^{n-1} (N_{FeII} - 1)^n}{n} \right) = 0 \\
 \frac{\partial F}{\partial N_{MII}} = & - \sum_{i=1}^2 N_{Ci} v_{MIIC} - kT \left(\frac{(-1)^{n-1} (N_{MII})^n}{n} + \sum_{n=1}^{\infty} \frac{(-1)^n (N_{MII})^{n+1}}{N_{FeII}^{n+1} (n+1)} - \sum_{n=1}^{\infty} \frac{(-1)^{n-1} (N_{MII} - 1)^n}{n} \right) = 0 \\
 \frac{\partial F}{\partial N_{FeI_1}} = & - \sum_{i=1}^2 N_{Ci} v_{FeI_1C} - kT \left(\frac{(-1)^{n-1} (N_{FeI_1})^n}{n} + \sum_{n=1}^{\infty} \frac{(-1)^n (N_{FeI_1})^{n+1}}{(N_{MI_1})^{n+1} (n+1)} - \sum_{n=1}^{\infty} \frac{(-1)^{n-1} (N_{FeI_1} - 1)^n}{n} \right) = 0 \\
 \frac{\partial F}{\partial N_{MI_1}} = & - \sum_{i=1}^2 N_{Ci} v_{MI_1C} - kT \left(\frac{(-1)^{n-1} (N_{MI_1})^n}{n} + \sum_{n=1}^{\infty} \frac{(-1)^n (N_{MI_1})^{n+1}}{N_{FeI_1}^{n+1} (n+1)} - \sum_{n=1}^{\infty} \frac{(-1)^{n-1} (N_{MI_1} - 1)^n}{n} \right) = 0 \\
 \frac{\partial F}{\partial N_{FeI_2}} = & - \sum_{i=1}^2 N_{Ci} v_{FeI_2C} - kT \left(\frac{(-1)^{n-1} (N_{FeI_2})^n}{n} + \sum_{n=1}^{\infty} \frac{(-1)^n (N_{FeI_2})^{n+1}}{(N_{MI_2})^{n+1} (n+1)} - \sum_{n=1}^{\infty} \frac{(-1)^{n-1} (N_{FeI_2} - 1)^n}{n} \right) = 0 \\
 \frac{\partial F}{\partial N_{MI_2}} = & - \sum_{i=1}^2 N_{Ci} v_{MI_2C} - kT \left(\frac{(-1)^{n-1} (N_{MI_2})^n}{n} + \sum_{n=1}^{\infty} \frac{(-1)^n N_{MI_2}^{n+1}}{N_{FeI_2}^{n+1} (n+1)} - \sum_{n=1}^{\infty} \frac{(-1)^{n-1} (N_{MI_2} - 1)^n}{n} \right) = 0 \\
 \frac{\partial F}{\partial N_C} = & - \sum_{i=1}^2 (N_{FeII} v_{FeIIC} + N_{MII} v_{MIIC}) - \sum_{i=1}^2 (N_{FeI_i} v_{FeI_iC} + N_{MI_i} v_{MI_iC}) - \\
 & - \sum_{i=1}^2 (N_{FeI_2i} v_{FeI_2C} + N_{MI_2i} v_{MI_2C}) - \sum_{i=1}^2 2N_{Ci} v_{CC} - kT \left(\sum_{n=1}^{\infty} \frac{(-1)^{n-1} (1 - N_C)^n}{n} \right) = 0
 \end{aligned} \tag{3}$$

To obtain an asymptotic estimate of system (3) solution it is sufficient to consider the first two terms of expansion in the logarithm expanding.

The results of the equations solution are shown in Fig. 3. With the growth of the temperature, the content of manganese and silicon in carbide Fe_3C increases (Fig. 3).

The analysis of the results allowed determining the solubility of carbon, manganese and silicon in Fe_3C carbide, i.e. it was found that there is a slight increase in carbon content in cementite (up to 28.79% (atoms)). Manganese can replace up to 12% of iron atoms, and silicon – up to 4.5% of iron atoms, subject to the temperature, what is in a good agreement with the experimental data.

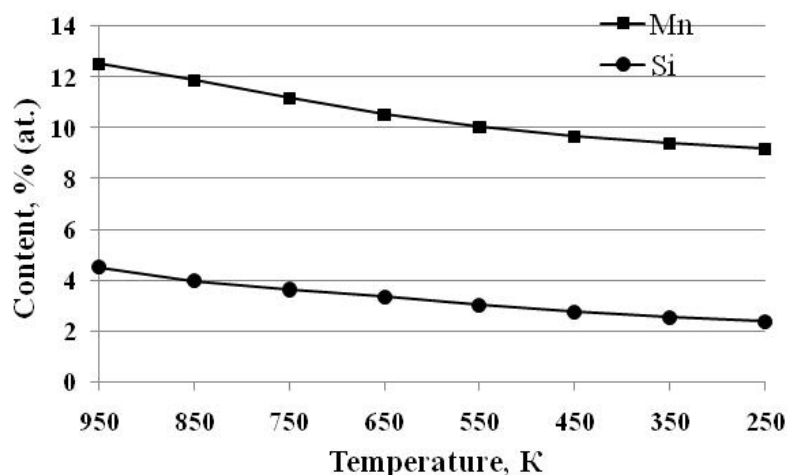


Fig. 3. Dependence of the content of manganese and silicon in Fe_3C carbide on the temperature

CONCLUSION

The research was carried out on the alloys containing carbon (0.55-0.60% (wt.), silicon (0.95-1.0% (wt.), manganese 0.8-0.9% (wt.)), the rest was iron. To determine the structural state of the alloys the microstructure and X-ray diffraction analyzes were performed. For the first time it was shown experimentally that the alloys of the Fe-Mn-Si-C system containing carbon (0.57% (wt.), silicon (0.97% (wt.)), manganese (0.85% (wt.)) have better mechanical characteristics, namely, higher numerical value of strength and hardness, as well as of plasticity and fracture toughness, as compared to the alloys with a different content of carbon, manganese and silicon. Thus, the results obtained in this paper show that to improve the mechanical properties of the wheels to be used in the railway transport, the alloys containing carbon (0.57% (wt.), silicon (0.97% (wt.)), manganese (0.85% (wt.)) can be used. The microstructure of this alloy contains up to 95% of the bulk fraction of pearlite, whose constituent is cementite. Therefore, to explain the good mechanical properties of the alloy the solubility limit of carbon, manganese and silicon in cementite Fe_3C was determined using the quasi-chemical method. For the first time the expression for free energy of Fe_3C cementite doped with manganese and silicon was obtained, and the limit of solubility of carbon, silicon and manganese in this phase was determined. It is ascertained that there is a slight increase in carbon content in cementite (up to 28.79% (atoms)), the manganese can replace up to 12% of iron atoms, and silicon – up to 4.5% of iron atoms, subject to the temperature.

The work was carried out within the framework of the project “Resurs” KC063.18 “Expansion of chemical composition and technology solutions for manufacture of railway wheels for different application and their maintainability” NAS in Ukraine.

ORCID IDs

Natalia Filonenko <https://orcid.org/0000-0003-1219-348X>, Alexander Babachenko <https://orcid.org/0000-0003-4710-0343>,
Ganna Kononenko <https://orcid.org/0000-0001-7446-4105>

REFERENCES

- [1] A.P. Huliacv, *Металловедение [Metalsscience]*, (Moscow, Metallurgiya, 1986), p. 538. (in Russian)
- [2] Jae Hoon Jang, In Gee Kim and H.K.D.H. Bhadeshia, *Materials Science Forum*, **638-642**, 3319-3324 (2010), <https://doi.org/10.4028/www.scientific.net/MSF.638-642.3319>
- [3] Bengt Hallstedt, Dejan Djurovic, Jörg von Appen, Richard Dronskowski, Alexey Dick, Fritz Körmann, Tilmann Hickel and Jörg Neugebauer, *CALPHAD: Computer Coupling of Phase Diagrams and Thermochemistry*. **34**(1), 129–133 (2010), <https://doi.org/10.1016/j.calphad.2010.01.004>.
- [4] I.G. Wood, L. Vočadlo, K.S. Knight, D.P. Dobson, W.G. Marshall, G.D. Price and J. Brodholt, *J. Appl. Cryst.* **37**, 82-90 (2004), <https://doi.org/10.1107/S0021889803024695>
- [5] S.V. Tverdokhlebova, *Visnyk Dnipropetrovskogo nacionalnogo universitetu. Serija Fizika. Radioelektronika*, **14**(12/1), 100-104 (2007).

- [6] O.V. Akymov and S.M. Nury, Eastern-European Journal of Enterprise Technologies, 6(11/78), 35-40 (2015).
 [7] Moshe Ron, Hanan Shechter and S. Niedzwiedz, Journal of Applied Physics. 39265-39285 (1968).
 [8] V.A. Kozheurov, *Статистическая термодинамика [Statistical thermodynamics]*, (Moscow, Metallurgiya, 1975), p 75. (in Russian).
 [9] O.Yu. Beryoza, N.Yu. Filonenko and O.S. Baskevich, Physics and Chemistry of Solid State. 13(3), 968-973 (2012).

ДОСЛІДЖЕННЯ РОЗЧИННОСТІ СИЛІЦІУ ТА МАНГАНУ В ЦЕМЕНТИТІ СПЛАВІВ НА ОСНОВІ ЗАЛІЗА

Н.Ю. Філоненко^{1,2}, О.І. Бабаченко², Г.А. Кононенко²

¹ДЗ «Дніпропетровська державна медична академія МОЗ України»
49044, Україна, м. Дніпро, вул. Володимира Вернадського, 9

²Інститут чорної металургії ім. З. І. Некрасова НАН України (ІЧМ НАНУ)
49107, Україна, м. Дніпро, пл. Ак. Стародубова К.Ф., 1

У роботі отримано вираз для вільної енергії цементиту та визначена розчинність мангану та силіцію в цементиті Fe₃C в залежності від температури. Дослідження проводили на сплавах з вмістом карбону 0,55-0,60 % (мас.), силіцію 0,95-1,0 % (мас.), мангану 0,8-0,9% (мас.), решта – залізо. Виплавку сплавів системи Fe-Mn-Si-C проводили в печі в алундових тиглях в атмосфері аргону. Швидкість охолодження виливки складала 10 К/с. Для визначення структурного стану сплавів використовували мікроструктурний та рентгеноструктурний аналізи. Окрім цього, в роботі були визначені механічні характеристики сплавів, що досліджували в даній роботі, а саме, залежність границі міцності, відносного видовження, відносного звуження, ударної в'язкості та твердості від хімічного складу сплаву. Отримані в даній роботі результати показали, що найкращі мікроструктурні та механічні характеристики має сплав на основі заліза з вмістом карбону 0,57 % (мас.), силіцію 0,97 % (мас.), мангану 0,85 % (мас.). Основною структурною складовою всіх сплавів, які досліджували є перліт (до 95 % об'ємної частки). У сплавах були виявлені дрібнодисперсні включення карбідів Fe_{2,7}Mn_{0,3}C та Fe_{0,25}Mn_{1,4}C_{0,6} та Fe₉SiC_{0,4}, об'ємна частка яких складала до 1,5 %, інше – ферит. Цементит має великий вплив на фізико-механічні характеристики сплавів. За допомогою квазіхімічного методу була визначена вільна енергія цементиту, легovanого манганом та силіцієм, а також була отримана залежність граничного вмісту кремнію і марганцю в цементиті в залежності від температури. Встановлено, що має місце підвищений вміст карбону в цементиті (до 28,79% (ат.)). Манган може заміщати до 12% атомів заліза, а силіцій до 4,5% атомів заліза в залежності від температури. Отримані в роботі розрахункові дані добре узгоджуються з експериментальними даними інших авторів.

КЛЮЧОВІ СЛОВА: сплави системи Fe-Mn-Si-C, цементит, вільна енергія цементиту, розчинність мангану та силіцію в цементиті

ИССЛЕДОВАНИЕ РАСТВОРИМОСТИ КРЕМНИЯ И МАРГАНЦА В ЦЕМЕНТИТЕ СПЛАВОВ НА ОСНОВЕ ЖЕЛЕЗА

Н.Ю. Филоненко^{1,2}, А.И. Бабаченко, А.А. Кононенко²

¹ГУ «Днепропетровская государственная медицинская академия МОЗ Украины»
49044, Украина, г. Днепр, ул. Владимира Вернадского, 9

²Институт черной металлургии им. З. И. Некрасова НАН Украины (ИЧМ НАНУ)
49107, Украина, г. Днепр, ул. Ак. Стародубова К.Ф., 1

В работе получено уравнение свободной энергии цементита и определена растворимость марганца и кремния в цементите Fe₃C в зависимости от температуры. Исследования проводились на сплавах с содержанием углерода 0,55-0,60 % (мас.), кремния 0,95-1,0 % (мас.), марганца 0,8-0,9 % (мас.), остальное – железо. Виплавку сплавов системы Fe-Mn-Si-C проводили в печи в алундових тиглях в атмосфері аргону. Скорость охлаждения отливки составляла 10 К/с. Для определения структурного состояния сплавов использовали микроструктурный и рентгеноструктурный анализы. Кроме этого, в работе были определены механические характеристики сплавов, а именно, зависимость предела прочности, относительного удлинения, относительного сужения, ударной вязкости и твердости от химического состава. Полученные результаты показали, что оптимальную микроструктуру и более высокие механические свойства имеет сплав на основе железа с содержанием углерода 0,57 % (мас.), кремния 0,97 % (мас.), марганца 0,85 % (мас.). Основная структурная составляющая во всех исследованных сплавах – перлит (до 95 % об'ємної доли). В сплавах были обнаружены микродисперсные включения карбидов Fe_{2,7}Mn_{0,3}C та Fe_{0,25}Mn_{1,4}C_{0,6} та Fe₉SiC_{0,4}, объемная доля которых составила до 1,5 %, остальное – феррит. Как известно, структурной составляющей перлита является цементит. Цементит оказывает значительное влияние на физико-механические свойства сталей. С помощью квазихимического метода была определена свободная энергия цементита, легированного кремнием и марганцем, а также была получена зависимость предельного содержания кремния и марганца в цементите в зависимости от температуры. Установлено, что имеет место повышенное содержания углерода в цементите (до 28,79 % (ат.)). Марганец может замещать до 12 % атомов железа, а кремний – до 4,5 % атомов железа в зависимости от температуры. Полученные в работе расчетные данные хорошо согласуются с экспериментальными данными других авторов.

КЛЮЧЕВЫЕ СЛОВА: сплавы системы Fe-Mn-Si-C, цементит, свободная энергия цементита, растворимость марганца и кремния в цементите

PACS: 61.50.Ah, 64.10.-h

SOLUBILITY OF BORON AND CARBON IN FERRITE OF THE Fe-B-C SYSTEM ALLOYS

 **Natalia Filonenko**^{1,2}

¹State Institution "Dnipropetrovsk Medical Academy of Health Ministry of Ukraine"
9, Vernadsky Str., Dnipro, 49044, Ukraine

²Z.I. Nekrasov Iron and Steel Institute of National Academy of Sciences of Ukraine
1, Akademika Starodubova Square, Dnipro, 49107, Ukraine

E-mail: nafph2016@gmail.com

Received March 11, 2019; revised March 29, 2019; accepted April 12, 2019

Investigation was carried out for Fe-B-C alloys with carbon content of 0.0001–0.01 % (wt.) and boron content of 0.0001–0.01 % (wt.), the rest is iron. To determine the structural state of alloys we use the microstructure analysis, X-ray microanalysis and X-ray structure analysis. The level of microstrains, dislocation density and the coercive force of ferrite is determined, and it is shown that structure imperfection grows with boron content increase in the alloy. The obtained results enable to suggest that boron atoms in a solid solution of α -iron occupy substitutional-interstitial positions depending on boron content. In the paper it is shown experimentally, that at room temperature solubility limit of boron and carbon in the ferrite is 0.00012 % (wt.) and 0.006 % (wt.). When boron and carbon content increases further, the following phases are formed: Fe₂B, Fe₃(CB) and Fe₂₃(CB)₆. In this paper by means of quasi-chemical method we obtain for the first time temperature dependence of the free energy for α -iron solid solution, as well as solubility limit of carbon and boron. Maximum mass fraction of carbon may be up to 0.016 % (wt.), and maximum boron mass fraction – up to 0.00025 % (wt.). At room temperature the boron solubility limit in ferrite is 0.0001 % (wt.), and carbon one is 0.004 % (wt.). The calculated numerical values of the solubility of boron and carbon in ferrite of the Fe-B-C system alloys are less than that of the experimental results. This can be explained by the fact that boron atoms interact more actively with structure imperfections than carbon atoms. At high temperatures the solubility of carbon and boron in given phase increases.

KEYWORDS: ferrite, solubility of boron and carbon, Fe-B-C system alloys

It is known that boron has a low solubility in iron-based solid solutions [1-2], but authors suggest different values for boron solubility in α -iron solid solution of the Fe-B system. Thus, authors of work [1] indicate that boron solubility in solid solution of α -iron in the Fe-B system is 0.004 % (wt.) at 983 K, and 0.08 % (wt.) at 1179 K. The authors of [2] note that the maximum solubility of boron in ferrite is 0.002 % (wt.) at the temperature of 1184 K. The other solubility of boron is pointed out by the authors of Ref. [3]: from 0.0035 % (wt.) to 0.00000038 % (wt.) when the temperature decreases from 1179 K to 983 K. In [4] the boron solubility is 0.0003-0.0067% (wt). The authors of [5] report the numerical value of boron solubility is 0.0019 % (wt.) at the temperature of 773 K.

According to [2], the boron solubility in δ -iron is 0.15 % (wt.), and according to [3] - 0.16 % (wt).

It is known that maximum solubility of carbon in the Fe-C system in δ -iron is 0.1 % (wt.) at 1772 K, and in α -iron – 0.02 % at 973 K, and 0.01 % (wt.) at room temperature [6-7], whilst the authors of work [3] note the value 0.025 % (wt.) at the temperature of 996 K.

At the moment, there is no information in the literature on the solubility limits of boron and carbon in α -iron of the Fe-B-C alloys.

The objective of this paper is to determine the solubility limits of boron and carbon in ferrite of the Fe-B-C system alloys.

MATERIALS AND METHODS

Investigation was carried out for the specimens with carbon content of 0.0001–0.01 % (wt.) and boron content of 0.0001–0.01% (wt.), the rest is iron. The following components were used to obtain the Fe-B-C system alloys: carbonyl iron (with iron content of 99.95 % (wt.)), amorphous boron (with boron content of 97.50 % (wt.)), graphite (with carbon content of 99.96 % (wt.)). Smelting of specimens was performed in a Taman furnace with in alundum crucibles in argon atmosphere. The cooling rate of alloys was 10 K/s. To determine the chemical composition of alloys, chemical and spectral analysis was used [8]. Microhardness was measured by PMT-3 device.

The phase composition of alloys was determined by X-ray microanalysis by means of JSM-6490 microscope with ASID-4D scanning head and "Link Systems 860" software energy-dispersive X-ray microanalyser, as well as by means of optical microscope "Neophot-21". X-ray electron probe analysis was carried out using internal standards. The X-ray and X-ray diffraction analysis was performed with DRON-3 diffractometer in monochromated Fe-K α radiation.

RESULTS AND DISCUSSION

The study of boron and carbon content in the Fe-B-C system alloys shows that boron and carbon maximum content in α -iron solid solution at room temperature can take such numeric values: 0.000 12% (wt.) and 0.006 % (wt.). At this boron and carbon content there is no formation of boron- and carbon-bearing phases except for ferrite (Fig. 1).

With boron content increase in alloy there boride are formed on the boundaries of ferrite grains, and with carbon content increase in alloy the formation of pearlite on the boundaries of ferrite grains occurs (Fig. 2).

If the content of boron or carbon in the alloy is greater than 0.0012 wt. % (boron) 0.004 wt. % (carbon), then the Fe_2B , $\text{Fe}_3(\text{CB})$, $\text{Fe}_{23}(\text{CB})_6$ phases are formed in the alloy [9].

It is known that the lattice parameter of bcc iron at room temperature is 2.862 Å [6]. Under boron and carbon doping of alloys the change in the lattice parameter of ferrite is observed (Table 1).

The results shown in Table enable to qualitatively evaluate the structure imperfection of ferrite depending on content of boron and carbon in the alloy. As boron content increases in the alloy, the microstrain degree, the density of dislocations in ferrite and the coercive force grows.

An increase in the coercive force for alloys containing higher content of boron and carbon can be explained by change in the density of dislocations and decrease in the size of the crystallites. The results (Table 1) show unique correlation relationship between the characteristics of the H_c , on the one hand, and the microstrain degree and density of dislocations, on the other hand, in all the specimens examined.

In addition, the results represented in Table 1 show that doping of ferrite only with boron leads to increase in the size of crystallites L , the density of dislocations ρ , the microstrain degree and the coercive force H_c compared with carbon doping. The obtained results can be explained by the fact that boron atoms in α -iron solid solution occupy substitutional-interstitial positions depending on boron content, which is in line with the results of other authors [10-11].

The structure of ferrite represents as body-centered lattice and pertains to the space group $O_h^9 - \text{Im}3\text{m}$ with eight atoms in the first coordination shell [12]. For each atom of the bcc lattice there are six tetrahedral and three octahedral pores. Two of the six atoms surrounding the octahedral pore, are closest compared to others [13]. The arrangement of carbon atoms in the bcc lattice can be described as the arrangement of the atoms of carbon or boron in the octahedral pore, which have four nearest metal atoms at a distance of 2.02 Å and two at the distance of 1.43 Å, each metal atom has eight neighbors located at the distance of 2.48 Å from each other (Fig. 3).

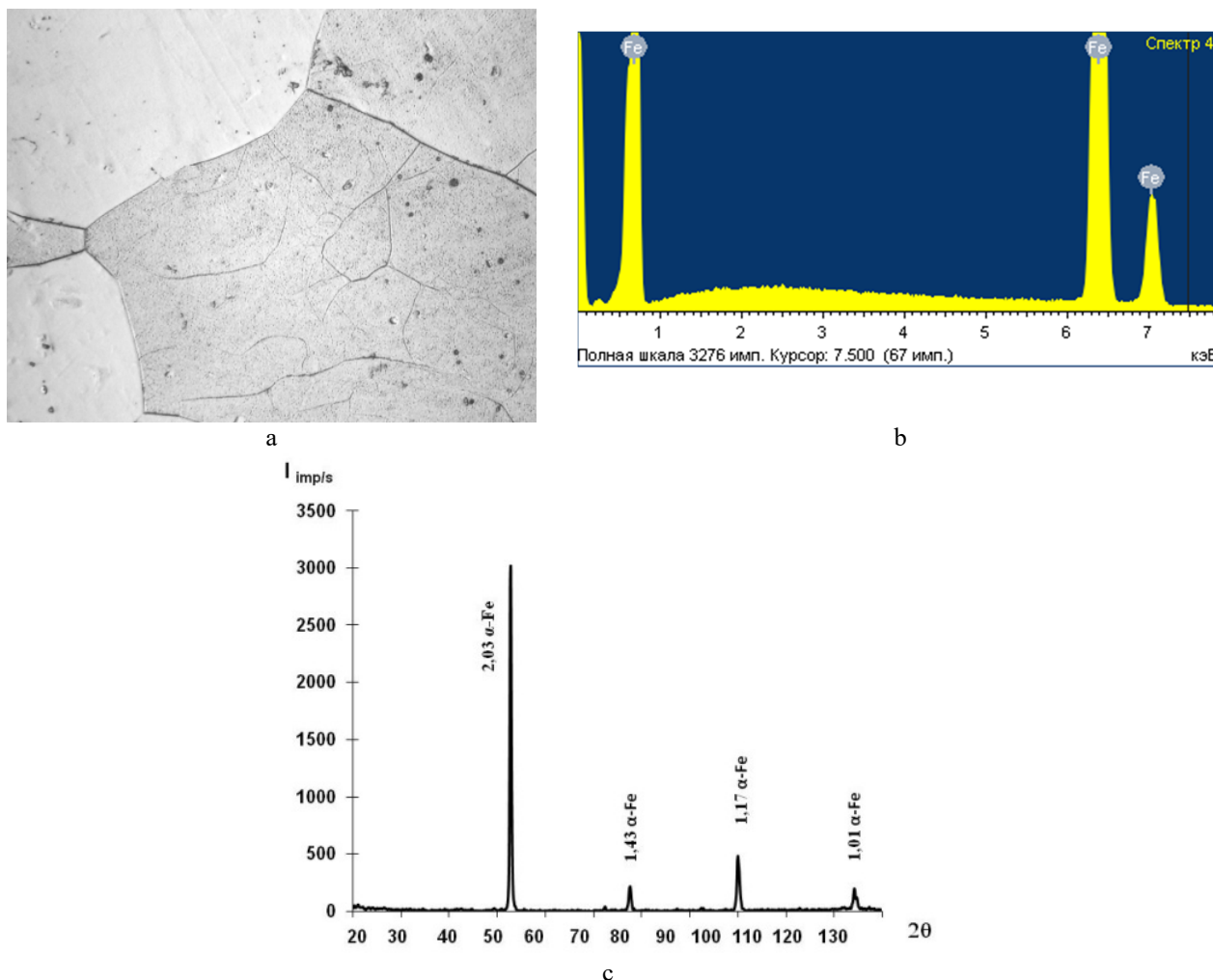


Fig. 1. Iron-based alloy with boron content of 0.0012 % (wt.) and carbon content of 0.004 % (wt.): a) microstructure, $\times 800$, b) microspectrum analysis curve, c) diffractogram

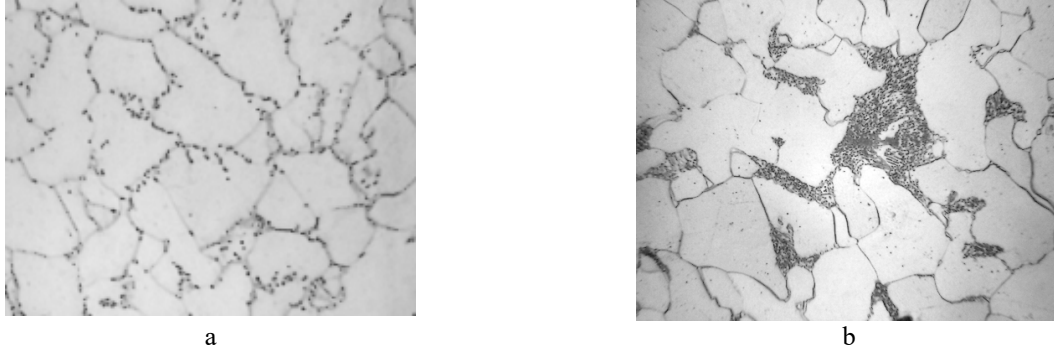


Fig. 2. Microstructure of alloys with: a) 0.005 % (wt.) boron and 0.004 % (wt.) carbon, b) 0.0012 % (wt.) boron and 0.04 % (wt.) carbon, $\times 500$

Table 1

Dependence of lattice parameter of ferrite a , crystallite size L , density of dislocations ρ , microstrain degree and coercive force H_c in ferrite on the boron and carbon content in alloy

Content, % (wt.)		a , Å	H_c , A/cm	L , Å	Microstrain degree of ferrite	ρ , cm^{-2}
Boron	Carbon					
0.0001	0.001	2.8614	4.6	1006	$4.84 \cdot 10^{-4}$	$6.91 \cdot 10^{10}$
0.0001	0.005	2.8610	5.8	1097	$4.98 \cdot 10^{-4}$	$7.52 \cdot 10^{10}$
0.001	0.001	2.8623	6.9	1114	$5.62 \cdot 10^{-4}$	$4.77 \cdot 10^{10}$
0.001	0.005	2.8629	7.54	1230	$5.23 \cdot 10^{-4}$	$9.82 \cdot 10^{10}$
0.005	0.001	2.8633	8.21	1098	$6.45 \cdot 10^{-3}$	$10.1 \cdot 10^{10}$
0.005	0.01	2.8642	8.97	1087	$7.62 \cdot 10^{-3}$	$10.48 \cdot 10^{10}$
0.0001	-	2.8650	4.2	1123	$2.5 \cdot 10^{-3}$	$7.2 \cdot 10^{10}$
-	0.001	2.8616	3.9	1056	$1.11 \cdot 10^{-3}$	$2.3 \cdot 10^{10}$

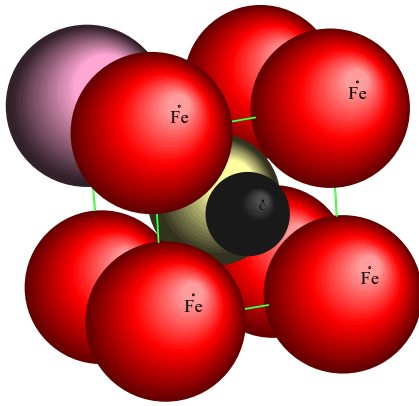


Fig. 3. Structure of ferrite

To calculate the solubility limit of carbon and boron atoms in the ferrite lattice, we use the quasi-chemical method with accounting for data on the boron and carbon position in α -iron solid solution [14].

The interaction of Fe-Fe, Fe-C, Fe-B and Fe-V atoms (where V is vacancy) can be taken into consideration as follows: the energy of interaction between eight atoms at the distance of 2.48 \AA is v_{FeFe} , v_{FeB_1} , v_{FeV} , between atoms at the distance of 2.02 \AA – v_{FeC} , v_{FeB_2} , v_{FeV_1} , and for two carbon or boron atoms located at the distance of 1.43 \AA – v'_{FeC} , v'_{FeV_1} and v'_{FeB_2} . For the values of the interaction energy of the atomic pairs, we use the results given in [9].

The free energy of ferrite can be determined by the formula

$F = E - kT \ln W$, where E is the internal, W is the thermodynamic probability of the atom location in the sites of the ferrite crystal lattice, $k = 1.38 \cdot 10^{-23} \text{ J/K}$ is Boltzmann constant, T is absolute temperature.

Thus, the free energy of ferrite is found as:

$$\begin{aligned}
 F = & - \sum_{i=1}^8 (N_{Fe} N_{B_1} v_{FeB_1} + N_{Fe} N_{Fe} v_{FeFe} + N_V N_{Fe} v_{FeV}) - \sum_{i=1}^4 (N_{Fe} N_C v_{FeC} + N_{Fe} N_{B_2} v_{FeB_2} + N_{Fe} N_{V_1} v_{FeV_1}) - \\
 & - \sum_{i=1}^2 (N_{Fe} N_C v'_{FeC} + N_{Fe} N_{B_2} v'_{FeB_2} + N_{Fe} N_{V_1} v'_{FeV_1}) - \\
 & - kT ((N_V + N_{Fe} + N_B) (\ln(N_V + N_{Fe} + N_B) - 1) - N_{Fe} (\ln N_{Fe} - 1) + N_V (\ln(N_V - 1) - \\
 & - N_{B_1} (\ln N_{B_1} - 1) + (N_{V_1} + N_C + N_{B_2}) (\ln(N_{V_1} + N_C + N_{B_2}) - 1) - N_C (\ln N_C - 1) - \\
 & - N_{B_2} (\ln N_{B_2} - 1) - N_{V_1} (\ln(N_{V_1} - 1))),
 \end{aligned}$$

where $N_B = N_{B_1} + N_{B_2}$ is the number of boron atoms.

To calculate the solubility of carbon and boron in ferrite, we should find the solution of set of equations:

$$\frac{\partial F}{\partial N_{Fe}} = 0, \frac{\partial F}{\partial N_C} = 0, \frac{\partial F}{\partial N_{B_2}} = 0, \frac{\partial F}{\partial N_{B_1}} = 0, \frac{\partial F}{\partial N_V} = 0 \text{ and } \frac{\partial F}{\partial N_{V_1}} = 0 \quad (1)$$

The obtained set of equations (1) is transcendental. Usually the solution of such equations can be obtained graphically or numerically. But within this problem there is a good reason to consider an asymptotic solution of the equations. For this we write the logarithm appeared in each equation of the system (1) as Taylor expansion (this is admissible in accordance with its convergence conditions):

$$\begin{aligned} \frac{\partial F}{\partial N_{Fe}} &= -\sum_{i=1}^8 N_B v_{FeB_1} + 2N_{Fe} v_{FeFe} - \sum_{i=1}^4 (N_C v_{FeC} + N_V v_{FeV}) - \\ &- \sum_{i=1}^2 (N_C v'_{FeC} + N_{V_1} v'_{FeV_1}) - kT \left(\frac{(-1)^{n-1} (N_{Fe})^n}{n} + \sum_{n=1}^{\infty} \frac{(-1)^n (N_{Fe})^{n+1}}{(N_V + N_B)^{n+1} (n+1)} + \sum_{n=1}^{\infty} \frac{(-1)^n (N_{Fe} - 1)^n}{n} \right) = 0; \\ \frac{\partial F}{\partial N_C} &= -\sum_{i=1}^4 (N_C v_{FeC}) - \sum_{i=1}^2 (N_C v'_{FeC}) - kT \left(\frac{(-1)^{n-1} (N_C)^n}{n} + \sum_{n=1}^{\infty} \frac{(-1)^n (N_C)^{n+1}}{(N_{V_1} + N_{B_2})^{n+1} (n+1)} + \right. \\ &+ \left. \sum_{n=1}^{\infty} \frac{(-1)^n (N_C - 1)^n}{n} \right) = 0 \quad (2) \\ \frac{\partial F}{\partial N_{B_1}} &= -\sum_{i=1}^8 (N_{Fe} v_{FeB_1}) - \sum_{i=1}^4 (N_{Fe} v_{FeB_2}) - \sum_{i=1}^2 (N_{Fe} v'_{FeB_2}) - kT \left(\sum_{n=1}^{\infty} \frac{(-1)^n (N_{B_1} - 1)^n}{n} \right) = 0; \\ \frac{\partial F}{\partial N_{B_2}} &= -\sum_{i=1}^4 (N_{B_2} v_{FeB_2}) - \sum_{i=1}^2 (N_{B_2} v'_{FeB_2}) - kT \left(\frac{(-1)^{n-1} (N_{B_2})^n}{n} + \sum_{n=1}^{\infty} \frac{(-1)^n (N_{B_2})^{n+1}}{(N_{V_1} + N_C)^{n+1} (n+1)} + \right. \\ &+ \left. \sum_{n=1}^{\infty} \frac{(-1)^n (N_{B_2} - 1)^n}{n} \right) = 0. \\ \frac{\partial F}{\partial N_V} &= -8N_{Fe} v_{FeV} - kT \left(\frac{(-1)^{n-1} (N_V)^n}{n} + \sum_{n=1}^{\infty} \frac{(-1)^n (N_V - 1)^{n+1}}{(N_{Fe} + N_B)^{n+1} (n+1)} + \sum_{n=1}^{\infty} \frac{(-1)^n (N_V - 1)^n}{n} \right) = 0 \\ \frac{\partial F}{\partial N_{V_1}} &= -4N_{Fe} v_{FeV_1} - 2N_{Fe} v'_{FeV_1} - kT \left(\frac{(-1)^{n-1} (N_{V_1})^n}{n} + \sum_{n=1}^{\infty} \frac{(-1)^n (N_{V_1} - 1)^{n+1}}{(N_C + N_{B_2})^{n+1} (n+1)} + \right. \\ &+ \left. \sum_{n=1}^{\infty} \frac{(-1)^n (N_{V_1} - 1)^n}{n} \right) = 0. \end{aligned}$$

To obtain an asymptotic estimate of the system (2) solution, it is quite sufficient to consider the first two terms of the logarithm expansion.

The results of solving of the set of equations are presented in Fig. 4.

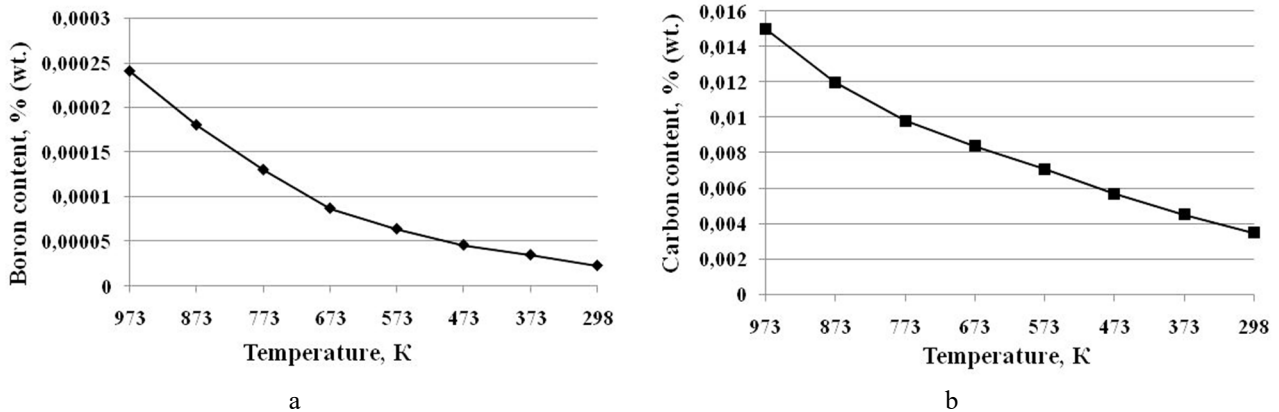


Fig. 4. Content of boron (a), carbon(b) in α -iron solid solution

The solubility of carbon in δ -iron is estimated to be 0.062 % (wt.) and boron solubility is 0.15 % (wt.). The analysis of the results enables to determine the solubility of carbon and boron in ferrite: it was revealed that up to 0.016 % (wt.) of carbon atoms can get into the pores in the ferrite lattice depending on temperature. According to the

calculations, the maximum content of boron in ferrite can be up to 0.00025 % (wt.). At room temperature the boron solubility in ferrite is 0.0001 % (wt.), and the carbon one is 0.004 % (wt.). The obtained results can be explained by the fact that boron doping of the iron-based alloys leads to displacement of the eutectoid point to the left in the state diagram of Fe-C and to the increase in the pearlite volume ratio, meaning, the carbon atom more likely to be located surrounded by iron atoms than by boron atoms [10-11]. Besides, boron atoms in the position of interstitial into the crystal lattice of α -iron have a greater binding energy with iron atoms than that with carbon atoms [10-11]. The effect of boron atoms in the position of interstitial in α -iron solid-solution on carbon atoms promotes the formation around the boron atoms of carbon-depleted zones [10-11]. The resulting values of the solubility of boron and carbon in ferrite of the Fe-B-C system alloys are less than those of other authors. This can be explained by the fact that boron is a horophilic element and interacting more actively with dislocations than carbon atoms [15]. Therefore, according to the results of experimental studies, the values of carbon and boron content is slightly higher.

CONCLUSION

It was shown that the solubility limit of boron and carbon in α -iron solid solution according to experimental data is 0.00012 % (wt.) and 0.006 % (wt.) at room temperature. As boron and carbon content grows, the formation of Fe_2B , $\text{Fe}_3(\text{CB})$, $\text{Fe}_{23}(\text{CB})_6$ phases occurs.

In the paper, using the quasi-chemical method, the temperature dependence of the free energy of α -iron solid solution is determined for the first time, as well as the solubility limit of carbon and boron in ferrite is calculated. The ferrite can contain up to 0.016 % (wt.) of carbon, and up to 0.00025 % (wt.) of boron, depending on the temperature. At high temperatures the solubility of carbon and boron in this phase increases.

The work was performed within the specific project “Resurs” KC063.18 “Development of chemical composition and technological decisions for the manufacture of railway wheels for different application and their maintainability” of the NAS of Ukraine.

ORCID IDs

Natalia Filonenko  <https://orcid.org/0000-0003-1219-348X>

REFERENCES

- [1]. N.P. Lyakishev, Yu.L. Pliner and S.I. Lappo, *Борсодержащие стали и сплавы [Boron-bearing steels and alloys]* (Metallurgiya, Moscow, 1986), p.191. (in Russian)
- [2]. A.E. Vol, *Строение и свойства металлических систем [Structure and properties of binary metal systems]*, (Fizmatgiz, Moscow, 1959), p. 856. (in Russian)
- [3]. O.A. Bannykh and M.E. Drytsa, *Диаграммы состояния двойных и многокомпонентных систем на основе железа [Phase Diagrams of Binary and multicomponent Systems based on of the iron: Handbook]*, (Metallurgiya, Moscow, 1986), p. 439.
- [4]. Yu.B. Kuzma and N.F. Chaban, *Двойные и тройные системы, содержащие бор: Справочник [Boron-bearing binary and ternary systems]*, (Metallurgiya, Moscow, 1990), p. 317. (in Russian)
- [5]. N.P. Lyakishev, *Диаграммы состояния двойных металлических систем: Справочник [Phase Diagrams of Binary Metal Systems: Handbook]*, (Mashinostroenie, Moscow, 2001), p. 498. (in Russian)
- [6]. A.P. Huliyev and A.A. Huliyev, *Металловедение [Metal science]* (Midalliance, 2011), p. 644 c. (in Russian)
- [7]. B.N. Arzamasov, V.Y. Makarova and H.H. Mukhynandets., *Металловедение [Metal science]* (Moscow, BMSTU, 2001), p. 648. (in Russian)
- [8]. S.V. Tverdokhlebova, *Visnik Dnipropetrovs'kogo universitetu. Seriâ Fizika, radioelektronika*, **14**(12/1) 100-104 (2007). (in Russian)
- [9]. O.Yu. Bereza, N.Yu. Filonenko and O.S. Baskevich, *Physics and Chemistry of Solid State*, **13**(3), 968-973 (2012).
- [10]. N.Yu. Filonenko and I.M. Spiridonova *Physics and Chemistry of Solid State*, **10**(3), 609-612 (2009).
- [11]. N.Yu. Filonenko, O.S. Baskevych and V.V. Soboliev *Journal Scientific Bulletin of National Mining University*, **4**, 74-78 (2012).
- [12]. M.P. Shaskolskaya, *Кристаллография [Crystallography]*, (Vysshaya Shkola, Moscow, 1984), p.376. (in Russian)
- [13]. Iu.S. Nechaev, *Advances in Physical Sciences*, **181**(5), 493-490 (2011).
- [14]. Z.A. Matysina and M.I. Milyan *Теория растворимости примеси в упорядоченных фазах [Solubility theory residual element in ordered phase]*. (DGU, Dnepro, 1991). p.180. (in Russian)
- [15]. V.H. Havrylova, Y.F. Tkachenko and A.V. Belostochnyi, *Reporter of the Priazovskyi State Technical University. Section: Technical sciences*, **18**, 90-95 (2008).

РОЗЧИННІСТЬ БОРУ ТА КАРБОНУ В ФЕРИТІ СПЛАВІВ СИСТЕМИ Fe-B-C

Н.Ю. Філоненко^{1,2}

¹ДЗ «Дніпропетровська державна медична академія МОЗ України»
49044, Україна, м. Дніпро, вул. Володимира Вернадського, 9

²Інститут чорної металургії ім. З.І. Некрасова НАН України (ІЧМ НАНУ)
49107, Україна, м. Дніпро, пл. Ак. Стародубова К.Ф., 1

Дослідження проводили на сплавах системи Fe-B-C з вмістом карбону 0,0001-0,01 % (мас.) і бору 0,0001-0,01 % (мас.), інше – залізо. Для визначення структурного стану сплавів використовували мікροструктурний, мікροрентгеноспектральний та рентгеноструктурний аналізи. Визначено рівень мікροнапружень, щільність дислокацій та коерцитивна сила фериту та показано, що зі збільшенням вмісту бору в сплаві дефектність структури зростає. Отримані результати дозволяють висунути

припущення, що атоми бору в твердому розчині α -заліза в залежності від вмісту бору займають позиції проникнення-заміщення. В даній роботі експериментально показано, що при кімнатній температурі межа розчинності бору та карбону в фериті складає 0,00012 % (мас.) та 0,006 % (мас.). При подальшому збільшенні вмісту бору та карбону відбувається утворення наступних фаз Fe_2B , $Fe_3(CB)$, $Fe_{23}(CB)_6$. В роботі вперше з застосуванням квазіхімічного методу отримано залежність вільної енергії твердого розчину на основі α -заліза від температури та визначено межу розчинності карбону та бору. Максимальна масова частка карбону може складати до 0,016 % (мас.), а бору до 0,00025 % (мас.). При кімнатній температурі межа розчинності бору в фериті складає 0,0001 % (мас.), а карбону 0,004 % (мас.). Розраховані числові значення розчинності бору та карбону в фериті сплавів системи Fe-B-C мають менші числові значення ніж за експериментальними результатами. Це можна пояснити тим, що атоми бору більш активно взаємодіє з дефектами структури ніж атоми карбону. Зі збільшенням температури розчинність карбону та бору в даній фазі зростає.

КЛЮЧОВІ СЛОВА: ферит, розчинність бору та карбону, сплави системи Fe-B-C.

РАСТВОРИМОСТЬ БОРА И УГЛЕРОДА В ФЕРРИТЕ СПЛАВОВ СИСТЕМЫ Fe-B-C

Н.Ю. Филоненко^{1,2}

¹ГУ «Днепропетровская государственная медицинская академия МОЗ Украины»
49044, Украина, г. Днепр, ул. Владимира Вернадского, 9





²Институт черной металлургии им. З.И. Некрасова НАН Украины (ИЧМ НАНУ)
49107, Украина, г. Днепр, ул. Ак. Стародубова К.Ф., 1

Исследования проводились на сплавах системы Fe-B-C с содержанием углерода 0,0001-0,01% (мас.), бора 0,0001-0,01% (мас.), остальное – железо. Для определения структурного состояния сплавов использовали микроструктурный, микрорентгеноспектральный и рентгеноструктурный анализы. Определен уровень микронапряжений, плотности дислокаций и коэрцитивная сила феррита и показано, что с увеличением содержания бора в сплаве дефектность структуры увеличивается. Полученные результаты позволяют выдвинуть предположение, что атомы бора в твердом растворе α -железа в зависимости от содержания занимают позиции проникновения-замещения. В работе экспериментально показано, что при комнатной температуре предельное содержание бора и углерода в твердом растворе феррита составляет 0,00012 % (мас.) и 0,006 % (мас.). При дальнейшем повышении содержания бора и углерода образуются следующие фазы: Fe_2B , $Fe_3(CB)$, $Fe_{23}(CB)_6$. В работе впервые с применением квазихимического метода получили зависимость свободной энергии твердого раствора на основе α -железа от температуры и определили предел растворимости углерода и бора. Максимальное массовое содержание углерода при комнатной температуре может составлять до 0,016 % (мас.), а бор до 0,00025 % (мас.). При комнатной температуре предел растворимости бора в феррите составляет 0,0001 % (мас.), а углерода 0,004 % (мас.). Рассчитанные значения растворимости бора и углерода в феррите сплавов системы Fe-B-C имеют меньшее числовое значение, чем по результатам эксперимента. Это можно объяснить тем, что атомы бора более активно взаимодействуют с дефектами структуры, чем атомы углерода. С повышением температуры растворимость углерода и бора в данной фазе увеличивается.

КЛЮЧЕВЫЕ СЛОВА: феррит, растворимость бора и углерода, сплавы системы Fe-B-C

PACS: 02.70.Uu, 07.05.Tp, 14.20.Dh

GEANT4 MODELING OF ENERGY SPECTRUM OF FAST NEUTRONS SOURCE FOR THE DEVELOPMENT OF RESEARCH TECHNIQUE OF HEAVY SCINTILLATORS

 Viktoriia Lisovska¹,  Tetiana Malykhina^{1*},
 Valentina Shpagina²,  Ruslan Timchenko¹

¹Kharkiv V.N. Karazin National University
4, Svobody sq., 61022, Kharkiv, Ukraine

²National Science Center "Kharkiv Institute of Physics and Technology"
1, Akademichna str., 61108, Kharkiv, Ukraine

*E-mail: malykhina@karazin.ua

Received April 14, 2019; revised June 6, 2019; accepted June 19, 2019

The proposed work demonstrates the results of creating and investigating the mathematical model of the source of fast neutrons. Computer modeling of the energy spectrum of fast neutrons was carried out for ²³⁹PuBe neutron source. The model of the source of fast neutrons has been developed. Neutrons in this model have an energy spectrum from 100 keV to 11 MeV with 100 keV step. Simulation is performed by the Monte-Carlo method. The model carrier is a computer program developed in the C++ programming language in the Linux operating system environment, using the Geant4 toolkit. All necessary classes describing low-energy models were used for the simulation of the passage of neutrons through materials of detectors. Those take into account the elastic scattering, inelastic scattering, radiative capture and fission. We consider these processes because models of processes implemented in our software will be also used for other problems of neutrons transport, for example, for passing neutrons through various substances, and for conducting virtual laboratory works. The PhysicsList class of our program contains classes G4NeutronHPElastic, G4NeutronHPElasticData, G4NeutronHPInelastic, G4NeutronHPInelasticData, G4NeutronHPCapture, G4NeutronHPCaptureData, etc. based on the NeutronHP model for neutron interactions at low energy, as well as the neutron data library G4NDL4.5. Diagrams containing energy spectra of a source of fast neutrons modeled in two ways are presented in the paper. The analysis of the obtained energy spectra is carried out. Virtual nuclear physics experiments are carried out with the aim of testing the elaborated neutron-matter interaction model. The processes occurring in scintillator substances during the passage of fast neutrons through them, have been studied. 10⁹ neutrons were used as primary particles emitted isotropically, and we used our simulation results of ²³⁹PuBe neutron source to describe the initial energy spectrum. The created model of ²³⁹PuBe neutron source can be used for the investigation of scintillation detectors Bi₄Ge₃O₁₂, CdWO₄, Gd₂SiO₅ and others, as well as studying their characteristics. Processes in heavy oxide scintillators substance during the registration of fast neutrons can be studied using the developed model. It is shown that for registration of the flow of neutrons from ²³⁹PuBe neutron source, using Bi₄Ge₃O₁₂ or CdWO₄ scintillators is more preferable. Results of the virtual nuclear physical experiments satisfy the published experimental data.

KEY WORDS: ²³⁹PuBe neutrons source, scintillation detectors, fast neutrons registration

With the aim of environmental monitoring and control of radiation hazard facilities, the devices for neutrons detection are developed by leading research centers [1]. Various classic methods are applied for registration of neutrons depending on neutrons energy. If neutrons energies exceed 10 MeV, its registration is based on the usage of compound with carbon and the study of interactions of neutrons with carbon nuclei [2]. Registration of neutrons with energies from 100 keV to 10 MeV is performed by scattering them on hydrogen-containing substances, and consequent registration of recoil protons.

The possibilities of detection of fast neutrons flux by heavy inorganic scintillators are investigated by scientists of V.N. Karazin Kharkiv National University in collaboration with scientists from Kharkiv Institute of Scintillation Materials [1].

In developing of devices for radiation detection, the usage of mathematical modeling allows to conduct a model experiment, and investigate the characteristics of developed detectors. The laboratory detector's experiments are carried out in harmful and dangerous working conditions due to the ionizing radiation. Computer simulation allows us to evaluate some technical parameters of the device being developed. Therefore, computer simulation is an important stage of detectors developing.

FORMULATION OF THE PROBLEM

The possibility of practical usage of heavy inorganic scintillators for neutron detection is investigated in the work [1]. However, for practical use of detectors it is necessary to estimate contributions of various mechanisms and processes that occur in the matter of these scintillators. This task can be solved using mathematical modeling and analysing its results.

The laboratory experiments were carried out with ²³⁹PuBe neutron source; therefore an important phase of investigations is the development of mathematical model of the neutron radiation source. The goal of our work is computer simulation of the energy spectrum of ²³⁹PuBe neutron source that will be used in programs for simulation of the passage of fast neutrons through matter.

There are published articles [3, 4] where one can see the experimental energy spectra of $^{239}\text{PuBe}$ neutron sources. However, these data have the too wide energy step and therefore can cause significant systematic errors in virtual experiment, which use them without preliminary processing.

DEVELOPING OF THE MODEL FOR FAST NEUTRONS TRANSPORT

For study of the processes in components of the experimental facility used for fast neutrons detection, the mathematical modeling of fast neutrons passage through matter was carried out. The modeling was carried out using the Monte Carlo method.

The mathematical model is a computer program developed by our team for the simulation of passage of neutrons from $^{239}\text{PuBe}$ neutron source through various substances. The program developed in C++ language with using Geant4 toolkit [5]. Description of the model includes physical and chemical properties of the materials of various facility components, its location and relative position as well as neutron source parameters. The special module contains description of neutron source. For developing of neutron source model the neutron source energy spectra from articles [3, 4] were digitized. Spectra in these works have the form of a histogram with wide (data from [3]) and non-uniform (data from [4]) step of energy.

For the purpose of obtaining a uniform energy step, the data was interpolated by Lagrange polynomials [6] after digitizing. Lagrange polynomial interpolation is a convenient method for such problems. The interpolation was carried out consistently with quantity of nodes from 5 to 7. The fragmentation into smaller segments is necessary to avoid accumulation of errors in the process of interpolation [6]. The obtained data was used as input for G4PrimaryGenerator class [7], which is mandatory in each computer program based on Geant4 toolkit.

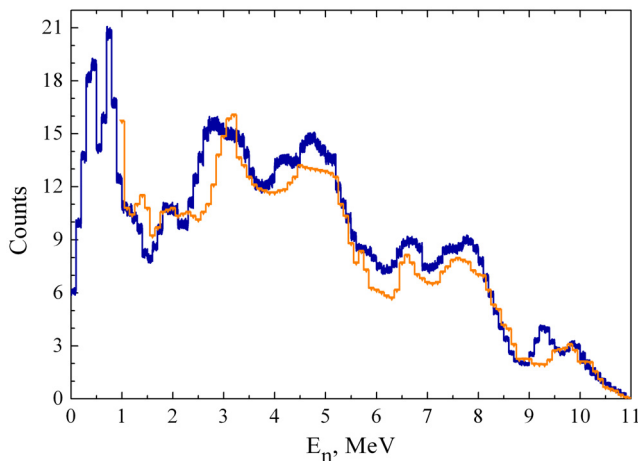


Fig. 1. The result of the G4PrimaryGenerator module: simulated neutron source spectra obtained from data [3] (light line in the chart) and [4] (dark line in the chart).

Figure 1 illustrates neutron source energy spectra modeled from two data sets [3, 4]. Energy spectra in Figure 1 were obtained as a result of the implementation of the G4PrimaryGenerator module as well as the G4GeneralParticleSource module, which uses two data sets [3, 4] as input data.

The G4GeneralParticleSource class [7] was applied for high-energy neutrons transport. This class allows specifying the spectral, spatial and angular distributions of primary neutrons. The flux of 10^7 primary neutrons was simulated with interpolated energy spectra in order to obtain a suitable statistics. Neutrons were radiated isotropically in this model experiment.

Energy spectra of primary neutrons (Fig. 1) are results of work of G4PrimaryGenerator module, and were written in steps of 100 keV for each sets of initial data, obtained as a result of interpolation [3, 4]. Thus, obtained data is given to a form convenient for further use by modules of our programs.

It should be noted that spectrum of primary neutrons based on data from work [4] is more preferable for further calculations because it contains energy data of primary neutrons in the energy range from 100 keV to 11 MeV. Unlike this energy spectrum, the spectrum based on [3] does not contain data from 100 to 1000 keV.

Our program has a user-friendly interactive mode. We have provided a number of keywords in the program, using which one can “turn on” or “turn off” some processes (previously specified in our program). For example, the command `/process/inactivate/inelastic` entered by the user in an interactive mode allows one “turns off” from consideration the processes of inelastic scattering.

BRIEF DESCRIPTION OF PHYSICAL PROCESS MODELS AND CLASSES FOR LOW ENERGY NEUTRON TRANSPORT USED IN OUR PROGRAM

The high-precision low energy neutron transport is implemented in corresponding classes of the Geant4 toolkit, namely, G4NeutronHPElastic, G4NeutronHPCapture, G4NeutronHPFission, G4NeutronHPInelastic. According to [7], the cross section data for low energy neutron transport are organized in a set of files that are read in by the corresponding data set classes. The classes accessing the total cross section of the individual processes, i.e., the cross section data for high-precision low energy neutron transport, are G4NeutronHPElasticData, G4NeutronHPCaptureData, G4NeutronHPFissionData, and G4NeutronHPInelasticData [8].

The NeutronHP package in Geant4 describes high-precision neutron interactions [8] and contains information about cross sections, angular distribution of the emitted particles, energy spectra of the emitted particles, number of

neutrons per fission, fission product yields etc., this data is placed in G4NDL4.5 files which represent Geant4 Nuclear Data Files. A detailed description of the models of these physical processes is given in [7, 8].

SERIES OF VIRTUAL EXPERIMENTS

In further model experiments, the opportunity of signal recording of $^{239}\text{PuBe}$ neutron source from distance 1000 mm was investigated. Initially, in real-life experiments the lead shielding was used for protection against gamma rays emitted from the $^{239}\text{PuBe}$ neutron source (besides neutrons). A center of this lead screen was situated at half distance to the detector, and had thickness 50 mm. The transverse size of lead shielding was 65 mm \times 65 mm.

Figure 2 schematically demonstrates the arrangement scheme of facility elements. The proportions of the detector are 20 mm \times 20 mm \times 20 mm.

The first series of the virtual experiment simulated the conditions in which these practical experiments were carried out. The main aim of this virtual experiment is studying how the initial spectrum changes after passage through the lead shielding. The resulting neutrons spectrum at the distance of 1000 mm from $^{239}\text{PuBe}$ neutron source, as well as the initial spectrum, are shown in Figure 3.

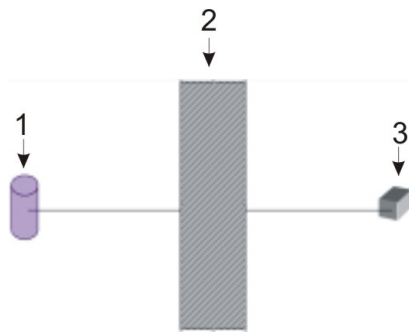


Fig.2. Arrangement scheme of facility elements in the first series of virtual experiments: 1 is neutron source; 2 is protective screen; 3 is detector

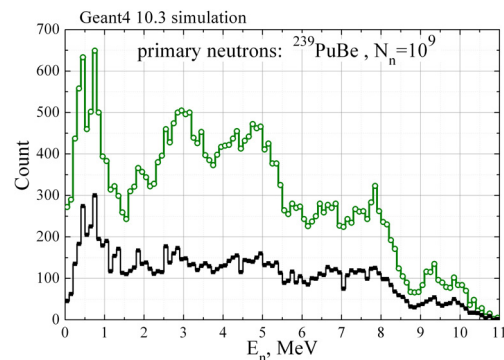


Fig. 3. Comparison of the initial neutrons spectrum (with using a protective Pb screen) and the result neutrons spectrum. Light line with empty circles is the initial spectrum; straight line is the result spectrum at the distance of 1000 mm from $^{239}\text{PuBe}$ neutron source

It can be seen (Fig. 3) that the general view of neutrons spectrum has been changed in energy range from 2 MeV to 5 MeV, however the quantity of neutrons before the detector (at the distance of 1000 mm from the source) significantly decreased. As a result of analysis of the virtual experiment for $N_n=10^9$ primary neutrons emitted from $^{239}\text{PuBe}$ neutron source, 31763 neutrons were observed before the detector without Pb shielding, and 11825 neutrons in case of using Pb shielding, this difference is explained by inelastic scattering.

The next series of virtual experiments was necessary for the development of a methodology for conducting real experiments, in which the number of neutrons detected at a distance of 1000 mm must be constant. Figure 4 schematically demonstrates the arrangement scheme of facility elements in the second series of virtual experiments. $^{239}\text{PuBe}$ neutron source is placed into a lead sphere. The radius of the sphere is 52 mm. The distance from the neutron source to the detector is 1000 mm.



Fig.4. Arrangement scheme of facility elements in the second series of virtual experiments: 1 is neutron source; 2 is a lead sphere; 3 is detector

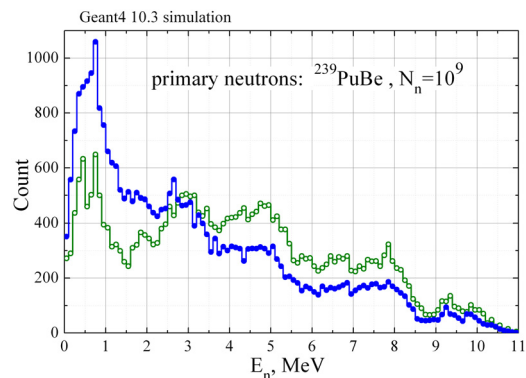


Fig. 5. Comparison of the initial neutrons spectrum ($^{239}\text{PuBe}$ source is into Pb sphere) and the result neutrons spectrum. Light line with empty circles is the initial spectrum; dark straight line is the result spectrum at the distance of 1000 mm from $^{239}\text{PuBe}$ neutron source

It can be seen (Fig. 5) that the general view of the result neutrons spectrum has been changed significantly in the energy range from 0.5 MeV to 5 MeV, especially in the energy range 0.5-2 MeV. As a result of analysis of the second

series of virtual experiments for $N_n=10^9$ primary neutrons emitted isotropically from $^{239}\text{PuBe}$ neutron source, 31763 neutrons were observed before the detector without the lead sphere, and 31694 neutrons in case of using the lead sphere surrounding the neutrons source.

ESTIMATION OF SECONDARY GAMMA QUANTA QUANTITY

The energy spectra of all secondary gamma quanta arising from the model experiment are shown in Fig. 6 (a).

Analyzing the simulation data, we found out that only negligible number of gamma quanta were registered by the LiI detector. It cannot affect the quality of detection of fast neutron flux. Figure 6 (b) illustrates the energy spectra of gamma quanta incoming in the detector.

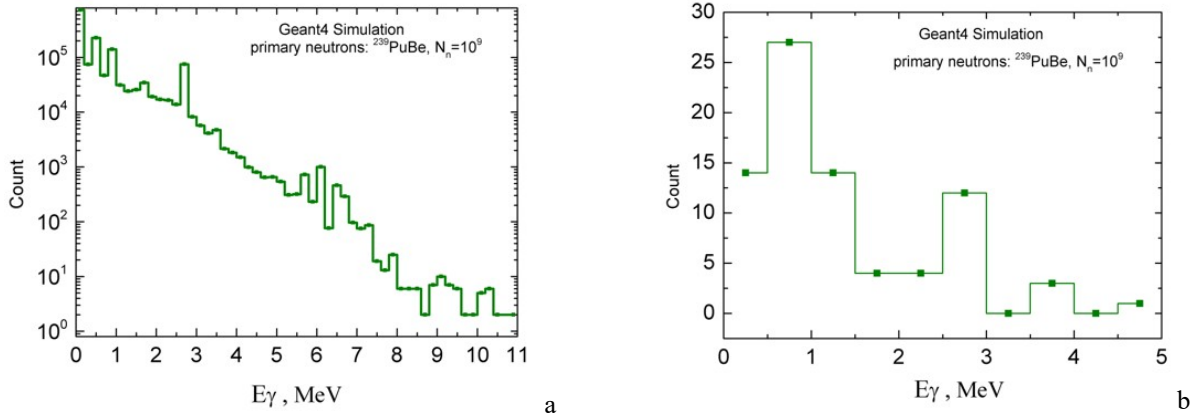


Fig. 6. Spectra of modeled secondary gamma quanta: (a) is spectrum for all gamma quanta; (b) is spectrum for incoming in detector gamma quanta

The total number of secondary gamma quanta produced in the process of model experiment is about 1.5×10^7 , while the number of gamma quanta registered by detector is 79.

The further laboratory tests confirmed the opportunity of applying heavy inorganic scintillators of small size for fast neutron flux registration from $^{239}\text{PuBe}$ neutron source.

COMPARISON OF RESULTS WITH PUBLISHED DATA

Experimental measurements and analysis of detection efficiency were carried out for fast neutrons from $^{239}\text{PuBe}$ neutron source using oxide scintillators: $\text{Bi}_4\text{Ge}_3\text{O}_{12}$, CdWO_4 , Gd_2SiO_5 as well as CsI(Tl) , NaI(Tl) , LiI(Eu) [9]. Fast neutrons registration efficiencies obtained experimentally [9] by heavy inorganic oxide scintillators ($Z > 50$) that have the same size, reach values from 42 to 48 percent and presented in Table 1. Results of measurements of the neutron fluxes registration efficiency by different scintillators in the equivalent energy range for electrons (gamma-quanta) of 20-300 keV [9] are presented in the right column of the Table 1.

Inelastic scattering reaction ($n, n'\gamma$) is a one of reliable mechanisms providing a high efficiency of fast neutron detection [7] by oxide scintillators. Figure 7 demonstrates modeled values of deposited energy in detectors.

Table 1.

Efficiency of fast neutron registration, % [9]

Scintillator (monocrystalline solid)	Z_{eff}	Efficiency of fast neutron registration, % reaction ($n, n'\gamma$)
BGO	75	48
GSO	59	46
CWO	66	42
CsI(Tl)	54	20
NaI(Tl)	51	18
$^6\text{LiI(Eu)}$	52	25

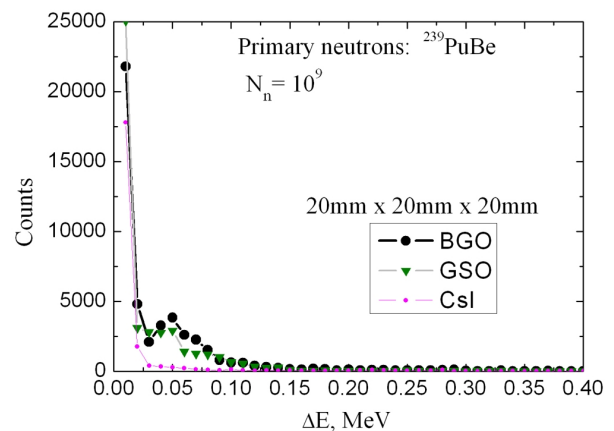


Fig. 7. Modelled values of absorbed energy in detectors for BGO, GSO, and CsI.

Small peaks are visible at $\Delta E \approx 0.05$ MeV for BGO and GSO scintillators. As a result of this analysis, the maximum peak value is 3830, therefore the statistical uncertainty of the Monte Carlo method is $1/\sqrt{3830} \approx 0.016$. This statistical uncertainty is acceptable for preliminary and estimational calculations.

Using preliminary virtual experiments, one can study mechanisms and reactions occurring in matter of scintillators during the registration of fast neutrons.

CONCLUSION

As a result of this work, the characteristics of the neutron source have been modeled and used for the study of response of scintillator detectors to neutron flux of $^{239}\text{PuBe}$ neutron source.





The convenient form of representation of fast neutrons energy spectrum from $^{239}\text{PuBe}$ neutron source has been obtained for use in computer programs for analyzing the characteristics of scintillators.

It is shown that the model based on data [4] is more preferable for further usage, because it contains neutrons with energies below 1 MeV in the initial spectrum. This is significant for neutron flux detection by heavy inorganic scintillators ($\text{Bi}_4\text{Ge}_3\text{O}_{12}$, CdWO_4 , Gd_2SiO_5 and others).

It is proposed to improve the methodology for conducting experiments for studying the response of heavy oxide scintillators by providing preliminary virtual experiments.

Based on conducted research, it can be concluded that heavy oxide scintillators, which at the same time are efficient gamma-detectors [9], allow to create highly efficient gamma-neutron detectors that provide high efficiency of fissile radioactive materials detection.

ORCID IDs

Viktoriia Lisovska  <https://orcid.org/0000-0003-1237-7959>, **Tetiana Malykhina**  <https://orcid.org/0000-0003-0035-2367>,
Valentina Shpagina  <https://orcid.org/0000-0002-6202-7474>, **Ruslan Timchenko**  <https://orcid.org/0000-0003-4983-9168>

REFERENCES

- [1]. V.D. Ryzhikov, B.V. Grinyov, G.M. Onyshchenko, L.A. Piven, S.V. Naydenov and O.K. Lysetska, *Functional Materials*, **3**(21), 345-351 2014, doi: 10.15407/fm21.03.345.
- [2]. Neutron interaction with matter, in <http://nuclphys.sinp.msu.ru/partmat/pm04.htm>.
- [3]. M.E. Anderson and R.A. Neff, *Nuclear Instruments and Methods*, **99**(2), 231-235 1972, doi: 10.1016/0029-554X(72)90781-1.
- [4]. G.I. Britvich, V.G. Vasil'chenko, Yu.V. Gilitsky, A.P. Chubenko, A.E. Kushnirenko, E.A. Mamidzhanyan, V.P. Pavlyuchenko, V.A. Pikalov, V.A. Romakhin, A.P. Soldatov, O.V. Sumaneev, S.K. Chernichenko, I.V. Shein and A.L. Shepetov, *Instruments and Experimental Techniques*, **47**, (5), 571-584 2004, doi: 10.1023/B:INET.0000.
- [5]. J. Allison, K. Amako, J. Apostolakis, P. Arce, M. Asai, T. Aso, E. Bagli, A. Bagulya, S. Banerjee, G. Barrand, B.R. Beck, A.G. ogdanov, D. Brandt, J.M.C. Brown, H. Burkhardt, Ph. Canal, D. Cano-Ott, S. Chauvie, K. Cho, G.A.P. Cirrone, G. Cooperman, M.A. Cortés-Giraldo, G. Cosmo, G. Cuttone, G. Depaola, L. Desorgher, X. Dong, A. Dotti, V.D. Elvira, G. Folger, Z. Francis, A. Galoyan, L. Garnier, M. Gayer, K.L. Genser, V.M. Grichine, S. Guatelli, P. Guèye, P. Gumplinger, A.S. Howard, I. Hrivnáčová, S. Hwang, S. Incerti, A. Ivanchenko, V.N. Ivanchenko, F.W. Jones, S.Y. Jun, P. Kaitaniemi, N. Karakatsanis, M. Karamitros, M. Kelsey, A. Kimura, T. Koi, H. Kurashige, A. Lechner, S.B. Lee, F. Longo, M. Maire, D. Mancusi, A. Mantero, E. Mendoza, B. Morgan, K. Murakami, T. Nikitina, L. Pandola, P. Paprocki, J. Perl, I. Petrović, M.G. Pia, W. Pokorski, J.M. Quesada, M. Raine, M.A. Reis, A. Ribon, A. Ristić Fira, F. Romano, G. Russo, G. Santin, T. Sasaki, D. Sawkey, J.I. Shin, I.I. Strakovsky, A. Taborda, S. Tanaka, B. Tomé, T. Toshito, H.N. Tran, P.R. Truscott, L. Urban, V. Uzhinsky, J.M. Verbeke, M. Verderi, B.L. Wendt, H. Wenzel, D.H. Wright, D.M. Wright, T. Yamashita, J. Yarba and H. Yoshida, *Nuclear Instruments and Methods in Physics Research*, **835**, 186-225 2016, doi: 10.1016/j.nima.2016.06.125.
- [6]. W. Press, S. Teukolsky, W. Vetterlong and B. Flannery, editors, *Numerical Recipes: The Art of Scientific Computing* (Cambridge University Press, 2007), <http://www.cambridge.org>.
- [7]. *Geant4 User's Guide for Application Developers* (CERN, 2018), in: <http://cern.ch/geant4-userdoc/UsersGuides/ForApplicationDeveloper/fo/BookForApplicationDevelopers.pdf>
- [8]. *Geant4 Physics Reference Manual* (CERN, 2018), in: <http://cern.ch/geant4-userdoc/UsersGuides/PhysicsReferenceManual/fo/PhysicsReferenceManual.pdf>
- [9]. *Наука про матеріали: досягнення та перспективи. Том 1, [Material Science: Achievements and Prospects. Volume 1]*, (Akademperiodyka, Kyiv, 2018), pp. 652.

GEANT4-МОДЕЛЮВАННЯ ЕНЕРГЕТИЧНОГО СПЕКТРУ ДЖЕРЕЛА ШВИДКИХ НЕЙТРОНІВ ДЛЯ НАПРАЦЮВАННЯ МЕТОДИКИ ДОСЛІДЖЕННЯ ВАЖКИХ СЦИНТИЛЯТОРІВ

В.В. Лісовська¹, Т.В. Малихіна¹, В.О. Шпагіна², Р.М. Тимченко¹

¹Харківський національний університет імені В.Н. Каразіна
майдан Свободи, 4, 61022, Харків, Україна

²Національний науковий центр Харківський фізико-технічний інститут
вул. Академічна, 1, 61108, Харків, Україна

В роботі представлені дослідження математичної моделі джерела швидких нейтронів. Проведено комп'ютерне моделювання енергетичного спектру швидких нейтронів від джерела $^{239}\text{PuBe}$. Розроблено модель джерела, що має енергетичний спектр нейтронів з кроком 100 кеВ у діапазоні енергій від 100 кеВ до 11 МеВ. Моделювання проведено методом Монте-Карло. Носієм моделі є комп'ютерна програма, розроблена мовою програмування C++ в середовищі операційної системи Linux з використанням бібліотеки класів Geant4. При моделюванні проходження нейтронів через речовини детекторів використовувалися всі необхідні класи, що містять моделі низьких енергій, і враховувалися процеси радіаційного захоплення, пружного розсіювання, поділу, непружного розсіювання, тому що програмно описані моделі процесів передбачається використовувати і для інших завдань, наприклад, проходження нейтронів через різні речовини, а

також для проведення віртуальних лабораторних робіт. При описі фізичних процесів у модулі PhysicsList розробленої програми використовувалися класи бібліотеки Geant4 G4NeutronHPElastic, G4NeutronHPElasticData, G4NeutronHPInelastic, G4NeutronHPInelasticData, G4NeutronHPCapture, G4NeutronHPCaptureData тощо, які засновані на модулях у складі пакету NeutronHP, і бібліотеки нейтронних даних G4NDL4.5. Представлені графіки, що містять змодельовані двома способами енергетичні спектри джерела швидких нейтронів $^{239}\text{PuBe}$. Проведено аналіз отриманих енергетичних спектрів. Для тестування моделі взаємодії нейтронів з речовиною проведені віртуальні ядерно-фізичні експерименти і досліджені процеси, що відбуваються у речовинах сцинтиляторів при проходженні через них потоку швидких нейтронів. У якості первинних частинок використовувалися 10^9 нейтронів з енергетичним спектром, отриманим в результаті моделювання $^{239}\text{PuBe}$ джерела нейтронів, і випромінюваних ізотропно. Розроблена модель $^{239}\text{PuBe}$ джерела нейтронів призначена для дослідження відгуку сцинтиляційних детекторів $\text{Bi}_4\text{Ge}_3\text{O}_{12}$, CdWO_4 , Gd_2SiO_5 , CsI та ін. на потік швидких нейтронів, а також дослідження важливих характеристик детекторів. У результаті проведення віртуальних ядерно-фізичних експериментів показано, що для реєстрації потоку нейтронів від джерела $^{239}\text{PuBe}$ більш перспективним є використання сцинтиляторів $\text{Bi}_4\text{Ge}_3\text{O}_{12}$ або Gd_2SiO_5 . Результати віртуальних ядерно-фізичних експериментів знаходяться у відповідності до опублікованих експериментальних даних.

КЛЮЧОВІ СЛОВА: $^{239}\text{PuBe}$ джерело нейтронів, сцинтиляційні детектори, реєстрація швидких нейтронів

GEANT4-МОДЕЛИРОВАНИЕ ЭНЕРГЕТИЧЕСКОГО СПЕКТРА ИСТОЧНИКА БЫСТРЫХ НЕЙТРОНОВ ДЛЯ НАРАБОТКИ МЕТОДИКИ ИССЛЕДОВАНИЯ ТЯЖЕЛЫХ СЦИНТИЛЛЯТОРОВ

В.В. Лисовская¹, Т.В. Малихина¹, В.О. Шпагина², Р.М. Тимченко¹

¹Харьковский национальный университет имени В.Н. Каразина

майдан Свободи, 4, 61022, Харьков, Украина

²Национальный научный центр Харьковский физико-технический институт

ул. Академическая, 1, 61108, Харьков, Украина

В работе представлены исследования математической модели источника быстрых нейтронов. Проведено компьютерное моделирование энергетического спектра быстрых нейтронов от источника $^{239}\text{PuBe}$. Разработана модель источника, имеющая энергетический спектр нейтронов с шагом 100 кэВ в диапазоне энергий от 100 кэВ до 11 МэВ. Моделирование проведено методом Монте-Карло. Носителем модели является компьютерная программа, разработанная на языке программирования C++ в среде операционной системы Linux с использованием библиотеки классов Geant4. При моделировании прохождения нейтронов через вещества детекторов использовались все необходимые классы, содержащие модели низких энергий, и учитывались процессы радиационного захвата, упругого рассеяния, деления, неупругого рассеяния, так как программно описанные модели процессов предполагается использовать и для других задач, например, прохождения нейтронов через различные вещества, а также для проведения виртуальных лабораторных работ. При описании физических процессов в модуле PhysicsList разработанной программы использовались классы библиотеки Geant4 G4NeutronHPElastic, G4NeutronHPElasticData, G4NeutronHPInelastic, G4NeutronHPInelasticData, G4NeutronHPCapture, G4NeutronHPCaptureData и др., основанные на модулях в составе пакета NeutronHP, и библиотеки нейтронных данных G4NDL4.5. Представлены графики, содержащие смоделированные двумя способами энергетические спектры источника быстрых нейтронов $^{239}\text{PuBe}$. Проведен анализ полученных энергетических спектров. Для тестирования модели взаимодействия нейтронов с веществом проведены виртуальные ядерно-физические эксперименты и исследованы процессы, происходящие в веществах сцинтилляторов при прохождении через них потока быстрых нейтронов. В качестве первичных частиц использовались 10^9 нейтронов с энергетическим спектром, полученным в результате моделирования $^{239}\text{PuBe}$ источника, и излучаемых изотропно. Разработанная модель источника $^{239}\text{PuBe}$ предназначена для исследования отклика сцинтилляционных детекторов $\text{Bi}_4\text{Ge}_3\text{O}_{12}$, CdWO_4 , Gd_2SiO_5 , CsI и др. на поток быстрых нейтронов, а также исследования различных характеристик детекторов. В результате проведения виртуальных ядерно-физических экспериментов показано, что для регистрации потока нейтронов от источника $^{239}\text{PuBe}$ более предпочтительным является использование сцинтилляторов $\text{Bi}_4\text{Ge}_3\text{O}_{12}$ или Gd_2SiO_5 . Результаты виртуальных ядерно-физических экспериментов находятся в хорошем соответствии с опубликованными экспериментальными данными.

КЛЮЧЕВЫЕ СЛОВА: $^{239}\text{PuBe}$ источник нейтронов, сцинтилляционные детекторы, регистрация быстрых нейтронов

PACS: 29.17.+w; 41.75.Lx

IMPROVEMENT OF PROPERTIES OF SELF-INJECTED AND ACCELERATED ELECTRON BUNCH BY LASER PULSE IN PLASMA, USING PULSE PRECURSOR

 Vasyl Maslov^{1,2*},  Denys Bondar²,  Iryna Levchuk¹,  Ivan Onishchenko¹

¹NSC "Kharkiv Institute of Physics and Technology" NASU

Kharkiv, 61108, st. Akademicheskaya 1, Ukraine

²V.N. Karazin Kharkiv National University

4 Svobody Sq., Kharkiv, 61022, Ukraine

*E-mail: vmaslov@kipt.kharkov.ua

Received April 8, 2019; revised April 15, 2019; accepted April 22, 2019

The accelerating gradients in conventional linear accelerators are currently limited to ~ 100 MV/m. Plasma-based accelerators have the ability to sustain accelerating gradients which are several orders of magnitude greater than that obtained in conventional accelerators. Due to the rapid development of laser technology the laser-plasma-based accelerators are of great interest now. Over the past decade, successful experiments on laser wakefield acceleration of electrons in the plasma have confirmed the relevance of this acceleration. Evidently, the large accelerating gradients in the laser plasma accelerators allow to reduce the size and to cut the cost of accelerators. Another important advantage of the laser-plasma accelerators is that they can produce short electron bunches with high energy. The formation of electron bunches with small energy spread was demonstrated at intense laser-plasma interactions. Electron self-injection in the wake-bubble, generated by an intense laser pulse in underdense plasma, has been studied. With newly available compact laser technology one can produce 100 PW-class laser pulses with a single-cycle duration on the femtosecond timescale. With a fs intense laser one can produce a coherent X-ray pulse. Prof. T. Tajima suggested utilizing these coherent X-rays to drive the acceleration of particles. When such X-rays are injected into a crystal they interact with a metallic-density electron plasma and ideally suit for laser wakefield acceleration. In numerical simulation of authors, performed according to idea of Prof. T. Tajima, on wakefield excitation by a X-ray laser pulse in a metallic-density electron plasma the accelerating gradient of several TV/m has been obtained. It is important to form bunch with small energy spread and small size. The purpose of this paper is to show by the numerical simulation that some precursor-laser-pulse, moved before the main laser pulse, controls properties of the self-injected electron bunch and provides at certain conditions small energy spread and small size of self-injected and accelerated electron bunch.

KEYWORDS: short laser pulse, plasma wakefield, electron acceleration, numerical simulation, self-injection of electron bunch

The accelerating electric fields in metal cavities of conventional accelerators are not more than ~ 100 MV/m for technical reasons, partly due to breakdown. Plasma can provide much more accelerating electric field which is approximately in 10^3 times larger than possible in metal cavities of conventional accelerators [1]. As plasma in experiment is inhomogeneous and nonstationary and properties of wakefield changes at increase of its amplitude it is difficult to excite wakefield resonantly by a long sequence of electron bunches [2, 3], to focus sequence [4-8], to prepare sequence from long beam [9-11] and to provide large transformer ratio [13-18]. In [4] the mechanism has been found and in [19-22] investigated of resonant plasma wakefield excitation by a nonresonant sequence of short electron bunches. Owing to successful development of laser physics [1, 23] the method of electron acceleration by short laser pulse in plasma is very perspective now. During last years, promising results have measured in experiments on electron acceleration by wakefield, excited by laser pulse in plasma [23]. The large accelerating wakefield, excited by laser pulse in plasma, provides possibility to decrease the dimensions and to cut the cost of accelerators. Important property of the accelerators, based on the laser-plasma interaction, is that short electron bunches can be self-injected and accelerated to high energy [23]. The electron bunch acceleration with small energy spread was observed at interaction of intense laser pulse with plasma.

The problem at laser wakefield acceleration is that laser pulse quickly destroyed because of its expansion. One way to solve this problem is the use of a capillary as a waveguide for laser pulse. The second way to solve this problem is to transfer its energy to the electron bunches which as drivers accelerate witness. A transition from a laser wakefield accelerator to plasma wakefield accelerator can occur in some cases at laser-plasma interaction [24].

Developed technology of compact intense lasers, which was awarded the Nobel Prize 2018, one can provide 100 PW laser pulses of a very small duration on the fs-timescale. Prof. T. Tajima concluded [25] that using this a femtosecond intense laser one can generate a coherent X-ray pulse. He also proposed [25] using these coherent X-rays to accelerate electrons. This X-ray, at injection into a crystal, can excite wakefield in a metallic-density electron plasma and ideally correspond for laser wakefield acceleration [25].

In [24, 26-28] it has shown that at certain conditions the laser wakefield acceleration is added by a beam-plasma wakefield acceleration.

At the laser acceleration of self-injected electron bunch by plasma wakefield the accelerating gradient about 50 GV/m has been obtained in experiments [23]. In numerical simulation [28], performed according to idea of Prof. T. Tajima [25, 29], on wakefield excitation by a X-ray laser pulse in a metallic-density electron plasma the accelerating gradient of several TV/m has been obtained. To solve the problem of laser pulse expansion, one can use a capillary discharge. The second method [23, 24, 26, 27] of solving this problem is fast energy transfer of driver laser pulse to self-injected electron bunch. This bunch becomes driver-bunch and accelerates next self-injected electron bunch up to larger energy.

It is important to form bunch with small energy spread and small size. We propose for the first time to use a laser pulse-precursor, moving directly in front of the main pulse, to control the parameters of a self-injected and accelerated electron bunch. Previously, no one used a precursor to control the parameters of a self-injected and accelerated electron bunch.

The purpose of this paper is to show by the numerical simulation that some precursor-laser-pulse, moved directly before the main laser pulse, controls properties of the self-injected electron bunch and provides at certain conditions small energy spread and small size of self-injected and accelerated electron bunch.

PARAMETERS OF SIMULATION

Fully relativistic particle-in-cell simulation was carried out by UMKA 2D3V code [30]. A computational domain (x, y) has a rectangular shape. λ is the laser pulse wavelength. The computational time interval is $\tau = 0.05$, the number of particles per cell is 8 and the total number of particles is 15.96×10^6 . The simulation of considered case was carried out up to 800 laser periods. The period of the laser pulse is $t_0 = 2\pi/\omega_0$. The s-polarized laser pulse enters into uniform plasma. In y direction, the boundary conditions for particles, electric and magnetic fields are periodic. The critical plasma density $n_c = m_e\omega_0^2/(4\pi e^2)$. The laser pulse is defined with a "cos²" distribution in longitudinal direction. The pulse has a Gaussian profile in the transverse direction. The longitudinal and transverse dimensions of the laser pulse are selected to be shorter than the plasma wavelength. Directly in front of the main pulse a laser pulse-precursor moves. Pulse-precursor has a lower intensity and smaller radius compared to the intensity and radius of the main pulse (see Fig. 1). Pulse-precursor consists of two pulses of different intensities and radii, so that the intensity and radius of the whole pulse grow along the pulse from first its front. Full length at half maximum of the main laser pulse equals λ and full width at half maximum equals 3λ . $a_0 = eE_{z0}/(m_e c \omega_0) = 2.236$; E_{z0} is the electric field amplitude. Full length at half maximum of the first pulse of the precursor equals 4λ and full width at half maximum equals λ , $a_{01} = eE_{z01}/(m_e c \omega_0) = 1$. Full length at half maximum of the second pulse of the precursor equals 2λ and full width at half maximum equals 2λ , $a_{02} = eE_{z02}/(m_e c \omega_0) = 1.732$. Coordinates x and y, time t, electric field amplitude E_z and electron plasma density n_0 are given in dimensionless form in units of λ , $2\pi/\omega_0$, $m_e c \omega_0/(2\pi e)$, $m_e \omega_0^2/(16\pi^3 e^2)$.

RESULTS OF SIMULATION

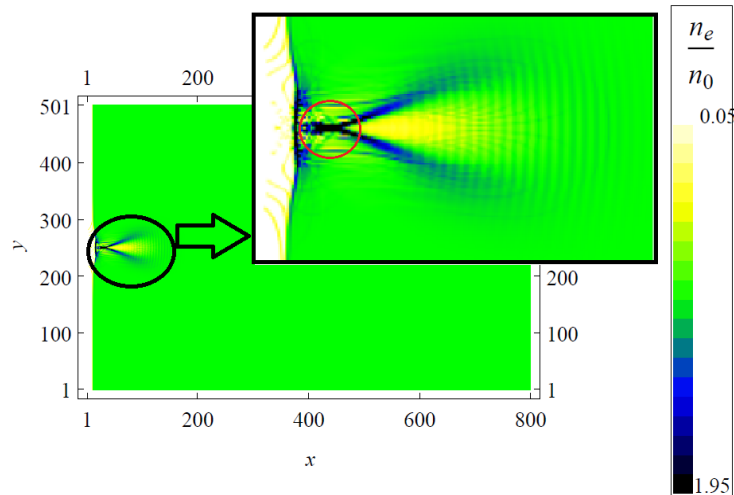


Fig. 1. Wake perturbation of plasma electron density n_e excited by laser pulse near the boundary of injection

We consider the wakefield excitation by laser pulse, shaped on intensity and radius. The intensity and radius grow from the first front of the pulse and then abruptly break off. Let us show that one can control the wakefield using a precursor. Namely, stochasticization of the wakefield is suppressed due to the adiabatic growth of intensity and radius of the pulse. Also one can control quality of the bunch. Namely, a point-kind bunch is formed.

From Fig.1 one can see that due to selected spatial distribution of intensity and radius of laser pulse near the boundary of injection the adiabatic structure, suitable for good self-injection, is formed.

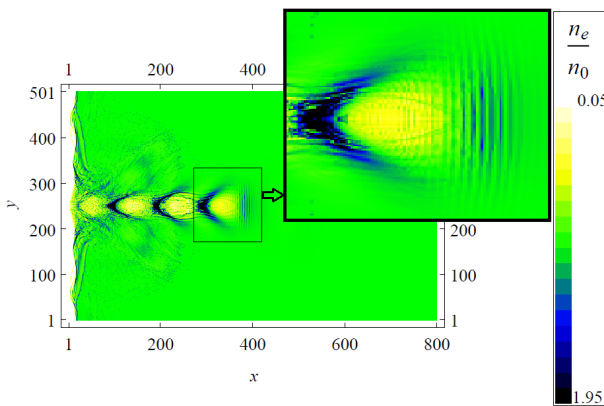


Fig. 2. Electron bunch self-injection at plasma wakefield excitation by laser pulse

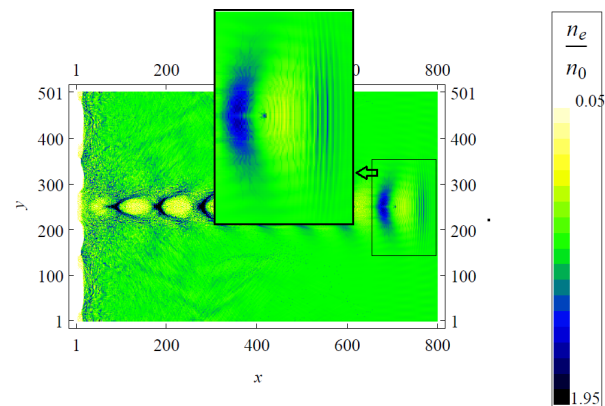


Fig. 3. Self-injected electron bunch acceleration by wakefield bubble, excited in plasma by laser pulse

It is seen from Fig. 2 that short electron bunch is self-injected. Fig. 3 demonstrates that point-kind electron bunch is accelerated.

Stochastization of the wakefield is suppressed due to the adiabatic growth of intensity and radius of the laser pulse (Fig. 4).

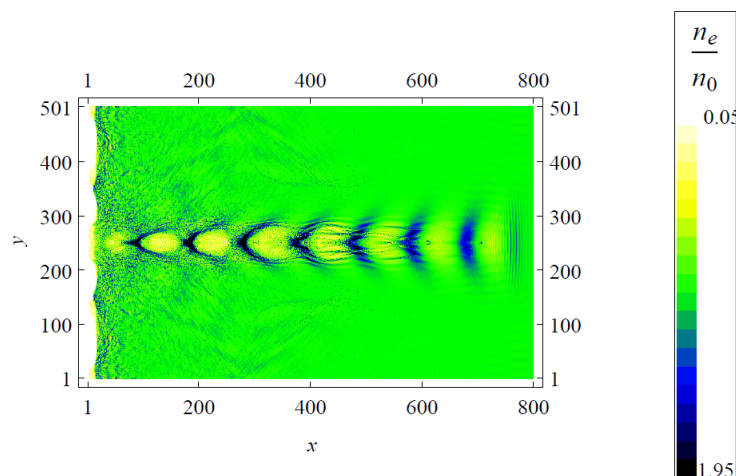


Fig. 4. Wakefield excitation and self-injected electron bunch acceleration in plasma by laser pulse

CONCLUSION

Thus, the authors for the first time used a laser pulse-precursor, moving directly in front of the main pulse, to control the parameters of a self-injected and accelerated electron bunch. Previously, no one used a precursor to control the parameters of a self-injected and accelerated electron bunch. It has been shown by the numerical simulation that some precursor-laser-pulse, moved directly before the main laser pulse, controls properties of the self-injected electron bunch and provides at certain conditions small energy spread and small size of self-injected and accelerated electron bunch.

ORCID IDs

Vasyl Maslov <https://orcid.org/0000-0002-4370-7685>, Denys Bondar <https://orcid.org/0000-0002-7358-4305>,
Iryna Levchuk <https://orcid.org/0000-0003-0542-0410>, Ivan Onishchenko <http://orcid.org/0000-0002-8025-5825>

REFERENCES

- [1]. A. Pukhov and J. Meyer-ter-Vehn, *Apl. Phys. B.*, **74**, 355-361 (2002), doi: 10.1007/s003400200795.
- [2]. K.V. Lotov, V.I. Maslov, I.N. Onishchenko and E.N. Svistun, *Problems of Atomic Science and Technology*, **6**, 114-116 (2008).
- [3]. K.V. Lotov, V.I. Maslov, I.N. Onishchenko and E.N. Svistun, *Plasma Phys. Cont. Fus.* **52**, 065009 (2010), doi: 10.1088/0741-3335/52/6/065009.
- [4]. K.V. Lotov, V.I. Maslov, I.N. Onishchenko and E.N. Svistun, *Problems of Atomic Science and Technology*, **3**, 159-163 (2012).
- [5]. V.I. Maslov, I.N. Onishchenko and I.P. Yarovaya, *Problems of Atomic Science and Technology*, **1**, 134-136 (2013).
- [6]. V.I. Maslov, I.N. Onishchenko and I.P. Yarovaya, *East European Journal of Physics*, **1**(2), 92-95 (2014).
- [7]. I.P. Levchuk, V.I. Maslov and I.N. Onishchenko, *Problems of Atomic Science and Technology*, **4**, 120-123 (2015).

- [8]. I.P. Levchuk, V.I. Maslov and I.N. Onishchenko, *Problems of Atomic Science and Technology*. **3**, 62-65 (2016).
- [9]. K.V. Lotov, V.I. Maslov and I.N. Onishchenko and M.S. Vesnovskaya, *Problems of Atomic Science and Technology*. **4**, 12-16 (2010).
- [10]. K.V. Lotov, V.I. Maslov, I.N. Onishchenko and M.S. Vesnovskaya, *Problems of Atomic Science and Technology*. **1**, 83-85 (2011).
- [11]. V.A. Balakirev, I.N. Onishchenko and V.I. Maslov, *Problems of Atomic Science and Technology*. **3**, 92-95. (2011).
- [12]. K.V. Lotov, V.I. Maslov and I.N. Onishchenko, *Problems of Atomic Science and Technology*. **4**, 85-89. (2010).
- [13]. K.V. Lotov, V.I. Maslov, I.N. Onishchenko and I.P. Yarovaya, *Problems of Atomic Science and Technology*. **3**, 87-91 (2011).
- [14]. V.I. Maslov, I.N. Onishchenko and I.P. Yarovaya, *Problems of Atomic Science and Technology*. **4**, 128-130 (2012).
- [15]. V.I. Maslov, I.N. Onishchenko and I.P. Yarovaya, *Problems of Atomic Science and Technology*. **6**, 161 –163 (2012).
- [16]. I.P. Levchuk, V.I. Maslov and I.N. Onishchenko, *Problems of Atomic Science and Technology*. **6**, 37 –41 (2015).
- [17]. I.P. Levchuk, V.I. Maslov and I.N. Onishchenko, *Problems of Atomic Science and Technology*. **6**, 43 –46 (2017).
- [18]. D.S. Bondar, I.P. Levchuk, V.I. Maslov and I.N. Onishchenko, *East Eur. J. Phys.* **5**(2), 72 –77 (2018).
- [19]. K.V. Lotov, V.I. Maslov, I.N. Onishchenko and E.N. Svistun, *Problems of Atomic Science and Technology*. **2**, 122-124 (2010).
- [20]. V. Lotov, V.I. Maslov, I.N. Onishchenko, E.N. Svistun and M.S. Vesnovskaya, *Problems of Atomic Science and Technology*. **6**, 114–116 (2010).
- [21]. K.V. Lotov, V.I. Maslov and I.N. Onishchenko, *Problems of Atomic Science and Technology*. **6**, 103 –107 (2010).
- [22]. K.V. Lotov, V.I. Maslov, I.N. Onishchenko and I.P. Yarovaya, *Problems of Atomic Science and Technology*. **4**, 73 –76 (2013).
- [23]. W. P. Leemans, A. J. Gonsalves, H.-S. Mao, K. Nakamura, C. Benedetti, C. B. Schroeder, Cs. Tóth, J. Daniels, D. E. Mittelberger, S. S. Bulanov, J.-L. Vay, C. G. R. Geddes, and E. Esarey, *Phys. Rev. Lett.* **113**, 245002 (2014), doi: 10.1103/PhysRevLett.113.245002.
- [24]. T. Tajima, *Eur. Phys. J. Spec. Top.* **223**, 1037–1044 (2014), doi: 10.1140/epjst/e2014-02154-6.
- [25]. V.I. Maslov, O.M. Svystun, I.N. Onishchenko and V.I. Tkachenko, *Nuclear Instruments and Methods in Physics Research A*. **829**, 422–425 (2016), doi: 10.1016/j.nima.2016.04.018.
- [26]. V.I. Maslov, O.M. Svystun, I.N. Onishchenko and A.M. Egorov, *Problems of Atomic Science and Technology*. **6**, 144-147 (2016).
- [27]. D.S. Bondar, I.P. Levchuk, V.I. Maslov, S. Nikonova and I.N. Onishchenko, *Problems of Atomic Science and Technology*. **6**, 76-79 (2017).
- [28]. D.S. Bondar, V.I. Maslov, I.P. Levchuk and I.N. Onishchenko, *Problems of Atomic Science and Technology*. **6**, 156 –159 (2018).
- [29]. S. Hakimi, T. Nguyen, D. Farinella, C.K. Lau, H.-Yu. Wang, P. Taborek, F. Dollar and T. Tajima, *Plas. Phys.* **25**, 023112 (2018), doi: 10.1063/1.5016445.
- [30]. G.I. Dudnikova, T.V. Liseykina, V.Yu. Bychenkov, *Comp. Techn.* **10**(1), 37 (2005).

ПОЛІПШЕННЯ ВЛАСТИВОСТЕЙ САМОІНЖЕКТОВАНОГО І ПРИСКОРЕНОГО ЕЛЕКТРОННОГО ЗГУСТКУ ЛАЗЕРНИМ ІМПУЛЬСОМ В ПЛАЗМІ ВИКОРИСТАННЯМ ПЕРЕДВІСНИКА

В.І. Маслов^{1,2}, Д.С. Бондар², І.П. Левчук¹, І.М. Онищенко¹

¹ Національний Науковий Центр «Харківський фізико-технічний інститут»

61108, Харків, вул. Академічна, 1

² Харківський національний університет імені В.Н. Каразіна

пл. Свободи 4, Харків, 61022, Україна

Зараз прискорюючі поля в звичайних лінійних прискорювачах обмежені ~ 100 мВ/м. Прискорення в плазмі забезпечує прискорюючі поля, які на кілька порядків більше, ніж в звичайних прискорювачах. У зв'язку з успішним розвитком лазерних технологій, лазерно-плазмові прискорювачі зараз викликають великий інтерес. За минуле десятиліття успішні експерименти по лазерному прискоренню електронів в плазмі кільватерним полем підтвердили перспективність цього прискорення. Очевидно, що великі прискорюючі поля в лазерно-плазмових прискорювачах дозволяють зменшити розмір і знизити вартість прискорювачів. Інша важлива перевага лазерно-плазмових прискорювачів полягає в тому, що вони можуть створювати короткі електронні згустки великої енергії. Були продемонстровані електронні згустки з невеликим розкидом по енергії при взаємодії інтенсивних лазерних імпульсів з плазмою. Також була вивчена самоінжекція електронних згустків в кільватерній порожнині, яка генерується інтенсивним лазерним імпульсом у щільній плазмі. Завдяки нещодавно розвиненій компактній лазерній технології можна генерувати 100-ПВт лазерні одно-періодні фемтосекундні імпульси. За допомогою потужного фемтосекундного лазерного імпульсу можна генерувати когерентний рентгенівський імпульс. Професор Т.Тадзіма запропонував використовувати ці когерентні рентгенівські імпульси для прискорення частинок. Коли такий рентгенівський імпульс інjektується в кристал, він взаємодіє з електронною плазмою металевої щільності і ідеально підходить для лазерного кільватерного прискорення. При числовому моделюванні авторів, виконаному на основі ідеї професора Т.Тадзіми, при збудженні кільватерного поля рентгенівським лазерним імпульсом в електронній плазмі металевої густини було отримано прискорююче поле кілька ТВ/м. При лазерному прискоренні самоінжектованного згустку електронів кільватерним полем в плазмі важливо сформуванати згусток з невеликим розкидом по енергії і невеликим розміром. У цій роботі числовим моделюванням показано, що певний імпульс-передвісник, що рухається перед основним лазерним імпульсом, контролює властивості самоінжектованого згустку і забезпечує за певних умов малий розкид по енергії і малий розмір самоінжектованого і прискореного електронного згустку.

КЛЮЧОВІ СЛОВА: короткий лазерний імпульс, кільватерне поле в плазмі, прискорення електронів, числове моделювання, самоінжекція електронних згустків

УЛУЧШЕНИЕ СВОЙСТВ САМОИНЖЕКТИРОВАННОГО И УСКОРЕННОГО ЭЛЕКТРОННОГО СГУСТКА ЛАЗЕРНЫМ ИМПУЛЬСОМ В ПЛАЗМЕ ИСПОЛЬЗОВАНИЕМ ПРЕДВЕСТНИКА**В.И. Маслов^{1,2}, Д.С. Бондарь² И.П. Левчук¹, И.Н. Онищенко¹**¹ *Национальный Научный Центр «Харьковский физико-технический институт»**61108, Харьков, ул. Академическая, 1*² *Харьковский национальный университет имени В.Н. Каразина**пл. Свободы 4, Харьков, 61022, Украина*

В настоящее время ускоряющие поля в обычных линейных ускорителях ограничены ~100 МВ/м. Ускорение в плазме обеспечивает ускоряющие поля, которые на несколько порядков больше, чем в обычных ускорителях. В связи с бурным развитием лазерных технологий, лазерно-плазменные ускорители в настоящее время представляют большой интерес. За прошедшее десятилетие успешные эксперименты по лазерному ускорению электронов в плазме кильватерным полем подтвердили перспективность этого ускорения. Очевидно, что большие ускоряющие поля в лазерно-плазменных ускорителях позволяют уменьшить размер и снизить стоимость ускорителей. Другое важное преимущество лазерно-плазменных ускорителей заключается в том, что они могут создавать короткие электронные сгустки большой энергии. Были продемонстрированы электронные сгустки с небольшим разбросом по энергии при взаимодействии интенсивных лазерных импульсов с плазмой. Также была изучена самоинжекция электронных сгустков в кильватерной полости, генерируемой интенсивным лазерным импульсом в плотной плазме. Благодаря недавно развитой компактной лазерной технологии можно генерировать 100-ПВт лазерные одно-периодные фемтосекундные импульсы. С помощью мощного фемтосекундного лазерного импульса можно генерировать когерентный рентгеновский импульс. Профессор Т.Тадзима предложил использовать эти когерентные рентгеновские импульсы для ускорения частиц. Когда такой рентгеновский импульс инжектируется в кристалл, он взаимодействует с электронной плазмой металлической плотности и идеально подходит для лазерного кильватерного ускорения. При численном моделировании авторов, выполненном на основе идеи профессора Т.Тадзимы, при возбуждении кильватерного поля рентгеновским лазерным импульсом в электронной плазме металлической плотности было получено ускоряющее поле несколько ТВ/м. При лазерном ускорении самоинжектированного сгустка электронов кильватерным полем в плазме важно сформировать сгусток с небольшим разбросом по энергии и небольшим размером. В этой работе численным моделированием показано, что некоторый импульс-предвестник, движущийся перед основным лазерным импульсом, контролирует свойства самоинжектированного сгустка и обеспечивает при определенных условиях малый разброс по энергии и малый размер самоинжектированного и ускоренного электронного сгустка.

КЛЮЧЕВЫЕ СЛОВА: короткий лазерный импульс, кильватерное поле в плазме, ускорение электронов, численное моделирование, самоинжекция электронных сгустков

PACS: 29.17.+w; 41.75.Lx;

UNIFORM FOCUSING OF SEQUENCE OF RELATIVISTIC POSITRON BUNCHES IN PLASMA

 **Vasyl Maslov**^{1,2,*},  **Denys Bondar**²,  **Iryna Levchuk**¹,  **Sofiia Nikonova**²,
 **Ivan Onishchenko**¹

¹NSC "Kharkiv Institute of Physics and Technology" NASU
Kharkiv, 61108, st. Akademicheskaya 1, Ukraine

²V.N. Karazin Kharkiv National University

4 Svobody Sq., Kharkiv, 61022, Ukraine

*E-mail: vmaslov@kipt.kharkov.ua

Received April 8, 2019; revised April 23, 2019; accepted May 31, 2019

Plasma-based accelerators sustain accelerating gradients which are several orders greater than obtained in conventional accelerators. Focusing of electron and positron beams by wakefield, excited in plasma, in electron-positron collider is very important. The focusing mechanism in the plasma, in which all electron bunches of a sequence are focused identically, has been proposed by authors earlier. The mechanism of focusing of a sequence of relativistic positron bunches in plasma, in which all positron bunches of a sequence are focused identically and uniformly, has been investigated in this paper by numerical simulation by 2.5D code LCODE. Mechanism of this identical and uniform focusing involves the use of wave-length λ , which coinciding with double longitudinal dimension of bunches $\lambda=2\Delta_b$, the first bunch current is in two times smaller than the current of the following bunches of sequence and the distance between bunches equals to one and a half of wavelength 1.5λ . We numerically simulate the self-consistent radial dynamics of lengthy positron bunches in homogeneous plasma. In simulation we use the hydrodynamic description of plasma. In other words the plasma is considered to be cold electron liquid, and positron bunches are aggregate of macroparticles. Positron bunches are considered to be homogeneous cylinders in the longitudinal direction. Positrons in bunches are distributed in radial direction according to Gaussian distribution. It is shown that in this case only first bunch is in the finite longitudinal electrical wakefield $E_z \neq 0$. Other bunches are in zero longitudinal electrical wakefield $E_z = 0$. Between bunches of this sequence longitudinal electrical wakefield and radial force are not zero $E_z \neq 0$, $F_r \neq 0$. The focusing radial force in regions, occupied by bunches, is constant along each bunch $F_r = \text{const}$. Between bunches the radial force is inhomogeneous $F_r \neq \text{const}$. All positron bunches of sequence are focused identically and uniformly.

KEYWORDS: electron bunch focusing, positron bunch focusing, plasma wakefield lens, particle acceleration, numerical simulation.

Plasma-based accelerators sustain accelerating gradients which are several orders greater than obtained in conventional accelerators [1-3]. Accelerating wakefield can be excited by single electron bunch [4, 5]. As plasma is inhomogeneous and nonstationary it is difficult to excite wakefield resonantly by a long sequence of electron bunches [6, 7], to focus sequence [8-12], to prepare sequence from long beam [13-15] and to provide large transformer ratio [16-22]. In [7] the mechanism has been found and in [23-26] investigated of resonant plasma wakefield excitation by a nonresonant sequence of short electron bunches.

Focusing of electron and positron beams by wakefield, excited in plasma, in electron-positron collider is very important [8-10, 27-30]. The focusing mechanism in the plasma, in which all electron bunches of a sequence are focused identically, has been proposed in [8-10]. However, investigations show that in a strongly nonlinear regime the value and spatial distribution of wakefield, excited by sequence of positron bunches, are different in comparison with the value and spatial distribution of wakefield, excited by sequence of electron bunches. Therefore this lens for relativistic positron bunches is researched in this paper by numerical simulation by 2.5D code LCODE [31]. Code LCODE treats plasma as a cold electron fluid and the bunches as ensembles of macro-particles. Electron beam is represented by a sequence of 4 and 10 electron bunches.

The article deals only with the focusing process. This regime can take place in the following cases:

- before the meeting point of colliding beams;
- during beam transport;
- in conditions with spatially separated processes of acceleration and focusing.

We use the cylindrical coordinate system (r, z) and plot wakefields, plasma and beam densities at some z as functions of the dimensionless value $\xi=(z-V_b t)$, V_b is the velocity of bunches.

Wakefield is normalized on $E_0=cm\omega_p/e$, where m is the electron mass, e is the elementary charge, c is the speed of light, and $\omega_p=(4\pi n_0 e^2/m)^{1/2}$ is the plasma frequency. Time t is normalized on ω_{pe}^{-1} , longitudinal momentum of bunches P_z – on $mc\gamma_b$, radius of bunches on c/ω_p , beam current I_b – on mc^3/e , emittance of bunches σ – on c^2/ω_p ; plasma electron density n_e and bunch density n_b are normalized on unperturbed plasma electron density n_0 , radial r and longitudinal z coordinates – on c/ω_p .

All bunches of sequence are focused identically and uniformly. By code LCODE we simulate the behavior of positron bunches of finite dimension in uniform plasma. The code simulate plasma electrons, using the hydrodynamic

equations. In other words the plasma electrons are considered to be cold electron liquid, and bunches are aggregate of macroparticles.

Aim of paper is to show that all relativistic positron bunches of sequence can be focused identically and uniformly and to derive conditions for achievement of identical and uniform focusing of relativistic positron bunches of sequence.

RESULTS OF SIMULATION

Let us study focusing of positron bunches of sequence by wave, which wave-length coinciding with double longitudinal dimension of bunches. This case is interesting, since at growth of bunch longitudinal dimension at fixed its current the amplitude of wakefield reaches highest value at $\lambda=2\Delta_b$. We apply the first bunch current is in two times smaller than the current of the following bunches of sequence $I_1=I/2, I_i=I, i=2, 3, 4 \dots$, spatial dimension from one bunch to another coincides with $1.5\lambda, \lambda$ is used wave-length of wakefield. In this case the distribution of excited longitudinal wakefield E_z , radial wake force F_r and magnetic field H_θ are of the form, shown in Fig. 1 for four bunches.

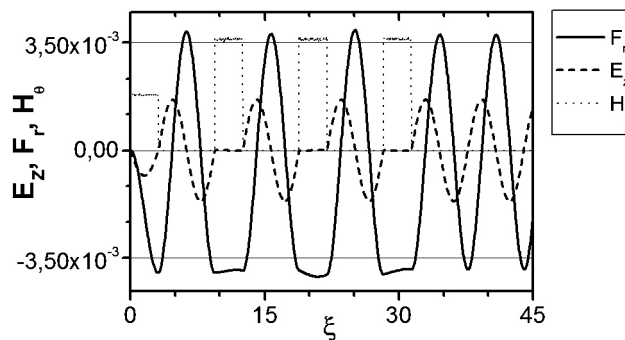


Fig. 1. Off-axis longitudinal wakefield E_z (---), off-axis radial wake force F_r (----)= $E_r-V_b H_\theta/c$ and off-axis magnetic field H_θ (.....) for $z=3, \gamma_b=5, I_b=0.3 \times 10^{-3}, n_b=0.1, \gamma_b$ is the relativistic factor of bunches, I_b is the maximal beam current. E_z, F_r, H_θ have been calculated for radius $r=r_b$

In Fig. 1 one can see positions of bunches by positions H_θ , because magnetic field is created by beam current. From Fig. 1 it is evidently, that first bunch is in $E_z \neq 0$ and it excites wakefield. All following bunches are in $E_z=0$ and they do not excite wakefield. Hence wakefield does not change from one bunch to another. However the sequence is focused since amplitude of transversal wake force is finite $F_r \neq 0$ in areas of bunches.

It is necessary to list the distinctive characteristics of the lens of this mechanism:

- 1) radial wake force F_r does not approximately depend on coordinate in regions, occupied by bunches (with the exception of first bunch), $F_r \approx \text{const}$, i.e. lengthy bunches are focused identically;
- 2) only first bunch is decelerated;
- 3) identical focusing force effects on all bunches (with the exception of first bunch);
- 4) longitudinal wakefield equal zero $E_z=0$ in regions, occupied by bunches (with the exception of first bunch).

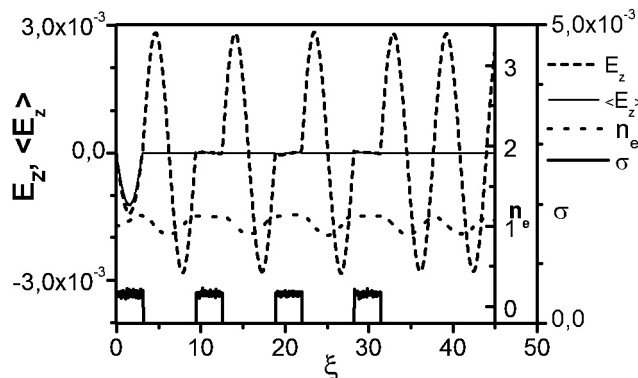


Fig. 2. On-axis plasma electron density n_e (.....) in wakefield, emittance of bunches σ (----), on-axis longitudinal wakefield E_z (---) and $\langle E_z \rangle = \int dr r E_z n_b / \int dr n_b$ (----) coupling rate of bunch with wakefield E_z for $z=3, \gamma_b=5, I_b=0.3 \times 10^{-3}, n_b=0.1$

Such ideal focusing (Fig. 3) is realized due to formation of flat elevations of plasma electron density n_e in areas of bunches (Fig. 2). These flat elevations compensate charges of bunches but magnetic field of current of bunches focuses them. In first bunch area (Fig. 2), the excited elevation of plasma electron density n_e is not uniform. As a result first

bunch nonuniform focusing is developed (Fig. 3). It is evidently from Fig. 2 that perturbation of density of plasma electrons n_e is periodic but non-sinusoidal: long elevations of n_e (as opposed to area of first bunch) are alternated by short decreases of n_e . The bunches are located in the regions of the elevations of n_e .

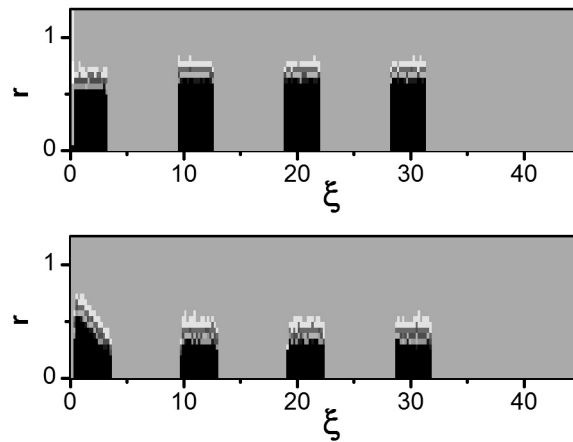


Fig. 3. The spatial (r, ξ) distribution of electron density n_b of bunches before focusing (near the boundary of beam injection, $z=3$) and after focusing (into the plasma on the distance $z=20$ from the boundary of beam injection) for $\gamma_b=5$, $I_b=0.3 \times 10^{-3}$, $r_b=0.1$. Black corresponds to the maximum density, and gray – to zero

In linear approximation relation $E_r \sim \partial_r E_z$ for transversal and longitudinal wakefields is known. But in our case it is erroneous (One can see Fig. 1). It is obviously from Figs. 1-2 that positive and negative perturbations of E_z are alternated, compensating each other. The latter leads to observed fact that along the final areas of dimension $\lambda/2$ of positions of bunches the longitudinal wakefield E_z is compensated. But in these areas of positions of bunches the transversal force F_r is finite $F_r \neq 0$.

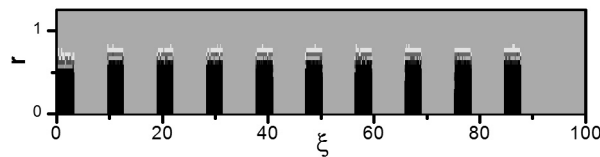


Fig. 4. The spatial distribution of electron density n_b of ten bunches before focusing for $z=3$, $\gamma_b=1000$, $I_b=0.3 \times 10^{-3}$, $r_b=0.1$. Black corresponds to the maximum density, and gray – to zero

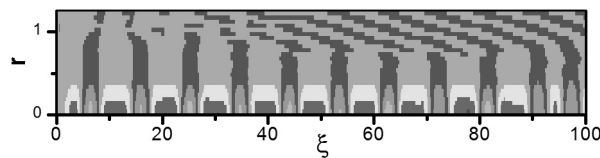


Fig. 5. Plasma electron density n_e in wakefield, excited by ten bunches for $z=3$, $\gamma_b=1000$, $I_b=0.3 \times 10^{-3}$, $r_b=0.1$

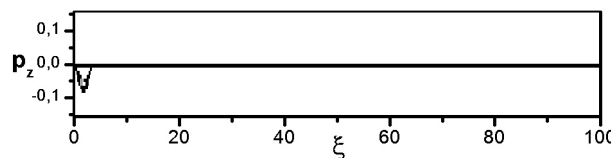


Fig. 6. Change of longitudinal momentum of bunches P_z at wakefield excitation for $z=80$, $\gamma_b=1000$, $I_b=0.3 \times 10^{-3}$, $r_b=0.1$, $p_z=P_{z-1}$

Let us show that similar behavior and dependencies are observed for another number of bunches. In particular, we simulate the case of ten bunches (one can see Fig. 4). Similar to the case of four bunches, the first bunch current is in two times smaller than the current of the following bunches of sequence $I_1=I/2$, $I_i=I$, $i=2, 3, 4 \dots$, spatial dimension from one bunch to another coincides with 1.5λ . One can see the plasma electron density n_e perturbation, excited longitudinal wakefield E_z , radial wake force F_r , magnetic field H_θ , average wakefield $\langle E_z \rangle$, momentum of bunches P_z in Figs. 4-8. One can see that behavior and dependencies are identical to the case of four bunches. Namely, Fig. 7

demonstrates that in the case of ten bunches also $\langle E_z \rangle$ for only bunch on front of sequence is finite and hence only bunch on front of sequence is decelerated (Fig. 6).

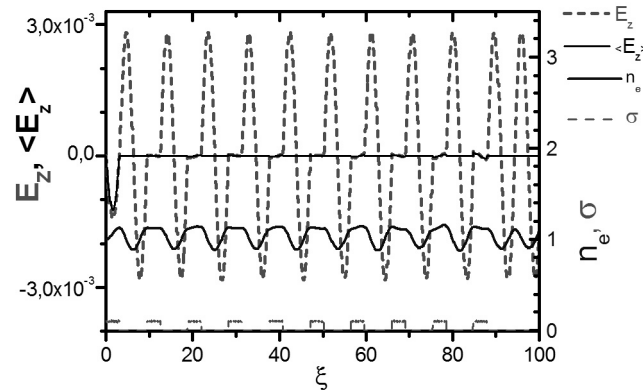


Fig. 7. On-axis plasma electron density n_e (—), emittance of bunches σ (·····), on-axis longitudinal wakefield E_z (- - -) and $\langle E_z \rangle$ (- · - ·) coupling rate of bunch with wakefield E_z for $z=3$, $\gamma_b=1000$, $I_b=0.3 \times 10^{-3}$, $r_b=0.1$

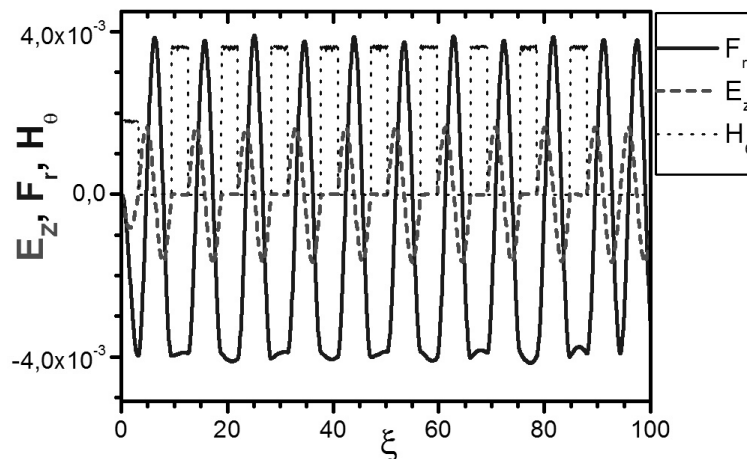


Fig. 8. Off-axis longitudinal wakefield E_z (- - -), off-axis radial wake force F_r (- · - ·) and off-axis magnetic field H_θ (·····) for $z=3$, $\gamma_b=1000$, $I_b=0.3 \times 10^{-3}$, $r_b=0.1$. E_z , F_r , H_θ have been calculated for radius $r=r_b$

Again one can see (Fig. 8) that only 1-st bunch is in finite $E_z \neq 0$. Other bunches are in zero longitudinal electrical wakefield $E_z=0$. Radial wake force F_r in regions, occupied by bunches, is finite (Fig. 8).

CONCLUSION

It has been shown that in considered conditions all relativistic positron bunches unlike a bunch at the front of sequence are focused equally and homogeneously (Fig. 3) similar to electron bunches. For this it is necessary that wave-length coinciding with double longitudinal dimension of bunches, the first bunch current is in two times smaller than the current of the following bunches of sequence, spatial dimension from one bunch to another coincides with 1.5λ . From results of simulations one can conclude that only bunch on the front of sequence interacts with wakefield. All next bunches are in areas, where longitudinal wakefield equals zero. Therefore only bunch on the front of sequence excites wakefield. The next bunches do not excite wakefield. Hence value of wakefield does not increase along sequence. Transversal force in areas of bunches is the same and homogeneous along bunches.

ORCID IDs

Vasyl Maslov <https://orcid.org/0000-0002-4370-7685>, Denys Bondar <https://orcid.org/0000-0002-7358-4305>,
Iryna Levchuk <https://orcid.org/0000-0003-0542-0410>, Sofiia Nikonova <https://orcid.org/0000-0003-3201-6077>,
Ivan Onishchenko <http://orcid.org/0000-0002-8025-5825>

REFERENCES

- [1]. E. Esarey, C.B. Schroeder and W.P. Leemans, Rev. Mod. Phys., **81**, 1229-1285 (2009), doi: 10.1103/RevModPhys.81.1229.
- [2]. A. Pukhov and J. Meyer-ter-Vehn, Apl. Phys. B., **74**, 355-361 (2002), doi: 10.1007/s003400200795.
- [3]. K.V. Lotov, V.I. Maslov, I.N. Onishchenko and E.N. Svistun, Problems of Atomic Science and Technology, **6**, 114-116 (2008).
- [4]. K.V. Lotov, V.I. Maslov, I.N. Onishchenko and E.N. Svistun, Plasma Phys. Cont. Fus., **52**, 065009 (2010), doi: 10.1088/0741-3335/52/6/065009.

- [5]. K.V. Lotov, V.I. Maslov, I.N. Onishchenko and E.N. Svistun, *Problems of Atomic Science and Technology*. **3**, 159-163 (2012).
- [6]. V.I. Maslov, I.N. Onishchenko and I.P. Yarovaya, *Problems of Atomic Science and Technology*. **1**, 134-136 (2013).
- [7]. V.I. Maslov, I.N. Onishchenko and I.P. Yarovaya, *East European Journal of Physics*. **1**(2), 92-95 (2014).
- [8]. I.P. Levchuk, V.I. Maslov and I.N. Onishchenko, *Problems of Atomic Science and Technology*. **4**, 120-123 (2015).
- [9]. I.P. Levchuk, V.I. Maslov and I.N. Onishchenko, *Problems of Atomic Science and Technology*. **3**, 62-65 (2016).
- [10]. K.V. Lotov, V.I. Maslov, I.N. Onishchenko and M.S. Vesnovskaya, *Problems of Atomic Science and Technology*. **4**, 12-16 (2010).
- [11]. K.V. Lotov, V.I. Maslov, I.N. Onishchenko and M.S. Vesnovskaya, *Problems of Atomic Science and Technology*. **1**, 83-85 (2011).
- [12]. V.A. Balakirev, I.N. Onishchenko and V.I. Maslov, *Problems of Atomic Science and Technology*. **3**, 92-95. (2011).
- [13]. K.V. Lotov, V.I. Maslov and I.N. Onishchenko, *Problems of Atomic Science and Technology*. **4**, 85-89. (2010).
- [14]. K.V. Lotov, V.I. Maslov, I.N. Onishchenko and I.P. Yarovaya, *Problems of Atomic Science and Technology*. **3**, 87-91 (2011).
- [15]. V.I. Maslov, I.N. Onishchenko and I.P. Yarovaya, *Problems of Atomic Science and Technology*. **4**, 128-130 (2012).
- [16]. V.I. Maslov, I.N. Onishchenko and I.P. Yarovaya, *Problems of Atomic Science and Technology*. **6**, 161-163 (2012).
- [17]. I.P. Levchuk, V.I. Maslov and I.N. Onishchenko, *Problems of Atomic Science and Technology*. **6**, 37-41. (2015).
- [18]. I.P. Levchuk, V.I. Maslov and I.N. Onishchenko, *Problems of Atomic Science and Technology*. **6**, 43-46. (2017).
- [19]. D.S. Bondar, I.P. Levchuk, V.I. Maslov, I.N. Onishchenko, *East Eur. J. Phys.* **5**(2), 72-77. (2018).
- [20]. K.V. Lotov, V.I. Maslov, I.N. Onishchenko and E.N. Svistun, *Problems of Atomic Science and Technology*. **2**, 122-124 (2010).
- [21]. V. Lotov, V.I. Maslov, I.N. Onishchenko, E.N. Svistun and M.S. Vesnovskaya, *Problems of Atomic Science and Technology*. **6**, 114–116 (2010).
- [22]. K.V. Lotov, V.I. Maslov and I.N. Onishchenko, *Problems of Atomic Science and Technology*. **6**, 103–107 (2010).
- [23]. K.V. Lotov, V.I. Maslov, I.N. Onishchenko and I.P. Yarovaya, *Problems of Atomic Science and Technology*. **4**, 73-76 (2013).
- [24]. G. Hairapetian, P. Devis, C. Joshi, C. Pelegrin and T. Katsouleas, *Phys. Plasma*. **2**(2555) 1995, doi: 10.1063/1.871217.
- [25]. Ya.B. Fainberg, N.I. Ayzatsky, V.A. Balakirev, A.K. Berezin, A.N. Dovbnaya, V.I. Karas', V.A. Kiselev, V.A. Kushnir, A.F. Linnik, V.V. Mitrochenko, V.D. Stepin, I.N. Onishchenko, A.P. Tolstoluzhsky and V.V. Uskov, in: *Proceedings PAC'97*, Edited by M. Comyn, M.K. Craddock, M. Reiser, J. Thomson (IEEE, Vancouver, 1997). **2**, pp. 651-653, doi: 10.1109/PAC.1997.749794.
- [26]. J.-H. Röckemann, L. Schaper, S.K. Barber, N.A. Bobrova, G. Boyle, S. Bulanov, N. Delbos, K. Floettmann, G. Kube, W. Lauth, W.P. Leemans, V. Libov, A.R. Maier, M. Meisel, P. Messner, P.V. Sasorov, C.B. Schroeder, J. van Tilborg, S. Wesch, and J. Osterhoff, *Phys. Rev. Accel. & Beams*. **21**, 122801 (2018), doi: 10.1103/PhysRevAccelBeams.21.122801.
- [27]. C. O'Connell, F.-J. Decker, M.J. Hogan, R. Iverson, P. Raimondi, R.H. Siemann, D. Walz, B. Blue, C.E. Clayton, C. Joshi, K.A. Marsh, W.B. Mori, S. Wang, T. Katsouleas, S. Lee, and P. Muggli, *Phys. Rev. Accel. & Beams*. **5**, 121301 (2002), doi: 10.1103/PhysRevSTAB.5.121301.
- [28]. M.C. Thompson, H. Badakov, J.B. Rosenzweig, G. Travish, R. Fliller, G.M. Kazakevich, P. Piot, J. Santucci, J. Li, and R. Tikhoplav, *ALP Conference Proceedings*, **877**, 561 (2006), doi: 10.1063/1.2409184.
- [29]. S.Yu. Kalmykov, L.M. Gorbunov, P. Mora and G. Shvets, *Phys. Plasmas*. **13**, 113102. (2006), doi: 10.1063/1.2363172.
- [30]. G.V. Sotnikov, R.R. Kniaziev, O.V. Manuilenko, P.I. Markov, T.C. Marshall and I.N. Onishchenko, *Nuclear Instruments and Methods in Physics Research A*. **740**, 124-129 (2014), doi: 10.1016/j.nima.2013.10.087.
- [31]. K.V. Lotov, *Phys. Plasmas*. **5**(3), 785-791 (1998), doi: 10.1063/1.872765.

ОДНОРІДНЕ ФОКУСУВАННЯ ПОСЛІДОВНОСТІ РЕЛЯТИВІСТСЬКИХ ПОЗИТРОННИХ ЗГУСТКІВ У ПЛАЗМІ

В.І. Маслов, Д.С. Бондарь, І.П. Левчук, С.А. Ніконова, І.М. Онищенко

¹ Національний Науковий Центр «Харківський фізико-технічний інститут»

61108, Харків, вул. Академічна, 1

² Харківський національний університет імені В.Н. Каразіна

пл. Свободи 4, Харків, 61022, Україна

Плазмові прискорювачі забезпечують прискорюючи поля, які на кілька порядків більше, ніж у звичайних прискорювачах. В електрон-позитронних колайдерах дуже важливе фокусування електронних і позитронних пучків за допомогою кільватерного поля, збудженого в плазмі. Механізм фокусування в плазмі, при якому всі електронні згустки послідовності фокусуються однаково, був запропонований авторами раніше. Механізм фокусування послідовності релятивістських позитронних згустків в плазмі, при якому всі позитронні згустки послідовності фокусуються однаково і однорідне, досліджується в даній роботі шляхом числового моделювання з використанням 2.5D коду LCODE. У цій схемі фокусування необхідно, щоб довжина кожного згустку дорівнювала половині довжини хвилі $\xi_b = \lambda/2$, заряд першого згустку дорівнює половині заряду інших згустків послідовності, а відстань між згустками дорівнює півтори довжини хвилі 1.5λ . Числовим моделюванням досліджується самоузгоджена радіальна динаміка довгих згустків позитронів в однорідній плазмі. При моделюванні ми використовуємо гідродинамічний опис плазми. Іншими словами, плазма вважається холодною електронною рідиною, а позитронні згустки являють собою сукупність макрочастинок. Згустки позитронів розглядаються однорідними в поздовжньому напрямку циліндрами. Позитрони в згустках розподіляються в радіальному напрямку згідно гауссівському розподілу. Показано, що в цьому випадку тільки перший згусток знаходиться в кінцевому поздовжньому електричному полі $E_z \neq 0$. Решта згустків знаходиться в нульовому поздовжньому електричному кільватерному полі $E_z = 0$. Між згустками цієї послідовності поздовжнє електричне кільватерне поле і радіальна сила не дорівнюють нулю $E_z \neq 0$, $F_r \neq 0$. Фокусуюча радіальна сила в областях, зайнятих згустками, є постійною уздовж кожного згустку $F_r \neq \text{const}$. Між згустками радіальна сила неоднорідна. Всі позитронні згустки послідовності фокусуються однаково і однорідно.

КЛЮЧОВІ СЛОВА: фокусування згустків електронів, фокусування згустків позитронів, плазмова кільватерна лінза, прискорення частинок, чисельне моделювання.

ОДНОРОДНАЯ ФОКУСИРОВКА ЦЕПОЧКИ РЕЛЯТИВИСТСКИХ ПОЗИТРОННЫХ СГУСТКОВ В ПЛАЗМЕ**В.И. Маслов, Д.С. Бондарь, И.П. Левчук, С.А. Никонова, И.Н. Онищенко**¹ *Национальный Научный Центр «Харьковский физико-технический институт»
61108, Харьков, ул. Академическая, 1*² *Харьковский национальный университет имени В.Н. Каразина
пл. Свободы 4, Харьков, 61022, Украина*

Плазменные ускорители обеспечивают ускоряющие поля, которые на несколько порядков больше, чем у обычных ускорителей. В электрон-позитронных коллайдерах очень важна фокусировка электронных и позитронных пучков с помощью кильватерного поля, возбужденного в плазме. Механизм фокусировки в плазме, при котором все электронные сгустки последовательности фокусируются одинаково, был предложен авторами ранее. Механизм фокусировки последовательности релятивистских позитронных сгустков в плазме, при котором все позитронные сгустки последовательности фокусируются одинаково и однородно, исследуется в данной работе путем численного моделирования с использованием 2.5D кода LCODE. В этой схеме фокусировки необходимо, чтобы длина каждого сгустка была равна половине длины волны $\xi_b = \lambda/2$, заряд первого сгустка равен половине заряда остальных сгустков последовательности, а расстояние между сгустками равно полутора длины волны 1.5λ . Численным моделированием исследуется самосогласованная радиальная динамика длинных сгустков позитронов в однородной плазме. При моделировании мы используем гидродинамическое описание плазмы. Другими словами, плазма считается холодной электронной жидкостью, а позитронные сгустки представляют собой совокупность макрочастиц. Сгустки позитронов рассматриваются однородными в продольном направлении цилиндрами. Позитроны в сгустках распределяются в радиальном направлении согласно гауссовскому распределению. Показано, что в этом случае только первый сгусток находится в конечном продольном электрическом поле $E_z \neq 0$. Остальные сгустки находятся в нулевом продольном электрическом кильватерном поле $E_z = 0$. Между сгустками этой последовательности продольное электрическое кильватерное поле и радиальная сила не равны нулю $E_z \neq 0$, $F_r \neq 0$. Фокусирующая радиальная сила в областях, занятых сгустками, является постоянной вдоль каждого сгустка $F_r \neq \text{const}$. Между сгустками радиальная сила неоднородна. Все позитронные сгустки последовательности фокусируются одинаково и однородно.

КЛЮЧЕВЫЕ СЛОВА: фокусировка сгустков электронов, фокусировка сгустков позитронов, плазменная кильватерная линза, ускорение частиц, численное моделирование.

PACS :12.19. – g ; 12.90. + b

FORMALIZATION OF COGNITION PROCESS AS AN ADDITIONAL COMPONENT RESPONSIBLE FOR DEVELOPMENT OF THEORETICAL PHYSICS

Jarosław Kaczmarek

Institute of Fluid-Flow Machinery, Polish Academy of Sciences

80-231 Gdańsk, ul. J.Fiszera 14, Poland

E-mail: jarekk@imp.gda.pl

Received December 21, 2018; accepted 22 January 2019

Theoretical physics has attained stage when new methodological approaches should be taken into considerations. In particular they should introduce larger discipline in theoretical speculations. In this paper one introduces concept of cognition manifold as methodological framework for development of description of reality by theoretical physics with the aid of theoretical speculations. One assumes that this is a way for constructing fundamental and universal physical theories. The cognition manifold is composed of basis which represents models of our space as a medium and fibres representing models of processes in corresponding space. Models are based on accessible experimental results and also on new assumptions and hypotheses obtained by theoretical speculations. In order to maintain discipline in these speculations one considers status of assumptions and theories spanned on cognition manifold as a function defined on elements of fibres. One accentuates importance of selforganizing reasoning as more appropriate for recognition of reality in comparison with precise pure mathematical proof. One considers also proof with respect to reality. This paper is considered as an attempt to formalization of cognition process what is manifested by three main components: cognition manifold, status of assumptions and theories and concept of selforganizing reasoning.

KEYWORDS: methodology of constructing universal physical theories, cognition manifold, formalization of cognition process

1 Introduction

Contemporary theoretical physics manifests various attempts to description of reality. However, no clear methodology for doing this is elaborated. On the one hand one applies mathematics with precise proofs neglecting analysis to what degree this mathematics reflects reality. On the other hand one constructs many simplified models which reflect directly experimental results.

In both cases we should not be satisfied. Mathematics is a system placed on the inside of our brain and as such is not associated directly with reality. Simplified models which are constructed in accordance with chosen set of experimental results lead to theories which are not universal.

We try in theoretical physics to construct fundamental and universal theory as far as it is possible. This is so since universal theory is real success for our civilization. By means of universal theory we can predict many phenomena as well as to develop various applications.

One suggests that theoretical physics should consider two aspects: the first one is related to correct application of mathematics within physical theory and the second one is related to quality of fitting of the applied mathematical theory to reality.

Various methodologies are suggested within philosophy of physics. Let us mention rejection of theories by falsification [3]. This method is usually too radical since approximation of reality by theory is usually not entirely perfect. Then corresponding rejection could be associated with loss of context for further development of theoretical description. As a result of this development of theoretical physics could be stopped.

On the other hand introduction of a paradigm [4] allows us to continue development until more complete recognition of theory within this paradigm is obtained. Then, development of theoretical physics is more fluent. However rejection of paradigm with time seems also be too radical since

correctness of approximation of reality by theories are not usually entirely investigated. Let us mention range of validity of theory with respect to correctness of approximation of reality. This aspect is usually not investigated. We would say that each theory which had partial success approximates reality to some degree. Therefore such a theory should not be entirely rejected. Instead of this placement of theory with respect to its quality should be better determined taking into account especially its range of validity.

Let us note that fitting of theory to reality is usually estimated by accordance of theoretical results with experimental results. However, when we come to more fundamental theories usually related to smaller scales then conjugation of interpretation of experimental results and theory increases. We are not able to carry our precisely experiments in small scale and related to chosen particular phenomenon. We are usually forced to decipher obtained experimental results from more complex processes modelled within a given theory. Thereby, accordance of theoretical results and experimental results as well as interpretation of obtained experimental results depend on theory applied.

Let us consider an example. We observe that system of cosmological objects expands. It means that in the past all they should be close one to another. This leads to concept of Big Bang. Something small exploded and as a result of this we have to do with expanding system of astronomical objects. One assumes in theories that this explosion was associated with explosion of space and corresponding inflation associated with creation of pairs of particles and antiparticles. These particles, owing to unknown asymmetry, create contemporary matter.

On the other hand we can assume that we can admit explosion of space in very dense matter on the inside of giant black hole. Then we have to explain why such explosion of space could happen. This is possible when we neglect model of point-like particle. Then annihilation of electron and positron is associated with emission of electromagnetic radiation and also joining of components of electron and positron what leads to explosion of space in place of annihilation. Such a model of explosion of space and corresponding Big Bang model is based on three-positron structure of proton and is discussed in [16]. Within this model we understand what was exploded and why.

We frequently encounter interpretation of experimental results by one chosen theory. Let us mention that one suggests that neutrino have mass. This is interpretation obtained with the aid of the standard model and related to experimental observation that neutrino change their type with time during their motion. However we can admit the situation when neutrino can change their type and have mass equal to zero when we apply the vacuum medium mechanics [17].

We see that the same experimental results on expansion of system of astronomical objects and evolution of type of neutrino can lead to entirely different theoretical interpretations. Therefore we have to consider whether our methodology of modelling of reality is appropriate and whether we can improve this methodology.

By above comments we see that theoretical speculations in relation to physical reality have too large freedom. This is manifested by fact that considerable number of theories can lead to the same results as experimental observations having in mind also quantitative accordance of these results with theoretical prediction. The question is how we can reduce this excessive freedom in creation of theoretical models.

It seems that development of theoretical physics should be supported by formalization of cognition process. This is so since theoretical physics acts on front of cognition in order to recognize reality better. However our possibilities of recognition of reality are connected with our biology. In particular our brain is created in order to improve our cognition. On the other hand, it is not clear to what degree our brain is the only tool for recognition of reality by formal theories. Perhaps we are not able to identify other kinds of perception which take part in supporting of power of our cognition. Perhaps our emotions considered as a driven force for cognition process can be associated with not well understood forms of perception and will be difficult to formalization within a theory.

However taking into account all possible sources of cognition we cannot accept attitude associated with relinquishment of formalization of cognition process. This formalization should be continued as far as it is possible and should lead to placing of other possible mechanisms of cognition more precisely.

In order to provide context for discussion of quality of description of reality by theory one discusses

in [1], [2] ways describing how theory could appear in our world. To this end one introduces there evolving dynamical system within which logic and mathematics could appear as a result of interactions with external world. Important aspect of this approach is associated with interpretation of implication as related to action of the dynamical system in environment. As a result of this one introduces the notion "status" of assumptions applied to construction of theory and "status" of theory as property which is responsible for quality of approximation of reality by this theory. Consequently the notion of status joins our mathematics considered as internal system in our brain with external world. This in turn allow us to estimate criteria for determination which assumptions and theories are better fitting to reality in comparison with other ones.

Whole methodology based on formalization of cognition process was elaborated during formulation of vacuum medium mechanics. This theory is aimed at satisfying contemporary requirements for fundamental and universal theory. These requirements are related especially to description of dynamics for the smallest scale applied in modelling. This in turn is of key importance for determination of mechanisms of biological evolution or source of precision for theoretical nanotechnology.

Contemporary theories are based predominantly of geometry and symmetries and dynamics of processes on the smallest scales are seen as secondary importance. Furthermore scale of averaging applied in these theories are not well formalized. As a result of this various interpretations of experimental results are done for reality which is not seen by corresponding theories. Let us mention in this place the Higgs particle. Existence of particle in this place is really detected. However, this elementary particle is not observed directly. Instead of this one observes products of its decay. On the other hand this particle is produced during collisions of protons. It means that it is created directly near particles. However the standard model as quantum theory which replaces elementary particles by waves does not see processes directly near particles. Therefore the standard model is not appropriate theory for interpretation whether detected particle is the Higgs boson with complicated functions assigned to it.

We see in this place overinterpretation obtained with the aid of the standard model. All this justifies necessity of formalization of cognition process which should be seen as supporting construction of fundamental and universal theories.

2 A framework for formalization of cognition process based on dynamical systems

2.1 On emerging of mathematics within evolving dynamical systems

We discuss here some results from [1], [2] in order to provide sufficiently large context for discussion of formalization of cognition process.

We assume that our brain and whole biological organism is a dynamical system which can evolve. Thereby, we should look for context for discussion of quality of cognition process by theory based on dynamical systems.

We introduce here dynamical system which can undergo evolution and is able to generate cognition process. Let us assume namely that our dynamical system contains the following subsystems: the neural network dynamical system (N), motor system (M), sensor system (S), environmental dynamical system (E) and the main dynamical system (\mathcal{M}).

All introduced subsystems interact by assumption. Source of activity follows from the main dynamical system. It can interact with environmental dynamical system immediately or by means of neural network, motor and sensor systems.

We distinguish the following groups of variables of our dynamical system: $x_E, x_N, x_M, x_S, x_{\mathcal{M}}$. In particular, for description of interactions we distinguish subgroups of variables which take part in these interactions directly. They are specified within the following dynamical systems

$$\dot{x}_E = A_E(\bar{x}_E, x_{EM}, x_{ES}, x_{EM}; x_{ME}, x_{SE}, x_{ME}), \quad (1)$$

$$\dot{x}_M = A_M(\bar{x}_M, x_{ME}, x_{MN}; x_{EM}, x_{NM}), \quad (2)$$

$$\dot{x}_S = A_S(\bar{x}_S, x_{SE}, x_{SN}; x_{ES}, x_{NS}), \quad (3)$$

$$\dot{x}_N = A_N(\bar{x}_N, x_{NM}, x_{NS}, x_{NM}; x_{MN}, x_{SN}, x_{MN}), \quad (4)$$

$$\dot{x}_M = A_M(\bar{x}_M, x_{ME}, x_{MN}; x_{EM}, x_{NM}). \quad (5)$$

Particular groups of variables specify parts of subsystems interacting. We discuss the notation for the first subsystem as example, where $x_E = \{\bar{x}_E, x_{EM}, x_{ES}, x_{EM}\}$. Variables $\{x_{EM}, x_{ES}, x_{EM}\}$ are designed to describe interaction with other subsystems. On the other hand x_{ME}, x_{SE}, x_{ME} represent subgroups of variables of remaining subsystems within the first one also in order to describe corresponding interactions.

We do not specify here how such a dynamical system evolves. This is not necessary for our considerations at this moment. However we accentuate this fact since it is important for future investigations on this line as well as for further discussion. Consequently, we introduce here an abstraction level for our considerations. Particular determination of the dynamical system could be seen as entirely separate problem and perhaps even branch of knowledge. This could be associated with considerations related to biology. However, corresponding determination of the dynamical system can also have entirely abstract form and can be considered within pure mathematics.

Subsystems are designed to describe particular properties of the whole system. Consequently, the external dynamical system describes behaviour of an environment in which the subsystem $S_A = S_M \cup S_N \cup S_M \cup S_S$ acts. Driven force for such an action is generated by the subsystem S_M . It can interact with the environment directly or realize an action by means of neural network system and motor and sensory system.

Concept of subsystems suggest that S_M represents the highest level of complexity of an autonomous system which can be interpreted as a living organism for instance. It has to survive in the environment. Therefore this system generates an action. In particular this action is associated with an attractor defined within the main dynamical system.

Whole system $S_T = S_E \cup S_M \cup S_N \cup S_M \cup S_S$ is called here the total system. Then, S_E stand for environment dynamical system and S_A is called here the autonomic dynamical system.

Introduced above dynamical system is intended to describe a kind of brain surrounded with some functional subsystems in an abstract form. In particular, having in mind such a concept, the neural network system is introduced.

Logic appears when we have at our disposal a system of formulas and ability to determination of the true. In order to construct the system of formulas we have first to define terms [22].

Terms have to be considered here within the neural network system. We assume that they are associated with action of motor and sensor systems by means of the functions π_{SN} and π_{MN} . They transform the set of variables of the sensory system V_S and motor system V_M into set of variables of the neural network system V_N . Thus we have $\pi_{SN} : V_S \rightarrow V_N$ and $\pi_{MN} : V_M \rightarrow V_N$. Both functions are determined by means of previously introduced dynamical system (1)-(5).

The set of terms induced by dynamical systems S_M, S_S is defined by

$$T = \pi_{MN}(V_M) \cup \pi_{SN}(V_S). \quad (6)$$

The set T contains variables associated with motor and sensor systems expressed within the neural network system.

When we construct theory then the set of terms T is contained in the set of formulas F [22]. Consequently, the question is how we define next elements of the set F . In order to do it we should have at our disposal relations as well as possibility of taking conjunction, alternative, negation and

implication. They should be expressed within the neural network. Therefore we should discuss a way on which such notions could happen in the neural network.

Let us notice that conjunction, alternative and negation seem to be relatively simple in order to express them in the neural network. The word "and" is easily understood as a primary notion. Negation appears also in a natural way as opposition to "satisfying a relation". Alternative has a similar level of complexity.

Implication seems to be more complicated and also more important for logic. Its role in proving of the true is crucial. Furthermore, it is not evident directly how to introduce implication. In classical logic the implication is introduced formally by assumed way of valuation. However, intuition associated with implication suggests a causality. This in turn suggests that implication is not entirely internal notion related to the neural network system. It should be associated with processes in the environment induced by the dynamical system S_A in order to reflect the causality. In this case environment play role of real world. Thereby, we should postulate a way for introduction of implication in our dynamical system.

We admit in general evolution of introduced subsystems. In particular this is the case for the neural network dynamical system. At this moment we do not discuss particular mechanisms of such an evolution. We expect in general that development attained by this evolution leads to possibility of generation of relations, formulas and methods of valuation of sentences. In particular relations could appear as a result of action of the main dynamical system which will be discussed below.

We decide which mechanism of evolution is admitted into considerations. Thereby, we discuss then an abstract system which could generate logic and a kind of thinking. Consequently, using such a way of modelling we should be motivated by concepts of phenomena which we would like to obtain as properties of our dynamical system. Let us discuss some properties related to logic which could appear during modelling of a reality.

Let \mathcal{A}_T be an attractor within the total system S_T defined predominantly by S_M and let $x_T = \{x_E, x_N, x_M, x_S, x_M\}$ belongs to the set of attraction of this attractor. Then evolution of x_T represents various processes undergoing selforganization.

Let us define the external process with respect to the main dynamical system as described by mapping $\pi_{ext}(x_T(t)) = \{x_E, x_N, x_M, x_S\}(t)$ following from (1)-(5).

DEFINITION 2.1: Induction of an external state process with respect to the main dynamical system by a process of the main dynamical system $x_M(t)$ immersed in the total state process $x_T(t)$ is called action of the main dynamical system.

Action is manifested by direct interaction of the main dynamical system with environment or by induction of processes in the neural network system and by this induction of action of the motor dynamical system in environment. In the second case we have to do with induction of a process in environment by S_M and next detection of changes in this environment by the sensor dynamical system.

We expect that actions of S_M are frequent sufficiently in order to provide considerable amount of data related to properties of environment. Then, results of each action are remembered within the neural network. When some properties of environment would happen repeatedly, then our model having by assumption property of optimization of energy consuming should manifest more strong remembering of effects corresponding to these properties. By this we expect generation of relations between state of variables which are present on the input of the motor system and output of the sensor system. Consequently we suggest generation of relations reflecting properties of the environment, within neural network system. Such relations can be applied for extension of the set of formulas F .

Let us introduce here implication by means of the action of the main dynamical system defined above. Thus we obtain

$$(x_{NM})_A \Rightarrow (x_{NS}), \quad (7)$$

where $x_{NM}, x_{NS} \in T$ and the symbol $_A \Rightarrow$ stands for operation of induction of action A of the system

S_M by means of states $\pi_{MN}^{-1}(x_{NM})$ and appearing of the response $\pi_{SN}(x_{SN}) = x_{NS}$ from the system S_S . Let us note that action A has to be considered beyond the neural network dynamical system.

Let us notice that our implication is indexed by kind of action A . Therefore we have to do here with a family of implications in fact. We can introduce more universal implication as

$$(x_{NM} \wedge A) \Rightarrow (x_{NS}), \quad (8)$$

In this case we have to do with two sentences on the left side of implication. The first one states that x_{NM} takes a value and the second one states that action have a determined kind. Then, implication follows the sentence that x_{NS} takes a determined value which can be written more formally using sentences

$$((x_{NM} = a) \wedge (A = A_G)) \Rightarrow (x_{NS} = b) \quad (9)$$

which is shortly written by (8).

Let us notice that we can also consider action of S_M which happen in neural network only. To this end we can distinguish subsystems within S_N . Then, let

$$S_N = \bigcup_i (S_{NMi} \cup S_{Ni} \cup S_{NSi}) \cup S_H, \quad (10)$$

where S_{NMi} is i -th motor subsystem within the neural network, S_{Ni} is i -th part of the neural network system, S_{NSi} is i -th sensory subsystem within the neural network. The S_H stands for a part of the neural network able to analyse information obtained by means of S_{NSi} following from action within the system S_{Ni} . The system S_H also generates action in S_{Ni} . Distinguishing of the subsystems enables us to discuss realization of action of the main dynamical system which is closed within part of the neural network.

Discussed above division of neural network into subsystems enables us to discuss implication similar to that one given by (7) which happens on the interior of the neural network only. We can consider the set of terms in relation to i -th subsystem by T_i . We assume as previously that they are associated with action of motor and sensor systems S_{NMi} , S_{NSi} by means of the functions π_{SNi} and π_{MNi} . They transform the set of variables of the sensory system V_{Si} and motor system V_{Mi} into set of variables V_H of the part S_H of the neural network system. Thus we have $\pi_{SNi} : V_{Si} \rightarrow V_H$ and $\pi_{MNi} : V_{Mi} \rightarrow V_H$.

The set of terms induced by dynamical systems S_{NMi} , S_{NSi} is defined by

$$T_i = \pi_{MNi}(V_{Mi}) \cup \pi_{SNi}(V_{Si}). \quad (11)$$

The set T_i contains variables associated with motor and sensor systems S_{NMi} , S_{NSi} expressed within the subsystem S_H .

Consequently, the implication followed by action within the neural network system can be expressed as

$$(x_{NMi} \wedge A_{NN}) \Rightarrow (x_{NSi}), \quad (12)$$

where A_{NN} represents a kind of action of S_H in the S_{Ni} .

Let us note that S_H represents a system which is able to analyse results of action and transfer of input into S_{NMi} . However, the action is induced in fact by the main dynamical system governing the S_H .

Having at our disposal action in neural network system we have also an opportunity to comparison of the action A from (9) with an action of type A_{NN} created within the neural network system. Then, a model of reality represented by A_{NN} is produced in case when effects of both actions are the same or similar within the neural network.

We have determined how implication appears within evolving dynamical system. By this we can imagine how proof of a theorem could happen. However, we see also that each step of the proof is

associated with an action of dynamical system. In case when this action happens in neural network system we have the problem to what degree each step of the proof fits to reality. Each step is associated with an approximation of reality. Thereby increasing of length of the proof should lower status of formula obtained by this proof.

2.2 Consequences of dynamical system approach for estimation of status of assumptions and theories

Having at our disposal context provided by dynamical systems as in [1], [2] we can discuss status of assumptions in relation to formulas induced by dynamical system as well as in relation to length of proof applied in inferring on form of these assumptions. We discuss also factors which decide on status of whole theory.

Let us discuss concisely some remarks obtained in [1] in order to illustrate how the term "status" can be usefull.

REMARK 2.1: Fundamental notions of theory describing reality should be related to maximum engagement by action of the dynamical system and its sensory system in order to obtain results which next can be interpreted as the simplest information by neural network system. Then, status of such a fundamental notion is viewed as high.

REMARK 2.2: Status of assumptions introduced into theory by means of proofs based on observed properties depends on length of the proof. The longer proof the lower status of assumption. This status could be increased when several independent proofs starting from independent facts would lead to the same conclusion inducing just this assumption.

Above remark follows from fact that implication is considered here differently from conjunction, alternative and negation. Implication is related to action of the dynamical system what shed light on role of proof in relation to reality. The length of the proof characterizes amount of action which when increases gradually decreases correctnees of approximation of reality. It means that recognition of reality is then less direct.

Frequently we obtain representation of a function describing a physical phenomenon as expansion in a series. Then, particular terms can be associated with a physical interpretation. This can be useful for introduction of fundamental assumptions into theory. However, expansion into series depends in general on option of a basis and this option can be in fact rather arbitrary. Therefore, physical interpretation is rather risky in this case. Consequently we come to the following remark:

REMARK 2.3: Fundamental notions obtained with the aid of expansion of a function into series have low status since this expansion depends on arbitrary option of a basis. This status could be higher in case when corresponding basis would have appropriate physical interpretation. However, in general, infinite series should not have good physical interpretation since there is small chance to assign appropriate interpretation to each term. Cutting of such a series to finite number of terms is also an arbitrary option with respect to physical interpretation.

Above remark suggests that we should avoid to construct physical theory with the aid of fundamental assumptions based on expansion of a function into a series. We have also remark related to status of whole theory as follows:

REMARK 2.4: We would say that status of theory depends on number of assumptions applied to construction of this theory, status of each assumption with respect to criteria discussed previously, range of validity associated with universality of theory and with status of logic.

Above remarks are useful for constructing universal and fundamental theories of our reality by pos-

sibility of estimation how theory fits to reality [1]. However, this methodology is not finished yet. Further ideas are expected. In this paper one introduces concept of cognition manifold which has several tasks. The first task is related to obtaining increasing of possibility of inference in relation to reality by making more clear whole methodology. The second task is related to creation of possibility of generation of context for description of reality. This context indicates how theories should evolve. Next task is associated with form of gathering of whole information on the subject how hitherto developed descriptions have been evolved. This task also supports development of the context.

Let us note that the term "status" is not entirely precisely determined. This is so since it estimates relation between internal theoretical system and external world. However we have at our disposal internal theoretical system only. By model of interactions of dynamical system with external world we can estimate what is better for recognition of reality. Consequently model of evolving dynamical system interacting with an environment allows us to understand better how the cognition process is continued. Such an understanding allows us in turn to estimate which ways of cognition are better and which are worse. This is manifested just by the term "status". Thereby we should not expect very precise definition of status. We expect rather possibility of estimation which status of assumption is higher and which is lower by inequality relation and some ordering.

We can see that obtaining of any criterion for estimation of status is success on way towards formalization of cognition process.

3 On inductive reasoning for theoretical descriptions of reality

Inductive reasoning is applied frequently to creation of various generalizations based on a set of experimental results. This kind of reasoning is important and frequently applied in pure theoretical physics. We would like to place this methodology within concept of cognition manifold as important method of reasoning.

Inductive thinking in relation to theoretical description is associated usually with property connected with an integer number and leads to a generalization of previous theory. Let us mention for instance inductive thinking, frequently applied in physics, on dimension of our space.

It would be convenient to have at our disposal more formal approach to this procedure as well as placement of this procedure in methodology of whole description of reality.

Let ϕ_{In} be a notion within a theory Th_n which is associated with an integer number n . Then generalization of theory Th_n to theory Th_{n+1} is associated with transformation of notion ϕ_{In} to the notion $\phi_{I(n+1)}$ and next development of theory Th_{n+1} which should contain $\phi_{I(n+1)}$. However this development of new theory is not arbitrary.

Theory Th_n is usually constructed taking into account a set of experimental results. Therefore the new theory also should be in accordance with this set of experimental results. We can express this fact by means of a mapping $P_{In} : Th_{n+1} \rightarrow Th_n$. Mapping P_{In} should express the property that approximation of reality corresponding to processes associated with property ϕ_{In} by theory Th_{n+1} is sufficiently well. In other words image of mapping P_{In} considered as a theory describes reality sufficiently well in sector where Th_n acts satisfactorily.

Consequently, we can illustrate scheme of inductive thinking placed within methodology of generating of new theories in the following general form

$$\begin{array}{ccc}
 n & \longrightarrow & n + 1 \\
 \uparrow & & \uparrow \\
 \phi_{In} & \longrightarrow & \phi_{I(n+1)} \\
 \uparrow & & \uparrow \\
 Th_n & \xleftarrow{P_{In}} & Th_{(n+1)}
 \end{array} \tag{13}$$

Within above scheme horizontal arrows are associated with sequential inductive steps. Vertical arrows are associated with assignation of notion undergoing induction for a given theory and also assignation of number representing step of induction for notion undergoing induction.

Let us discuss some examples of inductive reasoning. We can consider $\phi_{I_n} = U_n(\mathbf{X}_n)$, where U_n is an neighbourhood of a chosen point of space \mathbf{X}_n . Then, we can extend our theory to larger space by adding new set $\phi_{I(n+1)} = U_{n+1}(\mathbf{X}_{n+1})$. Then our space is expressed by

$$X = X_{n+1} = \bigcup_{i=1}^{n+1} U_i(\mathbf{X}_i) \quad (14)$$

and theories describing behavior of our space have the same form. It means that the mapping P_{I_n} represents cutting of theory from the set X_{n+1} to the set X_n . This kind of induction could be named transitive since definition of the mapping P_{I_n} and construction of theory $Th_{(n+1)}$ is direct and evident. On this way we extend our theory into whole space which has regions not attainable for us.

Another example can be associated with scale of averaging applied in modelling. Let $\phi_{I_n} = d_n$ be a distance which determines a volume on which properties of the medium are averaged. Then transition to next $\phi_{I(n+1)} = d_{n+1}$, where $d_{n+1} < d_n$ is not so direct as in previous case where theory was unchanged. Within smaller scale we see new phenomena. Then, mapping $P_{I_n} : Th_{n+1} \rightarrow Th_n$ can be considered for instance as $P_{I_n} = DR$, where DR is dimensional reduction procedure considered in [5] where multiscale modelling is discussed.

In this last case we see necessity of stopping of this inductive thinking for some $n = N$ associated with length d_N . Indeed our notion of a distance follows from possibility of recognition of this distance in our space by various phenomena including electromagnetic waves. The question is to what degree our space is three-dimensional with possibility of considering a distance in this space. In other words we have the problem how small distances we can consider at all in theoretical description.

Perhaps, for sufficiently small distances we have to activate another kind of inductive thinking. In particular this can be dimension of space. Then, $\phi_{I_n} = \dim X$, and P_{I_n} will represent projection of space from larger dimension space to smaller dimension space having in mind all processes expressed in theory Th_{n+1} . Then, we expect that image of mapping P_{I_n} should approximate processes described by theory Th_n appropriately.

Problem of stopping of inductive thinking is important. In last two cases generated theories in each step of inductive reasoning are not similar. Therefore such an induction is not direct. We should analyse which notions applied in theory have inductive character.

Let us consider notion of deformation applied in continuum mechanics. We consider there deformation function $\mathbf{x}(\mathbf{X}, t)$, where \mathbf{X} is a reference configuration. When we diminish scale then we should interpret medium together with corresponding reference configuration. We obtain relative motion of something with respect to something else. Usually in smaller scale we will interpret and model this background. However, when we introduce again the deformation function for this smaller scale then we should interpret again new background for still smaller scale. Thereby, so important notion for modelling of physical processes as deformation function provokes infinite step inductive thinking. Evidently we have to pose the question how to stop such an inductive thinking. We see that some notions are open with respect to inductive reasoning.

It seems that stopping of inductive reasoning needs deep analysis of notions which are fundamental for this induction. Let us mention for instance "distance" and "direction" as fundamental for inductive diminishing of scale. We could describe theoretically where from such notions appear in relation to processes which are entangled in corresponding notions. Let us mention stright propagation of light or motion of single elementary particles. All they are responsible for our understanding of our geometry. Then we should organize hypotheses more fundamental than direct description of these processes and by this estimate to what degree notions associated with our induction could be changed. This in turn could provide premises for stopping this kind of induction.

4 Concept of cognition manifold as theoretical environment for evolution of universal and fundamental physical theories

By means of theoretical physics we try to introduce an universal description of reality taking into account a set of observed properties or phenomena. We assume that this set should be large as far as it is possible. We try to construct models describing corresponding properties and phenomena in an unified manner. Methodology corresponding to this unified manner of description is not entirely clear and needs development. We are forced frequently to introduce various hypotheses which perhaps are not entirely verified by experimental results. Consequently, we would like to have at our disposal methods of estimation to what degree such hypotheses are appropriate in this unified description.

Methods of modelling need possibility of expression of particular observed property or phenomenon by means of theory based on a system of fundamental notions. Thereby, we should have at our disposal sufficiently complex theoretical environment for description of mentioned above properties and phenomena in order to express them correctly.

To this end, at first stage of our considerations, we introduce the set $\mathcal{B} = \{\{\tilde{X}_p, \lambda_p\}\}$ of models of our space, where \tilde{X}_p is a geometrical space composed of points and $\lambda_p = \{\lambda_{pi}\}$ is a set of variables which determines fundamental states of our space considered as fields $\{\lambda_{pi}(\mathbf{X})\}$, $\mathbf{X} \in \tilde{X}_p$ on the domain \tilde{X}_p . Consequently we use here the term "space" in various context. This should be commented more precisely.

We have not introduced time yet. Our variables which determine fundamental states correspond with admissible configurations which can be attained within \tilde{X}_p . Consequently fundamental notion is connected here with the change of state of our medium. Then various variables can represent changes of various states. They can be compared. This leads to definition of time.

Time can be defined as parameter which measures relative rate for changes of one state with respect to another one. By this we can introduce processes. Consequently time is not fundamental notion. Time appears in this case as parameter related to rate of one process with respect to another which can be considered as a reference process.

Time can be rescaled in theoretical considerations. The question is whether time is changed or rate of process is changed. These problems are not equivalent. In case when we assume that time is changed then we assume in fact that all rates of processes which can be considered as reference processes for time measurement undergo the same change. This is very strong assumption which needs experimental confirmation. Fulfilling of such a condition by reality seems to be rather improbable. Therefore, it seems more reasonable to consider time classically. Change of this point of view could be based on more carefull experiments related to rate of processes.

We consider mathematical context for modelling of various phenomena which is created in our brain. Then we have at our disposal various mathematical objects. In particular we can consider a point of three-dimensional space. On the other hand we consider context related to reality which is described by a mathematical theory. In accordance with previous discussion on status of mathematical notions and theories we see necessity of considering connections between reality and mathematical description. We have stated there that theory approximates reality.

Let us note that point is important object for mathematics. However in reality point is nothing. Mathematical point is applied to approximation of reality. We observe that our vacuum has various states manifested among others by electric field for instance. Thereby our space cannot be identified with an Euclidean three-dimensional space directly since such a space has no states. Therefore real space has to be identified with a medium which is associated with a geometrical space.

Consequently our Euclidean three-dimensional space is considered as domain of fields in vacuum medium and represents an element of mathematical approximation of reality considered as a medium. Then role of single point is assigned to possibility of expression of properties of this medium within assumed method of approximation.

Frequently, in theoretical physics one considers the problem whether our space is continuous or discrete. This is not well posed question. The question is how we approximate our space. Our brain

uses finite-dimensional neural network. Therefore we see better discrete objects by theory. Continuum description is a kind of approximation of reality. In particular we should apply continuum with finite-dimensional fields for correct approximation of reality [5], [10], where scale of averaging applied to modelling is introduced in formal way.

In general methods of approximation are associated with formalization of scale of averaging applied during modelling of processes. In large scale geometry is detected by our organism by determination of direction and a distance. In smaller scale we recognize these quantities by motion of particles and also by propagation of electromagnetic waves. Therefore we consider three-dimensional space as domain for our medium.

The question is whether we can violate assumption on this dimension. This has been discussed in context of inductive thinking. We should have at our disposal hypotheses creating foundations for changing dimension of domain of vacuum medium in relation to sufficiently small scale and also mapping P_{In} which joins the smaller scale models with larger scale models. Let us note that corresponding scale should be smaller than particles which determine direction by their motion. This scale should be smaller also than processes governing propagation of electromagnetic waves. However then we encounter new problem how to measure a distance. Some attempts in this direction have been done in [9].

Let us note that understanding of empty space is much more difficult than understanding of space considered as a medium. Therefore we have assumed that our space has to be considered as a medium.

At this moment of our considerations we do not introduce energy yet. Variables within λ_p determine all configurations of the vacuum medium and are rather of kinematical type. Energy can be expressed by means of these variables in what follows.

Let us consider a set of phenomena observed in reality and expressed as properties ϕ_k , $k \in I_N = \{1, 2, \dots, N\}$. We assume that corresponding properties and phenomena are characterized by evolution of variables λ_{pi} for a given p corresponding to p -th model. We introduce now, as a first stage, qualitative modelling what means that we do not determine of all constants within the model but we are concentrated on fact that the model is able to describe qualitatively the chosen property ϕ_k .

Let us mention for instance waving of components within vacuum medium [6], [7] or precession of electron [8] as separate phenomena for modelling. Models of these phenomena are introduced with the aid of accessible premises. It is difficult to determine immediately all properties of vacuum medium responsible for so important phenomena as evolution of wave function of electron or mechanisms of precession of electron. We try to introduce some qualitative models as first stage of description. Thereby introduced models are considered as starting point for modification of corresponding models as well as looking for opportunity for determination of constants of these models necessary in future development of whole theory of interacting phenomena.

Let us consider the phenomenon considered in reality and expressed by ϕ_k . Then various models which describe this phenomenon we denote by $m_{\phi_k i}$. Consequently they are equivalent with respect to property ϕ_k since they describe the same property. This can be expressed by the formula

$$m_{\phi_k i} \equiv_{\phi_k} m_{\phi_k j} . \quad (15)$$

Then whole equivalence class of corresponding models associated with the property ϕ_k is denoted by \mathcal{M}_{ϕ_k} . Consequently we introduce the set

$$\mathcal{M}_{\phi} = \bigcup_k \mathcal{M}_{\phi_k} . \quad (16)$$

The set \mathcal{M}_{ϕ} represents all models considered by theory for various phenomena observed. The question is how we should tend towards universal theory with the aid of models contained within the set \mathcal{M}_{ϕ} .

One suggests to consider the cognition manifold as composed of the set \mathcal{B} as basis on which some fibres represented by elements of \mathcal{M}_{ϕ} are determined. To each model we can assign its status.

Consequently, status of elements of fibres is a function which next is useful for characterization of status of whole theory constructed.

We should have better characterization of sets \mathcal{M}_{ϕ_k} and also \mathcal{B} . Let us discuss structure of the set \mathcal{B} in more details. Let us assume that we have several concepts of our space expressed by $\{\tilde{X}_p, \lambda_p\}$. To each \tilde{X}_p we can apply inductive generalizations having a number of steps.

Let us introduce set of multiindexes denoted by $\tilde{I}_L = \mathcal{I}_1 \times \mathcal{I}_2 \times \dots \times \mathcal{I}_L$, $\mathcal{I}_l = \{1, \dots, N_l\}$, $l = 1, \dots, L$, where l represents kind of induction applied, N_l represents number of inductive step of the same l -th kind. Particular multiindexes are denoted by $I_l \in \tilde{I}_L$. Thereby we have then that for each p we have $\{\{\tilde{X}_{pI_l}, \{\lambda_{pI_l i}\}\} : I_l \in \tilde{I}_L\}$. The multiindex $\{p, I_l\}$ belongs to $I_{\mathcal{B}}$. Then our \mathcal{B} takes the form

$$\mathcal{B} = \bigcup_{\{p, I_l\} \in I_{\mathcal{B}}} \{\tilde{X}_{pI_l}, \lambda_{pI_l}\}. \quad (17)$$

Consequently we admit several inductive steps of one kind and next several inductive steps of another kind indexed by l applied to one element of basis in order to generate next elements of this basis.

The aim of introducing of fibres \mathcal{M}_{ϕ_k} is to describe processes described in elements of \mathcal{B} taking into account various ways of modelling of these processes. In particular we should obtain possibility of estimation of status of introduced notions and hypotheses in models which appear in fibres.

Our models should have connections with reality. Thereby we should have at our disposal experimental results. We assume that we have at our disposal the set of sentences $\mathcal{E} = \{e_1, \dots, e_m\}$, which expresses just experimental results. Then, we can apply to the sentences e_i inferring based on an assumed logic. We can create by this inferring a mathematical minimal representation of phenomena expressed with the aid of e_i . It means that we introduce the most simple formulas to description of them without any additional postulates.

Minimal mathematical representation provides a system of assumptions which have high status. They are considered as starting point for formulation of various models of corresponding phenomena with the aid of additional assumptions having lower status.

We construct fibre on basis \mathcal{B} in relation to a chosen property ϕ_k . The fibre is indexed among others just by ϕ_k and is composed of models which have gradually increasing number of assumptions with increasing distance from basis.

We construct first the model m_{ϕ_k} for property ϕ_k with the aid of deductive skeleton expressed by a minimal representation of ϕ_k interpreted within \mathcal{E} . Within this skeleton we develop more detailed models $m_{\phi_k i}$ by means of additional hypotheses by application of new assumptions, inductive reasoning or abduction. We try to estimate status of introduced hypotheses which should gradually become lower when we go away from basis along fibres.

On this level of constructing of theories we have to do with speculative thinking. Let us mention a remark from [1] on this kind of reasoning. Let $St(A_1) < St(A_2)$ means that status of assumption A_2 is higher than status of A_1 . Let us consider the following remark:

REMARK 4.1: Speculative thinking needs changing of assumptions within the same theory. We should introduce hierarchy of assumptions by estimation of their status. Consequently, let $St(A_1) < St(A_2) < \dots < St(A_N)$ be set of assumptions of a given theory ordered with respect to their status. Then, we should first change assumptions of the lowest status during speculations and gradually do it going towards the largest status assumption A_N . Consequently, A_N should be the most stable during the speculative thinking. It means also that introduction of extra assumptions which makes constructing of theory more simple is interpreted as lack of discipline. We can admit sometimes corresponding extra assumptions. However, we should assign to them sufficiently low status.

Above remark manifests the fact that even in speculative thinking we are able to maintain a discipline and responsibility.

Let us introduce multiindex $M_s \in \bar{M}_s = \{\{\bar{M}_{s-1}, J_s\}, s \in N, \bar{M}_1 = J_1, J_s = \{q : q \in$

$\{1, 2, \dots, N_s\}$. Consequently, we denote model m_{ϕ_k} by $m_{\phi_k M_1}$. It means that on the first level we can introduce N_1 models based on minimal representation corresponding to ϕ_k . Perhaps the number N_1 should be equal to 1. This is so since perhaps minimal representation should be the only one.

Within the minimal mathematical representation we introduce additional hypotheses and assumptions in order to create new models indexed by $m_{\phi_k M_s}$. We do this since our theories are usually not complete with respect to their ability to description of reality. Experimental results cannot be related to all aspects of reality. Therefore within minimal mathematical representation which has just direct relation to experimental results we carry out theoretical speculations which seem to have connections with reality with some probability. We use to this end among others intuition in order to extend context for reasoning.

As a result of this activity we obtain the relation $m_{\phi_k M_{s-1}} <_{AH} m_{\phi_k M_s}$. The relation $<_{AH}$ means that the model $m_{\phi_k M_s}$ is obtained directly from the model $m_{\phi_k M_{s-1}}$ by adding to the last model additional assumptions. Adding of new set of assumptions can be continued on various ways. Each way is represented then by element of the set J_s .

Let us explain this more precisely. Consequently, J_1 represents set of theories $\{Th_i, i \in J_1\}$ each of them is constructed with the aid of set of assumptions $TA_i, i \in J_1$. Adding new assumptions modifies theories Th_i into Th_{ij} , where $j \in J_2$, which are based on set of assumptions $TA_{ij}, i \in J_1, j \in J_2$ and so on. We assume furthermore that no assumptions is added when $j = 1$. In other words theory $Th_{111..11}$ is identified with Th_1 as well as $Th_{111..51}$ is identified with $Th_{111..5}$ for instance. The last step allows us application of introduced multiindexes also for not modified theories. We identify all our models $m_{\phi_k M_s}$ with such theories assuming the same method of application of indexes.

By means of the method of indexing by multiindexes M_s we can characterize a group of subfibres assigned to the property ϕ_k . We define fibre associated with ϕ_k as set of models $\tilde{m}_{\phi_k n_1 \dots n_s} = \{m_{\phi_k n_1}, \dots, m_{\phi_k n_1 \dots n_s} : n_1 \in J_1, \dots, n_s \in J_s\}$. Then each subfibre is represented by set of multiindexes $\{n_1, \dots, \{n_1, \dots, n_s\}\}$ which in turn represents models with increasing complexity. When model for a given n_j is not modified with increasing s then we endow the same model with additional index equal to 1. Thereby some subfibres can be indexed by multiindex containing several numbers equal to 1. The model $m_{\phi_k n_1 \dots n_s}$ represents end of subfibre.

Consequently, the model $m_{\phi_k n_1}$ obtained at first stage of modelling when $s = 1$ has assumptions with the highest status since they are based on minimal mathematical representation. However, this model is usually not sufficiently complex in order to satisfy our expectations in modelling. Therefore we create additional new assumptions. Next models are then obtained by additional assumptions based on hypotheses, inductive thinking or abduction. Corresponding assumptions have gradually lower and lower status with increasing of number s . However status of whole models as theories increases since they describe reality better owing to their larger complexity

Lack of appropriate complexity in first constructed models follows from fact that assumptions based on minimal mathematical representation indicate new ways for modelling of more complex unknown world. Let us mention an example from [9]. Observed magnetic properties of electron discussed there leads to introduction of variables which characterize state of deep structure of vacuum medium. Properties associated with corresponding variables are considered just as minimal mathematical representation. This is so since the only premises which are taken into account follow from experimental results. We need then additional hypotheses in order to introduce more complete description.

On basis of the minimal representation we introduce in [9] deep structure of vacuum medium with states represented by magnetic field and two-ring field. Within this medium interacting magnetic monopoles can be considered. In particular network of bounded monopole-antimonopole pairs creates our space seen on more averaged level as homogeneous.

Let us assume that we have a set of properties $\phi_k(p, I_l)$. We assume that the index k is related to kind of property denoted by ϕ_k . Remaining indexes stand for indication of element of basis in which the property or phenomenon is expressed. We introduce our concept of cognition manifold by the following definition:

DEFINITION 4.1: By cognition manifold we understand the following object

$$\mathcal{M}_{COGN} = \left\{ \bigcup_{k, \{p, I_l\}, M_s} \tilde{m}_{\phi_k(\{p, I_l\}M_s)}, \mathcal{E}, \mathcal{S} \right\} = \{ \mathcal{M}, \mathcal{E}, \mathcal{S} \}, \quad (18)$$

where \mathcal{S} represents function which assigns status to each model.

Let us note that the function \mathcal{S} assigns status to each model considered as a theory of a given phenomenon. However we have introduced previously also status of assumptions. Status of a model m_i denoted by $\mathcal{S}(m_i)$ depends in general on status of assumptions $St(A_{ij})$ applied to formulation of this theory. Thereby we have assumed that $\mathcal{S}(m_i) = \Phi(\{St(A_{ij})\})$, where $\{A_{ij}\}$ is set of assumptions for i -th model.

Let us assume that we have estimated status of each model describing a given phenomenon $\phi_k(\{p, I_l\})$ as $S(m_{\phi_k(\{p, I_l\}M_s)})$. We define cross-section within the set \mathcal{M}_{COGN} as follows

$$\mathcal{C}(\mathcal{M}_{COGN}) = \{ \bar{m}_{\phi_k(\{p, I_l\})} : \bar{m}_{\phi_k(\{p, I_l\})} \leftarrow \max_{M_s} S(m_{\phi_k(\{p, I_l\}M_s)}), \{p, I_l\} \in I_{\mathcal{B}} \}, \quad (19)$$

where \leftarrow means operation of option of the model having the highest status within set of models placed at the end of each subfibre. The end of subfibre means that s stands for largest number attained during modelling. By taking the cross-section we chose one element within whole group of subfibres indexed by M_s and related to a given fibre indexed by ϕ_k . The option is based on estimation of status of the model and its comparison with status of other models within group of last elements of subfibres indexed by M_s and defined by application of the relation $<_{AH}$. In other words we assign one, the best model of a given phenomenon ϕ_k to a given fibre within our way of speculation. We do it for each phenomenon considered during description.

The set $\mathcal{C}(\mathcal{M}_{COGN})$ can be decomposed into the sets

$$\mathcal{C}(\mathcal{M}_{COGN}) = \bigcup_{\{p, I_l\}} \mathcal{C}_{\{p, I_l\}} = \bigcup_{\{p, I_l\}} \{ \bar{m}_{\phi_k(\{p, I_l\})} \}. \quad (20)$$

The set $\mathcal{C}_{\{p, I_l\}}$ represents models which together describe all chosen properties of reality associated with element of basis \mathcal{B} indexed by multiindex $\{p, I_l\}$. However, in order to construct model of all considered phenomena which can interact, we should join selected models. Consequently, by theory of reality composed of all models within $\mathcal{C}_{\{p, I_l\}}$ we understand

$$\mathcal{C}_{J\{p, I_l\}} = \{ \mathcal{C}_{\{p, I_l\}}, \mathcal{J}_{PROC} \}, \quad (21)$$

where \mathcal{J}_{PROC} means procedure of joining of models from $\mathcal{C}_{\{p, I_l\}}$. This procedure can be associated for instance with division of space represented by vacuum medium determined in basis \mathcal{B} into parts $V = \bigcup_m V_m$. Then joining of models can be realized by means of boundary conditions determined on ∂V_m . The procedure can be also associated with introduction of additional postulates for variables of joined models related to energy for instance and various forms of constitutive equations.

Our method of modelling by theoretical speculations rests on modelling of separate phenomena on speculative way and joining of corresponding models into one more universal theory. However we do our speculations on one plane determined by basis element of cognition manifold. Procedure of defining cross-section within cognition manifold is not simple. We have to take into account status of speculative theories. This should be done considering many sources for estimation of this status. Let us mention accordance with experimental results, status of mathematical theories applied, including status of logic, and methodology of introducing of assumptions. We should admit also the case when methods of joining of models corresponding to one element of basis can have impact on option of form of cross-section. Several comments on this subject will be done in what follows.

Summarizing we have introduced concept of cognition manifold which provides environment for introduction of new theories, their evolution and estimation of their relations with reality. We have to do here with set of theories indexed by elements of basis \mathcal{B} . The most universal and fundamental theory have to be selected just from this set.

5 Cognition manifold as manifestation of qualitative reasoning towards recognition of reality

By introduction of cognition manifold we accentuate role of qualitative reasoning. We do it by construction of qualitative models and corresponding equivalence classes for models describing the same phenomenon. The question is what for such a qualitative approach to description of reality is introduced.

In order to catch large set of phenomena within one theory we develop a strategy. This strategy rests on constructing a network of fundamental notions and models which would be large sufficiently in order to describe all phenomena. In this place we see tendency to construction of universal theory.

Evidently we are not able to carry out all experimental results in relation to whole reality. Therefore role of hypotheses is important on our way. On the other hand we cannot develop too precise models of particular phenomena since flexibility of modelling corresponding to larger context will be smaller.

Thereby having sufficiently large network of qualitative models we continue our strategy by going to next step which consists in shrinking of our network. We do it by various cross-sections within cognition manifold. Then we obtain more consistent and universal theories. When we are sufficiently satisfied having in mind consistency of our qualitative theory we go to the next step. This step rests on identification of constants in order to obtain fundamental and universal quantitative theory.

We would like to accentuate fact that reasoning based on qualitative properties can be entirely precise from formal point of view. This reasoning is based on appropriate definition of corresponding equivalence classes. These classes need not contain finished models. However, we should have evidence that corresponding models are realizable. Then, we have not to consider too large number of details within initial formulation of our theories. This in turn gives us opportunity for manipulation of larger network of theoretical models for recognition of reality.

When we try to describe reality in an unified manner we encounter obstacles. One of them is associated with very complex mathematics which represents precise reasoning with large number of details. The second one is related to option which way of description is appropriate having in mind considerable large number of possible descriptions and necessity of doing speculative hypotheses.

Above obstacles have opposite character. On the one hand we need precision in details. On the other hand we would like to find optimal way in this environment by manipulation of introduced descriptions. Therefore we are forced to find a compromise. Qualitative reasoning seems to be just such a compromise. It provides us considerable flexibility in modelling. When we obtain satisfactory qualitative description we can continue development of our description. We go then towards taking into account larger number of details within chosen representatives of corresponding equivalence classes representing qualitative properties. Finally we should obtain on this way precise mathematical description of whole reality.

Let us note that we frequently encounter in theoretical physics comments which suggest that qualitative reasoning is a preliminary stage in construction of physical theory. This in turn means that quantitative theory is more important as directly confirmed by experimental investigations and is seen then as serious achievement. Perhaps we should change this point of view.

Quantitative theory can be successful in some range of validity. However some phenomena do not exist within such a theory. It means that this theory has loss of quality in this region of description. In other words this theory is not universal. The question is what is more important for theoretical physics qualitative theory which describes all phenomena observed or quantitative theory which describes a part of phenomena only. Within this work one suggests that qualitative universal theory is more important against currently dominant point of view that quantitative theories are more important. This is so since qualitative universal theory is appropriate stage in development of theoretical physics leading to indeed universal theory.

Consequently qualitative reasoning can lead to preliminary stage of theoretical description. However such a reasoning can also be associated with very complex and by this advanced qualitative theory expressed within cognition manifold for instance.

Above discussion shows that we develop theoretical physics with the aid of mathematics. However larger efforts are done within this methodology in order to introduce flexibility in making assumptions. Role of this flexibility will be seen especially in next sections where proof with respect to reality is discussed. This situation differs from traditional mathematical physics where we consider rather stable set of assumptions. Then, in mathematical physics, we are interested in precise formulation of theory and formulation of various theorems precisely proved.

REMARK 5.1: Formalization of cognition process changes methodological situation for mathematical physics. One shifts accent from precise mathematical reasoning by theorems towards introduction of more flexible systems of assumptions leading in fact to larger number of theories. Then qualitative reasoning allows us to discuss simultaneously this larger number of theories and manipulate them in order to fit description to reality better. However finally, after stage of speculations, we will be interested in precise mathematical formulations of various theorems within the best theory selected.

6 An example of constructing of cognition manifold

6.1 Elements of cognition manifold characterized for vacuum medium related to scale S_{VM}

We discuss here a general framework for speculations within cognition manifold leading to vacuum medium mechanics. Within this section we try to show how process of modelling based on speculations is initiated. Considerations carried out here are related to scale of averaging S_{VM} smaller than size of stable elementary particles. Therefore such particles are considered as extended particles and are manifested by processes within vacuum medium. Then components of corresponding particles are represented by their densities.

In order to characterize methods of speculations related to vacuum medium carried out within cognition manifold we should introduce elements of basis of cognition manifold as first step.

Various cosmological investigations indicate that the space of the Universe is flat. Furthermore, investigations of background radiation show existence of a resting reference frame with respect to radiation in our space. In particular we are able to determine velocity of Earth with respect to this reference frame. Above observations suggests that vacuum medium is similar to solids. Just such a medium is able to maintain the reference configuration and corresponding reference frame. In case when vacuum medium would be similar to a fluid we could expect varying physical laws going from one point of space to another.

Our space is rather not empty. We can detect existence of electric field for instance what represents a state of our space. This means that we have to consider our space as a medium associated with geometrical space. Our physical laws seem to be the same in all points of space or in all neighbourhoods of corresponding points.

Creation of electron positron pair suggests that this process is associated with separation of some components. Possibility of annihilation of these particles supports this point of view since corresponding components can also be joined again. Consequently we should assume that our space is identified with a vacuum medium similar to solids, composed of various components which could be separated when higher energy is provided to this medium.

Having in mind above remarks we consider our vacuum medium as similar to solids for low energy with distinguished reference configuration corresponding to three-dimensional space E^3 , where we can introduce a Cartesian coordinate system.

The vacuum medium is considered as a mixture of four components [15] joined within an elementary unit identified at this moment with a point of space. Consequently elementary units have stable positions within our model of vacuum medium what reflects fact that we have intention to consider

the vacuum medium as similar to solids for low energy state.

Motivations for assuming four components follows from observation that the Maxwell equations exhibit a symmetry with respect to electric and magnetic field. This induces considering at least two components. However, creation of electron-positron pair indicates that a separation of components is associated with electric field only. Therefore, two components are assigned to electric field. By analogy to observed symmetry between electric and magnetic fields two other components are also assigned to the magnetic field.

We have assumed here that these components constitute four-component elementary units which create a stable medium for low energy states. In the continuum description applied here the elementary units correspond to points of space. However, in particular cases we can also assume that elementary units have a finite size which is more natural and convenient in our considerations.

We introduce densities which represent an amount of component related to a volume which can be discussed owing to the introduced coordinate system. Thus, we assume that ϱ_v , $\varrho_{\bar{v}}$, ϱ_w , $\varrho_{\bar{w}}$ and ϱ stand for densities of the components and the density of the united media, respectively. We have then

$$\varrho_v + \varrho_{\bar{v}} + \varrho_w + \varrho_{\bar{w}} = \varrho. \quad (22)$$

State of each elementary unit is described by displacements or a kind of polarization of discussed components within units. They are represented by vectors \mathbf{v} , $\bar{\mathbf{v}}$, \mathbf{w} , $\bar{\mathbf{w}}$. We assume that two pairs of the components are discriminated by special interactions. Components within each pair are able to move with respect to each other. As a result, we can reduce in some cases the number of variables by introducing the new ones: $\mathbf{u} = \mathbf{v} - \bar{\mathbf{v}}$ and $\mathbf{q} = \mathbf{w} - \bar{\mathbf{w}}$. At this moment it is also assumed that $\bar{\mathbf{v}} = -\mathbf{v}$, $\bar{\mathbf{w}} = -\mathbf{w}$.

The variables \mathbf{u} and \mathbf{q} are identified with the vector of the electric field intensity \mathbf{E} and the magnetic induction vector \mathbf{B} , respectively. Propagation of \mathbf{u} and \mathbf{q} through the vacuum medium is interpreted as electromagnetic wave.

In the paper [15] we have assumed that the medium ϱ can be decomposed into the sum $\varrho = a + b$ for higher energy, where

$$a = \varrho_v + \frac{1}{2}(\varrho_w + \varrho_{\bar{w}}) \quad (23)$$

and

$$b = \varrho_{\bar{v}} + \frac{1}{2}(\varrho_w + \varrho_{\bar{w}}). \quad (24)$$

This decomposition appears as a result of attaining by \mathbf{u} a critical value \mathbf{u}^* characteristic for the discussed medium.

These relations have symbolic character which accentuates that an internal structure is associated with such a decomposition process. Symbolic character means that we are not able to interpret this decomposition entirely. Some efforts on this way are done in next subsection where we discuss approach to modelling related to still smaller scale.

Components a and b create medium of electron and positron respectively when they rotate. In such a case the components are separated from the remaining part of the medium by a discontinuity surface. Then, motion of this surface determines of motion of electron or positron.

Deformation of the whole ϱ -medium is also considered. We describe this deformation by means of variable \mathbf{h} .

We also admit rotation of a part of the ϱ -medium separated by a discontinuity surface from remaining part of stable ϱ -medium. Such a state is identified with neutrino and motion of the discontinuity surface describes motion of the neutrino.

We have discussed concisely some assumptions related to vacuum medium what allows us to characterize states of this medium. Consequently we are able to characterize an element of basis of cognition manifold $\mathcal{B} = \{\mathcal{B}_p\} = \{\{\tilde{X}_p, \lambda_p\}\}$.

We can consider several elements of basis at this stage of considerations. Option of variant will depend on further steps of development of description of processes.

Let us introduce first element of basis \mathcal{B}_1 . We have introduced four-component vacuum medium similar to solids with geometry expressed by $\tilde{X}_1 = E^3$ and states $\lambda_1 = \{a, b, \varrho, \mathbf{u}, \mathbf{q}\}$.

When we take into account gravitation then we should consider various additional variants. They can be associated with existence of fifth component of vacuum medium or additional state of four-component vacuum medium. Then \mathcal{B}_2 can be extended from \mathcal{B}_1 by adding new component and also by adding new state corresponding to displacement \mathbf{h} . We can also consider new state corresponding to displacement \mathbf{h} without assumption on existence of additional component. Then \mathbf{h} is interpreted within existing components what leads to element \mathcal{B}_3 of basis of cognition manifold.

We see that various elements of basis can be determined at the same scale of averaging related to description of vacuum medium. More precise option of elements of basis should be carried out during modelling of processes.

We have introduced several elements of basis of cognition manifold. Next step consists in determination of fibres. They are based on division of space of states of vacuum medium into sectors. Let us discuss concisely various processes in vacuum medium.

We assume that each component $\varrho_v, \varrho_{\bar{v}}, \varrho_w, \varrho_{\bar{w}}$ considered separately attracts its own elements. Components a and b have the same property. Attraction between various kinds of components takes place for sufficiently small energy what leads to formation of the elementary units. Components a and b after separation also exhibit attraction which can lead, for some conditions, to recovering of the elementary units and thereby the four-component vacuum medium structure.

We could consider several energetic levels with different kinematics. The lowest energy is connected with displacements \mathbf{u} and \mathbf{q} only, which are considered as small. Higher energy levels are associated with elementary particles. Consequently, electron and positron are viewed as rotating a and b -media separated from ϱ by a discontinuity surface. Interactions between particles and electromagnetic field are determined with the help of boundary conditions given on the discontinuity surface.

One also admits coexistence of components a, b and ϱ in the same point of space. Such a state is considered as a nonequilibrium state of the vacuum medium and has to relax to a lower energy level. In particular when electron moves then motion of the separation surface is associated with production of an excess of b before the particle and transferring of a into the particle as well as stopping part of a behind the electron. This induces just nonequilibrium distribution of components around the particle. Consequently $\{a, b, \varrho\}(\mathbf{X})$ associated with moving particle is interpreted as the wave function.

Fibres of cognition manifold contain models related to distinguished processes denoted by ϕ . Let us note that we use the term processes. It means that time is introduced into considerations. This is done in way discussed in section where the cognition manifold is introduced and time is defined. Thereby within fibres we use all notions admissible for creation of theory since fibres are composed of models. In particular energy conservation law can be formulated and introduced in context of states corresponding to basis and defined next processes.

Let ϕ_1 be related to low energy processes without any separation of components. Then states are considered as $\{\mathbf{u}, \mathbf{q}\}$ and lead to description of electromagnetic waves and static fields.

When we admit separation of components then ϕ_2 can be associated with dynamics of separated component a for instance. However dynamics can be associated with relaxation of this excessive amount of component or with integration of it into electron. Then ϕ_2 could be divided and replaced by ϕ_2 and ϕ_3 . Then ϕ_3 represents states corresponding to internal dynamics of components within electron.

Let us mention that stable vacuum medium can be forced into rotation. Such a process can lead to creation of neutrino. Then ϕ_4 can be associated with state of vacuum medium corresponding to relative displacements of one part of ϱ -medium with respect to another and dynamics of a slip on discontinuity surface. Let us mention that we have to do here with additional variables corresponding to displacements. This suggests in turn that we have to do with next element of basis of cognition manifold.

We have shown above methods of option of fibres. Development of fibres is associated with creation of additional assumptions and models corresponding to various ϕ_k .

Whole theory of vacuum medium should consider a set of ϕ_k which represents all admissible states and processes within this medium. Let us note that assumptions related to form of energy conservation law for instance appear just during constructing fibres. In this place various forms of constitutive equations can be considered.

Let us discuss several examples from literature which can be represented by various ϕ_k . In [18] we consider behavior of static electric field in vicinity of electron considered as extended particle. One shows that such a field should be flat in some region and should take form of Coulomb field at larger distances from electron. In [8] one considers model of precession of electron with dominant mechanisms called there surface superfluidity property expressed by properties of the vacuum medium. Waving associated with nonequilibrium distribution of components within stable vacuum medium is discussed in [6]. Models of neutrino and their interactions are discussed in [17]. Processes on the inside of black holes are discussed in [16].

All above models discussed in literature and considered separately can be seen as interesting concepts having perhaps not too much with reality common. In traditional approach physicists should expect necessity of experimental confirmation of such hypotheses. However when we consider all above examples within methodology manifested by the cognition manifold then all they appear as consistent action towards recognition of reality. In case when we introduce estimation of status of assumptions and theories then such speculations are joined with a reality not necessarily by experimental observations. Furthermore such speculations can lead to seeing of entirely new reality within well known set of experimental results which is at disposal of physics.

Let us mention surface superfluidity property [8] as property of vacuum medium responsible for precession of electron. We assume that volume of component a in electron is considerably smaller than the same amount of a in ϱ . This is property with high status. Then interactions between a and a from ϱ have nonhomogeneous character owing to transition of attractive interactions through the discontinuity surface. Then we can expect dynamics leading to stationarization of corresponding interactions generating tangent to the surface forces. This in turn should be manifested by evolution of motion of a towards a constant slip velocity on border between a and ϱ . Status of such a point of view is relatively high owing to direct reasoning. This means that concept of surface fluidity property is justified even in case when we are not able to carry out experimental investigations.

Interpretations leading to description of entirely new reality happen just in development of vacuum medium mechanics. Within existing set of experimental results vacuum medium mechanics sees that proton is composed of three positrons [19], [9]. Neutrino can create unstable bounded states with charged particles [17]. All this leads to entirely new classification of elementary particles [9]. There are no quarks. Boson Z is not carrier of electroweak interactions in direct interactions between electron and neutrino. Big Bang model is considered as explosion of space on the inside of giant black hole [16] and leads to processes which are in accordance with astrophysical observations.

Estimation of status of various assumptions applied will be considered in discussion related to proofs with respect of reality in what follows.

6.2 Elements of cognition manifold characterized for vacuum medium related to scale $S_{DVM} < S_{VM}$

Various considerations related to dynamics of processes, especially related to biology, suggest that dynamics of wave function is of key importance for selforganization process [11], [10], [7]. Thereby dynamics of this function can be associated with driven force for biological evolution. Within vacuum medium model related to scale S_{VM} wave function is represented by $\{a, b, \varrho\}(\mathbf{X})$. Thereby understanding of physics of components in more detail seems to be important task.

In order to do it we should carry out inductive step to scale $S_{DVM} < S_{VM}$. Then we can have a hope to see structure of the wave function. We should look for premises for modelling of processes in so small scale.

Let us note that electron is considered as electric monopole since it generates electric field perpendicular to its surface. On the other hand we do not observe magnetic monopoles. However electron has magnetic properties. The question is where from such properties follow. We can introduce concept that magnetic monopoles are on the inside of electron and therefore they are responsible for its magnetic properties. However then electron should generate magnetic field in perpendicular to its surface direction. Such a point of view suggests that an anisotropy in vacuum medium could happen. Such anisotropy should be caused by states of vacuum medium related to additional components in comparison with introduced previously magnetic ones in structure of vacuum medium. Consequently we have to do here with reasoning related to smaller scale than S_{VM} since we try to see elements of vacuum medium within component a and also new components related to smaller scale and responsible for mentioned anisotropy.

By means of above reasoning we obtain a premise for assumption that perhaps electron is composed of magnetic monopoles as main elements of component a . Positron could be composed of antimonopoles as main elements of component b . Then stable vacuum medium should be composed of network of systems composed of monopole and antimonopole in bounded state. Consequently network of such systems has structure similar to solids. However we have to introduce description which ensures that propagation of external magnetic field from monopole is not continued in perpendicular to its surface direction. This is necessary since electron has not magnetic field with components perpendicular to its surface direction.

Mnople-antimonopole system moving approximately on a sphere without any polarization would be considered as an atom of ϱ -medium. Polarization of their motion on the sphere would lead to electric field. The polarization can be manifested by motion of monopoles around poles of sphere determined by an axis represented direction of electric field. Such an interpretation of electric field is justified by fact that electric field is associated with separation of components. Consequently, sufficiently strong polarization of monopole-antimonopole system leads to separation of them and providing monopole to electron in case of its motion. Thereby within deep structure of vacuum medium related to scale S_{DVM} electric field is not defined between monopoles.

Various concepts of state of deep structure of vacuum medium leading to creation of monopole are admissible. Let us assume that our monopole is produced as a result of separation of components $\varrho_{\mathbf{w}}$ and $\varrho_{\bar{\mathbf{w}}}$ owing to increasing of magnetic field \mathbf{w} and $\bar{\mathbf{w}}$ from

$$\varrho_{\mathbf{q}} = \varrho_{\mathbf{w}} + \varrho_{\bar{\mathbf{w}}} \quad (25)$$

considered as a part of the whole vacuum medium representing the background neglecting at this moment additional components. Background vacuum medium is understood here as vacuum medium without any monopoles.

We assume that the monopole is created after separation of its component and undergoes rotation taking shape similar to a sphere. This happens owing to nonlocal attracting forces within each component of the medium and forces which act on the surface of particle. This happens in similar way as for electron but forces considered here can have another character.

Consequently, we consider a monopole composed of $\varrho_{\mathbf{w}}$ separated from $\varrho_{\mathbf{q}}$ by a discontinuity surface $\mathcal{S}_{\mathbf{w}}$. Then, motion of this surface corresponds to motion of the monopole.

The surface $\mathcal{S}_{\mathbf{w}}$ is considered as a discontinuity surface for various fields describing state of the medium. In particular densities of components are changing on $\mathcal{S}_{\mathbf{w}}$ in a discontinuous way. Thereby, in order to analyze motion of our particle we should consider various balance equations taking into account discontinuity surface within assumed continuum description.

In order to prevent efficient propagation of magnetic field in perpendicular direction to surface of monopole we assume that additional components take part in near-to-surface of monopole processes. Such processes govern motion of surfaces of monopoles and propagation of magnetic field. Manifestation of the additional components is realized by the two-ring field.

We have discussed above some aspects of existence of magnetic components only. However we have postulated existence of components responsible for anisotropy of magnetic field near monopole. Let us

denote them by $c_{\mathbf{w}}$ and $c_{\bar{\mathbf{w}}}$. Two additional components are introduced since we accept symmetry related to behavior of monopoles and antimonopoles. We should characterize states of these components which should lead to discussed previously anisotropy.

Let us introduce the vector \mathbf{n}_η which can be interpreted as normal to surface of monopole. This vector determines plane tangent to surface of monopole. On this surface the two rings appear. On the other hand we consider each ring of the two-ring field as having radius denoted by η_e and η_i correspondingly. We introduce the variable η as follows

$$\eta \mathbf{n}_\eta = (\eta_e - \eta_i) \mathbf{n}_\eta. \quad (26)$$

Motivation for introduction of the two ring field are as follows: (a) the fact that the variable η should have opposite sign on surfaces of opposite monopoles what leads to two rings and (b) the fact that propagation of magnetic field in tangent to the surface of monopole direction should differ from propagation in normal to the surface direction which discriminates tangent plane. Thereby variables η_e and η_i are interpreted as states related to components $c_{\mathbf{w}}$ and $c_{\bar{\mathbf{w}}}$ correspondingly.

The property (a) is introduced in order to obtain possibility of modelling of explosion of space after creation of bounded state of monopoles based on repulsion following from properties of the two-ring field. Then after separation of components volume of dense component a in electron is considerably smaller than volume of network of bounded monopole and antimonopole systems with the same amount of a . Then component a within electron is considered as dense fluid composed of the same type of monopoles. For more detailed discussion see [9].

Let us note that variables in (26) are introduced as a minimal mathematical representation of properties (a) and (b). It means that existence of corresponding fields has relatively high status. This is so since properties (a) and (b) are closely related to observed properties and minimal mathematical representation, in similar way as in Remark 2.1, introduces the simplest relation without any additional assumptions. Consequently variables introduced by (26) are appropriate starting point for further speculations.

Having at our disposal description of states of vacuum medium related to scale S_{DVM} we can characterize an element of basis of cognition manifold $\mathcal{B}_{DVM} = \{\mathcal{B}_{DVMp}\} = \{\{\tilde{X}_{DVMp}, \lambda_{DVMp}\}\}$.

We have that element \mathcal{B}_{DVM1} is characterized by $\tilde{X}_1 = E^3$ as medium corresponding to space between monopoles. States of such a medium can be represented by $\lambda_{DVM1} = \{\mathbf{w}, \bar{\mathbf{w}}, \eta\}$.

Element \mathcal{B}_{DVM1} is seen as the simplest one. It seems that \mathcal{B}_{DVM2} should be related to $\lambda_{DVM2} = \{\mathbf{w}, \bar{\mathbf{w}}, \eta_e, \eta_i, \xi\}$, where ξ represents groups of variables which characterizes state of components $c_{\mathbf{w}}$ and $c_{\bar{\mathbf{w}}}$.

Let us note that we have to distinguish four-component deep structure of vacuum medium. This is obtained by means of premises elaborated and expressed within minimal mathematical representation from (26). One suggests furthermore that components $c_{\mathbf{w}}$ and $c_{\bar{\mathbf{w}}}$ are responsible for solids like structure of vacuum medium in small scale to largest degree. Thereby our speculations subordinated to a discipline following from cognition manifold methodology lead in fact to a discovery. This discovery has rather low status however allows us to continue cognition process.

On the other hand we encounter necessity of stopping of inductive reasoning. In case when monopoles appear as a result of separation of components from $\varrho_{\mathbf{q}}$ and corresponding rotation we have to do with relative motion and perhaps necessity of considering new background vacuum medium related to smaller scale than S_{DVM} .

In order to stop this process of inductive decreasing of scale perhaps we could admit the case when four components $\{\varrho_{\mathbf{w}}, \varrho_{\bar{\mathbf{w}}}, c_{\mathbf{w}}, c_{\bar{\mathbf{w}}}\}$ create solids like structure with various polarizations or small displacements. Then within such a medium we could admit structural phase transformations leading to various forms of reorganization of components and interactions between them. In this place we see role of fibres which need determination of energy for description of structural transformations perhaps admitted in various variants.

Consequently, monopole would correspond with state obtained after exceeding of a critical value for magnetic field. Furthermore transition to monopole would be associated with transformations

in components $\{c_w, c_{\bar{w}}\}$ leading to discussed previously anisotropy in neighbourhood of surface of monopole. In this case we avoid separation of magnetic components and its motion in a background. Thereby inductive reasoning is to some degree stopped since we do not consider new background medium.

All this provides premises for speculations on form of elements of basis of cognition manifold related to scale S_{DVM} and development of new models. Let us note that owing to introduction of inductive step towards smaller scale we have also imposed limitations on freedom in speculations by mapping P_{In} . By means of this mapping transition to scale S_{VM} is continued. It means that properties observed for scale S_{VM} have to be expressible in scale S_{DVM} . Let us mention for instance modelling of electromagnetic waves for scale S_{DVM} and verification of such a model for scale S_{VM} after averaging.

Let us notice that relations (23), (24) can be reinterpreted. Components $\varrho_v, \varrho_{\bar{v}}$ represent in fact magnetic monopoles in averaged way and therefore they are related to scale S_{VM} . Components $\varrho_w, \varrho_{\bar{w}}$ are related to background vacuum medium and by this to scale S_{DVM} . However they can be formally expressed also directly in scale S_{VM} . This explains why Maxwell equations are not entirely symmetrical with respect to electric and magnetic field.

7 Selforganizing inference as important for recognition of physical reality towards better theory

Concept of cognition manifold expresses fact that we are frequently present in theoretical environment generated by various hypotheses not necessarily well associated with direct experiment. Furthermore we should tend towards improvement of models by increasing of their status. We are accustomed to carry out precise mathematical proofs and consider obtained consequences as appropriate for description of reality. This follows from our traditional interpretations of mathematics as precise tool for reasoning. However, physical reality is approximated by precise mathematical theory only. In order to reflect this fact status of theory as well as various assumptions are introduced. The question is how we should follow going towards increasing of status of theory.

It seems that construction of more appropriate theory, having higher status, should be precluded by various theories of lower status. Theories of low status are then associated with hypotheses and their verification provides extension of context for determination of better theory. We would say that evolution towards theory better fitting to reality Th_F is seen as a selforganization process

$$Th_1 \rightarrow_{C_1} Th_2 \rightarrow_{C_2} \dots \rightarrow_{C_{F-1}} Th_F \equiv Th_R, \quad (27)$$

where Th_1 is theory considered as starting point for this process. This process should be sufficiently long in order to obtain a theory Th_R as the most close to reality.

The question is what circumstances induce transition $Th_k \rightarrow_{C_k} Th_{k+1}$. The answer to this question discussed in [1] states that each step of transition to better theory is associated with context C_k which provides premises for such a step.

Let us introduce mapping $I_{EX} : \mathcal{E} \rightarrow \mathcal{M}$ which assign interpretation of the sentence $e \in \mathcal{E}$ within models contained in \mathcal{M} . By interpretation we understand description of process within a given model which leads to result expressed by the sentence e . Consequently, we obtain the possibility of estimation of accordance of corresponding model with experimental observations.

We can consider the situation when $I_{EX}(\mathcal{E}) \subset \mathcal{M}$ and $D_{EX} = \mathcal{M} - I_{EX}(\mathcal{E}) \neq \emptyset$. It means that some models have no connection with obtained set of experimental observations.

We can identify our theory Th_1 with an $\mathcal{C}_{J\{p, I_i\}}$. Then, we can identify all constants of the theory by means of experimental results in case when $\mathcal{C}_{J\{p, I_i\}} \subset I_{EX}(\mathcal{E})$. Consequently, we would say that we can estimate status of our theory by direct identification path associated with mapping I_{EX} . Then development of context consists in formulation of new hypotheses which would be able to improve accordance with experimental results on qualitative and quantitative way.

However, we can also have to do with the case when $\mathcal{C}_{J\{p,I_k\}} \subset D_{EX}$. This can be the case when our models are related to very small scale when direct experiments cannot be carried out. However, then we can go along identification path associated with mappings P_{I_k} introduced in (13) towards regions belonging to the set $I_{EX}(\mathcal{E})$. Then in order to make this procedure more systematic the mapping P_{I_k} should be extended to mapping \tilde{P}_{I_k} . The mapping P_{I_k} realizes transition of a one model into larger scale model for instance, where experimental results can be expressed. The mapping \tilde{P}_{I_k} should realize transition from all models obtained in speculative way into model where experimental results can be attained. In other words \tilde{P}_{I_k} represents a family of mappings of P_{I_k} type.

Having at our disposal such mappings we can discuss incompatibility with experimental results since they can be transferred by means of mappings $\tilde{P}_{I_k}^{-1}$ into appropriate level of modelling creating just context \mathcal{C}_1 for our theory Th_1 . By this step we can analyse character of incompatibilities and possible methods of improvement of this situation. Let us note that the mapping \tilde{P}_{I_k} is usually not one-to-one. Therefore $\tilde{P}_{I_k}^{-1}$ can create new space for theoretical speculations.

We see in this place important role of mapping P_{I_k} . It is important to construct whole cognition manifold in way where each element of basis \mathcal{B} can be connected by corresponding mapping with element where current experimental results can be interpreted.

We can summarize this situation as follows. The mapping $I_{EX}(\mathcal{E})$ provides a projection of experimental results on cognition manifold. Then, theories which are placed on the outside of this projection can be joined with experimental results by an identification path associated with appropriate mappings within the cognition manifold. Then, confrontation of theory with experimental results by means of these mappings extends context of this theory.

Let us comment role of context in this case. We consider various aspects of fitting of theory to experimental results. We can analyse direct deviation of theoretical results from possible large spectrum of experimental results. However we can discuss also quality of accordance between theory and experiment. In other words we discuss whether all observed phenomena are represented within theory. Then context is associated with all points of view on questions where from deviations could follow or why some effects are present within theory or not. This in turn can be starting point for creation of new hypotheses.

The context \mathcal{C}_1 can be developed also by all possible ways and additional concepts relating to more general points of views. Corresponding discussion can lead to reformulation of hypotheses which would have at this moment higher status since they take into account additional information. All this leads to determination of new theory Th_2 which is starting point for development of the context \mathcal{C}_2 .

We can also try to extend the set \mathcal{E} by extension of experimental investigations. However this task becomes more and more difficult for more fine processes where experimental investigations are more strongly conjugated with theoretical investigations. This elucidates role of mapping $I_{EX}(\mathcal{E})$ which join experimental results with currently developed models. Thereby interpretation of experimental results depends on models introduced. This in turn can suggest new kinds of experiments.

Summarizing we see that selforganizing inference on properties of reality, manifested by starting point theory and development of context for generation of new theory with better status, is an alternative to traditional inference based on precise mathematical proof what is frequently applied in theoretical physics. We would like to accentuate by this comment that changing of theory by introduction of new assumptions perhaps, in many cases, is more appropriate than obtaining of pure mathematical consequences with the aid of a long proof. Role of long mathematical proof in description of reality will be discussed also in connection with proof with respect of reality in what follows.

The question is why we discuss the term "selforganizing reasoning". This name follows from fact that we start from a chosen theory. Then modification of this theory towards new theory follows from a context elaborated on various ways including estimation of status. Obtained sequence of theories should go towards theory corresponding to the best approximation of reality. Thereby, changing of such a final theory will be very difficult. This is a kind of a fixed point.

Cognition manifold creates a methodological environment for selforganizing reasoning towards better recognition of reality by theory. Within this theoretical environment we can create new hypotheses

for changing of theories, estimate accordance of theories with experimental results and estimate status of theories which can be applied to defining a kind of distance from appropriate approximation of reality.

REMARK 7.1: We accentuate the term "selforganizing reasoning" since we have to do here with evolution of theories towards a theory corresponding to a fixed point. We can consider also a kind of distance from this fixed point and expressed with the aid of status of theory.

8 Remarks on connections between measurement theory and creative reasoning

Measurement theory describes our possibility in measurement of various quantities. Then, obtained results have to be interpreted with the aid of description of measurement applied. The most known result of measurement theory within theoretical physics is represented by Heisenberg uncertainty principle.

We encounter frequently in theoretical physics very strong connection between creation of hypotheses and the uncertainty principle. Frequently this principle is applied to proof of various theorems or justification of new hypotheses. In case of uncertainty principle we manipulate various type waves for measurement of quantities. In other words, in theoretical physics, we have to do with constraints imposed on thinking following from the uncertainty principle.

Let us note however that our measurement depends on current technical capabilities. On the other hand new hypotheses can be related to reality which perhaps is not accessible for our measurement directly. Perhaps our possibilities in measurement in a future can be based on entirely new phenomena and can be much more precise. Let us mention in this case properties of neutrino described within vacuum medium mechanics [17]. Neutrino described within vacuum medium mechanics has no wave function. This follows from considerably larger system of fundamental notions than that one applied to formulation of the quantum mechanics. Thereby uncertainty principle should not be taken into account in interactions of neutrino with other elementary particles. As a result of this we come to various conclusions on radius of various charged elementary particles when we apply scattering experiments of these particles with neutrino or scattering with electrons for instance.

It seems that measurement theory should be devoted to description of a system of interacting objects. One of them represents measurement apparatus which has various states and we are able to manipulate part of these states. The second one is a system which has also various states. These states can be measured quantitatively when both objects interact and we can decipher corresponding values owing to description which is at our disposal.

We see in this place that our measurement depends on description of corresponding interacting objects. We can obtain relation between various states of this system. Let it be $\mathcal{R}_M(Z_1, \dots, Z_N)$, where Z_1, \dots, Z_N are quantities which can be measured. The relation \mathcal{R}_M determines a set to which quantities Z_1, \dots, Z_N belong.

Let us notice that we can introduce to description of our system new quality associated with new hypotheses where we apply quantities which cannot be measured at this moment. This can mean that we are able to indicate a subsystem within $\mathcal{R}_M(Z_1, \dots, Z_N)$. However we are not able to manipulate new introduced variables. Thereby precision of our measurement is determined as previously by the relation $\mathcal{R}_M(Z_1, \dots, Z_N)$. Our technical possibilities are not improved. However we come to the conclusion that values Z_1, \dots, Z_N which appear within the set $\mathcal{R}_M(Z_1, \dots, Z_N)$ do not take all admissible values which are present there. It means that we cannot infer directly from measurement theory which values can be attained by real states. Consequently we come to the following remark:

REMARK 8.1: Measurement theory should not create constraints on creation of new hypotheses related to reality or in other words on our reasoning. Measurement theory should be considered as separate theory which allow us estimate to what degree we are able to measure various quantities in relation to recognized reality. Consequently this theory can be helpful in identification of constants

which appear in theories. However, application to inferring in direction to new description is not appropriate since such an inferring should not depend on our current technical capabilities for measurement.

9 Remarks on reductionism and emergence

Reductionism and emergence are notions which are frequently applied in philosophy of physics and philosophy in general [12], [13]. In particular one estimates that contemporary theoretical physics has success based on methodological reductionism. It means the attempt to reduce explanations to smaller constituents and to explain phenomena completely in terms of interactions between fundamental entities [13]. Theoretical reductionism is considered within the methodological reductionism, wherein one theory with limited predictive power can be obtained as a limiting case of another theory [13].

Emergence is understood as involving new, sometimes novel properties of a whole that are not shared by its isolated parts [13]. Problems of emergence in physics are discussed frequently in literature. Let us mention [14] for instance. One suggests that complexity leads sometimes to entirely new quality which cannot be derived from more elementary level.

It seems that both reductionism and emergence are notions which are not entirely clear. It follows from fact that they are placed on border of formal cognition. Within this work we do efforts towards formalization of cognition process as far as it would be possible. Therefore some comments on reductionism and emergence are justified.

By this paper we promote reductionistic approach to theoretical physics including also description of complex systems. This is manifested especially by concept of construction of fundamental theory. We assume namely necessity of determination of form of space considered as a medium. It means that we would like to have at our disposal states of this medium expressed with the aid of variables.

Introduction of corresponding variables is associated with determination of set of fundamental notions where we estimate status. Attaining high status of assumptions is easier in this place since we have to do with simpler objects. Summarizing promotion of reductionism is expressed here by starting first from determination of variables. Then, relations appear as next stage of modelling what is manifested by notion of cognition manifold.

Emergence in this context should be understood as construction of physical theory starting from relations at first stage, neglecting at this moment determination of precise role of corresponding variables at the fundamental level. In particular corresponding relations can use variables related to larger scale. This approach is justified in complex systems. We observe some properties and try to describe them directly by relations. As a result of this we obtain a theory. However this theory is usually not fundamental. Furthermore, we should not expect that such a theory will have sufficiently large range of validity.

Let us note that cognition process can lead to situation when it is difficult to introduce new variables directly on the most fundamental level. It would be the case when our modelling of reality is advanced and new concepts are difficult to obtaining however some relations could be observed and introduced into description as difficult to understanding. We can accept such a situation temporarily.

It seems that cognition process should be continued in spite of all towards finding fundamental assumptions as far as it is possible and constructing of theory with the aid of these assumptions. Perhaps we attain then new situation when we would have to do with necessity of considering very large number of assumptions. Perhaps we would be forced in this case to decipher chaotic phenomena for instance.

Efforts of this kind are done in [11] where the term precursor of evolutionary property is introduced. The term precursor of evolutionary property means processes in molecular system, described by fundamental laws and involved in biological evolution process, which are responsible for appearing of this particular property when biological evolution attains an assumed level of complexity where the property can be manifested.

Finding of precursors is task associated with creation of hypotheses related to fundamental level in

order to modify the fundamental theory. It means that the term precursor manifests using additional context following from more complex processes, for obtaining new premises for making assumptions. In this case more complex processes are considered as experiments which have additional quality in comparison with experiments related to the simplest processes.

CONCLUSION 9.1: Emergence is understood here as generation of theories by construction of relations based on observed properties. Corresponding relations can have variables which represent various scale states. These states can be difficult to understanding. One suggests to consider corresponding relations as placed in zone represented by image of a mapping \tilde{P}_{I_k} related to a smaller scale. Then $\tilde{P}_{I_k}^{-1}$ represents area where pressure towards deciphering fundamental assumptions can be generated. This in turn could lead to obtaining finally theoretical speculations within structure corresponding to cognition manifold.

This kind of pressure on development of theories can create premises and hypotheses leading to perhaps unexpected consequences. Introduction of precursors manifest just this approach. It is also admissible that we attain the stage of description where further recognition of reality will not be possible.

Let us comment here role of mappings \tilde{P}_{I_k} . They are introduced in discussion on inductive reasoning. When this induction is related to diminishing of scale then we have to do with mapping which represents averaging procedure. Such an approach is elaborated in case when we consider formalization of scale of averaging applied to modelling of physical reality [5], [10]. Then theoretical reductionism is not necessarily associated with obtaining another more general theory which leads, as a limiting case, to that previous one.

We apply averaging procedure going from theory having entirely new set of assumptions and variables not directly related to previous one which is modified. It means that we admit the case when we do a jump to entirely new assumptions without modification of previous theory. Then range of validity of previous theory becomes smaller and evolution of theory is not seen as continuous process. We express this possibility by considering various elements of basis of cognition manifold. Above comments extend in fact notion of theoretical reductionism and provide to it new context.

We have to do in theoretical physics with tendency to modification of existing theories in a continuous way. We understand by this modification of separate assumptions or adding new ones to existing assumptions within modified theory. This tendency is justified by fact that physicists try to maintain hitherto attained success in modelling of obtained experimental results. However, jump to new set of assumptions gives better chance for introduction of new quality. Let us mention concept of vacuum medium mechanics [15], [10] which is a jump from widely accepted quantum theories towards entirely new set of assumptions. As a result of this entirely new quality appears. This new quality is manifested in description of internal structure of proton as composed of three positrons [9], [10] or possibility of expression of mechanism of biological evolution on the most fundamental elementary particle level [10].

Emergence is seen within our approach as incapacity in our reasoning which we frequently have to accept. Therefore one suggests to give pressure towards changing this situation in accordance with Conclusion 9.1.

10 On proof with respect to reality

We use in theoretical physics mathematical theories which are designed to description of reality. Then, within corresponding theories we can carry out proof and by this we create theorems. The question is whether we are able to estimate status of theorems. In other words we should try to distinguish mathematical proof from proof with respect to reality.

Mathematical proof is understood in the same way as this is done in pure mathematics. However, each step of proof is associated with an action of dynamical system for recognition of reality. It means that increasing length of proof should lead to more complex action of dynamical system and therefore

approximation of reality becomes then less direct. Consequently status of obtained consequence should be lowered.

In order to estimate status of consequence we should discuss status of assumptions applied to proof. Let us note that in [1] one discusses properties of equivalence laws frequently applied in theoretical physics with respect to resolution of seeing of reality by theory. We have obtained there the following remark:

REMARK 10.1: Equivalence laws applied in physics reduce number of degree of freedom in theoretical description of reality. This follows from the fact that corresponding to this situation mapping which joins theoretical description with reality becomes then less similar to one-to-one mapping. It means that approximation of reality by theory is worse in case of application of equivalence laws what means lowering status of this description.

This remark provides an example of assumption which can be applied in a proof. When this is the case it makes status of a consequence lower. Taking into account previously discussed criteria for estimation of status of assumptions we should formulate the following remark in relation to status of consequences obtained with the aid of a mathematical proof:

REMARK 10.2: Status of a consequence obtained with the aid of mathematical proof within a physical theory should be lower than the lowest status of assumption considered in set of assumptions applied to obtaining of this consequence. Furthermore, the larger number of assumptions applied in various steps of proof the lower status of the consequence. It means also that longer proof leads to worse approximation of reality by obtained consequence.

Above discussion follows from fact that we try to formalize cognition process. Thereby a new quality in reasoning appears. Now we have to do with proofs with respect to reality as additional aspect of theoretical physics in comparison with mathematical proof hitherto applied.

Proof with respect to reality means that we carry our usual mathematical proof which is accompanied by additional process of estimation of status of each step of the proof. In case when status of consequence is very low we have to interpret this fact as premise for modification of assumptions of whole theory in order to obtain better description of reality.

Proof with respect to reality provides additional aspect of estimation of content of physical theory. Let us consider a set of assumptions TA . Then we can attain set of all consequences $C(TA)$ starting from the set TA by carrying out pure mathematical proofs in order to obtain the theory $Th = C(TA)$. However, taking into account proofs with respect to reality we admit a subset C_{PR} of all consequences $C(TA)$ only. This means that our theory describing reality Th_{PR} is smaller than Th .

In order to make theory Th_{PR} larger we should introduce new hypotheses. All this elucidates various aspects of methodology of construction of cognition manifold as well as methodology of obtaining cross-section within cognition manifold.

11 Examples of proof with respect to reality

11.1 On status of existence of virtual particles

Let us carry out an example of proof with respect to reality. We encounter in theoretical physics concept of virtual particles. Consequently we should estimate status for existence of such particles.

We can distinguish two aspects of existence of virtual particles. The first one is related to all assumptions which create environment for this concept. The second one is related to direct reasoning leading to justification of virtual particles.

Assumptions which create environment for this concept are associated with the Dirac equation. Let us discuss content of the Dirac equation with respect to its ability to description of reality. We

consider in this equation point-like particle which has charge and mass by assumption. Furthermore we accept wave particle duality what means that evolution of wave function entirely describes motion of this particle. The last aspect makes lower status of this description in accordance with Remark 10.1. Acceptance of wave particle duality means that we have decided to diminish resolution of our thinking to level where particles and waves are not distinguishable.

At this moment we are aware what degree of averaging of physical effects is assumed. Point-like particle means that all effects are averaged on whole particle. No internal dynamics is considered and no mechanisms of motion is introduced. Having such assumptions we are aware at this moment that resolution of this description is above internal properties of particle.

Derivation of discussed equation is based on quadratic relativistic relation between energy, mass and momentum as well as on acceptance of probabilistic interpretation of quantum mechanics.

The quadratic relativistic relation leads to situation when particles and antiparticles appear owing to taking roots of quadratic equation. Thereby, existence of particle-antiparticle pair is considered as assumption rather than consequence of this equation. In case when we would apply power of fourth order for relativistic relation between energy, mass and momentum then we have to do with four type particles.

Let us note that acceptance of probabilistic interpretation and introduction by this the probabilistic density also means that resolution of this theory is rather low and takes the level similar to level of measurability.

Joining of probabilistic density and quadratic relativistic relation is in fact risky. We impose stochasticity on perhaps unknown number of particles (particle-antiparticle system) with various properties including their interactions. At this moment we have no premises on such interactions. Then, we can expect difficulties with merging of two theoretical aspects leading to unknown and also perhaps unwanted effects. In other words we can have difficulties with interpretation of details related to reality by the Dirac equation. The Klein paradox can be interpreted just as such a difficulty.

Let us note that appearing of spin in the Dirac equation is rather strange. This follows from fact that no internal structure of particle or internal mechanisms of motion are assumed in accordance with above discussion. We can interpret this fact as introduction of spin in a phenomenological way by extra assumptions related to number of terms in development of the probability density expression. Freedom in this approach rests on fact that in case of application of larger number of terms we could obtain additional spins within this interpretation. Furthermore no justification is introduced on form of this development. See Remark 2.3 on status of assumptions introduced by development into series.

This in turn means that no serious efforts have been done in this place in order to describe such a really important phenomenon as spin. This also means that there is no chance for detailed description of spin phenomenon within the Dirac equation without essential extension of this approach.

At this moment we should decide whether we accept the Dirac equation as such or we should improve or better justify them. We have to do in theoretical physics with the second way. The Klein paradox leads to the conclusion that the Dirac equation can be treated in fact as a multiparticle equation, where virtual particles could appear and decay during a short time. This in turn justifies application of the quantum field theory description.

Summarizing status of the Dirac equation is rather low taking into account all assumptions applied in derivation of this equation. It does not mean that many experimental results should not fit quantitatively to predictions obtained by the Dirac equation. Accordance with large set of experimental results takes place since the Dirac equation provides large number of degree of freedom and by this allows us to fit this equation to reality in an area. However we should expect difficulties when we extend range of validity of such a theory. Indeed we have to do in theoretical physics with difficulties with spin of proton for instance. It means that when we apply the Dirac equation which describes just spin to this reality then it loses in this new environment whole quality. It justifies just low status of the Dirac equation.

Formally, existence of virtual particles is based on two steps. The first one applies indeterminacy principle which states that energy fluctuation can be considerable in sufficiently short time. This step

is in fact not admissible. We cannot infer that energy can have arbitrary value in sufficiently short time since this consequence is obtained by means of measurement theory which should not be applied to reasoning of this kind in accordance with previous discussion and Remark 8.1. Thereby this step of proof has very low status.

The second step is based on equivalence of mass and energy. This assumption allows us to change the fluctuating energy into massive virtual particles. However application of equivalence law means that this step of proof has low status in accordance with Remark 10.1.

Application of two successive steps of proof with very low status means that corresponding consequence has very low status. If we take into account additionally that assumptions which generate environment for concept of virtual particles have also not too high status then we come to the conclusion that status of existence of virtual particles is so low that we should entirely reject this concept.

11.2 On status of charge conservation law

In elementary particle physics we apply charge conservation law as law with rather high status. This status follows from accessible observations where this law is always satisfied. Our discussion in introduction suggests that we can discuss status of charge conservation law taking into account fitting of theory to reality based on experimental results and also additionally on methodology following from formalization of cognition process.

Let us discuss first status of notion of charge. This notion appears as a result of observations of electric field in vicinity of systems of charged particles interpreted within properties of Coulomb field. It has been noticed that an elementary state of electric field around single particle such as electron for instance can be seen as Coulomb field with constant e . This constant is interpreted as elementary charge.

Let us remark that notion of charge appears as a result of considerations related to state of environment of elementary particle and as such is assigned to elementary particle only. Considered elementary particle is seen as point-like particle. Consequently notion of charge does not represent deeper properties of elementary particle. We would say in accordance with Remark 2.1 that this notion is not interpreted as related to maximum engagement by action of the dynamical system and its sensory system in order to obtain results which next can be interpreted as the simplest information by neural network system.

We have to do in this case with rather low engagement by action of the dynamical system which represents our brain and experimental systems. This is so since experiments are relatively simple and theoretical description is also not too advanced especially in relation to smaller scales.

We can state that notion of charge is to some degree accidental and is assigned then to point-like particles. This notion is related to relatively large scale applied in modelling since analysis of electric field of elementary particles is carried out on larger distances from these particles.

Above analysis of status of notion of charge suggests that status of charge conservation law is perhaps low especially in relation to smaller scales.

We can also observe that charge conservation law can be seen as emergent property in system of elementary particles. Such a point of view is justified by fact that element of basis of cognition manifold corresponding to theoretical environment where this relation appears, is not determined sufficiently well. We have to do in this case with vacuum which is determined rather as geometrical space not interpreted directly as a medium. Various states are present in this geometrical space however without direct relation to properties of the medium and scale of averaging applied in modelling of processes in such a space is not formalized. Consequently we have difficulties with determination of mappings $\tilde{P}_{I_k}^{-1}$ in accordance with Conclusion 9.1 and deciphering fundamental states related perhaps to smaller scale.

The question is whether we could determine a fundamental notion with higher status than notion of charge which would be more appropriate for expression and discussion of charge conservation law.

We have discovered creation of pair of electron and positron by application of complex experimental systems what can be interpreted as "maximum engagement by action of the dynamical system". The simplest interpretation within our neuron network system states that some components are separated. Observation of annihilation of electron and positron suggests that some components are joined again in order to recover state of vacuum medium before creation of this pair. The simplest interpretation means that we do not understand particular properties of these components and we state existence of them only.

Consequently concept that our vacuum can be interpreted as multicomponent vacuum medium has high status in accordance with Remark 2.1. Separation of components is induced predominantly by electric field. Such point of view is justified by fact that electron and positron generate static electric field. Let us assume that one exists a critical value of intensity of electric field which is necessary for separation of components. Introduced assumption can be seen as direct consequence of existence of components. Thereby it is introduced by direct and short proof what means, in accordance with the Remark 2.2, that status of such an assumption is high.

Summarizing we introduce as fundamental assumption within vacuum medium mechanics [15], [18] the following relation

$$\mathbf{u}(\mathbf{X}) = \mathbf{u}^* , \quad \mathbf{X} \in S_a \quad (28)$$

where $\mathbf{u}(\mathbf{X})$ represents electric field intensity for points \mathbf{X} which belong to surface S_a of electron described within vacuum medium mechanics and \mathbf{u}^* is vector which has length corresponding to the largest value of this quantity admissible within the vacuum medium. Exceeding of this value induces separation of components. Electron is seen within vacuum medium mechanics as extended particle. Thereby on whole surface of this extended particles we have to do with the condition (28).

Consequently external electric field of elementary particle is determined by the condition (28) which has high status. Furthermore this condition is appropriately placed within whole theory by determination of basis of element of cognition manifold defined as four component vacuum medium [15] with well defined states. Scale of averaging applied in modelling is smaller than size of elementary particle. Therefore elementary particles are then extended objects with surfaces considered as a border between separated component and equilibrium vacuum medium.

Within context provided by vacuum medium mechanics charge conservation law can be derived. We can notice that this law can be violated when several charged particles can be so close that surface of whole such a system can be interpreted as one separation surface. Behavior of electric field in vicinity of such a surface is discussed in [18]. Such a field is flat at small distances from elementary particle and becomes Coulomb type field at larger distances. This property follows from the condition (28) and properties of components of vacuum medium.

We can state that charge conservation law can have low status especially for smaller scales. In particular within vacuum medium mechanics one assumes that proton has three-positron structure. Consequently disintegration of proton should be continued with breaking of charge conservation law. Status of such a model of proton is high and is discussed in [19], [9], [10].

11.3 On status of existence of quarks

Existence of quarks is inferred from experiments where various symmetries are observed in elementary particles. Furthermore one observes within experiments of scattering of electrons on protons and also neutrino on protons that proton has structure with three centers. These centers have been named partons and next identified with quarks.

Symmetries associated with properties of various type hadrons are determined by Gell-Mann Nishijima relation

$$Q = e(I_3 + \frac{1}{2}(B + s + c + b + t)) , \quad (29)$$

where Q is charge, e electron charge, I_3 is isospin, B is baryon number, and s, c, b, t are additional numbers called strange, charm, bottom and top.

Consequently we should estimate status of this relation as starting point for inferring existence of quarks. Let us notice that this relation is in similar situation as charge conservation law. It happens rather as emergent property since status of element of basis within cognition manifold is not sufficiently well determined. We have to do here with space introduced by geometry. Sometimes one suggests that this is a medium. Let us mention interpretation electron or positron by the Dirac equation as holes what suggests that vacuum is a kind of medium. On the other hand one considers fluctuation of vacuum. However the last concept is associated with existence of virtual particles. Existence of virtual particles should be rejected in accordance with previous discussion since they have very low status.

Summarizing determination of element of basis of cognition manifold as a medium which has well defined states is not clear as theoretical environment for the relation (29). Then we have to consider the relation (29) as emergent property and try to extend context for this relation taking into account mappings $\tilde{P}_{I_k}^{-1}$ in accordance with Conclusion 9.1.

Let us note that scale of averaging applied to modelling in relation to formula (29) is rather large. We have to do with point-like particles what means that averaging is carried out over whole particle and charge conservation law is maintained. Furthermore the relation (29) is satisfied only approximately. We encounter deviation of masses of particles from masses predicted by corresponding symmetries. Summarizing status of the relation (29) seems sufficiently large for larger scales above size of elementary particles. However problem with masses of particles suggests that status of this relation as fundamental assumption is considerably lowered.

Inferring on existence of quarks is based on rather long proof. First we should find representations of corresponding symmetry group in relation to existence of potentials. Next we have to find generators of corresponding symmetry group.

Let us also note that this inferring is continued towards lower scales. Indeed quarks have to be constituents of proton for instance. However the relation (29) considers point-like particles. It means that we should extend context by introduction of mappings $\tilde{P}_{I_k}^{-1}$ towards still smaller scale. Then however maintaining of charge conservation law is difficult in accordance with discussion from previous subsection. Necessity of assignation of fractional charges for quarks is important manifestation of these difficulties.

Summarizing status of existence of quarks is rather low owing to not too large status of the formula (29) in context related to various scales. Furthermore this relation is satisfied approximately only even for scale where it is directly formulated owing to not precisely fitting masses. Quarks appear as rather long proof continued towards lower scale where formal description is in fact not constructed what additionally lowers status of their existence.

11.4 On status of existence of bounded state of charged particle and neutrino

Existence of bounded state of charged particle and neutrino is not considered within current theoretical physics represented by the standard model. However we observe that muon μ^- decays into electron and two neutrino. The meson π^- decays into electron and three neutrino. Lepton τ^- decays into electron and four neutrino. Therefore it is difficult to avoid the question on better description of interactions of charged particles and neutrino.

This question is difficult to discussion since system of fundamental notions of the standard model is rather poor. In particular owing to application of wave particle duality elementary particles are represented within the standard model by waves. This leads in turn to avoidance of defining of elementary particles. In order to improve this situation vacuum medium mechanics is formulated on basis of larger set of fundamental notions [15], [6], [7], [8], [9], [16], [17], [18], [19].

In the Subsection 11.2 we have estimated status of existence of components of electron and positron as high. These components, when they are joined, create stable vacuum medium. Then separation of components of vacuum medium leads to creation of electron and positron as stable particles. However we can admit also additional method of creation of particles. Part of vacuum medium considered

as medium similar to solids can be forced to rotate without any separation of components. Such a rotation is possible since elementary particle is not point-like. Then elementary particle of this kind identified here with neutrino has no charge. Neutrino is in this case an extended elementary particle with border represented by discontinuity surface between rotating and stable vacuum medium. Model of neutrino within vacuum medium mechanics is discussed in [17].

Let us note that above considerations are simple and direct consequence of assumption that we have to do with multicomponent vacuum medium similar to solids. This assumption has high status what leads also to high status of neutrino introduced on this way.

When neutrino rotates near charged particle then static electric field of the charged particle is disturbed owing to this dynamics. This is so since propagating electric field within resting vacuum medium encounters rotating vacuum medium and gains by this its own dynamics. Thereby it is natural to expect that electromagnetic force can appear between charged particle and neutrino at small distances what can lead to unstable bounded state of these particles. More detailed description of this phenomenon is given in [17].

Thereby we have obtained possibility of existence of corresponding bounded state as direct and short proof. It means that such a possibility has sufficiently high status. Let us note that we have to do with muon μ^- having two neutrino and mass $M_2 = 105MeV$ in accordance with its decay, meson π^- with three neutrino and mass $M_3 = 139MeV$, lepton τ^- having four neutrino and mass $M_4 = 1776MeV$. On the other hand free electron has mass $M_0 = 0.5MeV$. It means that we have not at our disposal bonded electron and one neutrino. Masses of corresponding particles increase with increasing number of neutrino. This is justified by mechanism of motion of extended particle within vacuum medium mechanics [9]. Increasing number of neutrino shields more and more efficiently external electric field and by this makes acceleration of electron more difficult. It means that we predict existence of elementary particle representing bounded state of electron and neutrino with mass M_1 placed between $M_0 = 0.5MeV$ and $M_2 = 105MeV$.

Let us note that in papers [20] and [21] physicists have reported discovery of a new boson $E(38)$ with mass $38MeV$ which is not predicted by the standard model. Such a mass fits to our prediction. Therefore we could suppose that it could be electron with one neutrino.

Summarizing existence of bounded state of electron and neutrino is obtained by reasoning based on high status assumptions and direct and short proof. Furthermore experimental confirmation of existence of boson $E(38)$ additionally increases status of this point of view. All this suggests that unstable elementary particles should be composed of charged particles and neutrino [9] and this point of view has high status.

REMARK 11.1: Discovery of boson $E(38)$ is important manifestation of efficiency of presented here methodology based on formalization of cognition process. Prediction is carried out within vacuum medium mechanics for qualitative mathematical model of neutrino. Importance of this manifestation rests on fact that other fundamental physical theories do not predict this particle.

Above discussion is aimed at accentuating fact that discussed in this paper methodology of recognition of reality leads to qualitative theories which are predictive. Therefore methodology based on formalization of cognition process can lead to considerable advances in theoretical physics.

12 Final remarks

12.1 General summary

Formalization of cognition process is introduced here by several components. Let us mention them as follows:

1. Introduction of the term "status" of assumptions and theories. This is consequence of considering in [1] implication as associated with action of dynamical system in which mathematics is generated.

2. Formulation of notion of the cognition manifold which is aimed at introduction of methodological environment for generation of new theories describing physical reality.
3. Promotion of selforganizing reasoning based on development of context which contains fighting about recognition of premises from various sources, as appropriate for theoretical speculations and approaching by this to better recognition of reality.

Development of theoretical description can be continued by increasing of number s in creation of models $m_{\phi_k M_s}$ for a given element of basis \mathcal{B} within cognition manifold. Such a development is associated with speculations on the same level of understanding of our space by adding new assumptions and hypotheses related to evolution of processes. However we can also modify our understanding of space by inductive reasoning creating new elements of basis \mathcal{B} . We can go for instance towards smaller scale models of our space considered as a medium. Then by means of mapping P_{In} we can explain postulated models $m_{\phi_k M_s}$ related to previous element of basis. Option of way of development depends on our possibility of recognition of new premises. In the first case we have to do with simpler speculations. Transition to new element of basis \mathcal{B} needs usually more deep concepts and is usually more complicated. Cooperation of both ways simultaneously can considerably develop context related to modelling of reality.

Let us mention that cognition manifold should be applied also to gathering of information on previously introduced theories which become less important. Such a history supports development of context for new theories. In particular with the aid of obtained context we can select more optimal paths for continuation of development since we need not repeat the same ways.

The question is where from such a large necessity for theoretical speculations follows. It seems that in current theoretical physics we tend predominantly to physics associated with higher and higher energy. This is manifested by various facilities which are able to carry out experiments for high energy physics. However, low energy physics is very important. Let us mention physical foundations for theoretical biology or nanotechnology. In the paper [10] one indicates important role of attractor defined at the elementary particle level and governing selforganization manifested at the molecular level. This attractor is responsible for precision of nanotechnological processes as well as for biological evolution. Thereby we are able to express mechanism of biological evolution on the most fundamental elementary particle level.

Foundations for mechanism of this selforganization can be associated with high energy physics and low energy physics. Explanation of corresponding selforganization can be based on theoretical speculations and needs more subtle experimental results related to low energy physics. Experiments related to various states of vacuum medium associated with elementary particles are not carried out yet. Let us mention here for instance experimental investigations related to evolution of components responsible for state of corresponding wave function. Such experiments are difficult since theory and experiment are strongly conjugated for more subtle processes. Therefore they need more clear theoretical foundations frequently obtained with the aid of various hypotheses. We can expect that perhaps larger set of experiments can be necessary for extraction from them confirmation of formulated previously hypotheses. Then theoretical description has to be sufficiently complex in order to see this fine reality.

The title of this paper accentuates role of speculations in theoretical physics. We come to the conclusion that role of theory increases when we develop investigations towards more fundamental level. Indeed experiments are then less clear and need interpretation by theories which use hypotheses. All this elucidates the problem what is important in development of current theoretical physics.

The term qualitative theory is considered frequently as equivalent to preliminary stage of development of theory. Then, any theory which provides quantitative results is seen as more serious and advanced. However such a point of view is now not sufficiently justified. We should decide what is more important quantitative theory which is not universal or qualitative theory which can be universal in a future.

The first theory can be applied in some range of validity. The second theory gives us a hope for

description of all observed phenomena and perhaps to predict some new ones. Furthermore transition with time from qualitative to quantitative theory should be relatively easy. This step needs determination of constants which are provided by qualitative models only. Thereby, main efforts for construction of theory with large range of validity are done within qualitative speculations where we have to track down premises for making assumptions. This task seems to be the most difficult when we construct fundamental theory. Qualitative theory can be complex since it can be based on large number of equivalence classes corresponding to various partial phenomena. Let us also note that estimation of status of assumptions introduced can be difficult. Consequently it seems that the second aim related to formulation of qualitative theory is much more important for development of theoretical physics. We come to the following conclusion:

CONCLUSION 12.1: Construction of qualitative theory on way towards universal theory is much more important for development of theoretical physics than quantitative theories which fit to experimental results in some range of validity only. Therefore the main task for theoretical physics is to create activity by systematic speculations considered as method of recognition of reality. The term "systematic" means that speculations should be well placed within cognition manifold and selforganizing reasoning. Thereby the term qualitative theory can be associated with advanced theory and should not be identified with preliminary stage of development.

This paper expresses tendency towards formalization of cognition process as additional aspect of modelling in comparison with application of precise mathematics to description of reality only. In theoretical physics the cognition process is not formalized yet. Premises for application of mathematics follow in current theoretical physics from philosophy of physics and philosophy of sciences in general. This means that within this paper partial formalization of some aspects of philosophy of physics is carried out. I suggest necessity of shifting this formalization as far as it is possible ahead. This in turn should be helpful in determination of resolution of seeing of reality by theory, thereby also by our brain, so precisely as it would be possible.

Consequently one suggests to carry out formalization of cognition process in order to obtain better comprehension of theoretical description in relation to reality. It seems that space for more systematic theoretical speculations should be enlarged maintaining discipline as far as it is possible just owing to introduced formalization.

12.2 New possibilities for development of theoretical physics

Let us remark that elaborated here methodology was applied to formulation of vacuum medium mechanics. This creates new situation for development of theoretical physics. Vacuum medium mechanics sees reality within current set of experimental results which differs from reality described by other fundamental theories including the standard model.

The vacuum medium mechanics sees proton as composed of three positrons [19], [9]. Neutrino can create unstable bounded states with charged particles [17] what changes point of view on weak interactions. Now such interactions have electromagnetic character induced by rotation of neutrino within static electric field of charged particle. All this leads to entirely new classification of elementary particles [9]. There are no quarks. Boson Z is not carrier of electroweak interactions in direct interactions between electron and neutrino. Big Bang model is considered as explosion of space on the inside of giant black hole [16] and leads to processes which are in accordance with astrophysical observations. Gravitational field can be interpreted as phenomenon on the most fundamental level having clear influence on motion of particles. Dark energy is interpreted directly as energy of gravitational field generated by external black hole wall created after the Big Bang. Then accelerated expansion of universe is interpreted as attraction of visible matter by mass of external black hole wall and no inflation is considered. Unification of all elementary particle interactions is obtained directly.

We have also to do with entirely new quality within vacuum medium description. Annihilation of electron and positron produces electromagnetic radiation and additionally also explosion of space.

This property is not manifested in current fundamental theories since particles are considered there predominantly as point-like. Another new quality is related to concept of chain state of particles with the same charge [6], [7] which has high status. This leads to electronic interactions which are not described by quantum theories. Consequences are serious. We are able to suggest mechanism of biological evolution considered on the most fundamental physical level [11], [10], [7]. Furthermore such processes allow us to discuss source of precision for molecular nanotechnology [10].

New opportunity for further investigations is also associated with possibility of continuation of cognition process by considering deep structure of vacuum medium related to scale $S_{DVM} < S_{VM}$ with a hope of better understanding of mechanisms of evolution of wave function as well as better understanding of whole vacuum medium.

Let us notice that traditional point of view on development of theoretical physics suggests that we need new experiments for confirmation of various phenomena seen within vacuum medium mechanics. This situation differs from situation of the standard model where we have at our disposal large number of such experiments.

Indeed some additional experiments for vacuum medium mechanics could be useful especially in relation to disintegration of proton. Some of them are done or can be reinterpreted. Let us mention here discussion on arguments supporting model of three-positron structure of the proton [19]. Entirely new experiment gives evidence for existence of boson E(38) what supports directly the vacuum medium mechanics. However we encounter entirely new circumstances discussing experimental confirmation of vacuum medium mechanics. At this moment existing experiments support to larger degree vacuum medium mechanics than the standard model.

Let us mention in this place decay of pion for instance. Products of this decay suggests directly that pion is composed of electron and three neutrino. The standard model states that it is composed of two quarks what has a justification within this theory. However direct observation having larger status is removed by the standard model as less important. Similar situation happens in interpretation of neutrino. The standard model treats neutrino traditionally by wave particle duality as a wave. However no wave properties of neutrino is confirmed directly by experiment in similar way as this is done for electron for instance. It suggests directly that resolution of seeing of reality by the standard model is low and is not based on assumptions related to clear observations.

Introduction of larger system of fundamental notions within vacuum medium mechanics allows us interpret neutrino better [17], [9]. This in turn allows us to interpret decay of pion as confirmation of existence of bounded state of electron and three neutrino. Similar situation is related to neutron, its decay and interpretation of its composition as bounded state of proton, electron and neutrino within vacuum medium mechanics [9].

Above concise discussion states that improved methodology enables us to take over existing experimental results of physics in order to justify vacuum medium mechanics to larger degree than the standard model. We see in this place also increasing role of conjugation of theory and experimental results in interpretation of reality.

Consequently new possibilities for development of theoretical physics rest on development of various speculation lines in accordance with assumed methodology which takes into account estimation of status of assumptions and theories. Development of vacuum medium mechanics is an example of such a way. Furthermore new possibilities for development rest also on development of methodology which would elucidate better essence of conjugation of theory and experimental results. Continuation of development in this direction should improve our interpretation of experimental results.

12.3 New possibilities for development of philosophy of science

This paper creates a new quality also for philosophy of physics. We observe in literature various attempts for elaboration of methodology for construction of physical theories, let us mention [23], [24] for instance. We observe there structuralist approach which perhaps is the most close to that one presented in this work. However we can indicate important difference.

Structuralist approach formalizes theoretical description of reality. However methods of changing of theories in order to reflect reality better are not entirely clear. Nevertheless some comments on this matter are done. This is so since cognition process is not formalized. As a result of this methodology discussed in [23], [24] is referred to examples of existing theories and does not provide pressure on direct development of theoretical physics.

We would say that this work provides new opportunity for development of philosophy of physics which consists in formalization of cognition process. Cognition theory is a part of philosophy of science. Thereby formalization of this process is an important task for philosophy. Let us mention that we should have attitude which force us to formalization of all what is possible. Then "metatheoretical" reasoning should be continued beyond border determined by area of this formalization. It means that we should avoid "metatheoretical" reasoning in area which could be formalized.

The term cognition is related also to cognitive psychology. On the other hand theory of knowledge called epistemology is applied in philosophy. We have to do in this paper with mixing of both terms. Cognition considered here happens owing to action of a dynamical system in an environment. The term "status of assumptions" is associated to some degree with perception. This perception happens owing to motor and sensory system of our dynamical system. However it also happens on the inside of neural network system between its subsystems [1]. This in turn can lead to interpretation of various aspects of mathematics created there.

We would say that we try to introduce point of view that mathematics is considered here as a kind of sense for recognition of reality. By direct connections of mathematics with dynamical system we obtain a hope for physical interpretation of mathematics. This could be done when the dynamical system would be derived as a physical system. Then perception by mathematics could be perhaps better explained.

Formalization of cognition process discriminates two kinds of thinking. The first one is based on information processing and is related to larger degree to pure mathematics and power of brain. The second one is based on perception and is related to fitting of mathematical description to reality and to larger degree to sensitivity of brain. The last kind of thinking is perhaps more close to philosophy of science.

Within this context we come also to the conclusion that formalization of cognition process tends to improvement of resolution of seeing of reality by theory what is manifested just on way how mathematics is applied. In particular criteria for estimation of status of assumptions and theories should lead to improvement of this resolution.

Let us also note that owing to discussed above methodology we have a hope to formalize axiology in a future. This is so since owing to vacuum medium mechanics obtained with the aid of introduced methodology we can discuss formulation of theoretical biophysics which contains mechanisms of biological evolution based on the most fundamental physical processes [11]. Such a possibility can be discussed since we are able to define an attractor within molecular system and based on electronic processes which governs selforganization of biological molecules. This in turn gives foundations for defining a dynamical system which would realize cognition process associated with evolution on way discussed within this work. Then system of values within this dynamical system can be considered. Positive value is associated with action of this dynamical system which is in accordance with appropriate direction for evolution of a given organism. This in turn can be seen as opportunity for fundamental description of emotions as associated with created system of values.

We obtain also new situation related to general view on development of theoretical physics based on philosophy of physics. In accordance with [4] we have to do in theoretical physics with paradigms. Within paradigms evolution of theory is continued until it attains an appropriate stage. This stage of development indicates whether the theory can be removed or can become dominant as a result of comparison with other theories within other paradigms.

Paradigm approach has some deficiencies. It favors to larger degree organisation of groups of scientists. Progress in theoretical physics can be seen in such a case as of secondary importance since works within paradigms are preferred. Perhaps persons which try to introduce entirely new point of view

will not be accepted as not fitting to current paradigms and by this to organised groups of scientists. Consequently, paradigm approach stabilizes theoretical physics on current level of development. Pressure on cognition process associated with development of theoretical physics within this approach is in fact stopped owing to lack of appropriate mechanisms leading to development beyond the paradigms. This in fact has important consequences since estimation of quality of scientific work is not associated with fighting on new quality in theoretical physics.

The question is why such a situation appears. It seems that Kuhn did not see directly how new quality in theoretical physics appears by efforts of scientific workers. Instead of this various final steps have been analysed. Let us note that just each final step has its own history which is not seen directly, and is based on way how theoretical physicist is fighting and generates by this pressure on development. In particular new results appear with the aid of attained stage of scientific development of theoretical physicist and this development can take very large part of his scientific life. Thereby efficiency of scientific development has to be seen as important part of scientific work since just this development determines starting point for fighting on new results.

Summarizing this discussion, we see that paradigm approach is not introduced with the aid of analysis of methods of work of theoretical physicists taking into account all aspects of this work. This leads also to avoiding of introduction of systems of opinions which take into account methods of scientific work and real efforts related to doing progress. All this stabilizes current stage of development of theoretical physics and in fact acts against development. By this discussion one suggests also that philosophers of physics should to larger degree analyse scientific results considered as intermediate steps which lead to final important result instead of final results only what is done predominantly by historical analysis. Such an attitude makes better understanding how real progress is made. Formalization of cognition process seems support just such an approach.

This work suggests that we could consider speculation line placed within cognition manifold instead of paradigm. Then development of new line is natural and is not in contradiction with other speculation lines. Furthermore, even in case of rejection of a theory which is developed with the aid of speculative reasoning, corresponding speculation line is justified as separate tasks which should be finished with appropriate conclusions. All this is considerably better for scientific workers which create theories which perhaps will be rejected since they provide notwithstanding recognition of reality by extension of context with the aid of investigated speculation line.

It seems that speculation lines allow us to make better observations how development is continued by efforts of theoretical physicists and estimate amount of these efforts.

Above discussion indicates that development of context can be additional and important aim of investigations. With the aid of extended context, we could obtain perhaps new premises, which was not seen previously without this context. Struggle for obtaining of new premises is fundamental for creation of new speculation lines and estimation of status of assumptions and theories.

References

1. J. Kaczmarek, On methodology of constructing of physical theories, *Journal of Pure and Applied Mathematics: Advances and Applications*, **15**(1), 23-60 (2016).
2. J. Kaczmarek, On emergence of intelligence in biological systems and methods of modelling of reality necessary for development of theoretical biology, *Far East Journal of Applied Mathematics*, **75**(2) 101-150, (2013).
3. K. Popper, *The Logic of Scientific Discovery*, Taylor and Francis e-Library ed., (2005).
4. T.S. Kuhn, *The Structure of Scientific Revolutions*, University of Chicago Press, (1962).
5. J. Kaczmarek, A method of multiscale modelling considered as a way leading to unified mechanics of materials, *Acta Machanica*, **226**, 14191443 (2015), DOI 10.1007/s00707-014-1261-7.
6. J. Kaczmarek, Concept of the chain state of particles with the same charge, *Advanced Studies in Theoretical Physics*, **3**(1-4) 13-33, (2009).
7. J. Kaczmarek, On the role of the electronic chain state for evolution of molecular systems leading to a protocell, *Advanced Studies in Theoretical Physics*, **4**(9), 413-435 (2010).
8. J. Kaczmarek, Surface superuidity property as a mechanism responsible for rotation of the electron, *Advanced Studies in Theoretical Physics*, **6**(28), 1355-1369 (2012).
9. J. Kaczmarek, On structural classification of elementary particles within vacuum medium mechanics, *Malaysian Journal of Physics*, **36**(1), 1-19 (2014).
10. J. Kaczmarek, Problems Associated with Transferring of Engineering to Small Scale – Towards Theoretical Nanotechnology, *Acta Physica Polonica A*, **130**(6), 1295-1323 (2016).

11. J. Kaczmarek, On a general formulation of theoretical biophysics which accentuates dominant role of dynamics of processes over structures within biological systems, submitted.
12. Carl Gillett, Reduction and emergence in science and philosophy, Cambridge University Press (2016).
13. Hildegard Meyer-Ortmanns, On the Success and Limitations of Reductionism in Physics, in B. Falkenburg and M. Morrison (eds.), Why More Is Different, Springer-Verlag Berlin Heidelberg (2015).
14. Joana Rigato, Looking for Emergence in Physics, Firenze University Press, (2017).
15. J. Kaczmarek, Speculative mechanics: a concept for modelling the vacuum medium, Phys. Essays, **12**(4), 709-732 (1999).
16. J. Kaczmarek, Processes related to black hole state described within four-component vacuum medium model, Advanced Studies in Theoretical Physics, **3**(1-4), 35-63 (2009).
17. J. Kaczmarek, A prototype model of the free neutrino, Advanced Studies in Theoretical Physics, **2**(5-8), 13-33 (2008).
18. J. Kaczmarek, A model of electric field in the vicinity of charged particle, Advanced Studies in Theoretical Physics, **7**(24), 1165-1187 (2013).
19. J. Kaczmarek, Arguments supporting model of three-positron structure of the proton, Advanced Studies in Theoretical Physics, **5**(2), 63-75 (2011).
20. E.van Beveren, G. Rupp, Material evidence of a 38 MeV boson, arXiv:1202.1739 [hep-ph].
21. Kh.U. Abraamyan, A.B. Anisimov, M.I. Baznat, K.K. Gudima, M.A. Nazarenko, S.G. Reznikov and A.S. Sorin, Observation of the E(38)-boson, arXiv, (2012).
22. W.A. Pogorzelski, Classical functional calculus, PWN Warszawa (1981).
23. W. Balzer, C.U. Moulines, J.D. Sneed, An architectonic for science. The Structuralist Program, by D.Reidel Publishing Company (1987).
24. I. Niiniluoto, Is science progressive, Springer Science+Business Media Dordrecht, (1984).

ФОРМАЛІЗАЦІЯ ПРОЦЕСУ ПІЗНАННЯ ЯК ДОДАТКОВОГО КОМПОНЕНТА, ВІДПОВІДАЛЬНОГО ЗА РОЗВИТОК ТЕОРЕТИЧНОЇ ФІЗИКИ

Ярослав Качмарек

*Institute of Fluid-Flow Machinery, Polish Academy of Sciences
80-231 Gdansk, ul. J. Fiszer 14, Poland*

Теоретична фізика досягла етапу, коли слід враховувати нові методичні підходи. Зокрема, вони повинні впроваджувати більшу дисципліну в теоретичних спекуляціях. У цій статті представлено концепцію багатозначного пізнання як методологічної основи для розвитку опису реальності теоретичною фізикою за допомогою теоретичних міркувань. Можна припустити, що це спосіб побудови фундаментальних і універсальних фізичних теорій. Багатозначне пізнання складається з основи, яка представляє моделі нашого простору як середовища, і представляє моделі процесів у відповідному просторі. Моделі засновані на доступних експериментальних результатах, а також на нових припущеннях та гіпотезах, отриманих теоретичними міркуваннями. З метою підтримання дисципліни в цих міркуваннях розглядається стан припущень і теорій, що охоплюються багатозначним пізнанням як функція, визначена на елементах волокон. Наголошується важливість самоорганізації міркувань як такої, що більше підходить для розпізнавання дійсності порівняно з точним чистим математичним доказом. Розглядається також докази по відношенні до реальності. Ця стаття розглядається як спроба формалізації процесу пізнання, яка характеризується трьома основними компонентами: багатозначним пізнанням, статусом припущень теорії та концепцією самоорганізації міркувань.

КЛЮЧОВІ СЛОВА: методологія побудови універсальних фізичних теорій, пізнавальна різноманітність, формалізація процесу пізнання

Алла Таньшина

*К 100-летию юбилею НАН Украины & 90-годовщине основания ННЦ «ХФТИ»**... В Харькове была создана мощная школа современной теоретической физики.
Академик Б.Е. Патон, президент НАН Украины***ИНСТИТУТ ТЕОРЕТИЧЕСКОЙ ФИЗИКИ ИМЕНИ А.И. АХИЕЗЕРА***Продолжение. Начало в №4 (2018) – №1 (2019)***Стратегия развития**

Стратегия развития Института теоретической физики имени А.И. Ахиезера (далее – ИТФ) также прошла проверку временем: институту удалось сохранить актуальные научные направления и преемственность ведущих научных школ УФТИ – ХФТИ.

Конечно, были и есть проблемы. Но серьёзный международный рейтинг ИТФ помог ему устоять и в непростую постсоветскую эпоху, и в нынешние времена.

В «фокусе» сегодняшнего дня ИТФ – разработка актуальных и передовых рубежей современной физической науки. Структурные подразделения института являются наглядным показателем его научного потенциала:

- отдел статистической физики и квантовой теории поля;
- отдел диффузионных и электронных явлений в твердых телах;
- отдел квантово-электродинамических явлений и электродинамики адронов;
- отдел теории конденсированных сред и ядерной материи;
- отдел теоретико-групповых свойств элементарных частиц, теории ядра и нелинейной динамики;
- отдел электродинамики высоких энергий в веществе.

Но что самое важное – все научные отделы ИТФ имеют в своем штате талантливых (и весьма инициативных) молодых учёных, несмотря на то, что прошедшие годы не слишком-то благоприятствовали притоку молодёжи в науку. Более того – их творческие достижения отмечены научными наградами как отечественного, так и международного уровня.

Истина, которую исповедуют в ИТФ: главное не просто накопить знания и опыт, но и передать их достойной смене.

Очень здорово помогает и тот факт, что отношения в коллективе выстроены по-человечески доброжелательно и демократично.

И уже очевидно: ИТФ выдержал конкуренцию на постсоветском пространстве и накопил солидный научный потенциал.

На сегодняшний день научная идеология ИТФ – это и его традиции. И вот лишь некоторые из них:

- работа на передовых рубежах науки (*а эти рубежи необходимо знать!*);
- уважительное отношение к эксперименту;
- участие в актуальных научно-технических проектах Украины и мира;
- проведение общепитетутских и общегородских научных семинаров;
- воспитание научной смены;
- педагогическая деятельность.

Международное научное сотрудничество ИТФ

На протяжении последних лет были не только налажены научные международные связи ИТФ, утраченные с распадом СССР, но и значительно расширена география его научного сотрудничества.

Широкой международной кооперации способствуют и уже ставшие традиционными научные форумы ИТФ. (К примеру: с 1997 года проводятся международные конференции «Суперсимметрия и квантовая теория поля» (SUSY), а с 2001 – международные конференции «Квантовая электродинамика и статистическая физика» (QEDSP).)

Научный семинар ИТФ

По средам, в половине одиннадцатого...

Ещё в советские времена, по негласной традиции, апробация научных результатов на теорсеминарах ХФТИ была довольно весомой. Также и поныне ИТФ открыт для разумного сотрудничества и диалога с научным мировым сообществом.

И вот типичный пример. «Однажды, – как рассказывает Ю.П. Степановский, – на семинаре выступал мой однокурсник, приехавший из Дубны. Ему задавали много, как мне казалось, каверзных вопросов. После семинара

я хотел извиниться перед ним за то, что его немного потрепали слишком любознательные участники семинара. Но не успел.

“Ты знаешь, я тебе так завидую. Такого благожелательного** отношения к себе я ещё не разу не испытывал”, – сказал мне мой однокурсник» [1, с.301]. Подмечено, действительно, очень точно и без апломба.

Общегородской физический семинар ИТФ

Объясни нам это по-простому, по-рабоче–крестьянски...

Академик А.И. Ахиезер

По инициативе ИТФ с 2004 года в Харькове начал функционировать общегородской физический семинар «Современные проблемы физики». Далее со слов В.Д. Ходусова, профессора Харьковского национального университета имени В. Н. Каразина:

«В 2004 году по инициативе Н.Ф. Шульги на физико-техническом факультете Харьковского национального университета имени В.Н. Каразина начал работать общезнаменитый семинар “Современные проблемы физики”. Его цель – предоставить молодым ученым, и прежде всего студентам, возможность общения с ведущими учеными, чтобы они могли ощутить пульс современной науки. Необходимость такого семинара ощущалась уже давно многими учеными Харькова, потому что была потребность в неформальном общении на общезнаменитом уровне и желание не только поделиться своими достижениями, но и узнать, что делают другие.

Раньше такие семинары проводились в Харькове. В разное время ими руководили академики А.И. Ахиезер и И.М. Лифшиц. Но в 90-х годах они уже не проводились.

В феврале 2004 г. семинар открылся снова. Первый доклад сделал Н.Ф. Шульга. Семинар превзошел все ожидания. Аудитория была переполнена студентами всех курсов не только физико-технического, но и других факультетов университета. Также пришли известные физики и молодые научные сотрудники из многих физических институтов Харькова. В аудитории было более ста человек, некоторые даже сидели на ступеньках.

Теперь уже можно сказать – семинар удался и стал по-настоящему общезнаменитым.

И в этом большая заслуга академика НАН Украины Н.Ф. Шульги, который не только живо, но и с доброжелательным юмором его ведёт. Приятно слышать от студентов вопросы о том, когда будет следующее заседание и про что именно. Значит, им интересно. Семинар, кстати, проводится дважды в месяц».

Семинар молодых ученых ИТФ

Вновь созданный в стенах ИТФ семинар молодых ученых уже зарекомендовал себя как неформальная школа научного мастерства. Поскольку это реальный мастер-класс для молодёжи ИТФ: на равных, демократично и без пафоса.

И вот что рассказали сами участники этих семинаров.

Дмитрий Тютюнник: «Идею таких семинаров подал Н.Ф. Шульга, и мы ее сразу подхватили. Семинары молодых ученых решили сделать такими же традиционными, как общезнаменитые, но проводить их по четвергам, в одиннадцать. Здесь молодые сотрудники также имеют полную свободу научных тем для докладов и высказываний. Ведёт семинар профессор Ю.В. Слюсаренко.

Для начала мы решили доложить наиболее доступно собственные научные результаты. Это очень важно, т. к. часто один сотрудник не знает достаточно хорошо то, чем занимается другой. Список тем докладов получился достаточно разнообразным. Вот лишь некоторые из них: “Применение ферми-жидкостного подхода для изучения сверхтекучих состояний разнородной симметрии” (докладчик Сергей Шульга), “Когерентные эффекты в излучении при рассеянии пучков заряженных частиц” (докладчик Дмитрий Тютюнник), “Массоперенос и гетерогенные реакции в аэрозольных системах” (докладчик Дмитрий Копейченко) и т.д.

На каждом семинаре звучит достаточно много интересных вопросов, что помогает самому докладчику лучше понять свой материал. В настоящее время характер семинаров немного изменился. Мы теперь

* Невольно напрашиваются исторические параллели из воспоминаний П.А.М. Дирака:

«Хочу ещё рассказать кое-что о Нильсе Боре. Во время наших с ним дискуссий я узнал о том, какое недоразумение произошло когда-то между Бором и Томсоном. Бор сказал мне, что был горячим поклонником Томсона и меньше всего собирался критиковать его или обижать. Бору хотелось получить дальнейшие разъяснения по поводу атомных моделей Томсона, но он плохо знал английский язык и не мог задать свои вопросы столь вежливо, сколь хотел. В результате Томсон понял эти вопросы неправильно. Он решил, что его критикуют, и разозлился.

Происшедший инцидент сильно и надолго огорчил Бора. Мне кажется, что он всю жизнь расстраивался из-за этой истории и в дальнейшем всегда боялся, как бы она не повторилась. Когда бы он ни расспрашивал очередного автора о его работе, он неизменно повторял: “Я вовсе не собираюсь критиковать Вас, я просто хочу знать”. Это выражение: “This is not to criticize but only to learn” – стало в Копенгагене крылатым» [2, с.33]. Небезынтересен также исторический нюанс из воспоминаний академика А.И. Ахиезера: «Дирак был избран почетным членом ученого совета УФТИ, Капица и Гамов являлись научными консультантами института».

планируем сообщать на семинарах новости науки, докладывать и разбирать некоторые интересные вопросы теорфизики. В планах на будущее также неформальные лекции по избранным главам теор- и матфизики, касающихся КЭД и др.».

Денис Копейченко: «Многие из нас были знакомы друг с другом еще во время учебы на физтехе. Устроившись на работу в Институт теоретической физики, все разошлись по разным отделам и занимаются своей тематикой. Семинар же позволяет узнать: какие результаты в последнее время получены остальными. А в дальнейшем, возможно, поможет найти общие темы для совместных исследований».

Игорь Танатаров: «Семинары молодых ученых – хороший шанс для нас, молодых сотрудников, собраться, узнать что-то новое из тех областей, в которых работают другие, и свободно пообщаться по разным вопросам в физике (и не только). Впрочем, семинары эти оказались интересны не только для нас – так, и мой дедушка ходит их послушать, и другие старшие сотрудники. Сейчас с нетерпением ждём их продолжения в формате лекций по некоторым любопытным вопросам из квантовой механики».

Ещё одна особенность сегодняшнего дня ИТФ – это уже сложившиеся научные династии. По стопам отцов пошли Александр Пелетминский, Алексей Слюсаренко, Алексей Фомин, Игорь Танатаров, Сергей Ивашин и Сергей Шульга.

Педагогическая деятельность

Фундаментальной подготовке научных кадров весьма серьёзно способствует общение с активно работающими учеными. И со слов проректора по научной работе (1967-2013 гг.) Харьковского национального университета имени В. Н. Каразина члена-корреспондента НАН Украины Ильи Ивановича Залюбовского (1930-2013), «студенты слушают лекции из уст ведущих ученых Института теоретической физики. К тому же, как правило, наиболее творчески активные студенты привлекаются к актуальным научным изысканиям, что не так уж и маловажно в студенческой жизни».

Участие в актуальных научно-технических проектах Украины и мира

Тесная связь теории и эксперимента.

В этом была и есть великая сила УФТИ – ННЦ «ХФТИ».

Н.Ф. Шульга,

директор-организатор ИТФ

ИТФ участвует в постановке и разработке всех крупных научных программ и проектов ННЦ «ХФТИ» НАН Украины. Как подчеркивает генеральный директор ННЦ «ХФТИ» в 2004-2016 гг. академик Иван Матвеевич Неклюдов: «главнейшая из них – разработка государственной программы фундаментальных и прикладных исследований «Использование ядерных материалов, ядерных и радиационных технологий в различных отраслях экономики». А поскольку ННЦ «ХФТИ» является ядром нового отделения НАНУ и решением Совета национальной безопасности и обороны Украины определен в качестве головной организации по научному сопровождению работы атомных электростанций, нам, как говорится, и программу составлять, и ответ держать... Важно отметить, что для подготовки столь серьезной программы у коллектива есть и опыт, и традиции, и высококвалифицированные специалисты, и весьма перспективные наработки» [3].

Так, в частности, к работам по физике реакторов на быстрых нейтронах, так называемого реактора с медленным ядерным горением (или реактора Феоктистова), подключилась группа теоретиков-ядерщиков: Н.Ф. Шульга, В.В. Пилипенко, С.П. Фомин, Ю.П. Мельник, Л.Н. Давыдов и др.

Разработка такого типа реактора представляется чрезвычайно важной для энергетики Украины в будущем, так как работа такого реактора основывается на использовании урана-238, запасы которого в Украине огромны (работа обычных тепловых реакторов основывается на использовании урана-235, запасы которого быстро уменьшаются).

Кроме того, реактор с медленным ядерным горением является безопасным с точки зрения протекающих в нем физических процессов – **ядерный взрыв в таком реакторе невозможен**.

Представляется уместным вспомнить предысторию возникновения интереса теоретиков к этому направлению работ в контексте статьи нынешнего генерального директора ННЦ «ХФТИ», академика-секретаря Отделения ядерной физики и энергетики НАН Украины Николая Фёдоровича Шульги «Откуда шумеры узнали это староукраинское слово?», посвященной памяти замечательного физика-теоретика Николая Антоновича Хижняка:

«В 90-х годах в ННЦ «ХФТИ» приехала группа ученых, сотрудников Эдварда Теллера (Edward Teller) из Ливерморской лаборатории США (Lawrence Livermore National Laboratory, LLNL), с предложением подключиться к работам по подземному ядерному реактору.

Их большие интересовали материаловедческие проблемы такого реактора. Основная идея предложенного реактора заключалась в использовании в качестве топлива небогащенного урана, в который локально вводится небольшая часть обогащенного топлива (урана-235 или плутония). При этом подбираются условия, при которых в результате ядерных превращений по объему небогащенного урана распространяется волна повышенной плотности нейтронов, а значит и тепловыделения.

Скорость такой волны составляет порядка одного метра в год. Это означает, что если небогащенный уран будет находиться в цилиндре с диаметром один метр и длиной порядка 30 метров (именно с таким предложением приехали американские специалисты), то волна по такой среде будет распространяться 30 лет, пока не достигнет торца цилиндра противоположного торцу, где находится обогащенный уран.

Существенными особенностями такого реактора являются его безопасность и значительное (до 60%) выгорание топлива.

Сотрудница Э. Теллера сделала доклад по Монте-Карло моделированию ядерных процессов в реакторе, обратив внимание на то, что потенциал существовавших на тот момент времени в США компьютеров ограничивает возможности моделирования.

В этой связи у меня возникла идея о том, что упрощения при описании процессов в таком реакторе могут быть достигнуты путем некоторого огрубления задачи с помощью использования гидродинамического приближения.

С этой идеей я пришел к А.И. Ахиезеру, который хотя и не присутствовал на встрече с американскими учеными, но отслеживал, что там происходит.

Александр Ильич, выслушав, о чем идет речь, буквально вскрикнул: "Так это же задача на медленное горение – медленное ядерное горение!"

Дело в том, что существует быстрое и медленное горение. Быстрое горение – это детонация, взрыв. Медленное горение – это, например, когда мы поджигаем спичкой лист бумаги, и волна горения медленно распространяется по этому листу.

Отмечу в этой связи, что в 40-х годах А.И. Ахиезер вместе с И.Я. Померанчуком много работали над теорией ядерных реакторов. По заданию И.В. Курчатова они даже написали книгу по теории ядерных котлов (так раньше назывались реакторы), первый вариант которой, к сожалению, на долгие годы был засекречен. Затем А.И. Ахиезер утратил интерес к этой проблеме, занявшись другими задачами.

И вот как-то сразу почувствовалось, что идея о медленном ядерном горении вернула Александра Ильича к тем прекрасным годам, когда он работал вместе с И.Я. Померанчуком.

Александр Ильич сказал, что этой задачей обязательно и быстро нужно заниматься. Он также отметил, что без Николая Антоновича Хижняка ничего не получится, и сразу же отправил меня к Н.А. Хижняку, который находился в это время в больнице.

На следующий день я уже беседовал с Николаем Антоновичем. Идея о медленном ядерном горении ему очень понравилась. И работа «закипела»...

Здесь необходимо отметить, что к этому времени Николай Антонович уже много работал над проблемой безопасного реактора, но в несколько ином направлении. Он также предлагал использовать в реакторе небогащенное топливо, но перерабатывать его в тепло планировалось с помощью ускорителя. Сейчас эта идея интенсивно развивается Нобелевским лауреатом, бывшим директором ЦЕРНа К. Руббиа (Carlo Rubbia).

Работа, однако, вначале разворачивалась не очень быстро, что было связано и с отсутствием финансирования, и с необходимостью освоения новой области исследований, и с отсутствием необходимых вычислительных мощностей (компьютеры в ХФТИ тогда только появлялись).

Значительные продвижения произошли после получения гранта УНТЦ по этой теме и подключения в рамках гранта к проблеме теоретиков и экспериментаторов, имеющих опыт работы в области ядерной и радиационной физики (Ю.П. Мельника, Б.А. Немайшало, С.П. Фомина, Л.Н. Давыдова, Д.П. Белозерова и др.).

К сожалению, перед началом финансирования гранта ушел из жизни Александр Ильич Ахиезер, а после первого года работы по гранту умер Николай Антонович Хижняк, которые были движущей силой этого проекта.

Николай Антонович очень хотел, чтобы по этой теме была опубликована наша совместная статья. Такая статья появилась, но уже после смерти Николая Антоновича:

А.И. Ахиезер, Н.А. Хижняк, Н.Ф. Шульга, В.В. Пилипенко, Л.Н. Давыдов. Медленное горение // Вопросы атомной науки и техники. – 2001, – №6(2), – с.272-276». [4, с.62].

Продолжение следует...

СПИСОК ЛИТЕРАТУРЫ

- [1]. A.I. Akhieser, *Очерки и воспоминания [Essays and Memories]*, (Fact, Kharkiv, 2003), pp. 430, (in Russian)
- [2]. P. Dirak, *Воспоминания о необычной эпохе: Сб. статей [Memories of an unusual era: Collection of articles]*, edited by Ya.A. Smorodinskii (Nauka, Moscow, 1990), pp. 208. (in Russian)
- [3]. E. Sergienko, Всеукраинская техническая газета [Ukrainian technical newspaper], **39(91)**, (2004), (in Russian)
- [4]. Член-корреспондент НАН Украины Николай Федорович Шульга. К 60-летию со дня рождения [Corresponding Member of the National Academy of Sciences of Ukraine Nikolay Fedorovich Shulga. To the 60th birthday], edited by S.V. Peletinskii, (Kvant, Kharkiv, 2007), p. 64, (in Russian)

PACS: here you must specify PACS codes

INSTRUCTIONS FOR PREPARING MANUSCRIPT IN EAST EUROPEAN JOURNAL OF PHYSICS

¹N.N. Author, ²N.N. Co-author(s)

¹Affiliation of first author

²Affiliation of second author (if different from first Authors)

¹E-mail: corresponding_authors@mail.com, ¹ORCID ID

²E-mail: next_authors@mail.com, ²ORCID ID

Received January 4, 2019

Each paper must begin with an abstract. The abstract should be typed in the same manner as the body text (see below). Please note that these Instructions are typed just like the manuscripts should be. The abstract must have at least 1800 phonetic symbols, supplying general information about the achievements, and objectives of the paper, experimental technique, methods applied, significant results and conclusions. Page layout: the text should be printed on the paper A4 format, at least 5 pages, with margins of: Top - 3, Bottom, Left and Right - 2 cm. The abstract should be presented in English (only for foreign authors), Ukraine and Russian.

KEYWORDS: there, must, be, at least, 5 keywords

This is introduction section. This paper contains instructions for preparing the manuscripts. The text should be prepared in .doc format (using MS Word).

INSTRUCTIONS

The text should be typed as follows:

- title: Times New Roman, 12 pt, ALL CAPS, bold, 1 spacing, centred;
- authors: name, initials and family names; Times New Roman, 12 pt, bold, 1 spacing, centred;
- affiliation(s): Times New Roman, 9 pt, italic, 1 spacing, centred;
- abstract: Times New Roman, 9 pt, 1 spacing, justified;
- body text: Times New Roman, 10 pt, 1 spacing, justified; paragraphs in sections should be indented right (tabulated) for 0.75 cm;
- section titles: Times New Roman, 10 pt, bold, 1 spacing, centred, without numbering, one line should be left, blank above section title;
- subsection titles: Times New Roman, 10 pt, bold, 1 spacing, centred, without numbering in accordance to the section (see below), one line should be left blank above subsection title;
- figure captions: width of the figure should be 85 or 170 mm, figures should be numbered (Fig. 1) and titled below figures using sentence format, Times New Roman, 9 pt, 1 spacing, centred (if one line) or justified (if more than one line); one line should be left blank below figure captions;
- table captions: width of the table should be 85 or 170 mm, tables should be numbered (Table 1.) and titled above tables using sentence format, Times New Roman, 10 pt, 1 spacing, centred (if one line) or justified (if more than one line), tables should be formatted with a single-line box around the outside border and single ruling lines between rows and columns; one line should be left blank below tables;
- equations: place equations centred, numbered in Arabic (1), flush right, equations should be specially prepared in MathType; one line should be left blank below and above equation.

Additional instructions

Numerated figures and tables should be embedded in your text and placed after they are cited. Only black and white drawings and sharp photographs are acceptable. Letters in the figures should be 3 mm high. The figures should be presented in one of the following graphic formats: jpg, gif, pcx, bmp, tif.

REFERENCES

Cite references in AIP style (<https://guides.lib.monash.edu/citing-referencing/aip>). Numbering in the order of referring in the text, e.g. [1], [2-5], etc. References should be listed in numerical order of citation in the text at the end of the paper (justified), Times New Roman, 9 pt, 1 spacing.

Journal Articles

- [1]. T. Mikolajick, C. Dehm, W. Hartner, I. Kasko, M. J. Kastner, N. Nagel, M. Moert, and C. Mazure, *Microelectron. Reliab.* **41**, 947 (2001).
- [2]. S. Bushkova, B.K. Ostafyichuk and O.V. Copaiev, *Physics and Chemistry of Solid State.* **15**(1), 182-185 (2014). (in Ukrainian)
- [3]. M. Yoshimura, E. Nakai, K. Tomioka, and T. Fukui, *Appl. Phys. Lett.* **103**, 243111 (2013), doi: [10.7567/APEX.6.052301](https://doi.org/10.7567/APEX.6.052301).

E-print resources with collaboration research

- [4]. Aaboud et al. (ATLAS Collaboration), *Eur. Phys. J. C*, **77**, 531 (2017).
- [5]. OR: M. Aaboud et al. (ATLAS Collaboration), *Eur. Phys. J. C*, **77**, 531 (2017), doi: [10.1140/epjc/s10052-017-5061-9](https://doi.org/10.1140/epjc/s10052-017-5061-9)
- [6]. Sjöstrand et al., *Comput. Phys. Commun.* **191**, 159-177 (2015), e-print [arXiv:1410.3012](https://arxiv.org/abs/1410.3012).
- [7]. Amin et al. e-print [arXiv:1006.3075](https://arxiv.org/abs/1006.3075) (2010).
- [8]. Boudreau, C. Escobar, J. Mueller, K. Sapp, and J. Su, (2013), e-print [arXiv:1304.5639](https://arxiv.org/abs/1304.5639).

Books

- [9]. S. Inoue and K.R. Spring, *Video Microscopy: The fundamentals*, 2nd ed. (Plenum, New York, 1997), pp. 19-24.
- [10]. I. Gonsky, T.P. Maksymchuk and M.I. Kalinsky, *Біохімія Людини [Biochemistry of Man]*, (Ukrmedknyga, Ternopil, 2002), p. 16. (in Ukrainian)
- [11]. V.V. Mal'tsev, *Металлографія промислових кольорових металів і сплавів [Metallography of industrial nonferrous metals and alloys]*, (Moscow, Metallurgiya, 1970), p. 364. (in Russian)
- [12]. M. Garkusha, *Основи Фізики Нанієпровідників [Fundamentals of Semiconductor Physics]* (Vysshaja shkola, Moscow, 1982), in: <http://gagago.ru/g20-osnovi-fiziki-napivprovodnikiv-pidruchnik-dlya-tehniku.html>.

Book Chapters

- [13]. M. Gonzalez-Leal, P. Krecmer, J. Prokop and S.R. Elliot, in: *Photo-Induced Metastability in Amorphous Semiconductors*, edited by A.V. Kolobov (Wiley-VCH, Weinheim, 2003), pp. 338-340.
- [14]. A. Kochelap and S.I. Peкар, in: *Теорія Спонтанної і Стимульованої Хемілюмінесценції Газів [Theory of Spontaneous and Stimulated Gas Chemiluminescence]* (Naukova dumka, Kyiv, 1986), pp. 16-29. (in Russian)

Conference or symposium proceedings

- [15]. C. Yaakov and R.Huque, in: *Second International Telecommunications Energy Symposium Proceedings*, edited by E. Yow (IEEE, New York, 1996), pp. 17-27.
- [16]. V. Nikolsky, A.K. Sandler and M.S. Stetsenko, in: *Автоматика-2004: Матеріали 11 Міжнародної Конференції по Автоматичному Управлінню [Automation-2004: Materials of the 11th International Conference on Automated Management]* (NUHT, Kyiv, 2004), pp. 46-48. (in Ukrainian)

Patent

- [17]. I.M. Vikulin, V.I. Irha and M.I. Panfilov, Patent Ukraine No. 26020 (27 August 2007). (in Ukrainian)

Special Notes

1. Use International System of Units (SI system). 2. It is undesirable to use acronyms in the titles. Please define the acronym on its first use in the paper.
3. Refer to isotopes as ¹⁴C, ³H, ⁶⁰Co, etc.

Наукове видання

СХІДНО-ЄВРОПЕЙСЬКИЙ ФІЗИЧНИЙ ЖУРНАЛ

Номер 2, 2019

EAST EUROPEAN JOURNAL OF PHYSICS

№ 2, 2019

Збірник наукових праць
англійською, українською, російською мовами

Коректор – Коваленко Т.О.
Технічний редактор – Гірник С.А.
Комп'ютерне верстання – Гірник С.А.

Підписано до друку 24.06.2019. Формат 60×84/8. Папір офсетний.

Друк ризографічний.

Ум. друк. арк. 11,3. Обл.-вид. арк. 11,6
Тираж 70 пр. Зам. № Ціна договірна

61022, Харків, майдан Свободи, 4
Харківський національний університет імені В.Н. Каразіна
Видавництво

Надруковано Харківський національний університет імені В.Н. Каразіна
61022, Харків, майдан Свободи, 4, тел. +380-057-705-24-32
Свідоцтво суб'єкта видавничої справи ДК № 3367 від 13.01.09